

SPECTRAL CHARACTERIZATION AND TRANSMUTATION
OF ACTINIDES IN
GASEOUS CORE REACTORS

By

CINDY FUNG

A THESIS PRESENTED TO THE GRADUATE SCHOOL
OF THE UNIVERSITY OF FLORIDA IN PARTIAL FULFILLMENT
OF THE REQUIREMENTS FOR THE DEGREE OF
MASTER OF ENGINEERING

UNIVERSITY OF FLORIDA

2006

Copyright 2006

by

Cindy Fung

ACKNOWLEDGMENTS

I thank the members of my supervisory committee Dr. Samim Anghaie, Dr. Edward T. Dugan, and Dr. Jacob N. Chung for their guidance, encouragement, and support. Their scientific knowledge, dedication to their students, and kindness make the learning experience a pleasure. I would like to show deep gratitude for the financial support provided by the Department of Energy and the Office of Nuclear Energy, Science and Technology through the Advanced Fuel Cycle Initiative.

I am fortunate to have Dr. Anghaie as the chair of my supervisory committee. His great vision for the future of the nuclear industry and his pragmatic attitude are the foundations of this research. I am touched by his compassion and respect for his students, and most of all by his honesty.

It has been enlightening working with Dr. Dugan. His expertise in Gas Core Reactors was essential to the success of this research. I am very appreciative of Dr. Dugan's professionalism and dedication to his role as supervisory committee member.

I am grateful to have the support and love of my family and all those who love me; without them my accomplishments would be meaningless. I want to especially thank a close friend who encouraged me to do my best and helped me through times of doubt. His unconditional support was essential to the completion of this project.

TABLE OF CONTENTS

	<u>page</u>
ACKNOWLEDGMENTS	iii
LIST OF TABLES	viii
LIST OF FIGURES	xi
ABSTRACT	xiv
CHAPTER	
1 INTRODUCTION	1
The Fuel Cycle.....	2
Mining and Milling of Uranium Ore	2
Conversion of Yellowcake to Uranium-Hexafluoride	3
Enrichment of Uranium.....	3
Fabrication of Nuclear Fuel.....	3
Power Production	4
Spent Fuel Characteristics	4
Nuclear Waste History.....	6
Nuclear Waste Treatment	8
Reprocessing and Recycling.....	8
Advantages of the closed cycle	9
Disadvantages of the closed cycle.....	9
Storage and Disposal	10
Low level waste.....	10
High level waste	12
Advantages of the open cycle.....	14
Disadvantages of the open cycle	14
Nuclear Waste Challenges.....	15
Permanent Repository not Available.....	15
More Repositories are Needed	16
MRS not Available.....	16
Reprocessing Facility not Available.....	17
Waste Must be Isolated for 10,000 Years	18
Current Technology.....	19
Boiling Water Reactor	20
Pressurized Water Reactor	21

Developing Technologies	22
Accelerator Driven Systems (ADS)	23
Gaseous Core Reactor (GCR)	24
Thesis Objectives.....	25
2 THE GASEOUS CORE REACTOR.....	26
GCR Description And Modeling.....	26
Reactor Geometry.....	26
Reactor Materials.....	27
Gaseous fuel	28
Reflector/moderator	31
Assumptions	34
Power Conversion Systems	35
GCR Characteristics	36
Safety and Feedback.....	36
Reactivity Control	38
Core Neutronics.....	38
Advantages Of The GCR.....	39
Computational Tools	41
MCNP.....	41
ORIGEN	44
MONTEBURNS.....	45
3 ACTINIDES AND FISSION PRODUCTS.....	47
Origins	48
Actinides.....	50
92-Uranium (U).....	50
93-Neptunium (Np).....	51
94-Plutonium (Pu).....	53
95-Americium (Am).....	57
96-Curium (Cm).....	58
Fission Products.....	62
38-Strontium (Sr)	62
43-Technetium (Tc).....	63
53-Iodine (I)	63
55-Cesium (Cs)	64
Applications.....	65
Nuclear Fuel	66
Radioisotope Thermoelectric Generator (RTG).....	68
Improving Proliferation Resistance of Fissile Material.....	70
Nuclear Medicine: Diagnostic and Treatment.....	72
Spectral Influence On Transmutation.....	73
Important Isotopes	76
4 SPECTRUM DESIGN.....	78

Reflector Material.....	79
Reflector Savings Saturation Thickness.....	79
Cross Section Study.....	85
Reflector Thickness.....	89
Gaseous Fuel Pressure.....	97
Fuel Enrichment.....	102
Length-To-Diameter Ratio.....	105
Internal Moderation.....	108
Summary Of Sensitivity Studies.....	112
Gas Core Reactor Design.....	113
Minimization of the Critical Fuel Volume.....	113
Obtaining a Wide Range of Neutron Spectra.....	114
Reactor Dimensions.....	115
Reference LWR Description.....	117
Core Spectrum Characteristics.....	117
Thermal energy range.....	119
Epithermal energy range.....	123
Fast energy range.....	125
Spectral summary.....	126
Reflector Spectrum Characteristics.....	128
5 FUEL CYCLE ANALYSIS.....	131
Fuel Cycle Simulation.....	131
Burn Step Size.....	131
Feed Fuel.....	132
Removal of Elements.....	133
MONTEBURNS Output.....	134
Burnup Calculation.....	135
Issues with BeO Fuel Cycle Analysis.....	135
Neutron Spectrum.....	136
Actinide Inventory.....	139
92-Uranium (U).....	140
93-Neptunium (Np).....	142
94-Plutonium (Pu).....	148
95-Americium (Am).....	150
96-Curium (Cm).....	152
Waste Characteristics.....	152
Fuel Utilization.....	155
6 CONCLUSIONS AND RECOMMENDATIONS FOR FUTURE WORK.....	159
Fuel Cycle Analysis Conclusions.....	159
Recommendations For Future Work.....	160

APPENDIX

A	TABULATED DATA FROM GCR DESIGN PARAMETERS SENSITIVITY STUDIES	165
B	SAMPLE MCNP INPUT	170
C	SAMPLE MONTEBURNS FEED FILE.....	175
D	SAMPLE MONTEBURNS INPUT FILE.....	177
	LIST OF REFERENCES.....	179
	BIOGRAPHICAL SKETCH	184

LIST OF TABLES

<u>Table</u>	<u>page</u>
2-1. Summary of reflector/moderator material properties.....	34
3-1. Summary of actinides and their important properties.	60
3-2. Summary of fission products and their important properties.....	65
3-3. Neutronic parameters for U-235 and Pu-239 fueled LWRs.....	66
3-4. Summary of radioisotopes that are candidate fuel for RTG.....	70
4-1. Summary of the reflector thickness study and corresponding reflector saturation thicknesses. All results were obtained using a gas pressure of 155 bars and enrichment of 19.95 w/o.....	84
4-2. Average percentage of fissions caused by neutrons in three energy ranges with gas pressure at 155 bars and enrichment at 19.95 w/o (except tungsten at 95 w/o).....	93
4-3. The percentage of fissions caused by neutrons in three energy ranges with reflector thickness at saturation, gas pressure at 155 bars, and enrichment of 19.95 w/o (except tungsten at 95 w/o).	94
4-4. Reactor parameters used for gas pressure sensitivity study.	97
4-5. Percentage increase in the number of fissions caused by neutrons in three energy ranges due to increase in gaseous fuel pressure.	101
4-6. Percentage increase in the number of fissions caused by neutrons in three energy ranges due to increase in fuel enrichment.	104
4-7. Percentage increase in the number of fissions caused by neutrons in three energy ranges due to increase length-to-diameter ratio.	107
4-8. Reactor parameters used for gap thickness sensitivity study.	110
4-9. Percentage increase in the number of fissions caused by neutrons in three energy ranges for a three-cavity reactor relative to a single-cavity reactor due to increase gap thickness.	111

4-10. Percentage increase in the number of fissions caused by neutrons in three energy ranges for a three-cavity reactor relative to a reactor 0 cm gap thickness.	111
4-11. Final reactor designs for each reflector material.	115
4-12. Description of the reference PWR using 15x15 fuel assemblies.	117
4-13. Neutronic characteristics of final GCR designs compared to the reference PWR.	120
4-14. Core spectral characteristics for all GCR designs and the reference PWR.	120
5-1. Maximum fuel burnup attained for GCRs and the reference PWR. GCR values result from continuous feed of 19.95 w/o enriched fuel for 20 years.	140
5-2. Inventory of uranium isotopes at the end of 20 years.	141
5-3. Inventory of uranium isotopes per unit burnup at the end of 20 years.	141
5-4. Inventory of Np-237 and inventory per unit burnup at 20 years.	143
5-5. Percentage of neutrons with energy up to 1 MeV at 20 years.	145
5-6. Inventory of plutonium isotopes at the end of 20 years.	148
5-7. Inventory of americium isotopes and inventory per unit burnup at 20 years.	151
5-8. Inventory of curium isotopes at 20 years.	152
5-9. Inventory of actinides grouped by half life and inventory per unit burnup of at 20 years.	153
5-10. Inventory of long lived fission products and inventory per unit burnup at 20 years.	156
5-11. Fuel utilization summary of GCRs and the reference PWR.	156
A-1. Data from beryllium oxide reflector thickness sensitivity study.	165
A-2. Data from lithium-7 hydride reflector thickness sensitivity study.	165
A-3. Data from lithium-7 deuteride reflector thickness sensitivity study.	166
A-4. Data from graphite reflector thickness sensitivity study.	166
A-5. Data from tungsten reflector thickness sensitivity study.	166
A-6. Data from zirconium carbide reflector thickness sensitivity study.	167
A-7. Data from lead reflector thickness sensitivity study.	167

A-8. Data from gas pressure sensitivity study with pressures between 10 and 60 bars.	168
A-9. Data from fuel enrichment sensitivity study with enrichments between 2 and 20 w/o U-235.....	168
A-10. Data from length-to-diameter ratio sensitivity study with L/D ratios between 1 and 3.....	169
A-11. Data from gap thickness sensitivity study with gap thickness between 0 and 10 cm.....	169

LIST OF FIGURES

<u>Figure</u>	<u>page</u>
2-1. Cross-sectional views of a classical GCR (left), and a GCR with multiple fuel cavities.....	27
2-2. Model of the GCR with equivalent reflector thickness, neglecting control drum geometry and poison material.	28
2-3. Mole fractions of uranium-fluorine systems as a function of temperature at 1 atm.....	29
2-4. Bond dissociation energies for uranium halides.	29
2-5. A schematic representation of the GCR with MHD and combined power conversion cycles.	37
3-1. Activity of HLW from one ton of spent fuel.....	48
3-2. Distribution of fission products from U-235.....	49
3-3. Fission-to-capture cross section ratio for Np-237.	53
3-4. Production of Pu-238 with thermal interaction cross sections and decay half lives.	54
3-5. Production of Pu-239 with thermal interaction cross sections and decay half lives.	56
3-6. Production of Pu-240, Pu-241, Pu-242 with thermal interaction cross sections and decay half lives.	57
3-7. Production of Am-241, Am-242, Am-243 with thermal interaction cross sections and decay half lives.	58
3-8. Production and decay chains for curium isotopes with thermal interaction cross sections and decay half lives.	61
3-9. Fission yields from the fission of U-235 after various cooling times.	65
3-10. Capture cross sections for U-235 and Pu-239 at 300 K from ENDF/B-VI [39].	67

3-11. Fission cross sections for U-235 and Pu-239 at 300 K from ENDF/B-VI [39].	67
4-1. Saturation curves for (A) beryllium oxide, (B) lithium-7 hydride, (C) lithium-7 deuteride (D) graphite, (E) tungsten, (F) zirconium carbide, (G) lead.	80
4-2. Reflector thickness saturation curves for all materials at gas pressure of 155 bars and enrichment of 19.95 w/o, except tungsten is at 95 w/o.	85
4-3. Neutron capture cross section plot of reflector materials.	86
4-4. Ratio of capture to total cross sections for all reflector/moderator materials.	88
4-5. Percentage of fissions induced by neutrons in three energy ranges for (A) beryllium oxide, (B) lithium-7 hydride, (C) lithium-7 deuteride, (D) graphite, (E) tungsten, (F) zirconium carbide, and (G) lead reflected GCRs.	90
4-6. Percentage of fissions caused by neutrons in energy ranges: 0.625 eV-100 KeV, and > 100 KeV. The reflector is at saturation thickness, gas pressure is at 155 bars, with enrichment of 19.95 w/o for (A) zirconium carbide and (B) lead.	95
4-7. Gas pressure sensitivity study with BeO reflector. Shown is the effect of gas pressure on (A) k-effective, and (B) percentage of fissions caused by neutrons in three energy groups normalized to the average in each group.	98
4-8. Fuel enrichment sensitivity study with BeO reflector. Shown is the effect of enrichment on (A) k-effective, and (B) percentage of fissions caused by neutrons in three energy groups normalized to the average in each group.	103
4-9. Core length-to-diameter ratio sensitivity study with BeO reflector. Shown is the effect of L/D ratio on (A) k-effective, and (B) percentage of fissions caused by neutrons in three energy groups normalized to the average in each group.	106
4-10. Cross sectional view of a GCR model with three fuel cavities used in the gap thickness sensitivity study.	109
4-11. Gap thickness sensitivity study using 3 fuel cavities and a BeO reflector. Shown is the effect of gap thickness on (A) k-effective, and (B) percentage of fissions caused by neutrons in three energy groups normalized to the average in each group.	109
4-12. Average core spectrum obtained for each of the obtained for each of the reflector materials using design parameters in Table 4-11.	121
4-13. Average core spectrum obtained from each of the reflector materials for energies <2 eV.	122
4-14. Average core spectrum obtained from each of the reflector materials from 2 eV to 100 KeV.	124

4-15. U-235 and U-238 total cross section.	125
4-16. Average core spectrum obtained from each of the reflector materials for energies >100 KeV.	126
4-17. Average reflector spectrum of the reactor designs in Table 4-11.	129
5-1. Six group core spectra at (A) BOL (0 days), (B) 4.5 years, and (C) 20 years.	137
5-2. Total neutron flux as a function of fuel burnup.	139
5-3. Np-237 mass as a function of fuel burnup.	143
5-4. Mass of Np-237 feeders as a function of burnup.	144
5-5. Total neutron cross section for (A) U-237, (B) Pu-241, and (C) Am-241 compared to U-235 and U-238 capture cross sections.	146
5-6. Ratio of Pu-238 and Pu-240 mass to total Pu mass.	149
5-7. Fraction of fissile (Pu-239 and Pu-241) isotopes in Pu.	150
5-8. Am-241 mass as a function of fuel burnup.	151
5-9. Mass of actinides with half lives greater than 1E3 years and less than 1E4 years.	154
5-10. Mass of actinides with half lives greater than 1E4 years.	155
5-11. Burnup of the GCRs compared to the reference PWR.	157

Abstract of Thesis Presented to the Graduate School
of the University of Florida in Partial Fulfillment of the
Requirements for the Degree of Master of Engineering

SPECTRAL CHARACTERIZATION AND TRANSMUTATION OF ACTINIDES IN
GASEOUS CORE REACTORS

By

Cindy Fung

August 2006

Chair: Samim Anghaie

Major Department: Nuclear and Radiological Engineering

The objective of this research is to study the impact of GCR design parameter on the core spectral characteristics, characterize the relationship between neutron spectrum and actinide and fission product inventory, and analyze the Pu isotopic content from GCRs to address proliferation concerns. The actinides of interest are plutonium for proliferation concerns, in addition to neptunium and americium due to the waste disposal issues they cause. Computational tools include MCNP5, ORIGEN 2.2, and MONTEBURNS.

The reflector material and thickness are the most important design parameters in determining the core spectrum. The increase in the gaseous fuel pressure and enrichment increases the neutron population with energies greater than 2 eV. Among reflector materials studied, the beryllium oxide reflected GCR achieved the softest spectrum and the tungsten reflected system achieved the hardest spectrum.

The actinide inventory of Np-237 and actinides with half lives greater than 1,000 years can be minimized via transmutation using a high neutron flux level. The higher the neutron flux, the lower the inventory of these actinides. The majority of the GCR designs maintained a flux level on the order of $10^{15} \text{ cm}^{-2}\text{s}^{-1}$ while the PWR flux one order of magnitude lower. The inventory of the feeder isotopes to Np-237 including U-237, Pu-241, and Am-241 decreases with the increase in the neutron population with energies up to 1 MeV. This is due to the cross section characteristics of these isotopes in this energy range.

The PWR spent fuel yields a Pu mixture with better proliferation resistance characteristics than the GCRs for a given fuel burnup. Proliferation resistance characteristics of the GCRs improve with burnup.

Fuel utilization in the GCRs is superior to the PWR, except for the zirconium carbide reflected GCR. The achievable burnups in the GCRs are one order of magnitude greater than the PWR. The uranium required for 20 years of operation in the GCR is one order of magnitude less than that in the PWR. The ZrC reflected system is inferior to the PWR in the area of fuel utilization.

CHAPTER 1 INTRODUCTION

Nuclear power is a promising candidate for meeting growing energy demands, severing the world's dependence on dwindling fossil fuel supply. However, nuclear waste produced from current power reactors obstructs the growth of nuclear power into a major provider of economical and dependable source of energy. This research is intended to alleviate the environmental impact and stewardship burden posed by nuclear waste.

Nuclear waste consists of a broad range of unwanted materials generated from all activities involving radioactivity. These activities include, but are not limited to: power production, academic research, medical applications, national defense programs, and industrial applications. Waste is classified into five categories:

- high level wastes (HLW),
- low level wastes (LLW): classified into classes A, B, C and class greater than C,
- transuranic wastes (TRU),
- uranium mill tailings, and
- naturally occurring and accelerator-produced radioactive materials (NARM).

Examples of LLW include contaminated clothing and calibration sources. Most TRU waste is generated by Department of Energy (DOE) activities related to defense programs involving plutonium (Pu) separation [1]. Uranium Mill Tailings are from the mining and milling of uranium used in nuclear fuels. Disposal of NARM is regulated by

the states and most qualifies as LLW [1]. Spent fuel is classified as a HLW. For the rest of this thesis the term “nuclear waste” will be synonymous to “spent fuel” and HLW.

The Fuel Cycle

Spent fuel is the end product of the nuclear fuel cycle in the US. Knowledge of the fuel cycle will help define the challenges currently facing the nuclear industry. The cycle consists of the following stages.

Mining and Milling of Uranium Ore

Uranium (U) is a naturally-occurring element found at low levels in virtually all rock, soil, and water. Significant concentrations of uranium occur in some substances such as phosphate rock deposits, and minerals such as uraninite in uranium-rich ores [2].

Uranium ore is obtained from reserves using three methods:

- open-pit mining,
- underground mining, and
- in-situ leaching, widely used in the US.

The major uranium reserves in the US are located in New Mexico, Wyoming, Colorado, and Utah. Because of high ore grades in the Canadian and Australian reserves, it is more economical to import from these countries. Additionally, there is an abundance of highly enriched uranium from the dismantlement of nuclear weapons in Russia; thus, uranium mining activity in the US is limited.

The ore is transferred to a mill where it is ground, separated from organic materials, and concentrated. After the ore has gone through the milling process it is in the form of U_3O_8 , commonly called “yellowcake.”

Conversion of Yellowcake to Uranium-Hexafluoride

The yellowcake is purified to rid it of impurities such as boron, cadmium, chlorine, and many rare earth elements. Purification processes used are PUREX, and precipitation of uranium peroxide from uranyl salts and hydrogen peroxide. The yellowcake is converted to uranium-hexafluoride (UF_6) using the dry hydrofluor process or the wet solvent extraction process. Approximately 0.5% of the uranium is lost in this process.

Enrichment of Uranium

Natural uranium consists of 0.0055 % U-234, 0.720 % U-235, and 99.2745 % U-238 isotopes. The isotope U-235 has the highest probability of fissioning when encountering a thermal neutron. For various purposes such as neutron efficiency, and plant operation demands, UF_6 must be enriched in U-235. Current civilian maximum enrichment is 5 weight percent (w/o) U-235.

There are currently two widely used enrichment processes: Gaseous Diffusion, and Gaseous Centrifuge. The centrifuge method uses one order of magnitude less energy than the diffusion method. Other methods under development are Atomic Vapor Laser Isotope Separation, and enrichment by the Separation Nozzle.

Fabrication of Nuclear Fuel

Commercial power reactors use uranium dioxide (UO_2) as fuel. UF_6 is first converted into U_3O_8 through a precipitation process and then converted to UO_2 through calcinations. It is then ground and pressed into pellets. The pellets are sintered to give the UO_2 structural stability and the desired pellet porosity.

Stacked pellets are encased by zirconium alloy tubes. The tubes are organized into a specific configuration called a fuel “assembly” or fuel “bundle.” The fuel assembly is then sent to power plants.

Power Production

The fresh fuel replaces from one-quarter to one-third of the total number of fuel assemblies in the reactor. It is then used for power production or “burned.” One measurement of how efficiently the fuel is used is referred to as the fuel’s “burnup” and it is in units of gigawatt-days per metric ton of uranium (GWD/MTU). For current operating plants the average burnup of the spent fuel is 40-50 GWD/MTU. The spent fuel is sent to a pool lined with boron. Since the spent fuel is highly radioactive and generates decay heat, it must be kept in the pool to cool.

The US and other countries are similar up to this stage of the fuel cycle. The difference is the destiny of the spent fuel. Many countries such as France, the United Kingdom, Russia, Japan, and India reprocess spent fuel. With the presence of the reprocessing stage, this fuel cycle is referred to as the “closed cycle.” The US adopts the “open cycle”; the spent fuel is not reprocessed and shall be sent to a repository.

Spent Fuel Characteristics

Spent fuel contains three major categories of isotopes: actinides, fission products (FP), and activation products. The major actinides are the isotopes of U and Pu. The minor actinides are those with atomic number greater than 92 such as curium (Cm), americium (Am), and neptunium (Np). “More than 350 nuclides have been identified as fission products” [1:290]. Examples of fission products include cesium (Cs), technetium (Tc), samarium (Sm), iodine (I), strontium (Sr), and xenon (Xe). Activation products are structural materials that become radioactive under neutron irradiation.

Most of the original U-238 and about one-third of the U-235 remains in the spent UO₂ pellets [1]. However, with more efficient bundle designs, the use of burnable poisons and industry-wide improvement in reactor operation, the burnup of the fuel has

increased. This means that more of the fissile material is used to produce energy and the amount of U-235 left in the spent fuel is currently about one-quarter of the original amount; this number is steadily approaching one-fifth.

Other isotopes in the spent fuel such as U-233, U-235, Pu-239, and Pu-241 have high probability of fissioning. These isotopes are called “fissile.” A measure of this probability is referred to as a “cross section.” The cross section is a function of the neutron energy, and temperature of the medium. Because the fission cross sections of these isotopes are orders of magnitude higher than most elements, U and Pu are recovered during reprocessing. The recovered material is reintroduced into the reactor in the form of a Mixed Oxide Fuel (MOX).

Many minor actinides and fission products have high radiative capture cross sections emitting the extra energy in the form of radiation. Therefore, these materials are discarded during reprocessing.

If the spent fuel were to be disposed as HLW, it will be cooled until the decay heat production rate is such that heat removal via air convection and thermal radiation will suffice. For most types of fuels the level of radioactivity will decrease to an acceptable level for reprocessing between 5 and 25 years after it is discharged from the reactor [3]. The decay heat behavior of the discharged fuel depends on the irradiation history of the fuel and the time that has elapsed after discharge. Since most fission products have short half lives, the activity of the spent fuel due to fission products is mainly from the contributions of Sr-90 ($T_{1/2} = 28.79$ years) and Cs-137 ($T_{1/2} = 30.07$ years) [4]. Many actinides have considerably longer half lives than fission products; the activity decreases

more slowly with time. After 700 years the activity of actinides surpasses that of fission products [4]. According to Lamarsh,

... [in] the once-through cycle, the activity of the fuel persists for hundreds of thousands of years owing to the presence of TRU [actinide] material. [4:219]

With the open cycle, in the US spent fuel is intended to be sent to an ecological repository, Yucca Mountain, which is not yet ready for service. To understand the unique problems facing the US nuclear industry posed by the indeterminate future of nuclear waste one must first know a bit of history.

Nuclear Waste History

The first nuclear power plants were designed on the premise of operating in a closed cycle. The spent fuel pools were designed to be capable of storing at least four-thirds of a core's fuel bundles. However, the intention was to store the spent fuel (consisting of about one-fourth to one-third of the core) for a short period of time. The spent fuel will then be shipped to a reprocessing facility.

In the US three reprocessing facilities were built for commercial spent fuels. They were located in West Valley, NY, Morris, IL, and Barnwell, SC. The facility in West Valley started reprocessing fuel in 1965 [5]. In 1976 Nuclear Fuel Services, owners of the site, decided to leave due to operation costs. Since 1980, under the West Valley Demonstration Project Act, the West Valley site has been a DOE site for reprocessing activities.

The Barnwell site started construction in 1970. During this time weapons proliferation issues dominated public concerns. In 1977 President Carter decided to defer reprocessing and recycling of spent fuel indefinitely. The reprocessing facilities in Barnwell and Morris never operated [5].

In 1981 the Reagan administration revoked the ban on reprocessing. However, because of the lack of economic incentives, no efforts have been made to revive this aspect of the nuclear industry. Thus, there is no facility available to reprocess commercial nuclear fuels.

One major consequence of the Nuclear Waste Policy Act (NWPA) of 1982, and its amendments of 1987, is the federal government's assumption of the responsibility for the disposal of nuclear waste. The NWPA designated Yucca Mountain, Nevada as the site to be characterized for the first US repository for HLW. Yucca Mountain is located in a remote desert 100 miles from Las Vegas. It is within the federal protected land of the Nevada Test Site. "Some geological criteria considered are: type of rock, geologic stability, seismic activity, depth and lateral extent of the rock, groundwater flow, presence of or proximity to active faults, surface water bodies, and surface terrain characteristics" [1:314]. In 2002, Congress and President G.W. Bush approved development of the Yucca Mountain site. Expected opening of Yucca Mountain is in the year 2010.

NWPA also required the utilities to pay a fee to fund the HLW repository. The money collected will constitute the Nuclear Waste Fund. This is the only responsibility of the utilities regarding disposal of HLW. The cost of waste disposal is 1 mill (\$0.001) per kilowatt-hour of nuclear electricity generated.

Currently utilities in the US are awaiting the much anticipated opening of Yucca Mountain. Many plants have already run out of storage room, since they were not designed to store thirty years worth of spent fuel. In other countries, a different destiny

awaits the spent fuel. The next section will explore the many ways nuclear waste may be treated.

Nuclear Waste Treatment

There are two routes taken by the spent fuel: (1) it may be reprocessed or (2) it may be stored, intact, in a facility for many years. If the waste is reprocessed, isotopes of U and Pu are recovered from the spent fuel and recycled into MOX type fuel.

Reprocessing and Recycling

Reprocessing is the recovery of U and Pu from the UO_2 in spent fuel while fission products, minor actinides, and assembly structural materials such as cladding are disposed as HLW. Recycling is the reintroduction of this U and Pu back into a reactor for additional energy production.

At a reprocessing plant the spent fuel would first be disassembled. A solvent extraction process would separate the desired materials and the wastes. The wastes are treated as HLW. This waste contains more than 99% of the fission products and ~0.5% of the major actinides [1]. One of the solvent extraction processes is called Pu-U Recovery Extraction (PUREX). In this process U together with Pu are separated from the wastes. The U and Pu are then separated by reducing Pu into an organic-insoluble state [1]. This is the solvent extraction process of choice for existing commercial reprocessing plants for MOX fuels.

Other methods include Uranium Extraction (UREX), and Pyroprocessing. The UREX process extracts U, Tc, fission products, and minor actinides from the fuel, leaving behind Pu and Np. This is done in an attempt to increase proliferation resistance and reduce the volume of HLW [6]. Pyroprocessing is an electrometallurgical process developed specifically for fast reactors. It was used to treat Experimental Breeder

Reactor II (EBR-II) fuels at Argonne National Laboratory-West. This process may be used to treat commercial spent fuel with some modifications [7].

Advantages of the closed cycle

There are many advantages to implementation of a closed fuel cycle. Reprocessing and recycling of spent fuel would reduce the U_3O_8 requirements from commercial reactors by 40% [4]. Additionally, the uranium from spent fuel is still slightly enriched to 0.8-1.0 w/o compared to natural uranium of 0.711 w/o. Thus enrichment costs would decrease. With the recovery of the uranium from the spent fuel, the mass and volume of HLW would be reduced, thereby decreasing space demands on the long term repository [6]. Reprocessing would substantially reduce the volume of waste [4]. Furthermore, reprocessing of spent fuel will allow the waste to be converted into the desired solid form that effectively immobilizes radioactive particles. This will provide an effective and durable barrier between the waste and the biosphere [4].

Disadvantages of the closed cycle

A disadvantage of reprocessing that leads to strong public opposition is the fear of weapons proliferation. During reprocessing it may be possible to obtain pure Pu and weapons grade U. After the events of September 11th, terrorism in our backyard has become a reality, and the fear of nuclear war has grown. However, the basis for this fear is not confirmed. Recall that many countries have been reprocessing commercial fuels for 40 years [3]. Some even argue that leaving the U and Pu in the spent fuel may allow it to be recovered for illicit use in dirty bombs (after the fuel is allowed to decrease in activity) [3]. However, the main reason reprocessing is not practiced in the US is the lack of reprocessing facilities. This is simply due to economic reasons. Construction cost is the majority of the cost of nuclear power [1]. Reprocessing will at best decrease fuel

costs, and thus not improve the overall cost of electricity significantly. Spent fuel may be sent overseas for reprocessing, but because of proliferation concerns, this route is not taken.

Storage and Disposal

Since all activities involving radioactivity generate waste, storage and disposal of such waste is inevitable. Most waste can be treated as either LLW or HLW.

Low level waste

As far as the nuclear power is concerned, LLW is generated when materials are exposed to neutron radiation or materials are contaminated with radioactivity. A few examples of LLW are contaminated protective shoe covers and clothing, wiping rags, mops, filters, reactor water treatment residues, equipments, and tools. The radioactivity can range from just above background levels found in nature to very highly radioactive in certain cases such as parts from inside the reactor vessel in a nuclear power plant [8].

For the most efficient use of the disposal facilities volume reduction methods are encouraged. Volume reduction can be achieved by compaction, incineration or evaporation. Additionally, to ensure immobilization of the waste, avoiding leakage into the environment, the waste is solidified in cement, bitumen, urea formaldehyde (no longer permitted in the US), and Dow media.

Compacts. The disposal of LLW (except waste of class greater than C) is the responsibility of the state where the waste is generated. Most states have formed compacts to share disposal site. There are currently 10 compacts:

- Northwest: Alaska, Hawaii, Idaho, Montana, Oregon, Utah, Washington, and Wyoming
- Southwest: Arizona, California, North Dakota, and South Dakota

- Rocky Mountain: Colorado, New Mexico, and Nevada
- Midwest: Indiana, Iowa, Minnesota, Missouri, Ohio, and Wisconsin
- Central: Arkansas, Kansas, Louisiana, Nebraska, and Oklahoma
- Texas: Maine, Texas, and Vermont
- Central Midwest: Illinois, Kentucky
- Appalachian: Delaware, Maryland, Pennsylvania, and West Virginia
- Northeast: Connecticut, New Jersey, and South Carolina
- Southeast: Alabama, Florida, Georgia, Mississippi, Tennessee, and Virginia

Each compact may select a host state where a LLW disposal facility will be built.

Alternatively, a compact may ship their LLW to disposal sites outside the compact.

Disposal facilities. It is sufficient to dispose LLW in shallow burial grounds. All of the disposal sites in the US are open slit trenches about 1,000 ft long, 100 ft wide, and 20-50 ft deep. Disposal sites may also be above ground and covered with dirt. There are currently 3 operating LLW sites in the US located in Barnwell, SC, Hanford, WA, and Clive, Utah.

The Barnwell site opened in 1971. It was intended to be a reprocessing facility; however, the site was unable to obtain a reprocessing license before the ban on reprocessing was effective in 1977. Barnwell, operated by Chem-Nuclear Systems, is licensed to accept wastes of classes A-C, and it is already 90% full. Although South Carolina is part of the Northeast compact, this site accepts LLW from all states except those in the Northwest and Rocky Mountain compacts. Beginning in 2008 Barnwell will only accept waste from Connecticut, New Jersey and South Carolina.

The Hanford site has been used as a waste disposal facility since the late 1940s. It is managed by the DOE to receive LLW of classes A-C. This site only accepts waste from states in the Northwest and Rocky Mountain compacts.

The LLW site located in Clive, Utah is operated by Envirocare. This site was a DOE Vitro tailings disposal site from 1984 to 1988. In 1988 Envirocare acquired the land surrounding the Vitro tailings. The site disposed of NARM, uranium mill tailings, and mixed waste. In 2001 the site received its license to dispose class A waste. Envirocare accepts waste from all states and plans to operate for at least 25 years. After site closure, Envirocare will monitor the site for 100 years.

High level waste

HLW consists of spent fuel and the waste produced from reprocessing activities. Just as with LLW, liquid HLW is solidified. The methods employed are calcination, cementation, and vitrification; vitrification is the preferred solidification method because of its resistance to dissolution [1]. Spent fuel is to be disposed of intact. Some of the disposal options considered are deep geological disposal, transmutation, ice sheet disposal, sending waste into outer space, and sub-seabed disposal. Because of the effects HLW could have on the environment and the population if it leaked, the disposal site must involve containment of the waste with both natural and man-made barriers. In the US, the final disposal site for HLW is its deep burial in a stable geological repository. Because of waste accumulation, alternate forms of storage have been used such as dry cask storage and monitored retrievable storage (MRS) facilities.

Geological repository. Yucca Mountain in Nevada is chosen to be the first HLW repository. In 2002, the President approved the site for HLW disposal. Currently the DOE is in the process of preparing an application for the construction license of the

repository. Yucca Mountain is scheduled to open in 2010. The repository will operate from 100 to 300 years with the possibility of retrieving the waste [9]. The repository is expected to be permanently closed in 2116 [10].

On the surface the repository will look similar to a mine. The disposal facility is designed to isolate waste from the environment for at least 10,000 years. HLW will be sealed inside durable waste packages and stored in excavated tunnels. Corrosion resistant drip shields are placed over the packages to divert water away from the waste. The HLW will be placed under 1,000 ft of solid rock, and 1,000 ft above the water table. After the site closes the waste will no longer be retrievable. However, there will be perpetual monitoring of the site to ensure correct functioning. The tunnels will then be backfilled with the excavated rock.

Many nuclear plants have exhausted their spent fuel storage capacity, since they were originally designed to store 4/3 of the core. Since Yucca Mountain is not yet open, many plants have already re-racked the spent fuel pool to accommodate storage demands. However, this may not be enough, especially at older plants that have been in operation since the early 1970's. Thus, interim storage for spent fuel must be used.

Dry cask storage. The casks may be stored on the nuclear plant site or off site. Spent fuel that has decayed in activity is placed in these casks. These are designed to accomplish two functions:

- Shield radiation emitted from the spent fuel, and
- Adequately cool the spent fuel using natural or forced convection of a gas or air.

The casks may be made of steel or concrete. They have neutron-absorbing material, gamma shielding material, and cooling fins.

Monitored retrievable storage (MRS). The possibility of construction of a MRS facility is part of the NWPA. These are intended to serve as an interim storage facility until Yucca Mountain's opening. A MRS facility consists of a concrete pad on which dry casks will be stored. In 1985 three sites for a MRS facility were identified, all located in Tennessee. Because of strong local opposition, the 1987 amendments to the NWPA prohibited MRS sites in Tennessee. In 1996 a sparsely populated reservation of the Skull Valley Band of the Goshute Indians signed an agreement with a consortium of utilities to construct a MRS facility. They are located 70 miles from Salt Lake City, Utah.

Advantages of the open cycle

Due to the high level of radioactivity spent fuel has a high temperature. This makes it almost impossible to handle. Thus, it is naturally proliferation resistant. According to the Nonproliferation Alternative Systems Assessment Program (NASAP) initiated by President Carter, the open cycle is the most proliferation resistant. However the NASAP also concluded that no nuclear cycle is completely proliferation proof.

Disadvantages of the open cycle

The open cycle is wasteful of nuclear energy resources. A typical 1,000 MWe reactor discharges about 180 kg of fissile Pu, and 220 kg of U-235 each refueling [4]. If these materials were used in a reactor the energy produced would be equivalent to 1 million tons of coal [4]. Not only is the open cycle wasteful, it produces a greater amount of HLW than the closed cycle. With Yucca Mountain not even having a construction license from the Nuclear Regulatory Commission (NRC), nuclear waste issues have become one of the big challenges to the growth of the nuclear power.

Nuclear Waste Challenges

Nuclear waste is one of the many issues that must be resolved in order to progress onto the Generation IV (Gen-IV) goals of finding reactor concepts which are proliferation-resistant, sustainable and economical sources of energy, and safe and reliable technologies. The construction of a repository arouses much opposition due to the public's fear of radioactivity. Despite public opposition, nuclear waste is an issue that must be resolved. HLW accumulates every day. The majority of the waste is from defense programs that started during World War II. If left unresolved it will be a major obstruction to the nuclear renaissance. The states of California and Wisconsin prohibit the construction of a new nuclear plant before a HLW repository is available.

Permanent Repository not Available

Since the NWPA, HLW disposal is the responsibility of the federal government. After more than 20 years of characterization and feasibility studies the President approved the Yucca Mountain site, scheduled to start operation by 2010—12 years later than the law's target date [10]. As of early 2006—4 years before the scheduled opening of Yucca Mountain, the DOE has not submitted the application for construction of the site to the NRC. Once the license application is submitted, the NRC reviews it and public hearings will begin. The public hearing process is expected to take at least 3 years after the construction application is submitted. Construction begins when the license is granted. Upon completion of the construction, and before emplacement of waste, the DOE must apply for an operation license. Obtaining a license is not an easy task. For example, current operating plants took as little as 5 years and up to 12 years to construct due to licensing requirements. In the next four years, the DOE must submit a construction license application, go through NRC review and public hearings, construct

the facility, and apply for and receive an operation license. It seems that the DOE will yet again miss the targeted opening date, while nuclear waste accumulates each day.

More Repositories are Needed

A maximum of 63,000 MTHM is allotted to the disposal of commercial spent fuel. The rest of the 7,000 MTHM is for disposal of HLW generated by the DOE. HLW from defense and research activities has been accumulating since the mid 1940's. Civilian waste has been accumulating since 1957. As of December of 1999, there was 40,000 MTHM of civilian waste, and by 2035 it is projected to be doubled [11]. Thus, with more than 80,000 MTHM by 2035, Yucca Mountain will be full and a second repository will be needed. With the current status and projections, a 30 year time period is needed to build a repository from characterization studies to opening date. Thus, if the second repository will be open in time, site selection and characterization studies will need to start soon. Site selection for the second repository started in conjunction with the first repository. Due to a threatened moratorium on NWPA activities, Congress passed the amendments to NWPA in 1987. The amendment dictated that the secretary of the DOE shall report to the President and Congress after January 1, 2007 and no later than January 1, 2010, on whether a second repository is needed. This decision essentially deferred activities related to the second repository for 20 years. With the open cycle, waste accumulates faster than the federal government's ability to dispose of them.

MRS not Available

Even before the 2002 Presidential approval of the repository, spent fuel pools around the country had already started to store spent fuel in dry casks. The casks sit atop a pad of concrete on the plant site or off site. Some plants are even running out of room for the casks. Thus, utilities have formed consortiums to centralize dry cask storage at a

monitored retrievable storage facility. Feasibility of MRS has been considered since the NWPA of 1982. Three sites were identified in Tennessee. However, the congressional delegation of Tennessee strongly opposed. Thus, amendments of 1987 were passed and the MRS sites were nullified.

The search for MRS sites continued, but site selection is prohibited before the DOE recommends construction of a repository to the President. This may be due to “fears that the MRS would reduce the need to open the permanent repository and become a de facto repository itself” [10:1]. By law, construction of an MRS may not begin until the permanent repository has obtained a construction license; construction or operation of the MRS must cease if repository construction is interrupted. No more than 10,000 metric tons of waste may be stored at the MRS before the permanent repository begins operating, and no more than 15,000 metric tons thereafter [10]. Thus, to accommodate the current civilian waste, 4 MRS sites are need. As of today 1 MRS site has been selected with the Goshute Indians of the Skull Valley band located in Utah. Because Indian reservations are sovereign entities, the strong opposition from the state of Utah did not deter construction of the MRS. The facility will have a storage capacity of 40,000 MTHM—accommodating almost the entire nation’s spent fuel.

Reprocessing Facility not Available

The major disadvantage of the open cycle is the fast accumulation of waste. If reprocessing is practiced, the volume of waste would be significantly reduced, requiring only one repository for years to come. However, there are no reprocessing facilities available for civilian spent fuel, and the financial risks involved deter potential investors. Knowing that other countries such as France have been reprocessing spent fuel, one may wonder about the feasibility of having another country reprocess American spent fuel.

Countries such as Belgium, Germany, the Netherlands, Switzerland, and Japan send, or have sent their spent fuel to France for reprocessing. Since American nuclear plants are running out of storage room, and there are currently no operating storage facilities, reprocessing seems to be the answer to waste minimization. Americans have not utilized French reprocessing facilities for many reasons: proliferation concerns, it is more economical to do nothing, and legal hurdles of shipping radioactive materials to other countries. However, the author believes that a major factor for not reprocessing American spent fuel in France is an issue of pride. Since the dawn of nuclear energy, the US has long been considered the technological leader of this industry. Reprocessing American spent fuel in France is analogous to relinquishing this crown of prestige.

Waste Must be Isolated for 10,000 Years

One of the technical challenges for Yucca Mountain is the ability to prove that the HLW will be isolated from the biosphere for at least 10,000 years after the repository is closed. It is difficult to predict the corrosion behavior of metals for such a long period of time. It is even more difficult to predict climate changes. Since radioactive materials can be dissolved by water and eventually transported into the biosphere, the ability to accurately predict the amount of precipitation the site will receive is an essential part of the licensing process. Furthermore, the increase in precipitation will increase corrosion rate of the waste canisters. However, there is some evidence from the naturally occurring reactor in Gabon, West Africa that illustrates the locomotive behavior of the waste. Over the course of 2 billion years, the waste, only contained by natural barriers, moved less than 10 ft.

Waste isolation may not be a problem if the HLW consisted of mainly fission products. In November 2005 the American Nuclear Society (ANS) released a position

statement indicating that with the removal of long-lived heavy elements (i.e. the actinides), leaves “a small amount of fission product waste which requires assured isolation from the environment for less than 500 years” rather than the current regulatory demand of 10,000 years [12]. There are many ways that this could be accomplished. The actinides could be fissioned and produce fission products or they could be transformed into stable or short-lived isotopes through neutron capture and radioactive decay. The process of transforming these long-lived nuclides is called transmutation. It could be done in a reactor or the actinides may be bombarded by neutrons from an Accelerator-Driven System (ADS).

Transmutation is certainly a revolutionary concept. It allows the reduction of the volume of waste, improvement in the radiotoxic characteristics of waste, while at the same time generating power. Currently, the US nuclear utilities use light water reactors (LWRs) to generate power. LWRs are moderated and cooled with water (H_2O). There are 2 types of LWRs: the Boiling Water Reactor (BWR), and the Pressurized Water Reactor (PWR). Their differences are discussed in the next section.

Current Technology

In the US, nuclear fuel provides 20% of the electricity generated. There are 103 operating commercial power reactors operating in the US and approximately 443 reactors worldwide. Twenty-five reactors are under construction, mainly in Asia. All of these commercial reactors use a solid fuel in the form of UO_2 , and water as a moderator and coolant. Some examples of UO_2 -fueled, water-moderated reactors are: Boiling Water Reactor (BWR), Pressurized Water Reactor (PWR), and Canada Deuterium Uranium (CANDU), in which neutrons are moderated with heavy water (D_2O). Recently constructed plants, and those under construction, are evolutionary versions of these three

types of reactors that employ passive safety features such as in the case of the Advanced Boiling Water Reactor (ABWR), and the Next Generation CANDU. Only the BWR and PWR are currently operating in the US.

All LWRs consist of an arrangement of fuel bundles within a pressure vessel. The medium used for moderation of neutrons and cooling of the fuel is water. The current performance, as far as capacity factor, of the BWR and PWR are similar. The 2005 industry average capacity factor is 88.9% [13].

Boiling Water Reactor

As the name indicates, the water inside the reactor boils: it goes through a phase change and becomes a vapor. This occurs because the pressure and temperature conditions in the BWR are such that the water is saturated. The pressure in a typical BWR is about 1,000 pounds per square inch (psi). The average coolant temperature is about 560 K, and the average fuel temperature is 775 K (for 10x10 bundles, see below).

The operating BWRs in the US consist of six different phases, each with slight difference in system design. The BWR-6 core contains about 624 bundles. The latest BWR bundle is a rectangular arrangement of 10 fuel rods on each side, known as the fuel lattice. There are spaces in the bundle to increase the amount of moderator. Design of the water rods vary by vendor. General Electric's design features two offset water rods located towards the center of the bundle. Each water rod occupies the space of 4 fuel rods. The assembly is encased by zirconium alloy cans. The gap between the fuel lattice and the can is the water channel. The main reason why the channel exists is because of the boiling water. Since the temperature towards the center of the core is higher than the periphery, the water boils faster. If the channels were absent, the water will be drawn towards the center, creating lateral movement and resulting stability issues.

The reactivity is controlled using cruciform control blades. These blades are placed in the center of four bundles. Additionally, gadolinia (Gd_2O_3), a burnable poison is used. It is mixed with UO_2 in the pellet. Reactivity can also be indirectly controlled via coolant flow rate. Towards the beginning of the cycle (BOC) the flow in a BWR is less than at the end of cycle (EOC). The flow rate changes the moderator-to-fuel ratio in the core. An increased flow means that the heat generated by the fuel is distributed to a larger amount of water compared to a lower flow. Thus the moderator-to-fuel ratio is increased. Since all US reactors are undermoderated, the reactivity increases when the moderator-to-fuel ratio increases.

Since the coolant in a BWR is converted to water vapor, the vapor turns the turbine. The vapor is then condensed and is pumped back into the core. This means that the entire coolant loop is radioactive. Any coolant leak will expose workers to radiation.

Pressurized Water Reactor

The pressure in a PWR is about 2,250 psi, about twice that of a BWR. The average coolant temperature is about 580 K and the average fuel temperature is about 900 K (for a 17x17 assembly). Unlike the BWR, the coolant in the core does not boil.

The typical PWR core contains about 177 assemblies. The latest PWR assembly design involves a 17 by 17 lattice arrangement. The fuel rods are smaller in diameter than the BWR rods. The PWR assembly does not need a water channel since there is no boiling, and instability due to crossflow is not an issue.

Reactivity is controlled using boron in the moderator. This is a more homogeneous distribution of poison. However, with increased BOC enrichment, increased concentration of boron is also needed. At some threshold value, the presence of boron may cause the moderator temperature coefficient to become positive—this is forbidden

when the reactor is hot and critical. PWRs also use control rods that are placed within the assembly. The control rods are mainly used for power shaping and safety. Burnable poisons are also used in various forms. Westinghouse uses the integral fuel burnable absorber (IFBA). It is a thin coating of ZrB_2 on the fuel pellet. Unlike the BWR, it is not possible to use coolant flow rate to control reactivity, because of the absence of bulk boiling.

Since the coolant does not boil, the heat produced by the reactor is rejected through a steam generator. The primary coolant loop (reactor side), passes through a series of tubes inside the steam generator. On the other side of these tubes is water from the secondary side. The secondary side cools the primary coolant and in turn increases in temperature and eventually boils. The vapor then moves the turbine. Since the primary coolant is isolated from the rest of the plant (secondary side), maintenance activities should be safer and dose to workers should be lower than that of BWRs. This was the case years ago where the average occupational exposure for workers at PWR plants was much lower than at BWR plants. Today, the average exposure is quite similar. A disadvantage of the PWR is the need to repair leaks in the steam generator which is a high radiation environment.

Developing Technologies

There are many revolutionary reactor designs currently under research and development. Many reactors are designed to meet the Gen-IV goals: proliferation resistance, sustainability, economical source of energy, safety, and reliability. Others are designed to mitigate the issues of nuclear waste, using transmutation to convert long-lived nuclides into shorter-lived nuclides. Accelerator Driven Systems (ADS) and the

Gaseous Core Reactor (GCR) are designs that may help alleviate the disposal requirements of waste.

Accelerator Driven Systems (ADS)

ADS consist of a beam of high energy protons impinging on a target material producing a shower of spallation neutrons. The target material is a heavy metal as they contain an abundance of nucleons. Some target materials under consideration are lead (Pb), lead-bismuth (Pb-Bi), mercury (Hg), tantalum (Ta), and tungsten (W). The target is surrounded by a sub-critical arrangement of assemblies. The assemblies may be surrounded by a blanket containing actinides. The proton interaction with the target generates a neutron flux that is used to transmute the actinides.

An example of an ADS is an experimental facility that is part of the Japan Atomic Energy Research Institute (JAERI) R&D program called the Transmutation Experimental Facility (TEF). This system uses a Pb-Bi spallation target and coolant. The proton beam requires 27 MW of energy to sustain a k-effective of 0.97; the thermal power is 800 MW [14].

When compared to fission systems the advantages of ADS are:

- inherent exemption of criticality accidents
- the fastest neutron spectrum in the ADS gives some advantages in the rate of minor actinide burning, and
- ADS can use fuel with higher minor actinide content, theoretically up to 100% [15].

Some of the challenges encountered by this technology are:

- there is no fuel fabrication facility and not enough separated actinides to perform testing, and
- there is no industrial technology for reprocessing of the radiated assemblies [15].

- To maximize the transmutation rate the fuel should be MA based (or with some Pu). This poses major problems in terms of reactivity coefficients such as increase in void reactivity effect and decrease in Doppler effect. Also, the delayed neutron fraction is small. The addition of HEU mitigates these problems, but the transmutation rate will be reduced [16].

Gaseous Core Reactor (GCR)

The Gaseous Core Reactor (GCR) is the topic of this research. It is a cavity reactor that uses a homogeneous mixture of circulating gaseous fuel. Some fuels considered are enriched uranium tetrafluoride (UF_4) and uranium hexafluoride (UF_6). The reactor cavity is encased by a reflector that may also serve as a moderator.

Due to a low inventory and fully integrated fuel cycle, the GCR features exceptional sustainability and safety characteristics. Because of its flexibility in nuclear design, the GCR can achieve a wide range of conversion ratio from burner to breeder. Recycling of the fuel allows continuous transmutation of actinides, and possibly fission products, without reprocessing. When compared to the LWR, the GCR produces two orders of magnitude less fissile plutonium [17]. Additionally, the continuous transmutation of the actinides reduces the quality of the fissile plutonium inventory, making the GCR exceptionally proliferation resistant. The GCR is also inherently safe. Any loss of system pressure, core damage, or fuel leak will result in loss of reactivity.

This system is a promising solution to the current challenges of the nuclear industry. It efficiently produces power while at the same time reduces waste and eliminates the need for reprocessing. Inherent safety of cavity reactors and proliferation resistance of the isotope characteristics are additional advantages of the GCR. These features of the GCR make it an outstanding candidate for a Gen-IV reactor in the areas of sustainability, proliferation resistance, and safety. Additional information will be provided in the next chapter.

Thesis Objectives

The gaseous fuel allows great flexibility in the neutronic aspects of the reactor. A broad range of neutron spectra can be achieved. However, the relationship between the neutron spectrum and specific isotope inventory is not well understood. The three major objectives of this research are:

- Study the impact of GCR design parameter on the core spectral characteristics
- Characterize the relationship between neutron spectrum and actinide and fission product inventory
- Analyze the Pu isotopic content from GCRs to address proliferation concerns

The neutron spectrum producing the least amount of wastes, increasing proliferation resistance, and improving fuel utilization will be identified. Ways to control isotope inventory using the neutron spectrum will be identified focusing on the isotopes of Pu, long-lived minor actinides, and long-lived fission products.

CHAPTER 2 THE GASEOUS CORE REACTOR

The Gaseous Core is a cavity reactor that uses a homogeneous mixture of circulating gaseous fuel. The reactor cavity is encased by a reflector that may also serve as a moderator.

GCR Description And Modeling

The design of the reactor is simple and flexible. This allows easy control of the neutron spectrum and enhances safe features. Also, the ability of the gaseous fuel to withstand high temperatures yields high electrical conversion efficiency.

Reactor Geometry

There are some variations in the reactor design. The classical GCR consists of a cylindrical cavity with circulating gaseous fuel. A reflector which may also serve as an external moderator (depending on the material used) is placed on all sides of the cavity. Within the reflector/moderator there are rotating cylindrical control drums. Inside half of the control drum there is neutron poison material. The other half of the control drum contains reflector/moderator material (see Figure 2-1).

A variation on the classical GCR design is to have multiple cavities. Between the cavities there will be reflector/moderator material. This design will increase neutron moderation to help neutrons thermalize.

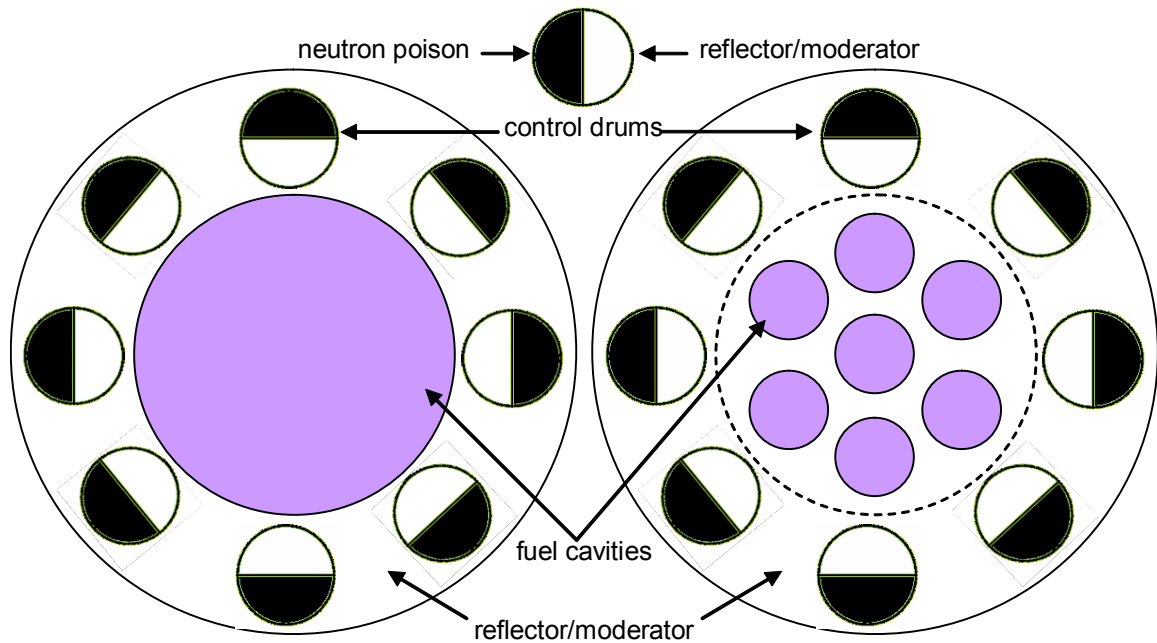


Figure 2-1. Cross-sectional views of a classical GCR (left), and a GCR with multiple fuel cavities.

There are also reflector liners, core wall cladding, coolant channels and other structures within the reactor. However, these have a small impact on the isotopic characteristics of the gaseous fuel and the eventual buildup of actinides and fission products; thus, these components are not modeled. The model of the GCR has a simplified geometry. Only the fuel cavity and reflector/moderator material are modeled. Since control drums are for operational concerns and there are infinite different drum configurations, the model neglects the control drum geometry and poison material. Thus, the reflector region will be modeled by a reflector volume equivalent to the volume present in the original GCR (see Figure 2-2).

Reactor Materials

Early studies of the GCR have been for space power applications. Thus, the materials analyzed are not materials traditionally used in civilian nuclear power systems.

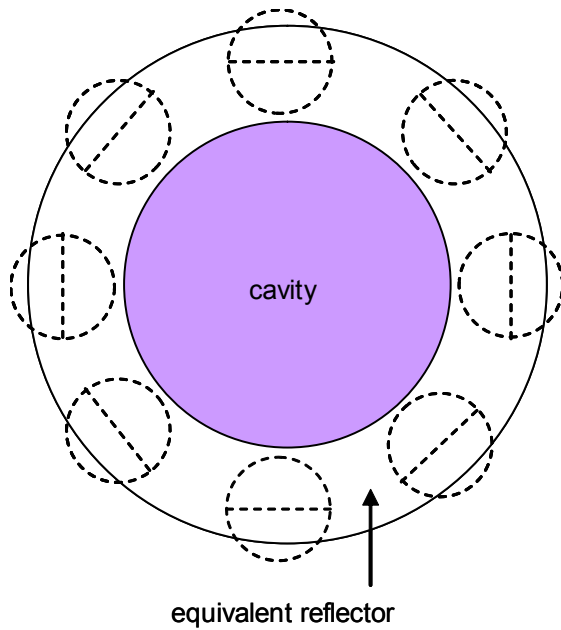


Figure 2-2. Model of the GCR with equivalent reflector thickness, neglecting control drum geometry and poison material.

Gaseous fuel

Previous research on GCR has used metallic uranium vapor, UF_6 , and UF_4 , as fuel. Materials studies by NASA and Nieskens and Stein found that UF_6 is chemically unstable as the temperature increases above 2,000 K (see Figure 2-3) [18, 19]. The boiling point of metallic uranium at 10-20 atm of pressure is 5,000 K; this high temperature presents materials issues and difficulties of addressing criticality during handling and recirculation of the fuel [20].

UF_4 has more desirable properties. It is thermodynamically stable, more chemically stable than UF_6 and at pressures of 10-20 atm, the boiling point is 2,000 K. The stability of UF_4 is illustrated in Figure 2-4 where UF_4 has higher bond dissociation energy. Thus, the current research will use UF_4 as the gaseous fuel. Figure 2-3 shows that UF_4 may decompose and release uranium and fluorine (F) atoms at temperatures greater than 3,000 K. This is due to the material exchange between oxygen (O) and F

atoms. Thus, control of oxygen concentration within the fuel is essential in suppressing O-F material transport [20].

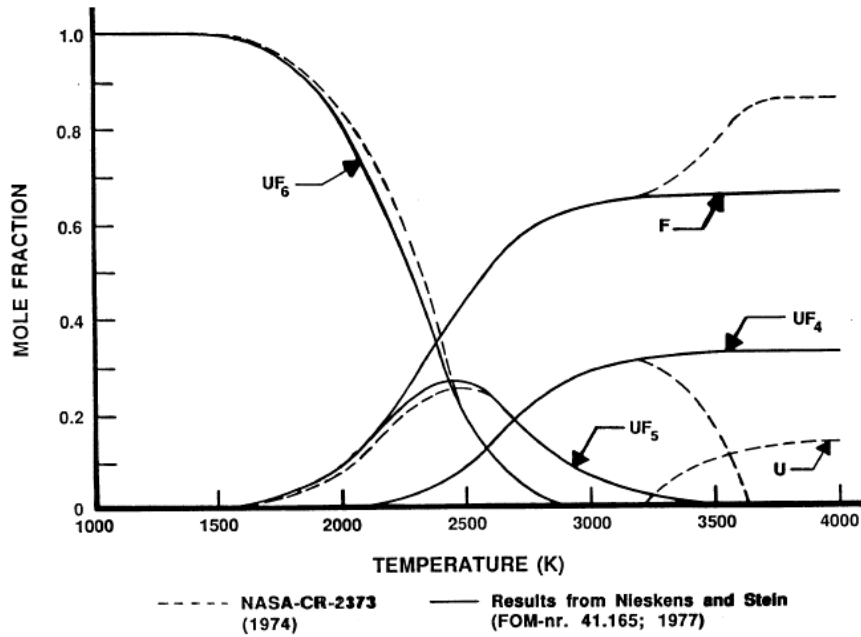


Figure 2-3. Mole fractions of uranium-fluorine systems as a function of temperature at 1 atm. Adapted from Maya et al [20].

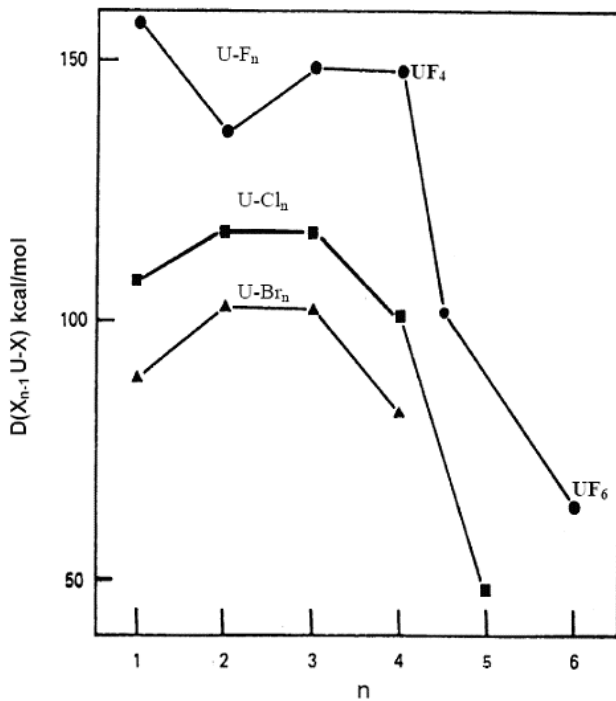


Figure 2-4. Bond dissociation energies for uranium halides. Adapted from reference [21].

For this research a wide range of spectra are needed. Thus, the fuel will not be limited by the current industry maximum enrichment of 5 weight percent (w/o). First, fuel enrichments greater than 5 w/o are technically possible. Many research reactors and US Navy submarines use U fuel enriched to 95 w/o. Second, the objective of this research is to find a viable solution to the waste problem which is a long-term industry goal. The results obtained may not be applicable to the immediate needs of the nuclear industry; however, due to the lack of industry experience with gas-fueled reactors, this is a concept that will take decades of R&D. Thus, the design of the GCR for this research is only limited by technical viability and not legislative ones.

One area of focus is on the proliferation resistance characteristics of the fuel. Uranium enriched to 20 w/o or greater is considered highly enriched uranium (HEU). HEU may be used in nuclear weapons, and thus requires safeguarding. Using HEU as fuel will defeat the current research objective of finding a proliferation-resistant power system. Thus, the fuel will be limited to less than 20 w/o enrichment.

The gaseous fuel in the model is assumed to behave like an ideal gas. The mass density of the fuel is a function of both core pressure and gas temperature:

$$\rho = \frac{MP}{RT} \frac{1}{100^3} \left[\frac{g}{cc} \right]$$

where M is the molecular mass of UF_4 , P is the system pressure in Pascals, T is the temperature in Kelvin, and R is the universal gas constant (8.3144 J/mol/K). The fuel in the core is assumed to be at its average temperature and density throughout the cavity. In reality this is not the case. Since the reflector is cooled, the fuel close to the reflector wall is at a lower temperature than the fuel towards the center of the core. However, due to

mixing of the gaseous fuel, temperature distribution is quite uniform relative to solid fuel in LWR. Results will not be skewed by small changes in temperature.

Since the scope of this research is concerned with actinide and fission product inventory, and operating temperatures are below 2,400 K, possible change in chemical composition of the fuel is neglected.

The fuel in the physical system circulates within the primary loop and flows within the reactor cavity. However, fuel in the model is assumed to be static due to code limitations. This will result in an overestimation of k-effective, mainly due to contributions from delayed neutrons. Physically, fuel circulating outside the core would be emitting delayed neutrons. In the model these delayed neutrons will contribute to the k-effective estimated by the code. The circulating delayed neutron phenomenon can have a strong effect on reactor dynamics and control. The impact on k-effective, on a percentage basis, is small; the impact on reactivity, on a percentage basis, can be quite large. Studies by Kahook show that this does not drastically affect the criticality in the core [22].

Reflector/moderator

Reflector materials are chosen to achieve the desired spectrum. It is desirable that the reflector material is compatible with the fuel and has a high melting point; however, this is not a requirement, since this research is only concerned with neutronic characteristics of the reactor. Previous studies on GCR have used beryllium (Be), beryllium oxide (BeO), graphite (C), heavy water (D₂O), water (H₂O), tungsten (W), rhenium (Re), molybdenum (Mo), tungsten carbide (WC), and molybdenum carbide (Mo₂C) as the reflector/moderator material. BeO will yield a relatively thermal spectrum. For a harder

spectrum other materials need to be considered. The following is a short description of the materials that may be used as a reflector/moderator.

Beryllium oxide. BeO is a white ceramic compatible with UF₄. It has a melting temperature of about 2,800 K, and nominal density of 3.01 g/cc [23]. However, the maximum continuous service temperature is 2,173 K. BeO has good thermal conductivity (330 W/m/K at 273 K) and is corrosion resistant; however, it is reactive with water at 1,273 K.

Since Be is a relatively light element, it serves as a neutron moderator. The (n, 2n) reaction in beryllium-9 is found to be significant with 10 to 12 percent of the neutrons generated coming from this interaction [21]. Thus, the use of Be increases neutron efficiency. One advantage of using BeO is that this material has some industry experience. It is often used for special nuclear reactor applications [21]. Because it is toxic when inhaled, BeO is one of the most expensive raw materials used in ceramics [24].

One advantage of using BeO rather than pure Be is the increase in melting temperature of the reflector material. The melting point of Be is much less than BeO at 1,560 K. This is dangerously close to the desired operating temperature of the reflector. Using BeO will give a very comfortable temperature margin. However, Be is a more effective neutron moderator than BeO. Since oxygen is not an efficient neutron moderator, the beryllium density is a good indicator of the relative effectiveness of the two moderator materials. The density of beryllium in BeO is about 1.08 g/cc while pure Be has a density of 1.85 g/cc. There are more atoms of beryllium per unit volume in pure Be than in BeO. Thus, less Be mass is needed to provide the same amount of moderation

than with the BeO. This may be of paramount importance for systems where achieving a low system mass is critical to its success, such is the case for space applications. For commercial power reactors a higher melting temperature provided by a BeO moderator far outweighs the mass savings provided by a pure Be moderator. Therefore, BeO is one of the candidate materials for further investigation in the current research.

Graphite is one of the allotropic forms of carbon. It has a black silvery color and is the most common and thermodynamically most stable form of carbon [23]. It has a melting temperature of 4,000 K, density of 2.5 g/cc, and it is compatible with UF₄ up to 3,000 K [21]. It has been used as moderator material in Russian reactors and Gas Cooled Reactors from General Atomics.

Lithium hydride. LiH is a grayish white crystalline solid. It has a melting temperature of 961 K, and a density of 0.778 g/cc. [25]. This is a flammable solid and reacts with water to form the corrosive lithium hydroxide and flammable hydrogen gas. It may also ignite spontaneously in air at elevated temperatures [26]. Because of the presence of hydrogen, LiH is expected to serve as a moderator, just as H in light water. Li is lighter than Be; however, ⁶Li which comprises 7.5 atom percent of natural Li has a significant thermal cross-section. Thus, LiH is not as efficient a moderator than light water. To improve the LiH moderating capabilities, ⁷LiH will be used as the reflector material.

Tungsten. W is a grayish white lustrous metal. It has a melting temperature of 3,700 K and a density of 19.2 g/cc [21]. It has the highest melting point and lowest vapor pressure of all metals and has good corrosion resistance [23]. This metal is compatible with UF₄ at temperatures up to 3,000 K [21]. Since W is much heavier than a neutron, it

is not expected to be a moderator. It is used to reflect enough neutrons back into the core to be able to sustain fission [21].

Zirconium carbide. ZrC is a ceramic with high strength, conductivity, hardness and corrosion resistant [27]. It reacts with water and acids and it is pyrophoric, spontaneously igniting in air [28]. It has a melting point of 3,523 K and density of 6.73 g/cc. It is also expensive because of the lack of a fully developed, commercially viable sintering process in its production [27].

Lead. Pb is a very soft and highly malleable metal. It has a very low melting point of 600 K and a density of 11.34 g/cc [23]. Adriamonje has studied the use of lead as a “moderating” material for transmutation and burning for actinides and fission products. The special kinematics in Pb results in a flat neutron lethargy distribution in the regime where captures can be neglected, together with a very “slow” moderation of neutrons, providing a harder spectrum, best suited for fissioning actinides [29]. In its adiabatic slowing down process, a neutron sweeps all energies down to about 100 eV with very small steps of constant $\Delta E/E$ of 0.01 in Pb [30], until it is captured with high probability by an isotope with a high resonance in its capture cross-section [29].

Table 2-1. Summary of reflector/moderator material properties.

material	melting temperature (K)	density (g/cc)	fuel compatibility
BeO	2,800	3.010	yes
⁷ LiH	961	0.778	n/a
C	4,000	2.500	yes
W	3,700	19.200	yes
ZrC	3,523	6.730	yes
Pb	600	11.340	n/a

Assumptions

Models of the GCR are based on the following assumptions and operating conditions:

- the reflector material and the gaseous fuel are assumed to be able to work together in the reactor, regardless of compatibility issues with the use of liners and cladding (not modeled here)
- both fission products and actinides may be removed from the fuel via filtration or chemical separation
- the fuel behaves like an ideal gas
- for comparison purposes, the GCR produces 3,000 MWt of energy, equivalent to the current LWR
- the fuel temperature is 2,000 K, limited by fuel boiling temperature, chemical stability, and power conversion system temperature requirements
- the reflector temperature is close to its melting temperature or at 1,500 K, whichever is lower. It is assumed that the reflector could be cooled to any temperature while the fuel is maintained at an average temperature of 2,000 K. In reality, this may or may not be possible.

Power Conversion Systems

There are two options for the power conversion cycles:

- a Brayton cycle with superheated Rankine heat recovery cycle, and
- a closed magneto-hydrodynamic (MHD) power generation cycle.

Because of the absence of solid-cladding temperature limitations, the operating temperatures of 1,800-2,400 K are only limited by the chemical stability of the fuel.

The first option utilizes a high temperature gas turbine in the Brayton cycle and a bottoming superheated steam Rankine heat recovery cycle. In this concept the released nuclear energy is processed and used to power the combined gas turbine and superheated Rankine cycle, achieving conversion efficiency close to 60% [31]. This is a significant improvement over the current LWR efficiency of 33%.

The MHD cycle directly processes and converts fission power at temperatures of 1,800-2,500 K. The rejected heat is used to power single or multiple gas turbines and/or superheated steam cycles. The MHD generator extracts energy directly from the gas core

fluid at the highest possible quality, with sufficient heat left over to drive two heat recovery cycles. When the MHD generator is combined with the first option (Brayton/Rankine), the conversion efficiency is close to 70% [31] (see Figure 2-5). In spite of the added efficiency, this is a relatively new technology that has not been successful in converting large scale energy conversion due to economical and chemistry issues. However, plant efficiency does not affect the current analysis since the comparison between the GCR and the LWR is based on the thermal power produced.

GCR Characteristics

Most previous studies on gas and vapor core reactors have been performed for space applications. These reactors were smaller in size and power output. However some studies were for terrestrial applications on surfaces of planets and moons that produced up to a few thousand MW of energy. Some studies have used UF_6 as fuel; however system pressures, temperatures, and geometries are similar in this research. Valuable information can be drawn from previous GCR studies, increasing the breadth of knowledge presented in this thesis.

Safety and Feedback

One major advantage of the GCR is its inherent safety features. Any loss of pressure, for example severing of a fuel pipe, will result in a sub-critical condition in the reactor. Analysis on a 100 MWt GCR was done by Dugan and Kutikkad [32]. For the startup and full-power transients considered the authors concluded that the Doppler fuel temperature and moderator temperature feedback are insignificant compared to the fuel density feedback. The fuel density feedback is capable of rapidly stabilizing the 100 MWt GCR within a few seconds, even when large positive reactivity insertions are imposed [32]. The fuel temperature affects the system reactivity through its effect on the

fuel gas density [32]. Recall that the reflector consists of a large block of material. Thus it has a large thermal inertia and any variations in the core power yield only small changes in the moderator temperature [33].

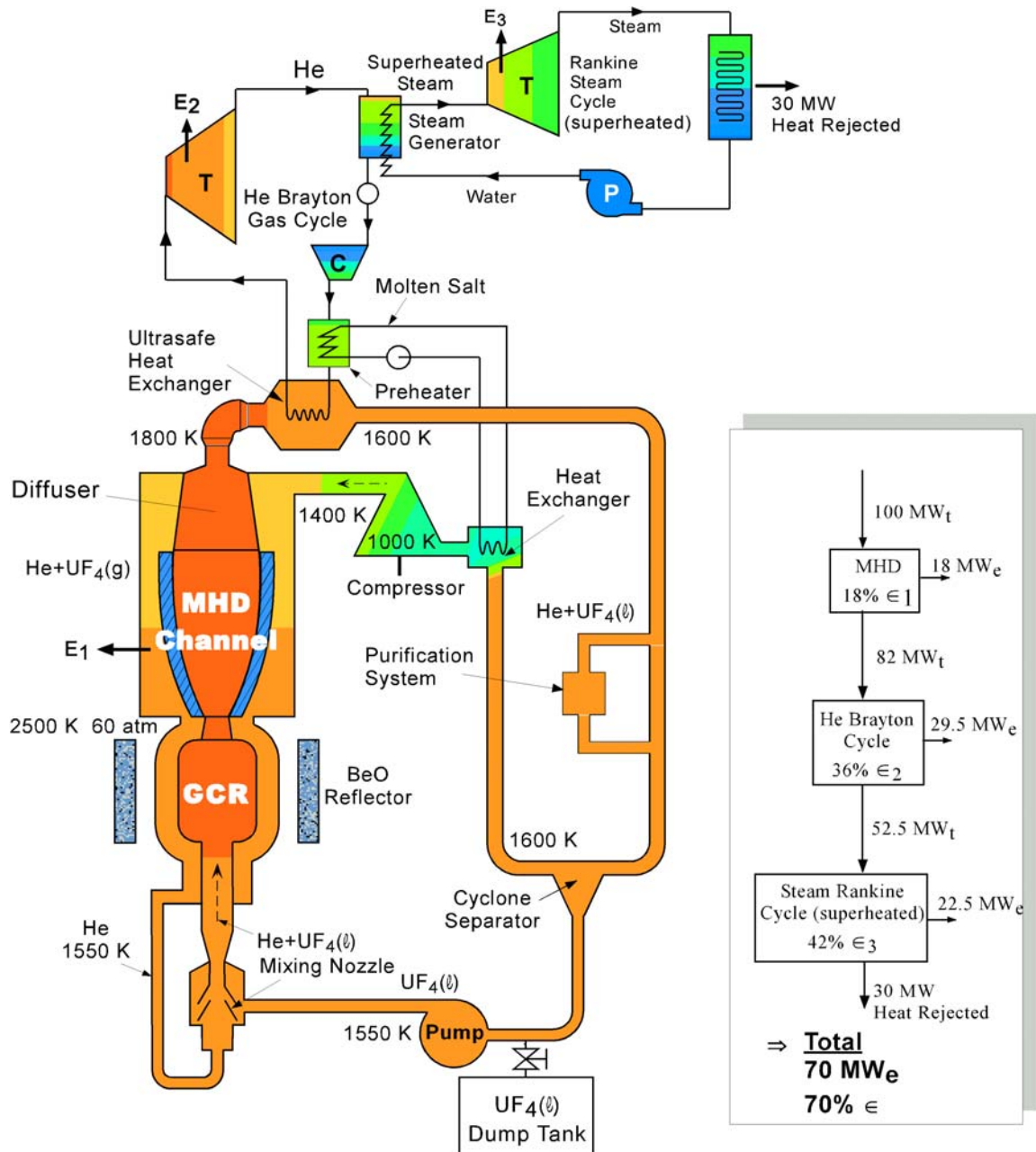


Figure 2-5. A schematic representation of the GCR with MHD and combined power conversion cycles. Adapted from reference [31].

Reactivity Control

A study on a high-temperature vapor core has found that the neutron multiplication factor eventually “saturates” with increasing gas density [33]. When the gas is saturated further increases in gas density will yield small increases in k-effective. To ensure prompt and effective power and reactivity control of the reactor it is desirable to operate below the saturation point where changes in gas density yield significant changes in k-effective.

Due to the strong fuel density feedback, external reactivity insertions alone are inadequate to bring about the desired power level changes [32]. Methods of reactivity control include:

- varying the fuel mass flow rate,
- varying system pressure, and
- rotating control drums.

The first two methods are prompt and effective in controlling reactivity. Rotation of control drums involves massive mechanical parts that may fail more frequently than for example the valve used to control fuel flow. There is an additional, very effective control mechanism and that is varying the external loop circulation time. The fuel mass flow rate can be maintained constant, but by changing the external loop circulation time, one can vary the delayed neutron precursor concentration re-entering the core and this can be extremely powerful.

Core Neutronics

GCR exhibit unique neutronic characteristics:

- a very large neutron mean free path (mfp)

- a generally flat neutron flux in the core and a significant flux variation in the reflector, provided the gas density is not real high
- complete establishment of the thermal spectrum in the reflector
- at high gas densities the flux has a moderate to high degree of nonlinear anisotropy
- at lower gas densities, flux anisotropy is mild and almost linear [34].

Unlike LWR, the neutron spectrum in the GCR can easily be altered. The reflector/moderator material can be processed into columns similar to the control drums. In place of the absorber material there would just be air or vacuum. By rotating these columns the effective reflector/moderator thickness changes; thereby changing the ratio of thermal to fast neutrons in the core.

Advantages Of The GCR

There are many advantages of the GCR over traditional nuclear systems. The fuel form alone provides unique benefits. Since the gaseous fuel is homogeneously dispersed within the core, the neutron flux becomes very flat. With the gaseous fuel mixing within the core, there is an even burn up of the fuel, improving fuel utilization.

Since fuel can be directly injected into the core, the reactor can be continuously refueled. This will eliminate plant down time and increase capacity factor. Additionally, the fuel form renders physical control mechanisms obsolete. The many ways that reactivity can be controlled makes operation very flexible. Instead of using control rods like in LWR, reactivity in the GCR is achieved by varying gas pressure, enrichment, mass flow rate or external loop circulation time. This would avoid mechanical failures of control drums, increase safety, and reduce reactor downtime related to repairs.

There is a twofold advantage to the absence of fuel cladding. One concern for the LWR is that the fuel temperature is so high that the cladding fails and reactivity leaks into

the cooling system. In the GCR, fuel temperature is only limited by the chemical stability of fuel. Thus, operating temperatures are much higher than in a conventional LWR, increasing electrical efficiency. Additionally, radioactive particles are not confined inside the cladding. This will allow continuous separation of fission products. In the event of an accident, the release of fission products will be minimal.

An important feature of cavity reactors is its inherent safety. Once the pressure boundary is breached during an accident scenario the core will lose pressure. The fuel particles will be too dissipated to maintain criticality, and the core will shut down without taking any operator action. Even if there was a prompt reactivity increase and the gas temperature increases, the moderator temperature will not be greatly affected. Since the moderator is external to the core and it is in the form of a large monolithic mass, the moderator has a large thermal inertia, avoiding overheating of the moderator.

The GCR has a very simple design. All the complexity associated with geometrical heterogeneity, i.e. control rods, cladding, structures, and burnable poisons, present in LWR cores is unnecessary in the GCR. Fuel cycle design and calculation becomes straightforward and simple.

Because of the ability to continuously refuel, the actinides that are produced achieve a higher burnup than those in LWRs. This gives the actinides more exposure to neutrons, allowing them to either fission or transmute into shorter-lived isotopes.

This system is a promising solution to the current challenges of the nuclear industry. It efficiently produces power while at the same time reduces waste and eliminates the need for reprocessing. Inherent safety of cavity reactors and proliferation resistance characteristics are additional advantages of the GCR.

Computational Tools

Due to the revolutionary nature of the GCR, many conventional computational tools are not suitable since both the codes and their libraries are designed for LWRs.

Thus, the following codes are used for this research.

MCNP

[Monte Carlo N-Particle] MCNP is a general-purpose, continuous-energy, generalized-geometry, time-dependent, coupled neutron/photon/electron Monte Carlo transport code. [35:1-1]

It is a stochastic code developed at Los Alamos National Laboratory, based on the Monte Carlo method where the interaction histories of individual particles are recorded. To achieve statistical significance, thousands or millions of histories may be needed, and thus this is a very time-consuming modeling method. However, MCNP is an all purpose modeling tool. It can generally model any geometrical configuration, and most subatomic particle behaviors including interactions that occur at high energies (hundreds of MeV) in MCNPX.

Interactions experienced by the particle are sampled from a probability density function with the help of a pseudo-random number generator. This is similar to throwing dice to determine which type of interaction occurs next in the particle's "random walk." Compared to deterministic methods where the solution to a governing equation is obtained, the Monte Carlo method is often viewed as a numerical experiment.

Dependant on user request different types of information may be extracted from the neutron histories. These quantities along with their statistical uncertainties are reported and include: particle current, energy deposition, detector response, charge deposition, and particle flux. For this research MCNP5 will be used to obtain the neutron flux inside the reactor cavity. This information will be used by ORIGEN for depletion calculations.

The cross section libraries available in MCNP are limited in temperatures. These libraries are obtained using a cross section processing code called NJOY. NJOY applies Doppler broadening to all interaction cross sections except for inelastic scattering for a specified temperature. Recall that the gas temperature is at 2,000 K. The two closest temperatures offered in the library for U-235 is at 1,200 K and 3,000 K. The library closest to the actual temperature of the medium is chosen. These cross section libraries used can be Doppler-broadened to the appropriate temperature using the free-gas thermal temperature (TMP) card in the MCNP5 input. The TMP card expects the medium temperature in the form of kT , kinetic energy in units of MeV. The change in cross section due to temperature is a result of the thermal motion (translation, rotation, and vibration) of the target nuclei. Generally, increase in temperature of a neutron absorbing medium increases resonance absorption probability.

The use of the TMP card will only affect the elastic scattering cross section. The total cross section also changes due to change in the elastic scattering cross section. This treatment of cross sections is an attempt to improve accuracy while minimizing the burden on calculation time and memory requirements. It is not a completely accurate way of Doppler-broadening cross sections. While the temperature effect on smoothly varying scattering cross section is treated correctly, the resonances in the scattering cross sections are broadened inaccurately and capture, fission, and other low-threshold absorption cross sections ($<1\text{eV}$) are not treated at all. For more information on temperature treatment refer to pages 2-28 and 3-130 of the MCNP5 manual [35].

Despite its shortcomings, the temperature treatment in MCNP5 provides a “quick fix” for the limited cross section temperatures offered in the library. Because of the

simple geometry of GCRs and homogeneity of the fuel, any errors associated with this method should be small and predictable. Results obtained from MCNP5 should be relatively accurate as long as the code is not used for temperature sensitivity calculations such as for obtaining fuel temperature or moderator temperature reactivity coefficients.

The temperature treatment does not alter the thermal scattering kernel, known as the $S(\alpha,\beta)$ tables. These tables are used to correctly model the physics of neutron scattering in a moderating medium, generally for neutron energies less than 4 eV. It provides inelastic scattering information and sometimes elastic scattering information. The $S(\alpha,\beta)$ tables are of paramount importance for moderating substances that scatter neutrons as a molecule or a crystalline solid, rather than as individual atoms. For example, to model neutron interaction in moderators such as water, BeO, and graphite, $S(\alpha,\beta)$ information is essential. As with cross section libraries, $S(\alpha,\beta)$ information is limited in both temperature and the number of moderators offered. Of the six reflector/moderator materials to be analyzed, $S(\alpha,\beta)$ tables are available for BeO and graphite.

For the materials which $S(\alpha,\beta)$ tables are unavailable none will be used in the model. The accuracy of the results obtained from these models depends on the neutron moderation characteristics of the reflector material. If the reflector material yields a hard spectrum, then the errors due to the lack of $S(\alpha,\beta)$ information for thermal neutrons are negligible. Most of the well known moderators are light elements such as hydrogen, deuterium, beryllium, and carbon. Carbon, in the form of graphite is about as high as one can go on the elemental chart and still get adequate neutron thermalization [21]. Thus, Pb and W, very heavy elements, will mostly serve as neutron reflectors, and the lack of

thermal scattering model will still produce acceptably accurate results. However, some of the constituents of ^7LiH and ZrC are light elements that may possess neutron moderating potential. If these materials produce a hard spectrum, then results should be relatively accurate. However, if these materials yield a soft spectrum, $S(\alpha,\beta)$ information is essential to the credibility of the results. This topic will be further investigated in chapter 3 where spectral information is available.

ORIGEN

ORIGEN, developed at Oak Ridge National Laboratory, is a point-depletion and radioactive-decay computer for simulating nuclear fuel cycles and calculation nuclide compositions [36]. The code uses a matrix exponential method to solve a large system of coupled, linear, first-order ordinary differential equations with constant coefficients.

ORIGEN contains a decay and photon data base of 130 actinides, 850 fission products, and 720 activation products. This data base is adequate for the majority of reactor designs. However, this is not the case for cross-section data since these are strongly dependant on the type of reactor and nuclide concentrations; this is especially true in the case of actinides [36]. Cross section data are available for:

- U and U-Pu cycle PWR and BWR
- alternative fuel cycle (thorium-based fuels: extended burnup) for PWR
- CANDU reactors
- U-Pu cycle Liquid Metal Fast Breeder Reactors (LMFBR)
- thorium LMFBR
- Fast Flux Test Facility
- Clinch River Breeder Reactor

It is apparent that data for gaseous fueled cavity reactors are not available in the ORIGEN cross section library. The next code allows the use of ORIGEN as the depletion tool even with absence of cross section data.

MONTEBURNS

This is a code developed at Los Alamos National Laboratory. It serves as a liaison between MCNP and ORIGEN. The user supplies three input files:

- an MCNP input file with the system material and geometry description at BOC
- a feed file containing the amount of and type of materials to be added or removed from the system
- an input file describing miscellaneous data such as the core thermal power, number of burnup steps, and a list of isotopes to be monitored and printed in the output

The code obtains one-group microscopic cross sections and fluxes from an MCNP run. It passes that information to ORIGEN. ORIGEN then burns those materials and outputs a new material composition. MONTEBURNS writes a new MCNP input file containing the adjusted composition and density of each material being analyzed. This is repeated until the user-specified burnup steps are complete.

A predictor step is executed in the middle of each burn step where ORIGEN is executed and one-group cross sections are calculated at the midpoint by MCNP. These cross sections are then used by ORIGEN to calculate material compositions for the end of the burn step. MONTEBURNS outputs information regarding the isotopes listed in the input file for each burn step; such information includes isotope build-up or destruction rate, radiotoxicity, activity, and heat load.

An important feature of MONTEBURNS is its ability to simulate continuous fuel feed. This may not be useful for LWRs because there is enough excess reactivity at BOC to maintain criticality throughout the cycle with the use of burnable poisons, control

blades, and chemical shim (for PWRs)—none of which are necessary in a GCR due to its simplicity in design. The main way to obtain enough reactivity in the GCR to maintain criticality is with the use of continuous fuel feed. This allows the actinides to stay in the GCR longer than in LWRs, increasing their chances of undergoing fission or transmutation. With other depletion codes, be it deterministic or stochastic, does not offer continuous fuel feed, an important advantage of the GCR.

MCNP5, ORIGEN2.2, and MONTEBURNS are the three computational tools used for this research.

CHAPTER 3 ACTINIDES AND FISSION PRODUCTS

It is essential to obtain an in-depth understanding of actinides and fission products in order for the results of the current research to be applied in a pragmatic manner. When discharged from the LWR, the concentration of these nuclides in spent fuel is dependant on individual irradiation histories. However, small differences in nuclide concentration will not change the long term effects on waste disposal.

The GCR actinide inventory will be compared to typical LWR spent fuel. To determine the isotopes that significantly affect the storage and disposal requirements on HLW, one needs to consider those that have longer half lives than natural uranium isotopes. The radioactivity of HLW is often compared to the radioactivity of natural uranium ore, as in Figure 3-1. Current LWR spent fuel will decay to the activity of natural uranium ore in about 10,000 years. This is the basis for setting the current repository requirements; the repository at Yucca Mountain is required to prove that it is capable of isolating HLW for 10,000 years, after which the activity of the waste is equivalent to naturally radioactive materials found in the environment.

Hence, the isotopes that have half lives less than hundreds of years do not affect scientists' ability to prove the repository's isolation capabilities and are not of great concern in the current research. The isotopes with half lives significantly longer than uranium decay very slowly (low activity) and are more or less considered stable. The isotopes that pose a threat to the success of the repository are those with half lives greater than about one thousand years and less than about $1E+9$ years. This research will focus on isotopes that are

problematic in the aspect of HLW, the isotopes that improve proliferation resistance, those that are fissile, and those that have important commercial applications.

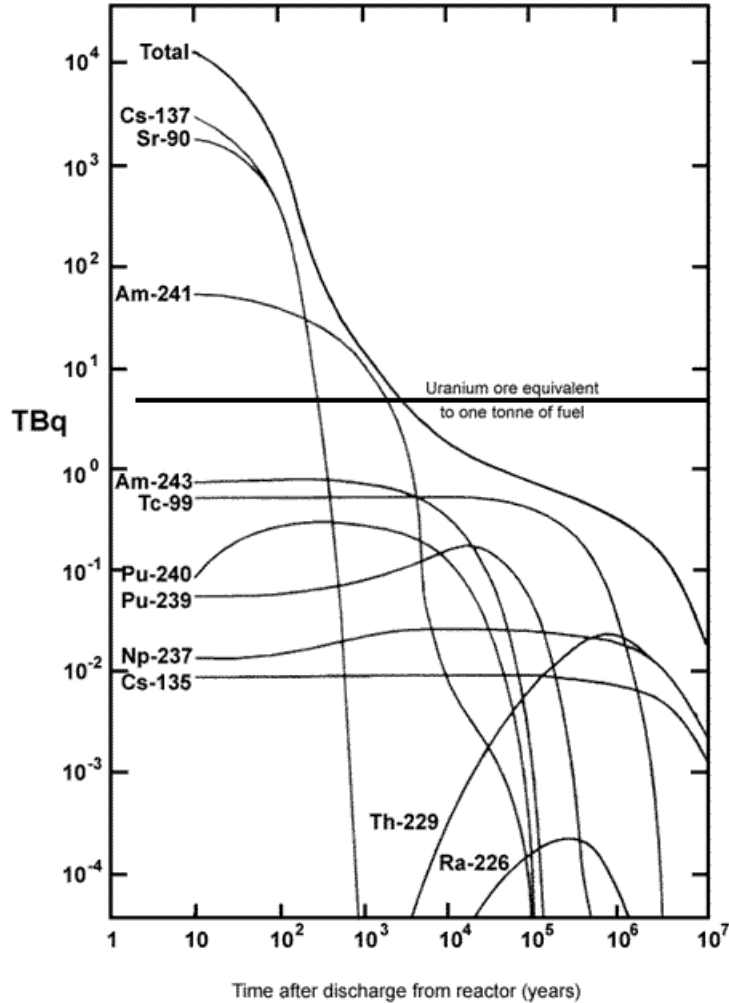


Figure 3-1. Activity of HLW from one ton of spent fuel. Source: IAEA, 1992, Radioactive Waste Management, courtesy of reference [37].

Origins

Actinides and fission products are a result of neutron interaction with uranium isotopes in a reactor. The actinide series consist of 15 chemical elements with atomic number between 89 and 103; of these only three are found in nature: actinium ($Z = 89$), thorium ($Z = 90$), and uranium ($Z = 92$). The rest of the actinides can only be artificially produced in

environments such as a nuclear reactor or a particle accelerator. Regardless of the origin of these nuclides, all actinides are radioactive; however, the latter half of the actinide series has decreasingly shorter half lives. In nuclear waste, most actinides are generated in the fuel from the capture of a neutron by U-238. The resulting isotope becomes a transuranic actinide through decay and/or sequential capture of other neutrons.

It is not so straightforward when identifying fission products. When an isotope encounters a neutron and fission occurs, it splits into two fragments and releases 2 or 3 neutrons, gamma rays, beta particles, and neutrinos. The two fragments are referred to as fission products. Figure 3-2 shows the probability distribution of fission products as a function of atomic mass number from the fission of U-235. The peaks of Figure 3-2 occur at atomic masses of approximately 95 and 140. This corresponds to elements of strontium through palladium and iodine through neodymium.

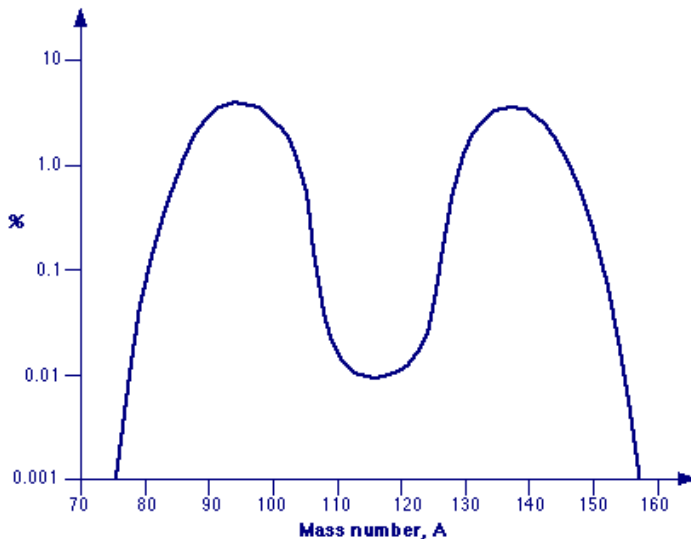


Figure 3-2. Distribution of fission products from U-235. Adapted from reference [37].

A nuclear reactor is a unique environment where an abundance of neutrons are available. Many nuclides may undergo neutron capture and release excess energy in the

form of gamma rays, alpha and beta particles. Some of these nuclides have large cross sections for such a reaction and are neutron poisons in a reactor such that they account for a large negative effect to the reactivity of the core. Well known examples of poisons in LWR are Xe-135 and Sm-149—both fission products. However, due to the current research objectives, only those nuclides that pose storage and disposal problems for HLW will be examined in this section.

Actinides

Actinides pose proliferation and waste disposal concerns; isotopes of U and Pu are fissile. While fission products are responsible for the initial activity of the waste, transuranics accounts for almost all of the activity in the spent fuel several hundred years after discharge. Most of the transuranics in nuclear waste are plutonium, neptunium and americium. These have long half lives on a similar time scale to uranium. They are the reason that the legislature requires spent fuel to be isolated at Yucca Mountain for more than a few thousand years if the waste were fission products alone [37].

92-Uranium (U)

Natural U contains three radioactive isotopes: 0.0055% U-234 ($T_{1/2} = 2.455E+5$ yrs), 0.72% U-235 ($T_{1/2} = 7.038E+8$ yrs), and 99.2745% U-238 ($T_{1/2} = 4.468E+09$ yrs). Other uranium isotopes that are found in spent fuel are U-236 ($T_{1/2} = 2.342E+7$ yrs), and U-237 ($T_{1/2} = 6.75$ days). In addition to the component of U-234 found in natural uranium, U-234 is a daughter of Pu-238, which is also found in spent fuel. Although the cross section for radiative capture is low (99.75 barns) relative to neutron poisons (greater than $E+4$ barns) in the reactor, this is the dominant mode of neutron interaction. Neutron capture in U-234 yields U-235.

Nuclear fuel in the US consists of enriched U-235, to a regulatory limit of 5 w/o for commercial power production. The thermal fission cross section of U-235 is 584.4 b with a fission-to-capture ratio of 5.9144. Highly enriched uranium (HEU), with U-235 content greater than or equal to 20 w/o, may be used in nuclear weapons. The first atomic bomb created during World War II used HEU. It was dropped on Hiroshima, Japan in 1945.

U-236 is a daughter of Pu-240, found in spent fuel. U-236 decays to Th-232. Th-232 is found in nature to be three times more abundant than uranium and as abundant as Pb. There is increased interest in using Th-232 as nuclear fuel. It absorbs thermal neutrons eventually producing U-233 ($T_{1/2} = 1.592E+5$ yrs), which is fissile and gives off more fission neutrons than U-235. Thorium isotopes appear in U decay chains but most are short-lived and on a mass basis are negligible [38]. When U-235 interacts with a neutron, about 14% of the time this interaction will result in a radiative capture event, becoming U-236. The main modes of neutron interaction in U-236 are elastic scattering (8.336 b) and radiative capture (5.295 b). Capture of another neutron converts U-236 to U-237.

U-237 is a daughter of Pu-241, and decays shortly to Np-237—a long-lived radionuclide. With a capture cross section of 452.4 b, U-237 becomes U-238. U-238 is the most abundant of the U isotopes, and it is fertile. Through neutron bombardment it becomes the source of all actinides produced in the nuclear fuel cycle.

93-Neptunium (Np)

Neptunium is only found in trace amounts in uranium ores. Its commercial use is in neutron detectors. Most Np isotopes are short-lived, except for Np-236 and Np-237. Np-236 has a half life of $1.54E+5$ yrs. It is also fissile with a fission cross section of 2,770 b and a fission-to-capture ratio of 3.9515. However, no significant amount is found in spent fuel.

The primary isotope of Np in spent fuel is Np-237. It is a daughter of U-237 and Am-241. It is very long-lived with a half life of 2.144×10^6 yrs. It eventually decays to stable bismuth.

Another isotope of interest is Np-238. In a reactor, Np-237 may capture a neutron and become Np-238. With a half life of 2.117 days, Np-238 decays to Pu-238. Pu-238 is used in radioisotope thermoelectric power generation (RTG) for space missions. Thus, one way to generate Pu-238 is to irradiate Np-237. However, Np-238 is fissile with a thermal fission cross section of 2,070 b and a fission-to-capture ratio of 4.5990. Generation of Pu-238 is difficult and expensive.

In September of 2002, Los Alamos National Laboratory (LANL) successfully brought a sphere of Np-237 to criticality. The system involves layers of enriched uranium surrounding a layer of Np-237. Since the thermal fission cross section of Np-237 is 22.49×10^{-3} b and the fission-to-capture cross section ratio is 1.3663×10^{-4} , achieving criticality with a bare sphere may require large amounts of Np-237. Thus, the experiment at LANL needed enriched uranium to sustain the chain reaction.

A simple calculation using MCNP5 indicates that the bare critical mass of Np-237 is about 63.31 kg. This small critical mass is unexpected. However, the MCNP simulation reveals that the average number of neutrons released from fission is 2.962; this high number of fission neutrons per fission event is because over 99% of the fissions are caused by neutrons with energies greater than 100 KeV.

The average energy of neutrons that cause fission is 2.176 MeV. At this energy, the fission-to-capture ratio becomes 31.92. Figure 3-3 shows the fission-to-capture ratio for Np-237 as a function of energy. At about 0.492 MeV the fission-to-capture ratio is 1.0. Since

fission neutrons are born at high energies, and the fission-to-capture ratio is greater than 1.0 at such energies, this is the reason Np-237 can become critical.

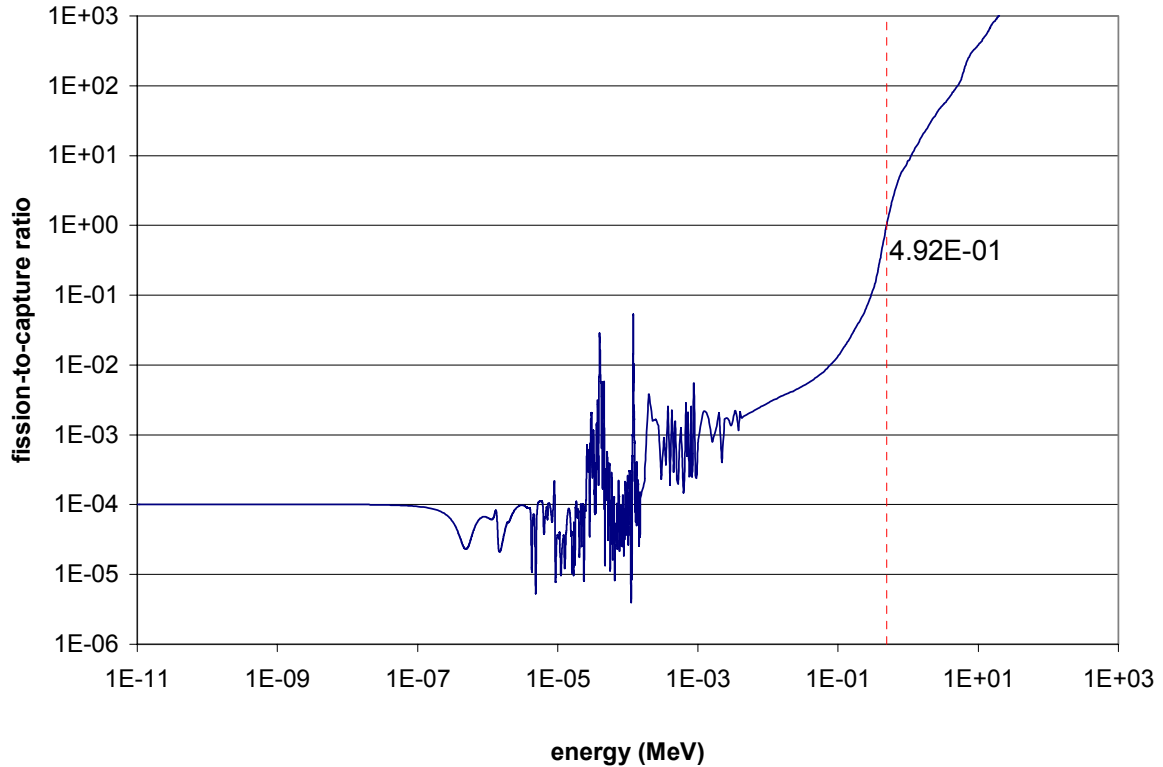


Figure 3-3. Fission-to-capture cross section ratio for Np-237. All values are at 300 K. Data interpreted from ENDF/B-VI [39].

94-Plutonium (Pu)

Plutonium is a very important transuranic element due to the relative ease in producing the fissile isotopes. The main uses for these fissile isotopes are for the production of energy in nuclear fuels (not currently practiced in the US), and military applications such as nuclear weapons. The bomb dropped on Nagasaki, Japan during WWII used Pu-239. Weapons-grade Pu contains more than 90% Pu-239. However, after international efforts aimed at the dismantlement of nuclear weapons, Pu from weapons stockpiles is down-blended and used as nuclear fuel.

From a chemical standpoint Pu is about as poisonous as Pb and other heavy metals [40]. When inhaled, Pu may cause cancer to the lungs, and skeleton. Additionally, Pu is a fire hazard when exposed to water or oxygen. Thus, Pu must be stored and handled in a dry inert atmosphere.

Pu also has very peculiar materials properties. Pu occurs in a variety of allotropes that differ in crystal structure and densities, readily changing phases. These six allotropes vary in density from 16.00 to 19.86 g/cc [41]. This makes Pu difficult to handle as far as machining is concerned.

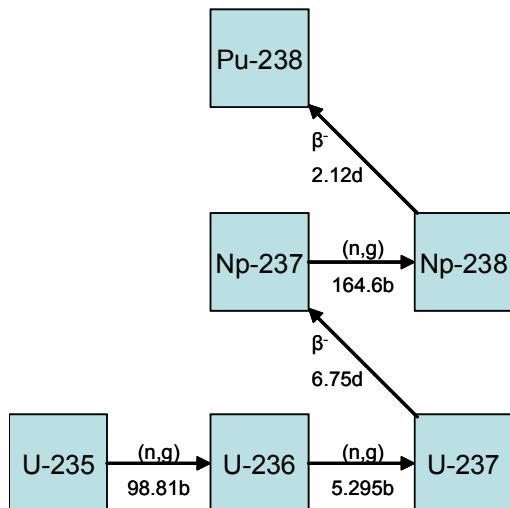


Figure 3-4. Production of Pu-238 with thermal interaction cross sections and decay half lives. Half life and cross section values are from reference [42]. Cross sections are taken at 0.0253 eV.

In a uranium-fueled reactor, Pu-238 production is mainly due to the reactions shown in Figure 3-4. This is due to the abundance of neutrons and U-235 isotopes, and the short half lives of the intermediate isotopes (U-237 and Np-238). However, relative to other Pu isotopes present in spent fuel, the amount of Pu-238 generated is the least. This is because some isotopes in the chain are fissile such as U-235 and Np-238. Thus, the chances that U-235 (fission-to-capture ratio of 5.9144) goes through all the interactions in Figure 3-4, become another fissile isotope, Np-238 (total thermal cross section of 2,533 b), and then

decay to Pu-238 are minimal. The interest in Pu-238 lies in its many applications, discussed in later sections.

Since Pu-239 is fissile, it contributes about one-third of the total energy output in a typical LWR [37]. The fission of all Pu isotopes accounts for 40 % of the total energy output over an equilibrium cycle. It has a long half life of 24,110 yrs, and decays to fissile U-235. Spent fuel contains the highest amount of Pu-239 among the transuranics. As shown in Figure 3-5, Pu-239 originates from a chain of interactions with U-238 at its head. The production of Pu-239 in a nuclear reactor is straightforward and painless. This is due to 3 reasons:

- There is an abundance of U-238 isotopes. The enrichment of civilian fuel is at most 5 w/o U-235. Thus, there is at least 95 w/o of U-238 in fresh fuel.
- U-238 and all of the intermediate isotopes are not fissile. Additionally, fission and capture cross sections for U-239 and Np-239 are very low (~37 b and ~39 b, respectively).
- Intermediate isotopes have very short half lives, and Pu-239 has a long half life.

This is why U-238 is known as a fertile isotope: it converts to a fissile nuclide after neutron interaction.

In countries where reprocessing is practiced, Pu along with the remaining U-235 is put back into the reactor in the form of MOX fuel. The Pu and U are separated from the spent fuel. Pu is sent directly to the fabrication plant. U is sent to an enrichment plant for re-enrichment. The MOX is a mixture of UO_2 and PuO_2 . Because of reactivity control issues with Pu fuel, Pu in MOX is mixed with depleted U. Typically only about one-third of the reactor contains MOX fuel, the rest of the reactor contains enriched UO_2 fuel.

Pu-239 has a thermal capture cross section of 270.3 b and a fission-to-capture ratio of 2.77, whereas U-235 has a fission-to-capture ratio of 5.91. Thus, a capture event is more

likely in Pu-239 than in U-235. When Pu-239 captures a neutron Pu-240 is produced. Pu-240 has a half life of 6,564 years, and decays to U-236. Pu-240 also emits spontaneous fission neutrons, and thus is considered a contaminant in nuclear weapons. Pu from commercial reactors contains at least 20% Pu-240 and is called “reactor-grade” plutonium.

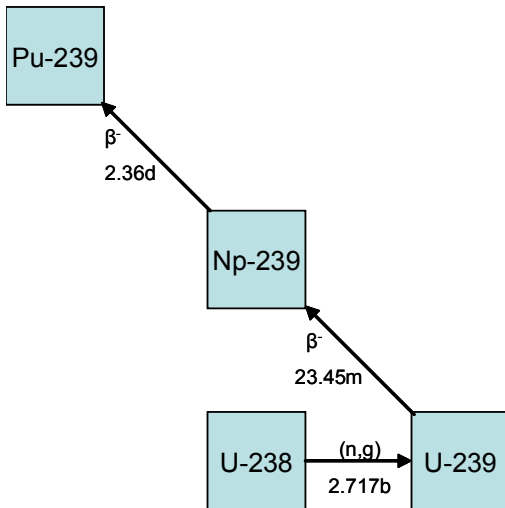


Figure 3-5. Production of Pu-239 with thermal interaction cross sections and decay half lives. Half life and cross section values are from reference [42]. Cross sections are taken at 0.0253 eV.

Pu-241 is a result of neutron capture by Pu-240. Since Pu-240 has a capture cross section of 289.4 b and a fission-to-capture ratio of 2.03E-04, neutron capture is the dominant mode of neutron interaction. Pu-241 has a short half life of 14.35 years and decays to Am-241 (99.9975%), and U-237 (0.0025%). Pu-241 is fissile like Pu-239, with a fission cross section of 1,012 b and fission-to-capture ratio of 2.80. However, unlike Pu-239, Pu-241 is harder to produce. It is a result of two consecutive captures, the first of which competes with fission. Nonetheless, capture cross sections of the intermediate isotopes are large enough that there is a significant amount of Pu-241 in spent fuel.

With another neutron capture (361.5 b) Pu-241 becomes Pu-242. This isotope has a half life of 373,300 years and decays to U-238. Pu-242 has a low neutron cross section of 27.11 b, with capture being the dominant mode of interaction. Like Pu-240, Pu-242 emits

spontaneous fission neutrons. Since the capture cross section of Pu-241 is relatively high, there is a significant amount of Pu-242 in spent fuel. Figure 3-6 shows the events leading to the production of Pu-240, Pu-241 and Pu-242.

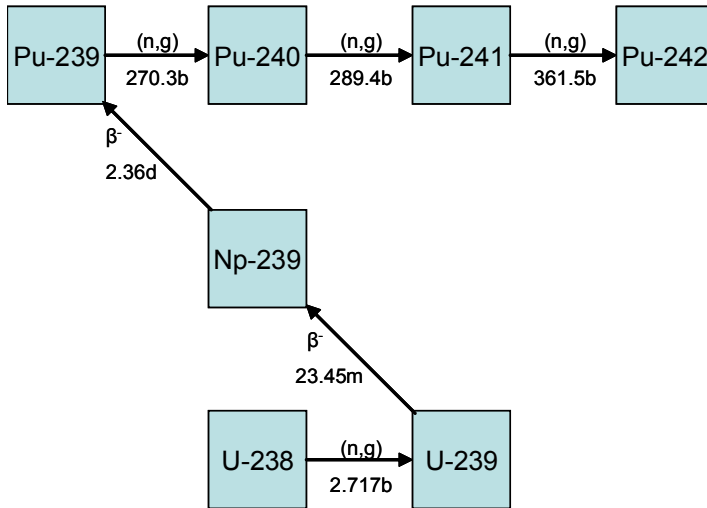


Figure 3-6. Production of Pu-240, Pu-241, Pu-242 with thermal interaction cross sections and decay half lives. Half life and cross section values are from reference [42]. Cross sections are taken at 0.0253 eV.

95-Americium (Am)

Am-241 comes from the decay of Pu-241. It has a relatively short half life of 432.2 years. However, its importance is that it decays to Np-237, a very long-lived actinide. The dominant mode of neutron interaction is capture with a thermal cross section of 600.4 b. Note in Figure 3-7 that no matter if Pu-241 experiences an α or a β^- decay, it eventually decays to the long-lived Np-237. Fortunately Pu-241 is fissile and its destruction is easily achieved in a reactor. Am-241 is used in smoke detectors, and as a gamma source for radiography.

Am-242 has large interaction cross sections and a short half life of 16.02 hours. The thermal fission and capture cross sections are 2,100 and 5,500 b respectively. Thus, the amount of Am-242 in spent fuel is minimal. However, its importance is that upon production of Am-242 in the reactor, it will immediately either fission or experience a capture event and

convert to Am-243. Am-243 has low interaction cross section, with capture being dominant (78.5 b). It has a half life of 7,370 years and decays to Np-239. Recall that Np-239 shortly decays to Pu-239. This is the reason that in Figure 3-1 the activity of Pu-239 builds up and reaches a maximum with time as the activity of Am-243 sharply decreases around the time frame of $1E+4$ years.

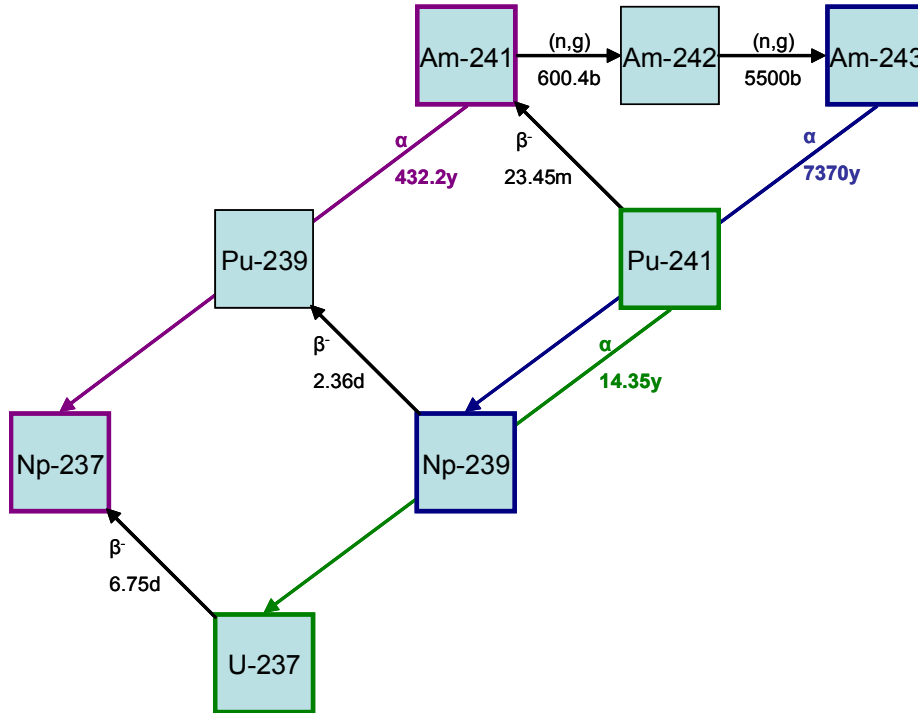


Figure 3-7. Production of Am-241, Am-242, Am-243 with thermal interaction cross sections and decay half lives. Alpha decays are highlighted. Half life and cross section values are from reference [42]. Cross sections are taken at 0.0253 eV.

96-Curium (Cm)

Because curium isotopes are alpha emitters, they can potentially be used as fuel for RTG, such is the case for Pu-238. Cm-242 is a daughter of Am-242. With a half life of 162.8 days, it quickly decays to Pu-238. The dominant mode of neutron interaction in Cm-242 is radiative capture with a thermal cross section of 15.90 b. As far as potential for fueling RTG, Cm-242 generates up to 120 watts of thermal energy per gram (W/g) [43], compared to 0.57 W/g from Pu-238 [44]. However, Cm-242 has too short of a half life and

because it emits a significant amount of spontaneous fission neutrons, it requires a thick radiation shield. Hence, Cm-242 is not suitable for space applications.

Neutron capture in Cm-242 will produce Cm-243. Cm-243 has a half life of 29.1 years, with daughters Pu-239 (99.71%) and Am-243 (0.29%). Cm-243 decays to a fissile Pu-239, and it is fissile itself; its fission cross section and fission-to-capture ratio are 617.4 b and 4.74 respectively. From Figure 3-7, Am-243 also eventually decays to Pu-239, albeit after a long half life. Cm-243 has a maximum energy density of ~ 1.6 W/g, but requires shielding for the gamma and beta particles from its decay products [43].

Cm-243 also has a significant capture cross section of 130.2 b. Such interaction would produce Cm-244. Another source for this isotope is neutron capture by Am-243 producing Am-244, with half life of 10.1 h, decaying to Cm-244. With these two sources, Cm-244 is the most abundant of the Cm isotopes found in spent fuel. Cm-244 has a half life of 18 years and alpha decays to Pu-240, or spontaneously fissions. Its dominant mode of neutron interaction is capture with a low cross section of 15.1 b. Of the Cm isotopes, Cm-244 is most often considered as a candidate for thermoelectric generation with a power density of ~ 3 W/g [43]. However, like Cm-242, Cm-244 also presents shielding issues due to spontaneous fission neutrons [45].

Cm-245 is the product of a neutron capture interaction with Cm-244. It has a long half life of 8,500 years and decays to Pu-241. Cm-245 is fissile with a fission cross section and fission-to-capture ratio of 2,001 b and 5.78 respectively. It also has a significant capture cross section of 346.4 b. Thus, there is little accumulation of Cm-245 in spent fuel.

Sequential captures produce Cm-246, Cm-247, and Cm-248, with half lives of 4,760 years, 15.6 million years, and 348 thousand years respectively. All three decay to Pu

isotopes. Cm-246 and Cm-248 have low neutron cross sections, with capture being dominant at 1.291 b and 2.57 b. Cm-247 is fissile; however the fission cross section is low at 81.79 b and the fission-to-capture ratio of 1.43. Like other Cm isotopes, these three isotopes are spontaneous fission neutron sources. This is especially true for Cm-248, where spontaneous fission is the mode of decay 8.26 % of time, and alpha decay 91.74% of the time. See Figure 3-8 for production and decay chains of Cm isotopes and Table 3-1 for a summary of the important characteristics of actinides.

Table 3-1. Summary of actinides and their important properties. Data from reference [42].

isotope	half life (years)	decay mode	decay product	cross section* (barns)		fission:capture ratio
				fission	capture	
U-234	2.46E+05	α	Th-230	0.006218	99.75	6.23E-05
U-235	7.04E+08	α	Th-231	584.4	98.81	5.91
U-236	2.34E+07	α	Th-232	0.06129	5.295	1.16E-02
U-237	1.85E-02	β^-	Np-237	1.702	452.4	3.76E-03
U-238	4.47E+09	α	Th-234	1.177E-05	2.717	4.33E-06
Np-237	2.14E+06	α	Pa-233	0.02249	164.6	1.37E-04
Np-239	6.45E-03	β^-	Pu-239	0	37	0
Pu-238	8.77E+01	α	U-234	17.89	540.3	3.31E-02
Pu-239	2.41E+04	α	U-235	747.4	270.3	2.77
Pu-240	6.56E+03	α	U-236	0.05877	289.4	2.03E-04
Pu-241	1.44E+01	β^- (99.998%) α (0.0025%)	Am-241 U-237	1012	361.5	2.80
Pu-242	3.73E+05	α	U-238	0.002557	18.79	1.36E-04
Am-241	4.32E+02	α	Np-237	3.018	600.4	5.03E-03
Am-242	1.83E-03	β^- (82.70%) EC (17.30%)	Cm-242 Pu-242	2100	5500	3.82E-01
Am-243	7.37E+03	α	Np-239	0.1161	78.5	1.48E-03
Cm-242	4.46E-01	α	Pu-238	5.064	15.9	3.18E-01
Cm-243	2.91E+01	α (99.71%) EC (0.29%)	Pu-239 Am-243	617.4	130.2	4.74
Cm-244	1.81E+01	α	Pu-240	1.037	15.1	6.87E-02
Cm-245	8.50E+03	α	Pu-241	2001	346.4	5.78
Cm-246	4.76E+03	α	Pu-242	0.1401	1.291	1.09E-01
Cm-247	1.56E+07	α	Pu-243	81.79	57.2	1.43
Cm-248	3.48E+05	α	Pu-244	0.37	2.57	1.44E-01

* at 0.0253 eV

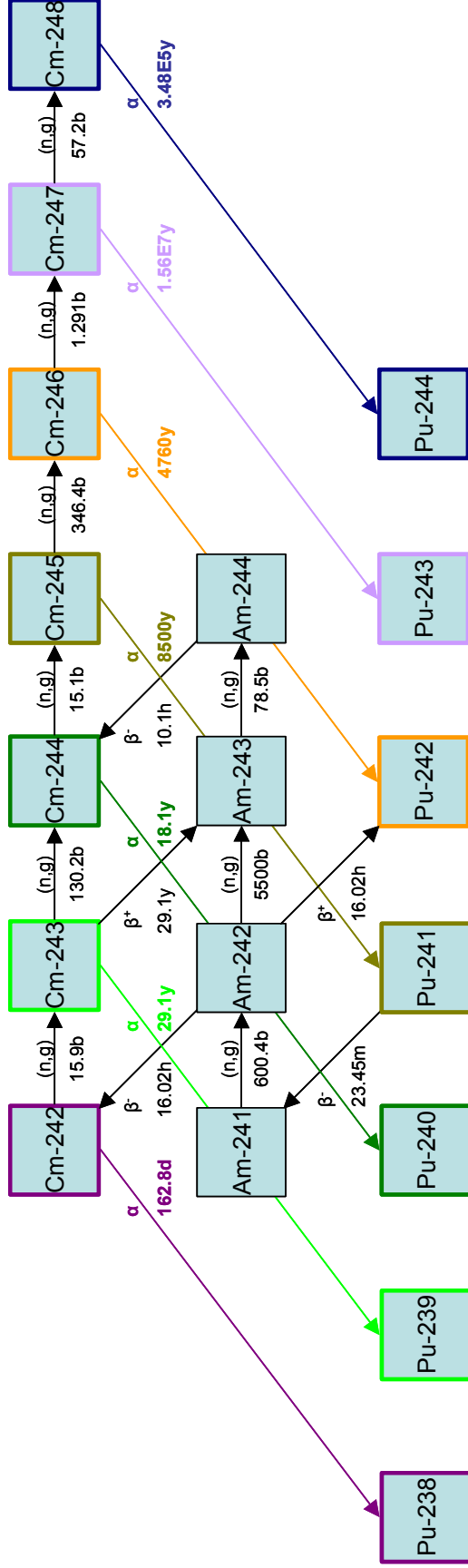


Figure 3-8. Production and decay chains for curium isotopes with thermal interaction cross sections and decay half lives. Half life and cross section values are from reference [42]. Cross sections are taken at 0.0253 eV.

Fission Products

The mass number of the fission products from the fission of U-235 is shown in Figure 3-2. The most common are isotopes of iodine, cesium, strontium, xenon, and barium [46]. Since the majority of fission products have short half lives relative to actinides, the initial activity of spent fuel is mostly due to the decay of fission products. Initially the activity is due to I-131 and Ba-140. After about four months isotopes such as Ce-141, Zr-95, Nb-95, and Sr-89 are responsible for most of the activity; after two to three years the largest share comes from Ce-144, Pr-144, Ru-106, Rh-106, and Pm-147. Sr-90 ($T_{1/2} = 29.1$ years) and Cs-137 ($T_{1/2} = 30.2$ years) are the main fission products in spent fuel [46].

Since most fission products are short-lived, they do not pose a threat to HLW disposal requirements. On the contrary, fission products can be harnessed for medical applications. Since the fuel is in a gaseous form, online separation of fission products from the fuel, lighter in mass than uranium and heavier actinides, is viable. This will also improve fuel utilization when fission products that are neutron poisons are removed from the fuel, eliminating their negative reactivity impact.

38-Strontium (Sr)

Strontium is an important fission product since it mimics calcium in the human body [47]. Accidental release of Sr into the biosphere could lead to Sr accumulation in bones and possibly cancer. One isotope, Sr-89, is used in radiotherapy of bone tumors. Sr-89 has a half life of 50.52 days and decays to stable Y-89. It has a low total neutron cross section of 6.12 b, with elastic scattering as the dominant mode of interaction (5.7 b). A longer lived isotope is Sr-90, with a half life of 28.79 years, and beta decays to Y-90. The fission yield of Sr-90 is about 6%. Sr-90 also has a low total neutron cross

section of 5.819 b, with elastic scattering as the dominant mode of interaction (5.804 b). Sr-90 is “one of the best long-lived high-energy beta emitters known [41],” and is often cited as a possible candidate fuel for RTG [45], generating about 0.93 W/g of energy [48]. It was used in a Soviet unmanned lighthouse called Beta-M and in some of the Systems for Nuclear Auxiliary Power (SNAP).

43-Technetium (Tc)

There are no natural isotopes of technetium. Tc-99m is the most widely used radioisotope for diagnostic studies in nuclear medicine [42]. The metastate has a half life of 6.01 hours and by internal conversion converts to Tc-99. Tc-99 has a half life of 211,110 years, and decays to stable Ru-99. Neutron interaction of Tc-99 is dominated by radiative capture, with a thermal cross section of 19.64 b. There is significant production of Tc-99 during the fission process [47]. The fission yield of Tc-99 is about 6%. It is one of the isotopes that is able to form anionic species and become very mobile in both solid and water [46], making its isolation from the biosphere difficult.

53-Iodine (I)

Similar to Tc-99, I-129 can form anionic species and become very mobile. Although I-129 has a low fission yield of about 0.7%, it has a very long half life of 15.7 million years, decaying to stable Xe-129. The dominant mode of interaction is neutron capture at 27 b. Upon transmutation, I-129 converts to I-130, with a significantly shorter half life of 12.36 hours.

The human body concentrates iodine in the thyroid gland [46]. Thus, radioactive isotopes such as I-131, are used to diagnose and treat thyroid disorders. A small dose is used for a thyroid function test while a large dose could destroy the thyroid [47]. I-131 has a higher fission yield of about 3%. This isotope has a half life of 8.0207 days and

decays to stable Xe-131. Its dominant mode of interaction is neutron capture with a cross section of 80 b.

55-Cesium (Cs)

A lot of cesium is produced during the fission process [47]. Cs acts like potassium in the human body, and thus becomes a biological hazard. Cs-135 is very long-lived with a half life of 2.3 million years, decaying to stable Ba-135. Neutron capture is the dominant mode of interaction with a cross section of 8.702 b. In contrast, Cs-136 has significantly shorter half life of 13.16 days.

Cs-137 has a half life of 30.07 years and decays to stable Ba-137. This isotope has a low interaction cross section of 3.78 b, with an elastic scattering cross section of 3.53 b. Cs-137 beta decays to a metastable state of Ba-137. The decay of Ba-137m to Ba-137 is responsible for all the gamma energy release. These gamma rays have a wide range of applications such as for cancer treatments, to measure correct patient dosages of radioactive pharmaceuticals, to measure and control the liquid flow in oil pipelines, to tell researchers whether oil wells are plugged by sand, and to ensure the correct fill level for packages of food, drugs and other products [42].

The yield of most isotopes of Sr, Tc, I, and Cs from the fission of U-235 caused by a thermal (0.0253 eV) are shown in Figure 3-9. Both I and Cs have isotopes with high fission yields such as I-134, Cs-133, Cs-135, and Cs-138.

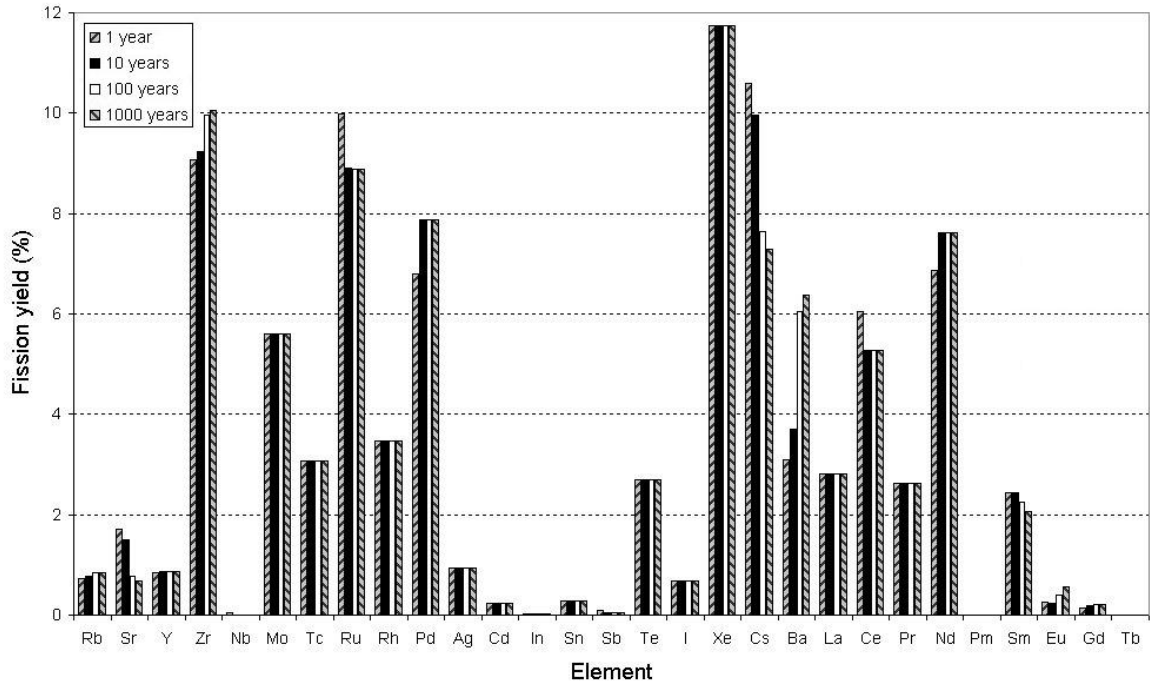


Figure 3-9. Fission yields from the fission of U-235 after various cooling times. Adapted from reference [46].

Table 3-2. Summary of fission products and their important properties. Data from reference [42].

isotope	half life (years)	decay mode	decay product	capture cross section* (barms)	fission yield
Sr-89	1.38E-01	β^-	Y-89	0.42	2.44E-02
Sr-90	2.88E+01	β^-	Y-90	0.015	2.95E-02
Tc-99	2.11E+05	β^-	Ru-99	19.64	3.06E-02
I-129	1.57E+07	β^-	Xe-129	27	3.59E-03
I-131	2.20E-02	β^-	Xe-131	80	1.44E-02
Cs-135	2.30E+06	β^-	Ba-135	8.702	3.27E-02
Cs-137	3.01E+01	β^-	Ba-137	0.25	3.13E-02

* at 0.0253 eV

Applications

The actinides and fission products created from the activation or fission of uranium in a nuclear reactor presents storage and disposal problems. However, some radioactive isotopes are used in a wide range of applications. This discussion will help define the list of isotopes to be analyzed when making comparisons to LWR.

Nuclear Fuel

Since U-235 and Pu-239 are used in nuclear fuel and weapons, it is behooving to investigate their relative effectiveness as fissile material. Table 3-3 compares the neutronic parameters of interest for the two isotopes when used as nuclear fuel.

Table 3-3. Neutronic parameters for U-235 and Pu-239 fueled LWRs. Adapted from reference [1].

parameter	units	U-235	Pu-239
σ_a	2200 m/s	682	1019
	Spectrum avg.	430	915
σ_f	2200 m/s	584	748
	Spectrum avg.	365	610
η	2200 m/s	2.07	2.11
	Spectrum avg.	2.07	1.9
β	delayed nt. fraction	0.0065	0.0021
l	neutron lifetime	μs 47	27

Pu-239 has a significantly higher capture and fission cross section than U-235.

This is clearly shown in Figure 3-10, where the average height of the resonances in Pu-239 is at about one order of magnitude greater than those of U-235. This can be observed in the resonance at the lowest energy (about 0.3 eV). Both capture and fission cross sections in Pu-239 are at least one order of magnitude greater than the U-235 capture and fission cross sections. Because of the higher absorption cross section of Pu-239, reactivity control mechanisms decreases in reactivity worth [1]. This is because LWRs are designed with the intention of using U-235 fuel. In order to used MOX fuel in an LWR the MOX assemblies are placed away from control rods.

Pu-239 has a higher fission cross section than U-235. This tends to produce power peaks [1]. Thus, MOX fuel should be placed away from water gaps where the moderator-to-fuel ratio is higher and the local neutron population is more thermal.

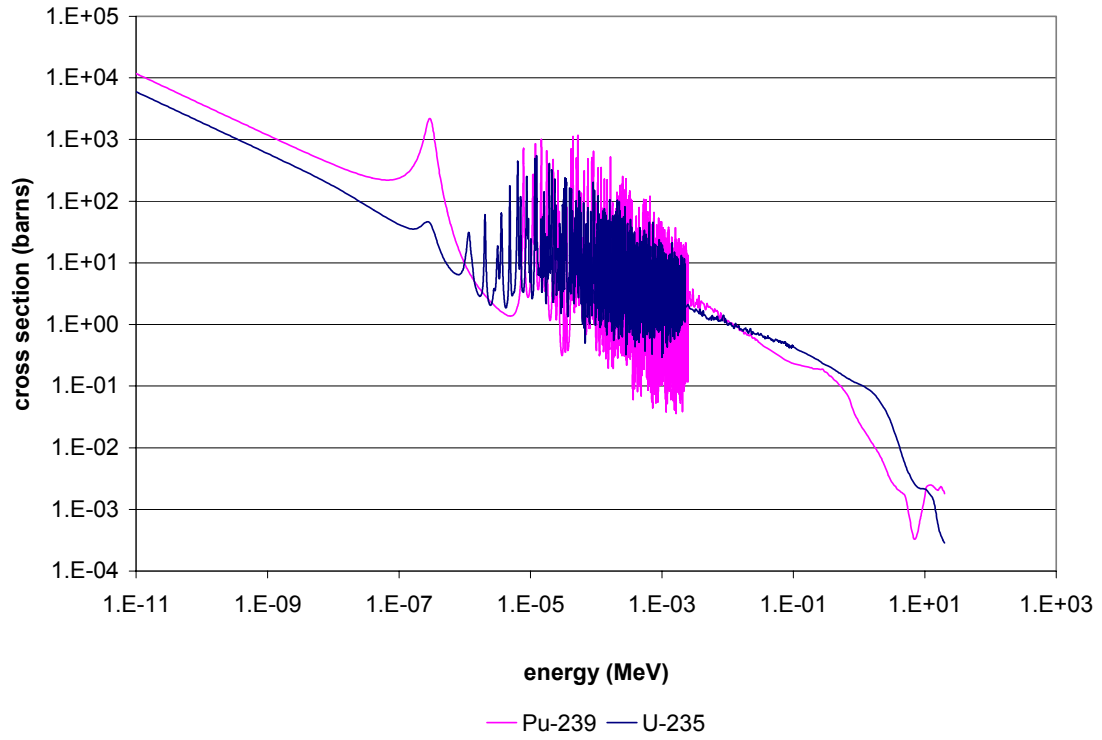


Figure 3-10. Capture cross sections for U-235 and Pu-239 at 300 K from ENDF/B-VI [39].

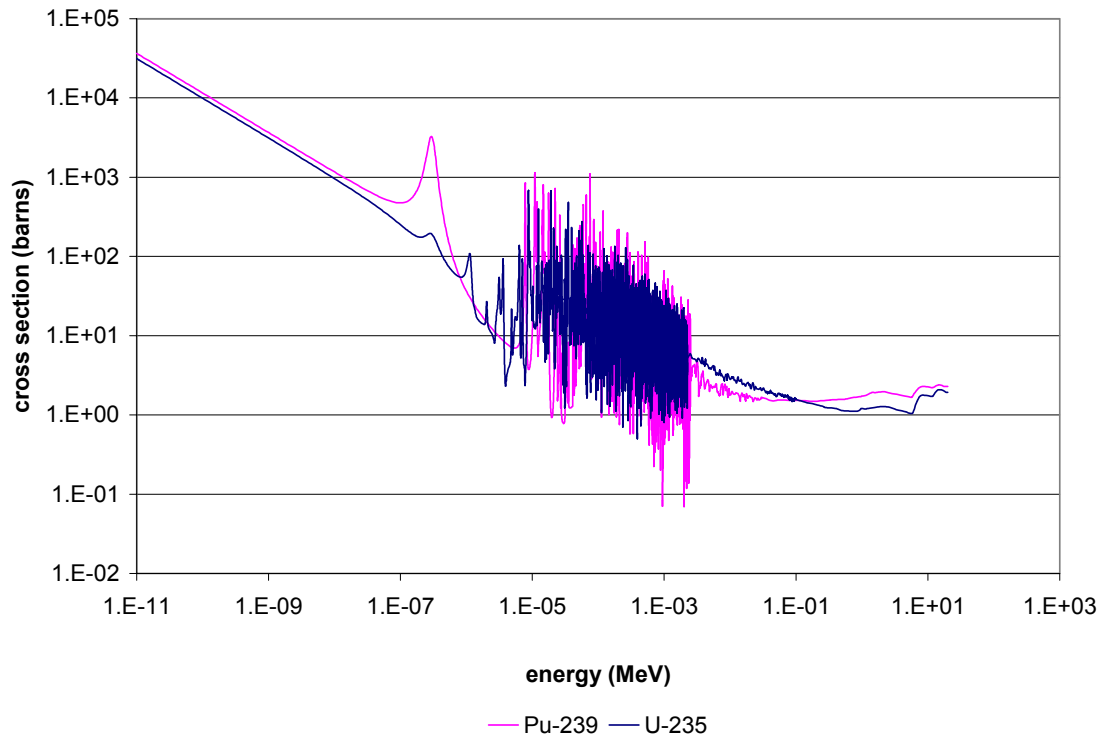


Figure 3-11. Fission cross sections for U-235 and Pu-239 at 300 K from ENDF/B-VI [39].

The average η is less for Pu-239 than U-235, thus more Pu-239 is needed than U-235 for the same reactivity worth. However, reactivity decreases slower with burnup in Pu-239 than U-235, so that to achieve the same burnup, less MOX fuel is needed than UO₂ fuel [1].

Both delayed neutron fraction and prompt neutron lifetime are less in Pu-239 causing kinetics safety concerns. To overcome these issues, the use of MOX in LWR follows two guidelines in France:

- The amount of MOX used must be less than 30% of the core.
- MOX rods are placed within the assembly in 2 or 3 zones with different enrichments in an attempt to flatten the power distribution [1].

Because LWRs were not designed for Pu fuel, use of MOX in LWR is limited to ensure safety. This is mainly due to reactivity control issues from the large absorption cross section of Pu-239. This would not be a problem if the number of control rods is increased. However, this may not be done in reactors that are now in operation.

Radioisotope Thermoelectric Generator (RTG)

An RTG harnesses the heat generated from radioactive decay and converts it to electricity using thermocouples. RTGs are used in unmanned missions that require a low amount of reliable electricity for long periods of time. Thus, RTGs are often used to power space missions. The ideal fuel consists of a radioactive material satisfying the following criteria:

- The half life must be long enough to supply continuous energy for a reasonable amount of time, but short enough to obtain the desired amount of energy. Typically, isotopes with half lives of several decades are used [45].
- For space missions, a high mass density is desirable since a low mass is crucial to its success. A high energy density is also preferred.

- The fuel must produce high energy radiation with low penetration, mainly through alpha emission. Beta and gamma radiation produce a significant amount of secondary radiation, increasing shielding requirements.

The most popular RTG fuels are Pu-238, Sr-90, and Cm-244 [45]. Pu-238 is the most commonly used fuel for RTG. Of these three isotopes, Pu-238 has the longest half life (87.7 years) and the lowest shielding requirements. Many times the fuel casing itself provides adequate shielding [45]. The energy density of Pu-238 is about 0.57 W/g [44]. The primary mode of decay is alpha emission to U-234, with low neutron and gamma levels [45]. Pure Pu-238 is difficult to produce, and hence very expensive. To produce Pu-238 one must first isolate Np-237 or Am-241 from spent fuel. Through neutron bombardment of either of these isotopes would transmute to Pu-238. Details on this process are in the previous section (see Pu and Cm sections) and clearly illustrated in Figure 3-4 and Figure 3-8.

Sr-90 has been used in some Russian terrestrial RTGs. It has a half life of 28.79 years, one-third of the Pu-238 half life. Sr-90 also has a lower density than Pu-238 and produces 0.93 W/g [48]. Although Sr-90 decays through beta emission, it also produces gamma radiation through bremsstrahlung secondary radiation production, increasing shielding requirements. One advantage is that it is produced in significant amounts as a fission product. Thus, it is cheaper than Pu-238.

Compared to Pu-238, Cm-244 has a high energy density of ~ 3 W/g [43] but has the shortest half life of the three candidate fuel isotopes. One major disadvantage is that Cm-244 emits a significant amount of neutron and gamma particles due to its tendency to spontaneously fission. Thus, Cm-244 requires heavy shielding, increasing the mass of the system. Table 3-4 summarizes important RTG properties of the three isotopes discussed.

Table 3-4. Summary of radioisotopes that are candidate fuel for RTG.

isotope	half life (years)	decay mode	energy density (W/g)
Pu-238	87.7	α	0.57
Sr-90	28.79	β^-	0.93
Cm-244	18.1	α	~3

Improving Proliferation Resistance of Fissile Material

Recall that weapons proliferation concerns in the 1970's led to the prohibition of commercial spent fuel reprocessing in the US. Proliferation is a topic that attracts great public concern and opposition towards nuclear technology. However, nuclear energy has many advantages compared to other forms of power generation such as fossil fuels, and renewable energy. It is reliable, limits greenhouse gas emissions, and competitively priced. Patrick Moore, a well known environmental activist, expressed on the subject of nuclear energy and weapons proliferation that "if we banned everything that can be used to kill people, we would never have harnessed fire" [49:B01].

One argument opposing reprocessing of spent fuel is that there is a possibility of obtaining pure Pu for illicit use. If this was the case, the Pu obtained from reprocessing of spent fuel contains many isotopes of Pu: Pu-238, Pu-239, Pu-240, Pu-241, and Pu-242. From the previous sections, we know that reactor grade Pu contains at least 20% Pu-240, and is considered a contaminant for nuclear weapons. This is because Pu-240 has a high rate of spontaneous fission (415,000 fissions/s-kg). Since Pu-240 emits neutrons randomly it makes it difficult to accurately initiate the chain reaction at the desired instant, reducing the bomb's reliability and power [40]. A 1% Pu-240 impurity in Pu-239 will lead to premature initiation of fission in gun type nuclear weapons, blowing the weapon apart before most of its fissions [40]. Thus, Pu obtained from reprocessing spent fuel is not suitable for nuclear weapons.

Other uses for this Pu may be to disperse it into the environment as a dirty bomb, since Pu is toxic and radioactive. The radioactivity comes from alpha particles that are released during decay. To avoid illicit use of Pu, methods of spiking and doping are used. When weapons materials are spiked with 5% Pu-238, the surface temperature is about 875 °C [1]. Since the melting point of explosives is ~200 °C [1], the presence of Pu-238 makes fissile Pu proliferation resistant. At these temperatures, handling this mixture would require special equipment that is too inconvenient for the Pu to be used for destructive purposes. Additionally, separation of Pu-238 from fissile Pu-239 is extremely difficult since the difference in mass is 1 amu, i.e. less by a factor of 3 than for uranium isotopes [44].

Spent fuel that has just been discharged from the reactor is inherently proliferation resistant. This is because it is highly radioactive and thus high in temperature. It must be cooled via convection of water; otherwise the cladding will melt and release a large amount of activity. This radiation will most likely cause acute radiation sickness or kill anyone conducting criminal activities.

The isotopic content of fissile materials can be used as a barrier against weapons proliferation. Isotopic impurities in weapons material will require a more complex weapon design, complications with material fabrication and handling, and/or enrichment [50]. These isotopes are effective when they alter the following attributes of the fissile material so that it is no longer an attractive option for weapons production:

- critical mass exceeding 800 kg is considered impractical for explosives,
- heat generation rate,
- spontaneous neutron generation, and
- radiation, especially gamma [50].

The most straightforward way to increase proliferation resistance of spent fuel is to increase the Pu-238 content. According to the International Atomic Energy Agency (IAEA), plutonium containing 80% Pu-238 content is exempt from safeguard. However, it was shown that even a 12% Pu-238 content is sufficient to deter proliferation activity [51]. As discussed in the previous section Pu-238 is not easy to produce. Another option is to also increase the content of the even-numbered Pu isotopes (238, 240, and 242). These isotopes have high decay heat and high emission rate of spontaneous fission neutrons, which serves as a proliferation deterrent. A study by Peryoga doped conventional LWR fuel with 1% Np or minor actinide. After the fuel is burnt, the Pu mixture would have a higher percentage of even numbered Pu isotopes. While the decay heat of the spent fuel is almost entirely due to Pu-238, the resulting Pu mixture is equivalent to having a 12% Pu-238 content (in terms of both specific decay heat and rate of spontaneous neutron emission) [51].

Nuclear Medicine: Diagnostic and Treatment

Many radioisotopes have important medical applications, especially in the diagnosis and treatment of cancer. For example, Y-90 is used to treat lymphoma, I-131 is used to treat thyroid cancer, and Cs-137 is used for brachytherapy and external radiotherapy.

Perhaps the most widely used radioisotope for diagnostic studies is Tc-99m [42], because of its half life, the gamma ray energy emitted, and its ability to bind to biologically active molecules [41]. Often in diagnostic tests radioisotopes are introduced into the human body, and a short biological and radioactive half life is desirable. Tc-99m has a half life of 6.01 hours, and is almost completely decayed in 24 hours. This isotope emits 140 keV gamma rays that are easily detectable by medical equipment. This isotope

is very effective for functional studies and is the basis for 31 radiopharmaceuticals used for the study of the brain, myocardium, liver, thyroid, lungs, gallbladder, kidneys, skeleton, blood, bone, spleen, and tumors [42, 52]. It can be incorporated into a monoclonal antibody, an immune system protein that binds to cancer cells, thereby helping to find tumors. When combined with other minerals Tc-99m can be used for imaging of organs and functional systems. For example, when combined with tin it attaches to red blood cells, mapping circulatory system disorders. Together with a phosphate ion, it can be used to gauge the damage of a heart attack to the heart, and its sulfur colloid is used for imaging the structure of the spleen.

Strontium isotopes are useful radiopharmaceuticals because strontium mimics calcium in the human body. Thus, it is ideal for the treatment of bone disorders. Radioisotopes of Sr are beta emitters that can deposit large amounts of localized energy. Sr-89 and Sr-90 emit a 1.495 MeV and a 0.546 MeV beta particle, respectively. Sr-89 is used for bone pain secondary to metastatic prostate cancer and for the treatment of bone cancer, osteogenesis, and osteoporosis (in Europe) [48]. Sr-90 is used to treat cancer, especially in superficial radio-therapy due to its longer half life and beta energy [48].

Spectral Influence On Transmutation

Waste from nuclear fuel contains fission fragments and actinides that have long half lives on the order of hundreds of thousands to millions of years. Transmutation of nuclear waste converts these to more stable materials that decay within a few hundred years. The goal of the current research is to find effective ways to burn and transmute actinides and fission products. The transmutation process is intimately related to the neutron spectrum and flux. Thus, knowledge of the effect of the neutron characteristics on transmutation efficiency is essential for the success of this research.

The consensus among transmutation researchers is that the key requirement for successful transmutation is the availability of a high neutron flux [16, 53]. Feasible condition for transmutation is a neutron flux on the order of $10^{15} \text{ cm}^{-2}\text{s}^{-1}$ [53]. However, the effect of the neutron spectrum on actinide burning and transmutation is complex and isotope dependent.

A general actinide inventory study in Gaseous Core Reactors was conducted by Norring. In Norring's research cores of three pressures 143.85, 119.32, and 26.5 bars were compared. The low pressure core with a thermal spectrum had the lowest total actinide inventory, as well as lowest inventory of isotopes with long half lives. This is due to the initial lack of production of actinides from the uranium. However, in this low pressure core specific isotopes are present in greater concentration (e.g. U-237, Cm-246, Cm-247, and Cm-248). Once actinides are produced, a harder spectrum is favorable to deplete them. Although the high-pressure core (with the hardest spectrum) is better at depleting actinides, the low-pressure core produces less [54].

The unexpected results from Norring's research may, in part, be due to the use of low enriched uranium (less than 6 w/o). The use of LEU causes an undesirable buildup of additional actinides [16] and plutonium. The Pu is advantageous from the fuel efficiency standpoint, but poses proliferation concerns.

Proliferation resistance requires minimal reprocessing during transmutation, deep burnup of the fissionable material, especially plutonium, and no fissile material breeding [55]. Because the fuel in GCR is a gas, reprocessing is not required. Additionally, all fissile plutonium (Pu-239 and Pu-241) can be destroyed in a thermal system because both capture and fission cross sections for thermal neutrons are an order of magnitude larger

than in a hard neutron spectrum where the average thermal neutron energy is greater than 1 eV [55]. Thus, to be completely proliferation resistant, the current research will investigate the use of uranium enriched up to 20 w/o to minimize both fissile material breeding and actinide buildup.

In terms of improving proliferation resistance, isotopes with high specific heat are desirable. One example of this is Pu-238. Another isotope with high specific heat is the minor actinide Cm-244 at 2.8 W/g. Curium isotopes have high emission of spontaneous fission neutrons [44]. Cm-245 is a more fissile than U-235 and Pu-239; its thermal cross sections for fission is 2,001 b, its cross section for capture is 346.4 b, with an average of 3.82 neutrons per fission [44], and a fission-to-capture ratio of 5.78. However, the delayed neutron fraction is 1.5 times less than that of Pu-239 [44].

For minor actinides the fission cross sections in the fast region are smaller than in the thermal region; however, fission-to-capture ratios are higher in the fast region [55]. A study by Baxter on Gas Cooled Reactors concludes that even though minor actinides are hard to fission at any energy level due to their low cross section, their destruction can be better in fast reactors than in thermal reactors, especially if a high neutron flux is provided. Fast neutrons are particularly effective in burning minor actinides such as neptunium and americium [56].

Fission products are generally short-lived. However, technetium and iodine are very-long lived and pose storage problems, especially Tc-99 and I-129. Fortunately they are relatively easy to convert to stable isotopes if there is an adequate supply of available neutrons [55]. Neutron capture in Tc-99 produces Tc-100 which beta decays with a half life of 15.8 s to stable Ru-100 [27]. The capture cross section of Ru-100 is small, and

Ru-101 and Ru-102 are also stable. A similar procedure can be used for I-129. With capture, I-130m (9 min) and I-130 (12.36 h) ends up as stable Xe-130.

A thermal spectrum is effective in reducing the initial buildup of actinides. It is effective in burning fissile plutonium, uranium and Cm-245. A thermal spectrum can also be used to enhance the production of Pu-238, a spiking agent that can be used to fortify the proliferation resistance of fissile Pu. Some ways that the thermal neutron population can be increased in the GCR is to increase moderation of neutrons in the center of the core. This is because thermal neutrons that are reflected into the core have short mean free paths. These neutrons do not have to travel very far from the reflector to cause fission. Thus, at the center of the core there are less thermal neutrons than fast neutrons. For efficient and effective minor actinide transmutation, a hard spectrum (average thermal neutron energy greater than 1 eV), and high neutron flux is needed [16]. Fast neutrons are especially effective in burning minor actinides such as Np and Am, and fission products such as Tc-99 and I-129. Some ways that a hard spectrum can be achieved in the GCR is to use reflector/moderator materials that have a significant capture cross section at thermal energies. This causes absorption hardening of the spectrum.

Important Isotopes

Since there are many isotopes that are produced in a reactor as a result of fission and/or transmutation, analysis of the isotope inventories will be difficult. Keeping in mind the objectives of this research are to minimize waste and improve waste radioactivity characteristics, the list of isotopes that need detailed analysis are based on the following criteria:

- The isotope is long-lived and produced in significant quantities in spent fuel.

- The isotope plays a major role in proliferation characteristics of the waste, including fissile material and those that are proliferation deterrent.
- The isotope has important applications.
- The isotope is a precursor or parent of isotopes that satisfy the above criteria.

It is necessary to realized that even if an isotope has important applications, such as Pu-238 in an RTG, it may not be possible to extract Pu-238 from the gas mixture with current technologies. However, the GCR is the technology of tomorrow. In the future, if and when the GCR becomes a reality, more advanced extraction may exist to allow production of pure Pu-238.

With the four isotope selection criteria in mind, the isotopes of focus are:

- uranium isotopes with mass numbers from 235 to 238
- neptunium-237
- plutonium isotopes with mass numbers from 238 to 242
- americium isotopes with mass numbers from 241 to 243
- curium isotopes with mass numbers from 242 to 248
- iodine-129
- cesium-135

The production and destruction patterns of these isotopes will be analyzed throughout the GCR fuel cycle.

CHAPTER 4 SPECTRUM DESIGN

The main objective of this research is to obtain a relationship between the neutron spectrum and the isotope-specific actinide inventory in the gaseous fuel mixture of Gaseous Core Reactors (GCR). To accomplish this task it is essential to study GCR designs with a wide range of neutronic spectra. Reactor designs that yield cores with most of the neutron population in a specific energy range are desired. Ideally, one can obtain reactors with neutron spectra that are thermal, epithermal, and fast. These regions do not have a standardized definition of their energy range. In general, energy ranges are defined as follows:

- thermal region: less than 2 eV
- epithermal region: 2 eV - 100 keV
- fast region: greater than 100 keV

There are various reactor parameters that could be changed to obtain the desired neutron spectrum. The effect of each parameter on the neutron spectrum is analyzed and presented in this section. Due to the scoping nature of these studies, the results may not have attained statistical significance. These studies are primarily used to develop a better understanding of the general behavior of GCR spectrum due to changes in reactor parameters. The trends are later used to obtain the desired spectra.

Additionally, the data obtained from sensitivity studies are default data presented in the MCNP5 output. The percentage of fissions caused by neutrons in three energy ranges will be used in the sensitivity studies. The energy ranges in these scoping studies are not the same as

what is previously defined as thermal, epithermal, and fast energy ranges. However, this data could provide insight to trends for some neutronic properties. These energy ranges are:

- less than 0.625 eV,
- 0.625 eV to 100 KeV, and
- greater than 100 KeV.

Note that a thermal energy limit of 0.625 eV is quite low for a GCR. A more appropriate upper energy limit is 2 eV. Because scoping studies are only used to determine behavioral patterns for selected neutronic parameters, the default percent fission breakout data will be used.

The data presented in graphical form in the following sensitivity studies is presented in tabular form in Appendix A. Due to the large amount of data in the cross section plots these are not included in Appendix A. However, cross section data can be obtained from the ENDF/B-VI database maintained by Brookhaven National Laboratory.

Reflector Material

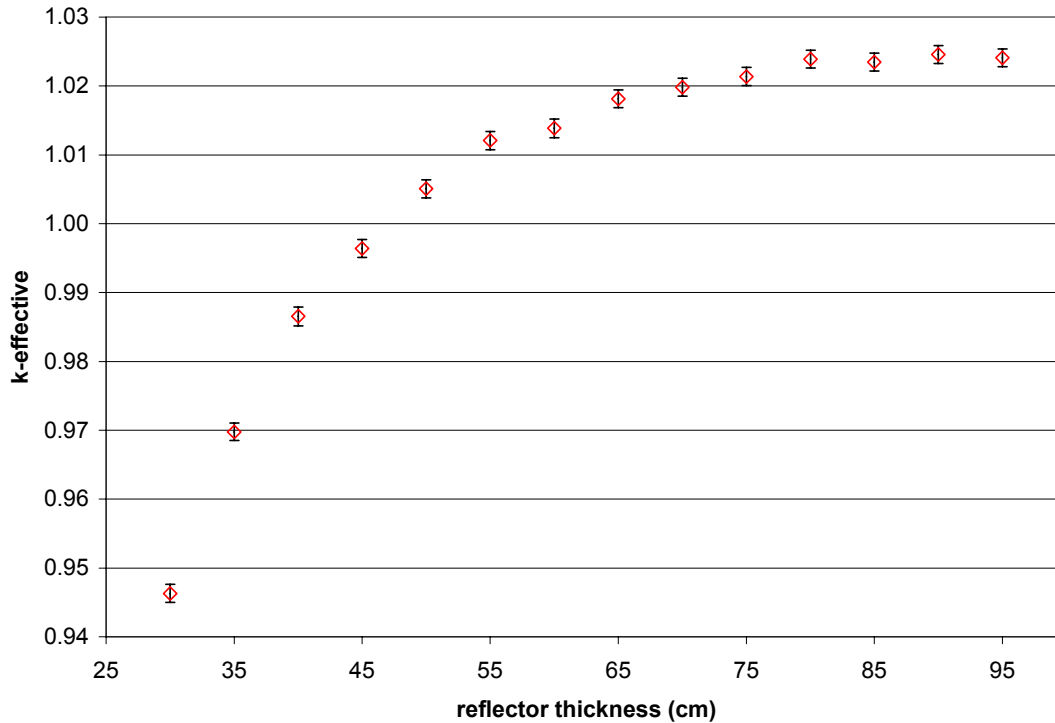
To compare the effectiveness of different materials as reflector/moderator materials, results of analysis for all cases are tabulated and discussed. The effects of the reflector thickness and temperature on the neutron spectrum are presented in the following sections.

Reflector Savings Saturation Thickness

To determine the criticality savings due to the presence of different reflector materials, the reflector thickness is varied and saturation curves are obtained for all materials. The reactors are square cylinders. The dimensions of the core vary in order to yield designs with a k-effective close to 1.0 for the various reflector thicknesses. Saturation curves with error bars are shown in Figure 4-1. Table 4-1 lists the saturation thickness for each material.

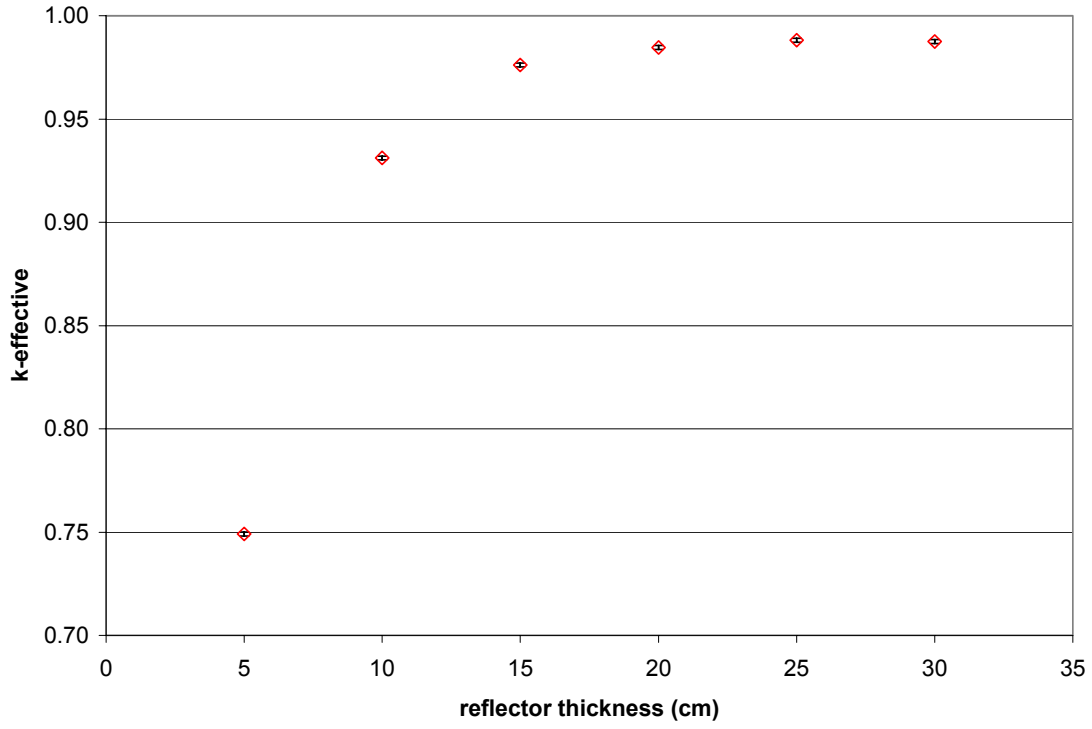
Notice that the plots in Figure 4-1 show the change in k-effective as a function of the change

in reflector thickness. The saturation thickness is the approximate thickness where the k -effective reaches its asymptotic value. The saturation thickness is a rough estimate of the reflector thickness where increases in the reflector thickness yields decreasingly small increases in k -effective, and thus no longer advantageous for further increases.

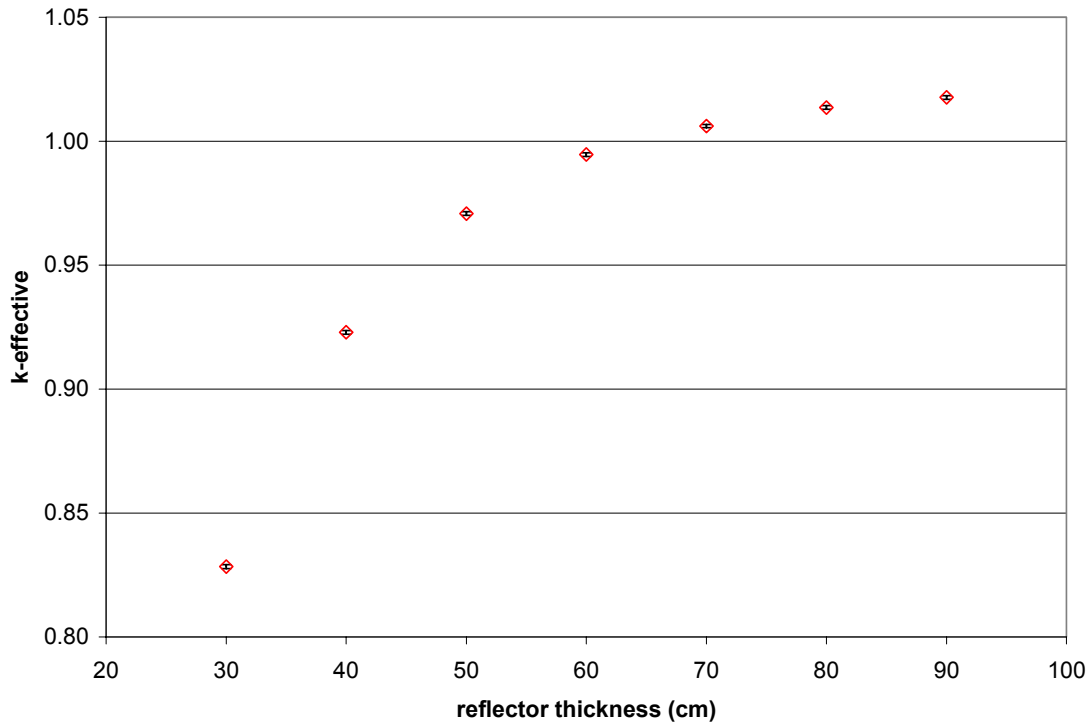


A

Figure 4-1. Saturation curves for (A) beryllium oxide, (B) lithium-7 hydride, (C) lithium-7 deuteride (D) graphite, (E) tungsten, (F) zirconium carbide, (G) lead.

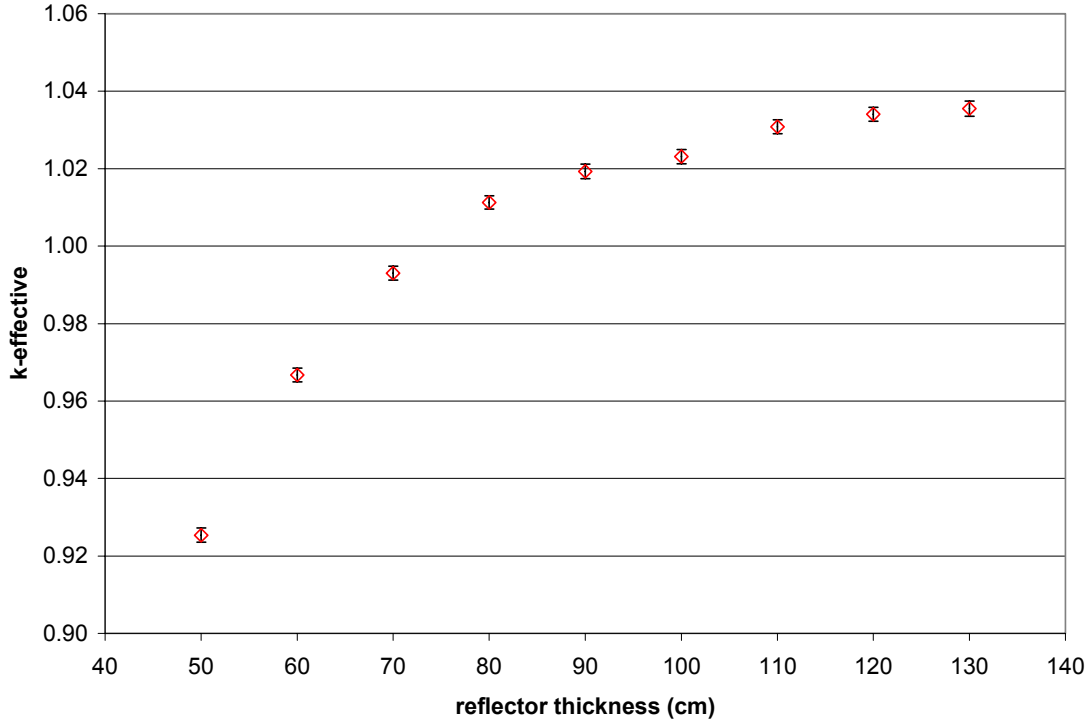


B

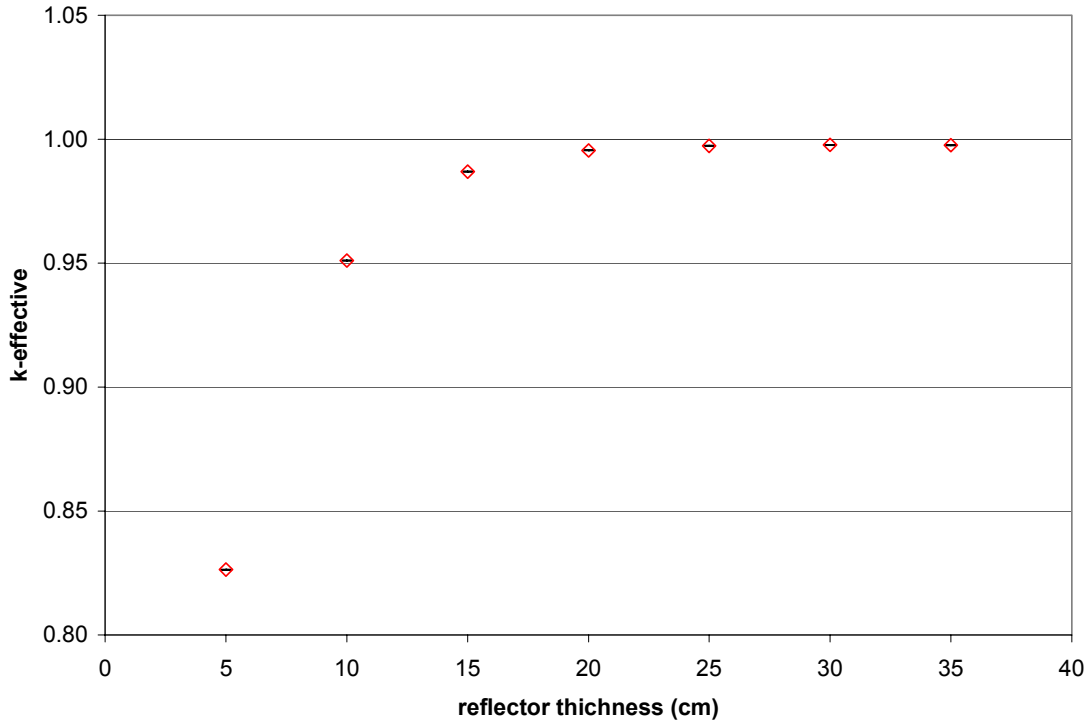


C

Figure 4-1. Continued.

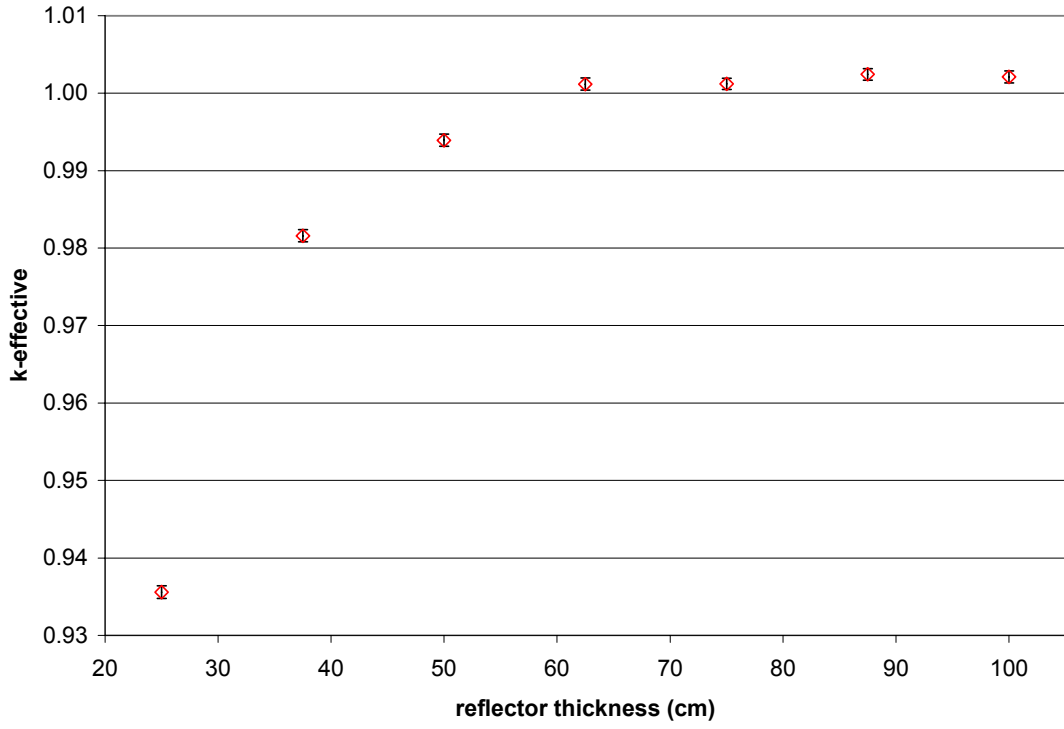


D

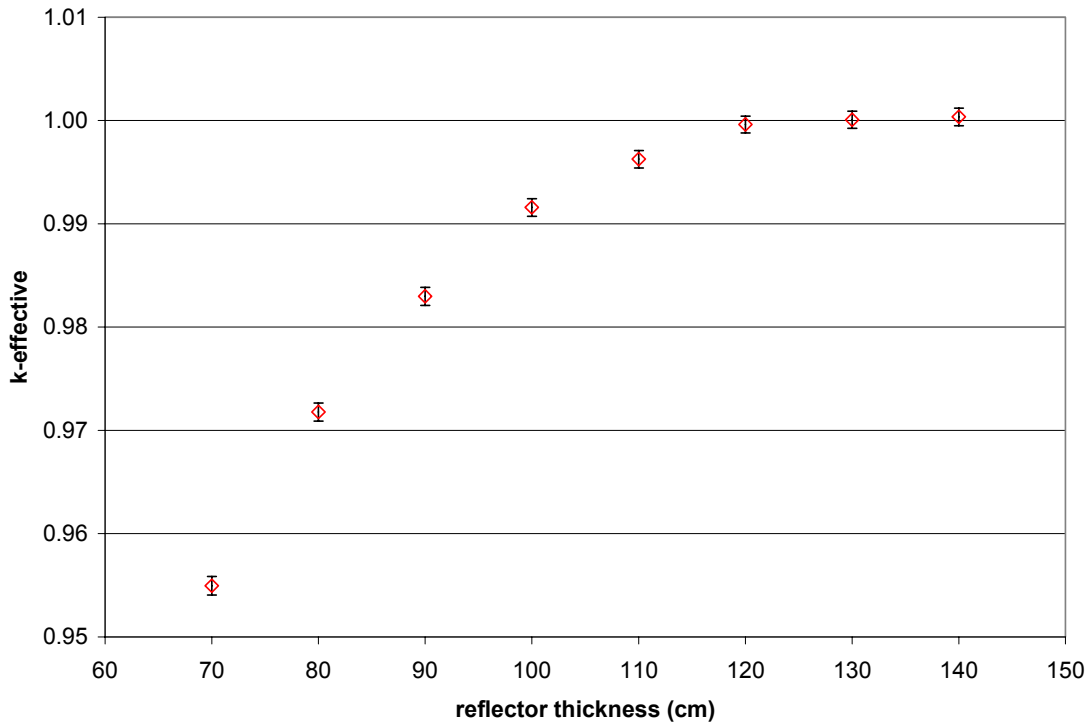


E

Figure 4-1. Continued.



F



G

Figure 4-1. Continued.

Table 4-1. Summary of the reflector thickness study and corresponding reflector saturation thicknesses. All results were obtained using a gas pressure of 155 bars and enrichment of 19.95 w/o.

material	reflector temperature (K)	core diameter (cm)	saturation thickness (cm)
BeO	1,500	44.814	80.0
^7LiH	750	856.778	20.0
^7LiD	750	150.000	80.0
graphite	1,500	59.221	110.0
W*	1500	450.555	20.0
ZrC	1,500	957.923	62.5
Pb	600	673.593	130.0

* A fuel enrichment of 95 w/o was used.

Results presented in Table 4-1 were obtained using a gaseous fuel temperature and pressure of 2,000 K and 155 bars, respectively. For all reflector materials investigated, a fuel enrichment of 19.95 w/o is sufficient for obtaining critical configurations, except for tungsten. Due to high neutron absorption cross section, a tungsten reflected GCR requires the use of high enriched uranium (~ 95 w/o) to achieve criticality. Even with this high enrichment, the core diameter is relatively large. Thus, there will be no further analysis of tungsten as a reflector material, and depletion analysis will not be performed.

Note that 600 K is the melting point of Pb. In practice the reflector would be operating safely below its melting temperature. However, a higher reflector temperature is expected to increase resonance absorptions and hence harden the spectrum. Thus, the reflector temperature is chosen at the highest temperature that Pb remains a solid. Recall that one of the assumptions listed in Chapter 2 is that the reflector can be cooled to any temperature. While the actual operating temperature of the Pb reflector will be lower than 600 K, this is done to get the hardest spectrum possible.

In an attempt to decrease the critical volume of ^7LiH , reflector saturation curves for ^7LiD is obtained. The fuel volume necessary for a critical configuration using ^7LiD is two

orders of magnitude less than the critical volume of ${}^7\text{LiH}$. This is mainly due to the decrease in the neutron capture cross section when hydrogen is replaced with deuterium (${}^2\text{H}$). The thermal capture cross section of deuterium is three orders of magnitude smaller than that of hydrogen.

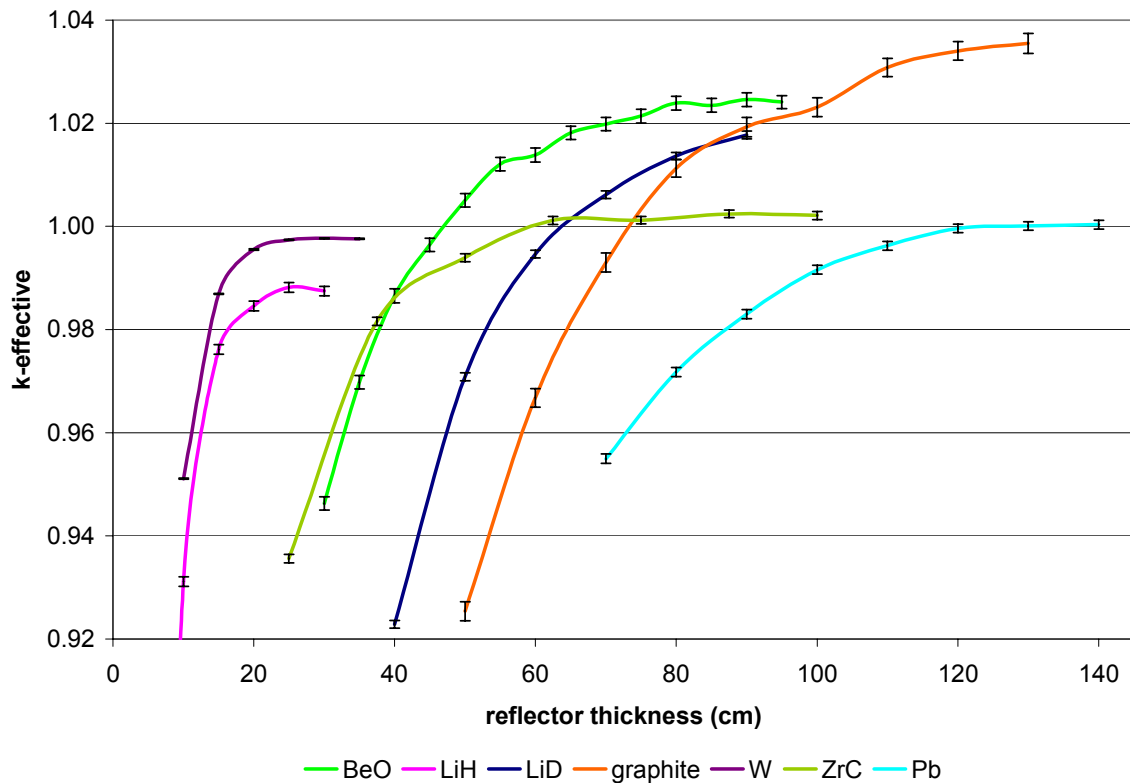


Figure 4-2. Reflector thickness saturation curves for all materials at gas pressure of 155 bars and enrichment of 19.95 w/o, except tungsten is at 95 w/o.

Cross Section Study

The larger fuel volumes necessary to achieve criticality are due to the large capture resonances in a few of the reflector materials. These resonances make it difficult for fission neutrons to thermalize, helping sustain the chain reaction. Moreover, fast neutrons have two competing events. These neutrons may be absorbed (absorption includes primarily capture and fission) or they may leak out of the system. Since fast neutrons have a large mean free path in the core, they have a higher probability of leaking from the system than thermal

neutrons. Hence, a more efficient way to sustain the fission chain is to allow fast neutrons to slow down to thermal energies through elastic collisions with moderator material. Since some of these reflector materials such as W, ZrC and Pb, have high capture resonances, as soon as the neutrons decrease in energy the probability of their removal by capture will increase. This leaves fast neutrons to sustain the chain reaction. Thus, the critical volume of such a system must be increased to compensate for the increased captures by the moderator/reflector and the leakage of fast neutrons.

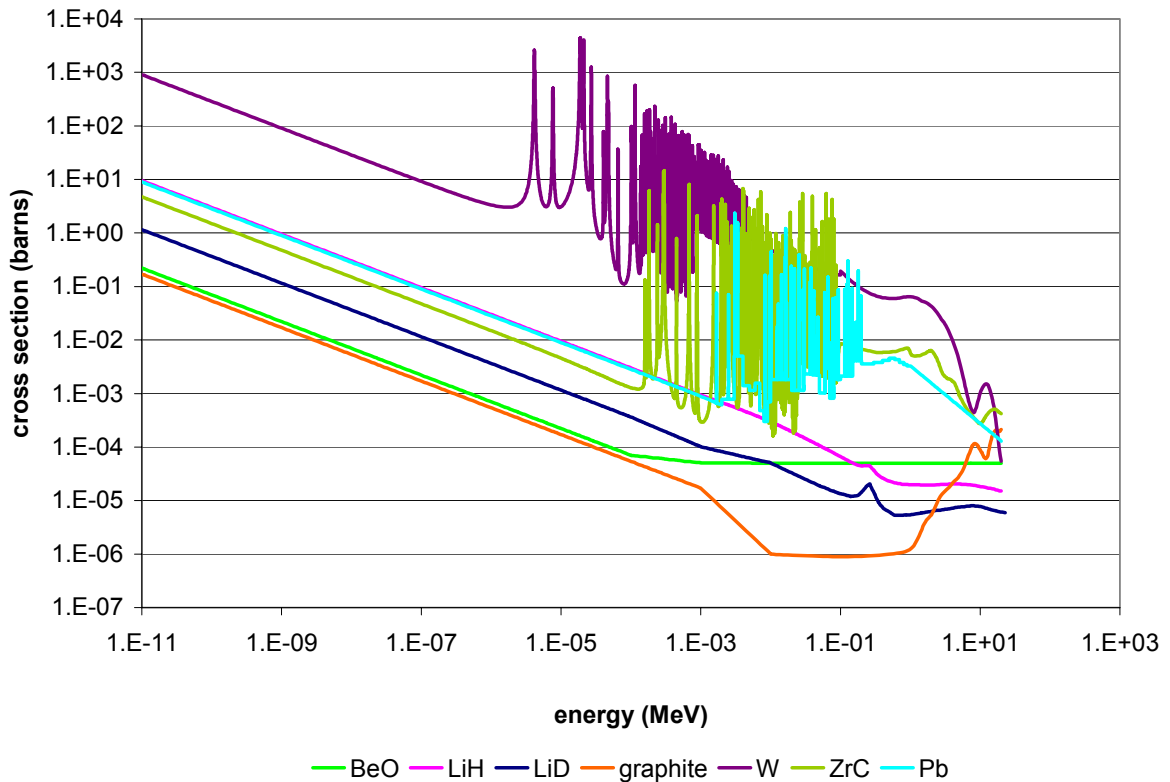


Figure 4-3. Neutron capture cross section plot of reflector materials. All values are at 300 K. Data interpreted from ENDF/B-VI [39].

The critical volumes in Table 4-1 are clearly explained by observing capture cross section plots of all the reflector/moderator materials studied. In Figure 4-3, the materials with the lowest capture cross sections are BeO and graphite. Indeed these materials required the smallest critical volumes. Notice that although BeO does not have the lowest capture

cross section, its critical volume is the lowest among the reflector materials. This is primarily because beryllium has a significant (n,2n) cross section, helping decrease the critical volume below that of graphite.

Tungsten had the highest resonance cross section among all the materials studied. The maximum capture cross section reached as high as 4,407.06 barns at 18.8 eV. This explains why using tungsten as reflector material requires fuel enriched to 95 w/o in order to obtain critical conditions. From this discussion above one can also deduce that a zirconium carbide reflected GCR requires large critical volume since it has very large capture resonances. In fact, ZrC requires a critical volume four orders of magnitude larger than BeO when the gas pressure is at 155 bars and fuel enrichment is 19.95 w/o. Notice the capture cross section of ZrC is lower than ^7LiH below $1\text{E-}4$ MeV. However, preliminary studies show that the neutron population in this energy range for ZrC is less than ^7LiH . This is because once neutrons are in the resonance region of ZrC most are captured and few survive to lower energy ranges. The large resonances in ZrC are the primary reason why it has the largest critical volume after tungsten.

Notice that ^7LiH has lower capture cross section than Pb for energies greater than a few KeV as shown in Figure 4-3. However, the critical volume of Pb is smaller than the critical volume required for ^7LiH . Another factor that contributes to the effectiveness of a moderator is its scattering cross section. Those with low capture cross section and high scattering cross section are more effective in moderating neutrons, making effective moderators and reflectors. To determine what other factors could affect the effectiveness of a reflector/moderator, the ratio between capture and total cross sections is plotted for all materials in Figure 4-4. In general, a higher capture-to-total cross section ratio means a less

effective reflector/moderator. Lead generally has a higher capture-to-total neutron cross section ratio than ${}^7\text{LiH}$, and this ratio is the same as for ${}^7\text{LiH}$ between tenths of an eV to keV. Thus, the effectiveness of a reflector/moderator must depend on another characteristic of the material.

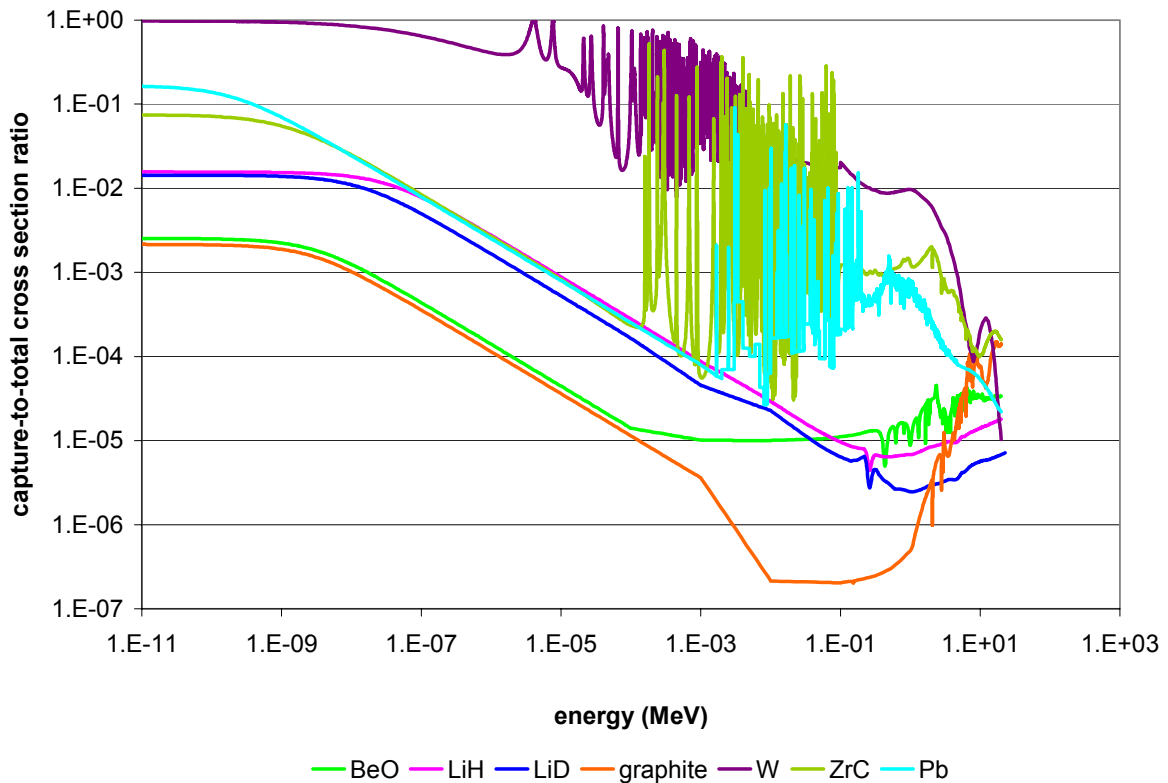


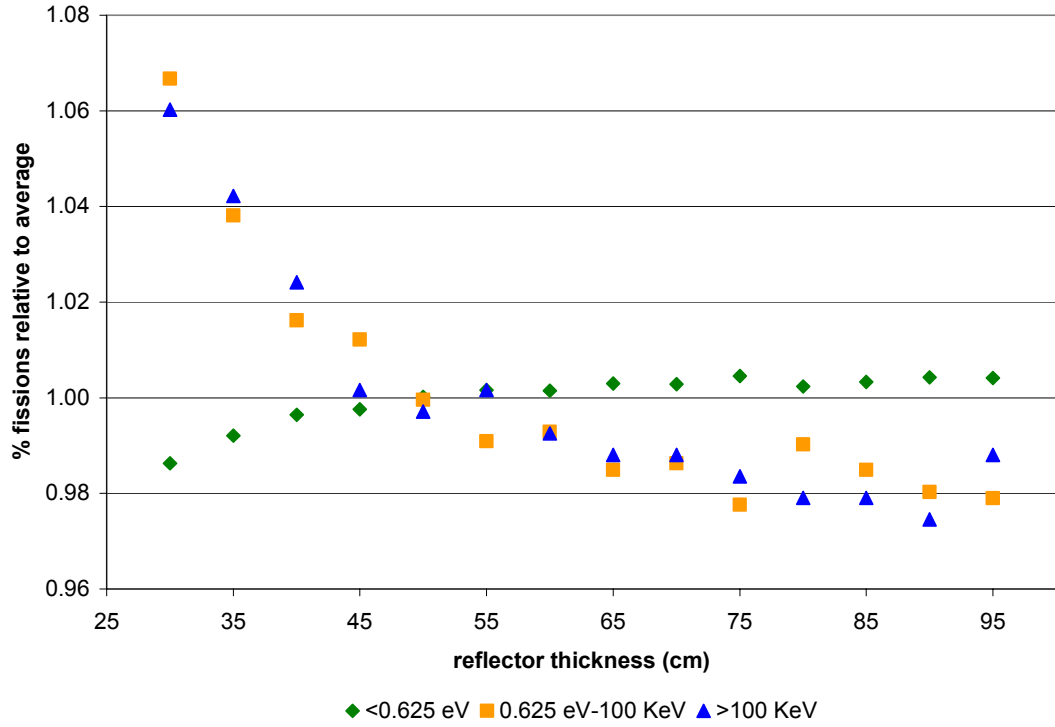
Figure 4-4. Ratio of capture to total cross sections for all reflector/moderator materials. All data is at 300 K. Data interpreted from ENDF/B-VI [39].

Another clue for determining what other factor affects the effectiveness of a reflector/moderator material can be found in both Figure 4-3 and Figure 4-4. The cross section plots in both figures for ${}^7\text{LiH}$ and ${}^7\text{Li D}$ show that these two materials are very similar. The capture cross section of ${}^7\text{LiH}$ is at most one order of magnitude higher than ${}^7\text{Li D}$. The capture-to-total ratio of ${}^7\text{LiH}$ is higher than that of ${}^7\text{Li D}$, but extremely similar, and even converging as the energy decreases. As expected, the critical volume for ${}^7\text{LiH}$ is higher than that of ${}^7\text{Li D}$. However, the critical volume for ${}^7\text{LiH}$ is at least two orders of magnitude

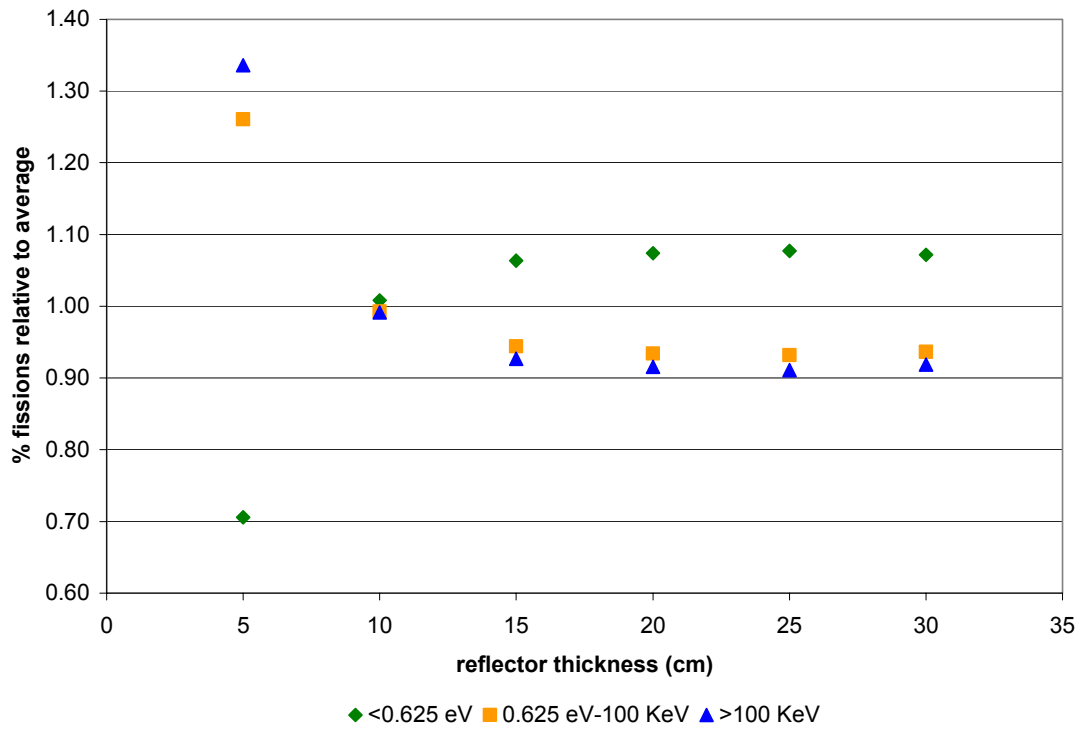
greater than the critical volume for ${}^7\text{Li D}$. This may be because the saturation thickness of ${}^7\text{Li D}$ is 4 times the saturation thickness of ${}^7\text{Li H}$. Neutrons have a better chance to thermalize and be reflected back into the core. Additionally, the thermal spectrum should be softer with the ${}^7\text{LiD}$ than with the ${}^7\text{LiH}$ and this reduces the critical volume. Using this same logic, the saturation thickness of ${}^7\text{Li D}$ is 61% of the saturation thickness of Pb. Thus, the decreased neutron leakage in Pb results in a smaller critical volume than when ${}^7\text{Li D}$ is used.

Reflector Thickness

Following the choice of reflector material, the reflector thickness is one of the important factors in determining the neutron spectrum of the reactor. However, if the thickness being used is the saturation thickness, then the most important factor is the reflector material neutronic characteristics. To determine the effect of the reflector thickness on the percent fission by energy region of the core, the reactor design and operating conditions for the saturation thickness study are used. For scoping calculations, three neutron energy ranges are used: (1) less than 0.625 eV, (2) between 0.625 eV and 100 KeV, and (3) greater than 100 KeV. The percentage of fissions caused by neutrons in these three energy ranges is determined for all configurations presented in the saturation thickness study. For comparison purposes, the results for each energy range are normalized to the average value in that range and presented in Figure 4-5 with the averages in Table 4-2. Absolute values are presented in tabular form in Appendix A.

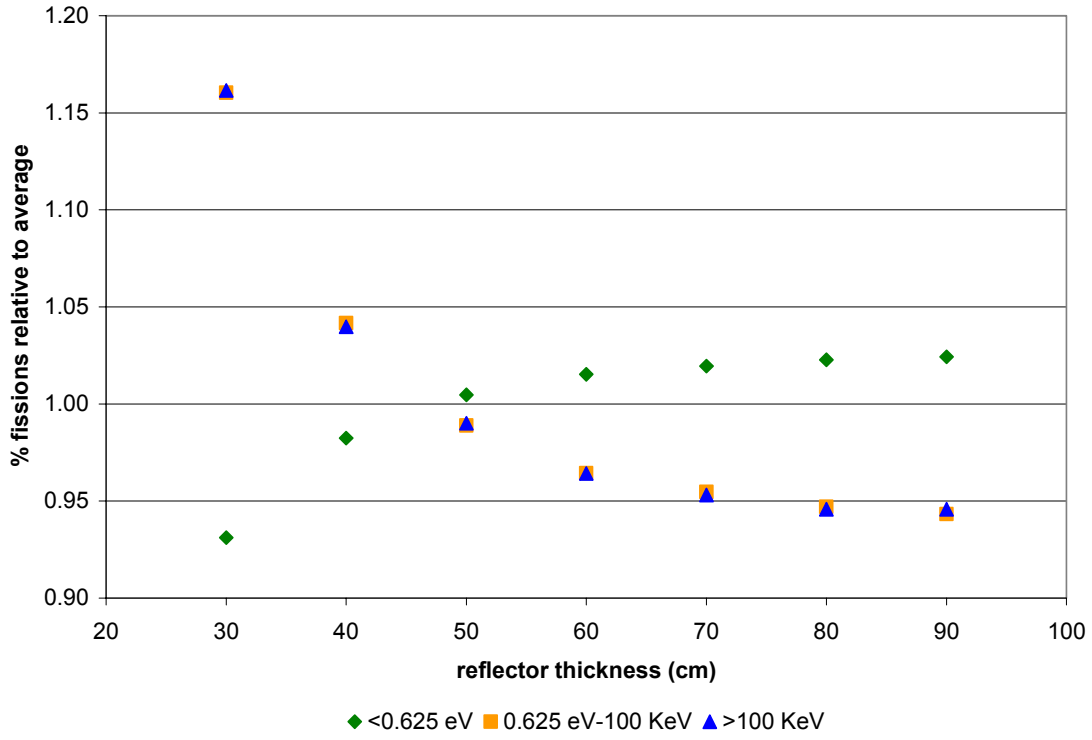


A

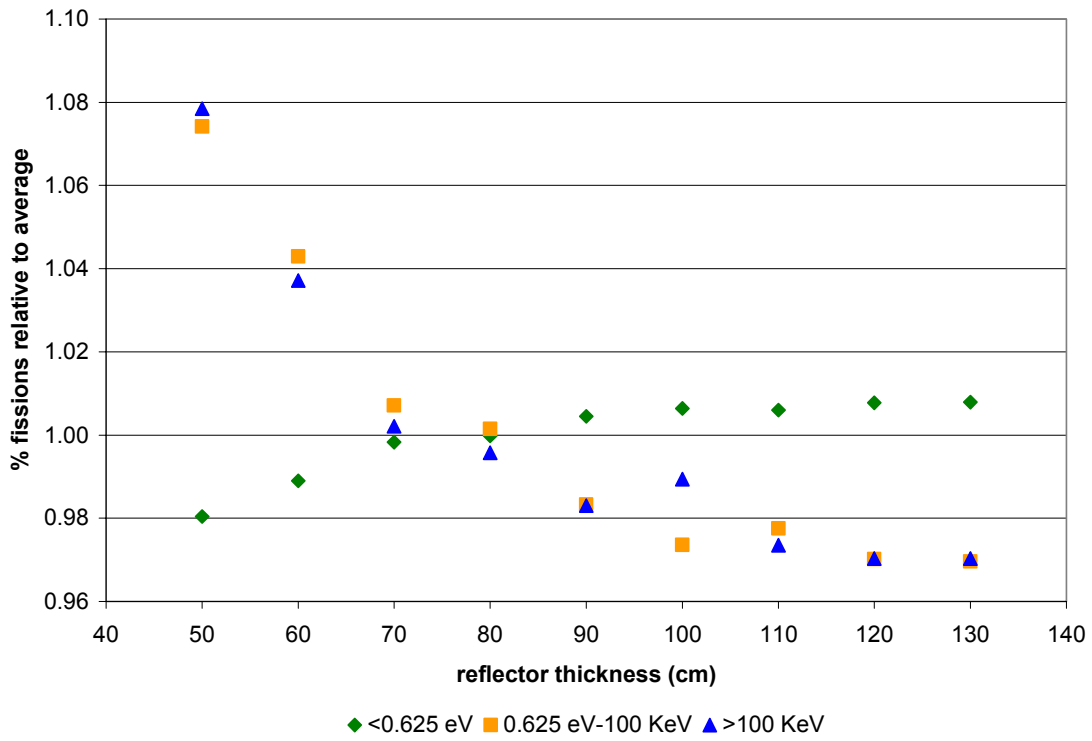


B

Figure 4-5. Percentage of fissions induced by neutrons in three energy ranges for (A) beryllium oxide, (B) lithium-7 hydride, (C) lithium-7 deuteride, (D) graphite, (E) tungsten, (F) zirconium carbide, and (G) lead reflected GCRs.

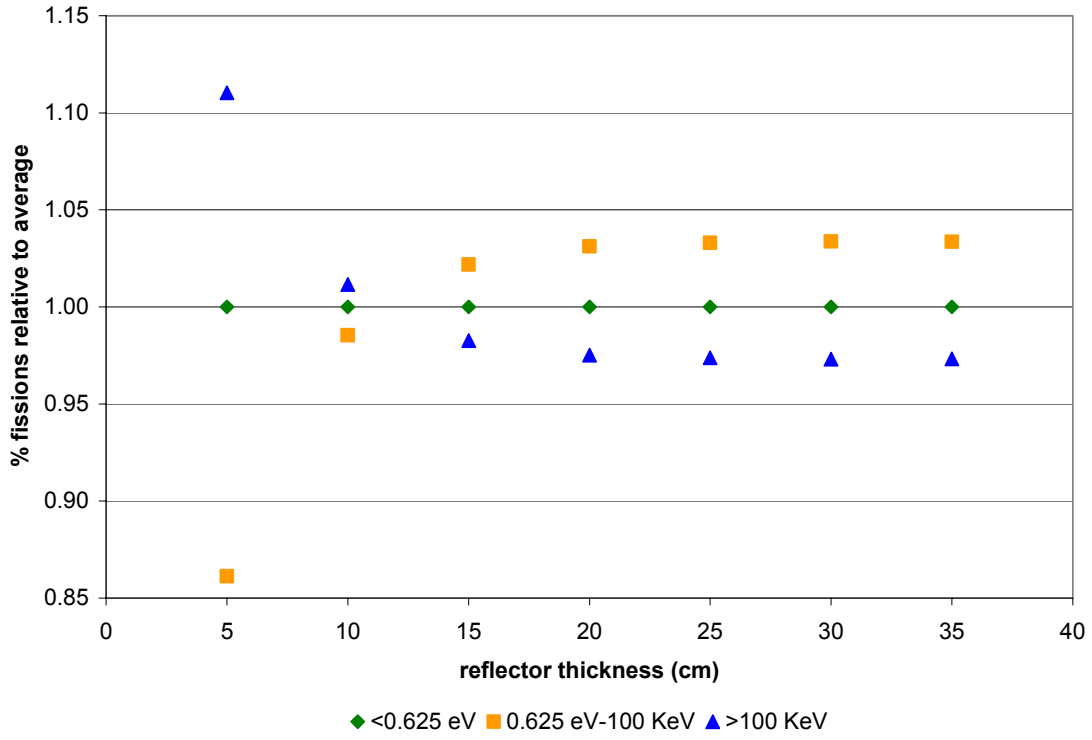


C

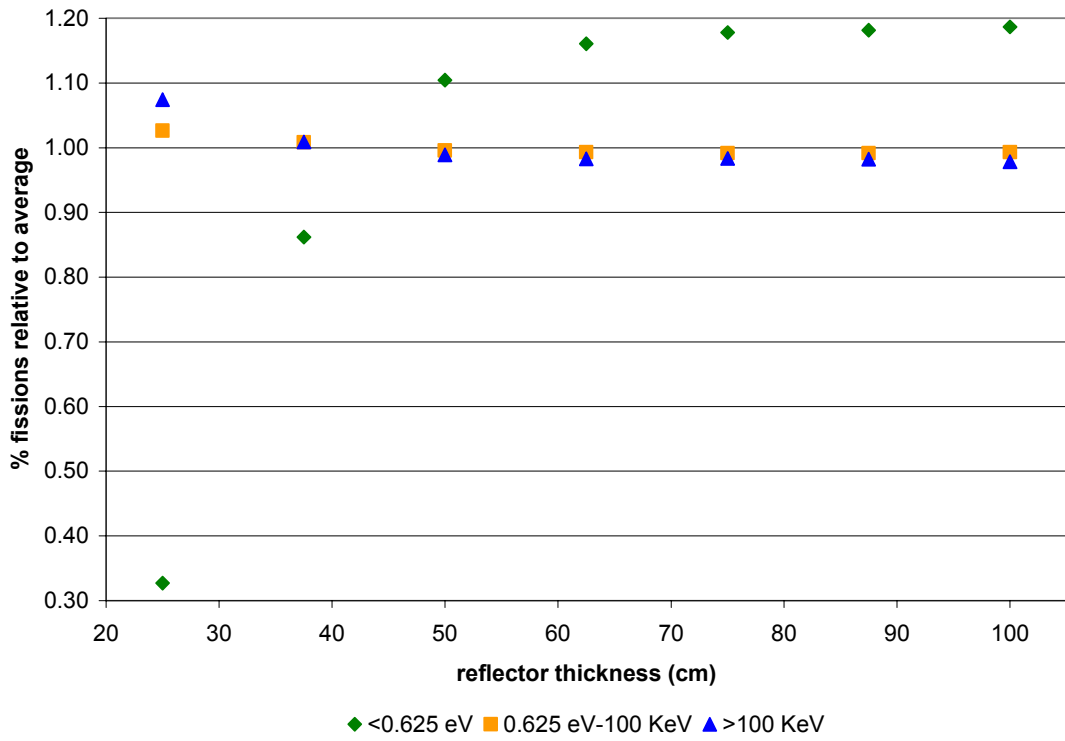


D

Figure 4-5. Continued.

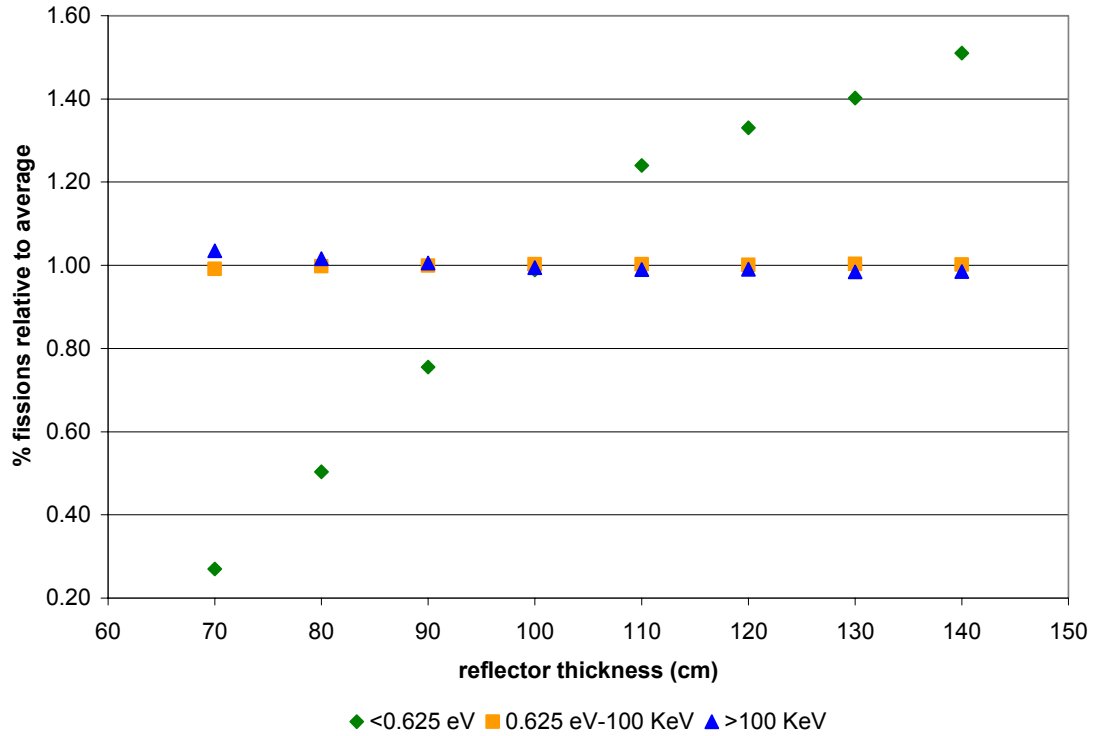


E



F

Figure 4-5. Continued.



G

Figure 4-5. Continued.

Table 4-2. Average percentage of fissions caused by neutrons in three energy ranges with gas pressure at 155 bars and enrichment at 19.95 w/o (except tungsten at 95 w/o). These are used to normalize data presented in Figure 4-5.

material	average % fissions caused by neutrons in this energy range		
	<0.625 eV	0.625 eV-100 KeV	>100 KeV
BeO	82.7364	15.0464	2.2164
⁷ LiH	49.6133	30.8050	19.5800
⁷ LiD	69.9657	24.6057	5.4243
graphite	79.2544	17.6044	3.1433
W	0.0000	44.3157	55.6843
ZrC	5.7214	65.9786	28.3000
Pb	0.5563	71.0450	28.3988

Figure 4-5 shows that the percent fission by energy region in the core is strongly dependant on the reflector thickness, for all reflectors involved. However, the primary determining factor is the moderating/reflector material. For true moderator materials, the moderator/reflector temperature is also very important. In most cases, the percentage of fissions caused by neutrons in the first energy range (< 0.625 eV) increases as the reflector

thickness increases. This is because increase in reflector thickness increases the number of mean free paths that the neutrons need to travel in order to exit the reflector. This increases the number of interactions the neutrons experience and thus increases the number of scatterings. Thus, more neutrons are thermalized and reflected back into the core resulting in more fission reactions. Similar to the effect of the reflector thickness on k-effective, the percentage of fissions caused by neutrons in the three energy ranges eventually reaches a point where further increase in reflector thickness results in small changes in these values. As far as increasing the thermal neutron population in the core, it is limited by reflector material and thickness. For each reflector material there is an upper limit to the relative number of thermal neutrons to neutrons with higher energies. At saturation thickness, the thermal neutron population is at its maximum.

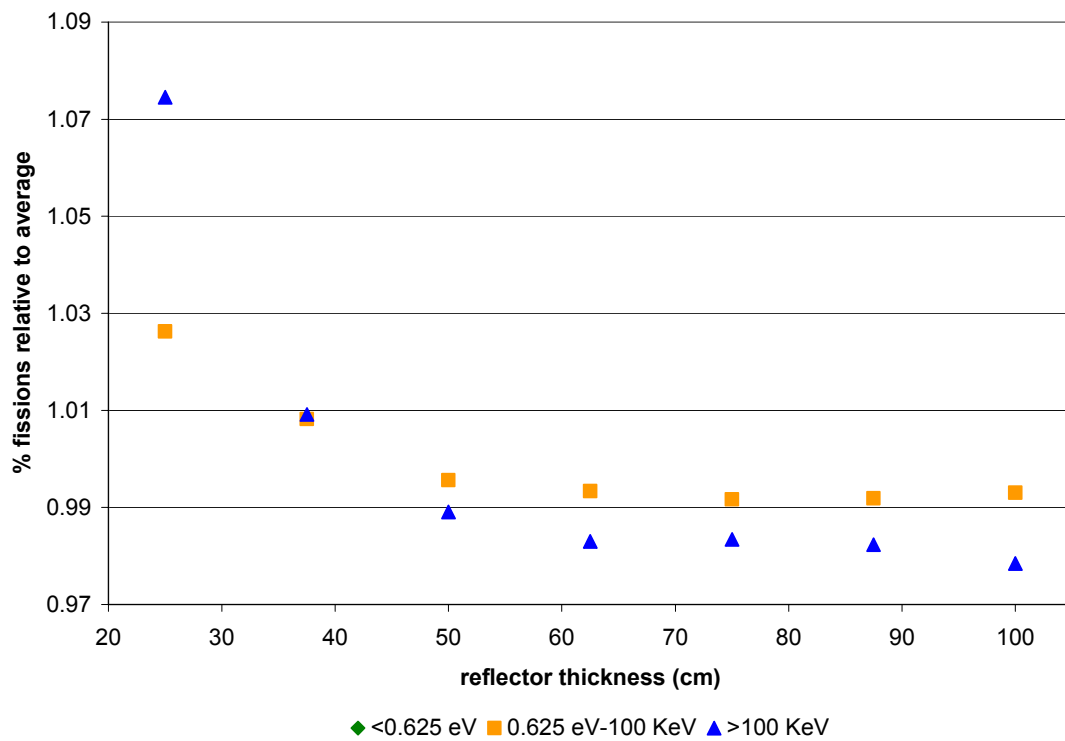
Table 4-3. The percentage of fissions caused by neutrons in three energy ranges with reflector thickness at saturation, gas pressure at 155 bars, and enrichment of 19.95 w/o (except tungsten at 95 w/o).

material	% fissions caused by nts in enrg range at saturation thickness		
	<0.625 eV	0.625 eV-100 KeV	>100 KeV
BeO	82.93	14.90	2.17
⁷ LiH	53.28	28.78	17.93
⁷ LiD	71.56	23.30	5.13
graphite	79.73	17.21	3.06
W	0.00	45.70	54.30
ZrC	6.64	65.54	27.82
Pb	0.78	71.28	27.95

Table 4-3 shows that in a BeO reflected system, the majority of the fissions occur in the thermal energy region (first energy range). The majority of the fissions in a Pb reflected system occur in the epithermal energy range (second energy range), and most of the fissions in a W reflected system occur in the fast energy range. Note that thermal neutrons have no significant presence and do not cause any fission in the W reflected GCR system. The capture cross section for natural tungsten is so large that as soon as the neutrons loose energy

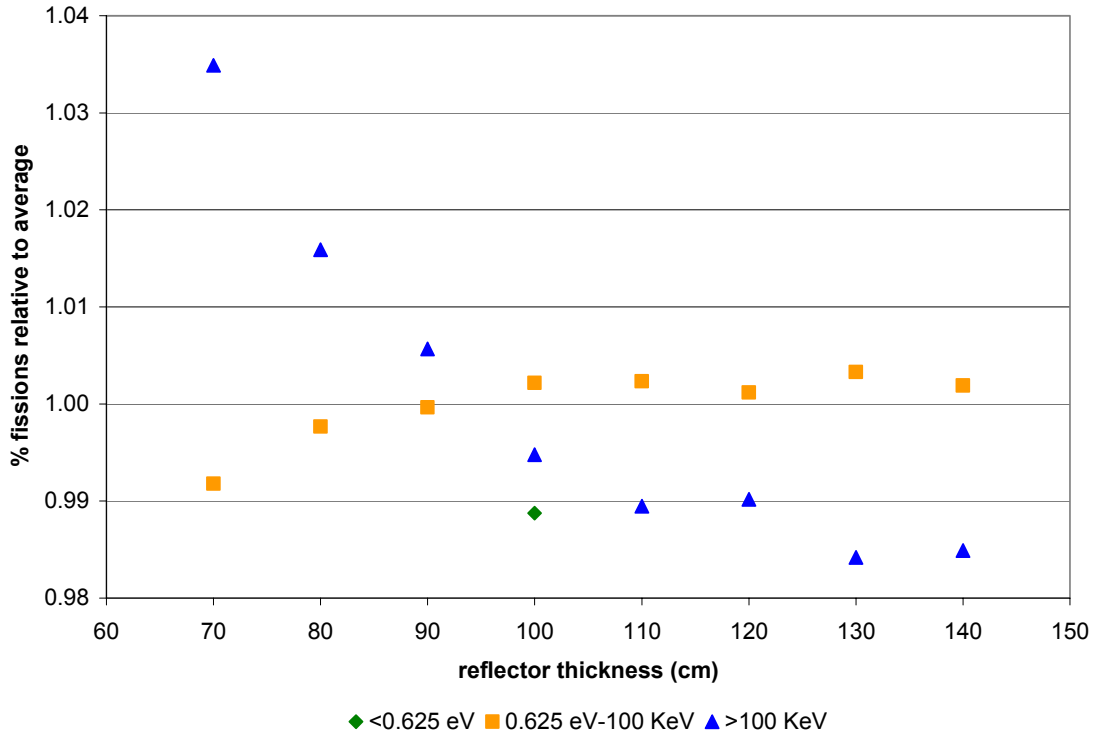
they are absorbed by the reflector material. In fact, capture is almost the only mode of neutron interaction towards low energies as shown in Figure 4-4 where the capture-to-total ratio approaches unity towards lower energies.

Although Figure 4-5 shows that for the energy ranges of 0.625 eV-100 KeV and greater than 100 KeV the plots for ZrC and Pb reflected reactors seem to follow a linear trend, this is only a matter of scale. For these energy ranges, these two materials follow trends similar to other reflector materials. All materials are similar in that the percentage of fissions caused by neutrons in different energy ranges asymptotically reaches a fixed distribution as the reflector approaches its saturation thickness.



A

Figure 4-6. Percentage of fissions caused by neutrons in energy ranges: 0.625 eV-100 KeV, and > 100 KeV. The reflector is at saturation thickness, gas pressure is at 155 bars, with enrichment of 19.95 w/o for (A) zirconium carbide and (B) lead.



B

Figure 4-6. Continued.

Each material naturally produces a spectrum with the majority of neutrons in one of the three energy ranges. The energy range that naturally dominates the neutron population reaches its saturation point before the reflector savings provided by the reflector saturates. This can be observed, for example, in the systems where the majority of the fissions are caused by neutrons with energies less than 0.625 eV, such as systems with BeO, ${}^7\text{LiH}$, ${}^7\text{LiD}$, and graphite reflectors. Recall from Table 4-1 that the reflector savings for these materials saturate at 80, 20, 80 and 110 cm respectively. Figure 4-5 shows that the percentage of fissions caused by neutrons with energy less than 0.625 eV reaches its asymptotic value at approximately 65, 15, 70, and 90 cm for BeO, ${}^7\text{LiH}$, ${}^7\text{LiD}$, and graphite, respectively.

The energy ranges that do not cause the majority of the fissions reach their asymptotic percentage values at approximately the same reflector thickness as the reflector savings

saturation value. This can be observed in . Table 4-2 indicates that for ZrC and Pb reflected systems, neutrons with energies greater than 100 KeV cause the second highest number of fissions. This energy group reaches its asymptotic percentage value at about the same thickness as the reflector savings saturation value of 60.5 and 130 cm for ZrC and Pb.

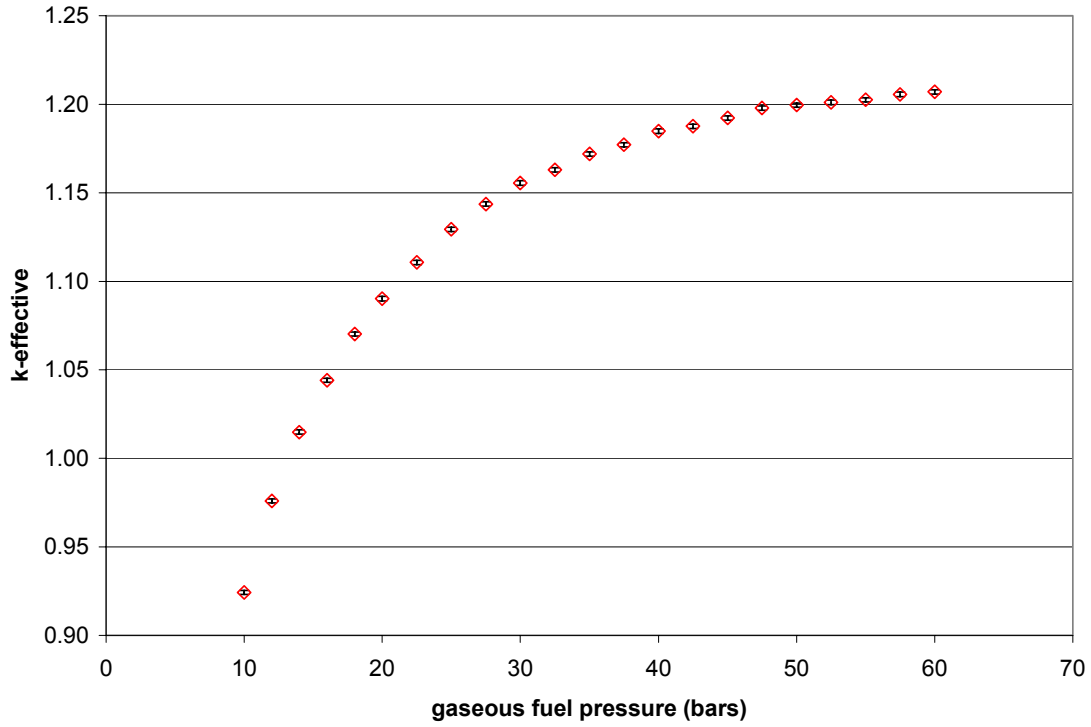
Gaseous Fuel Pressure

As can be observed from the reflector thickness studies, shifts in percentage fission by energy region follow similar trends regardless of the reflector material used. Using a BeO reflected GCR design, the trends observed will be applied to other reflector materials and this knowledge will be used to design the broad range of spectra used in depletion calculations.

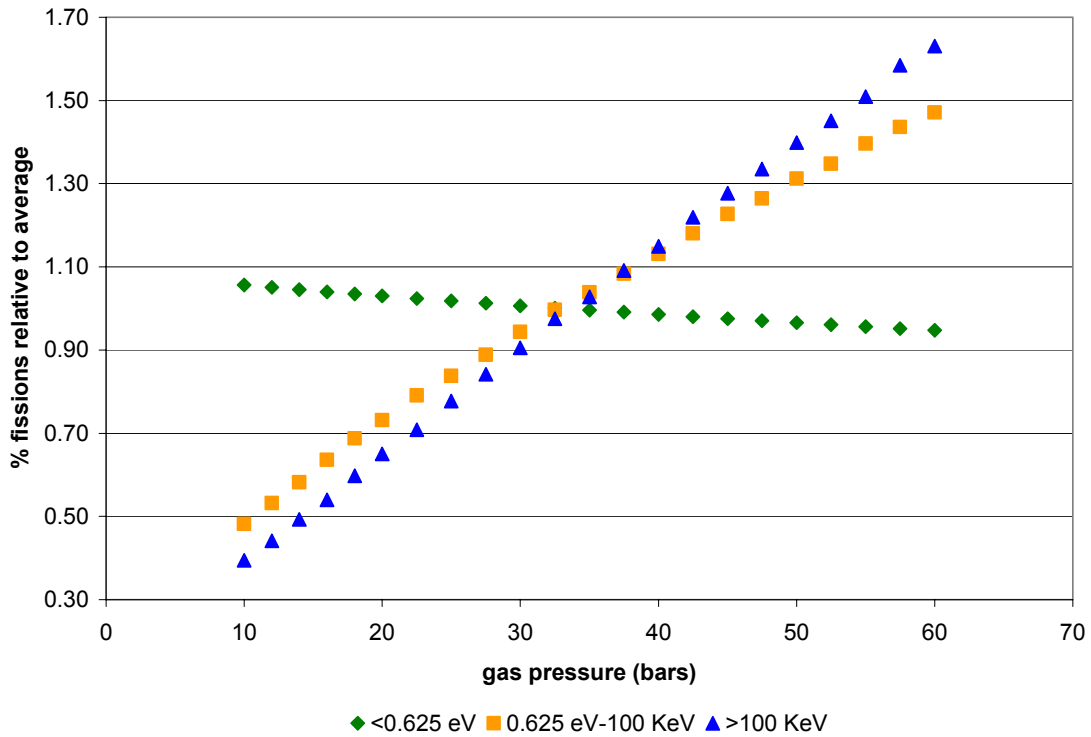
To determine the effect of the gas pressure on the spectral characteristics of the core, a BeO-reflected system is used. Description of the reactor dimensions and other design parameters are presented in Table 4-4. The dimensions used in the reflector savings studies were not used for the gas pressure study. This is because those dimensions would necessitate higher gas pressures to achieve criticality. Recall that a gaseous fuel pressure of 155 bars was used for the reflector savings studies. Since 155 bars is the upper pressure limit for GCRs (based on the operating pressure for PWRs), using the values in Table 4-4 would allow more flexibility in the range of pressure values used in this study.

Table 4-4. Reactor parameters used for gas pressure sensitivity study.

design parameter	value
core diameter (cm)	300
core length (cm)	300
reflector thickness (cm)	80
enrichment (w/o)	5
gas temperature (K)	2,000
reflector temperature (K)	1,500



A



B

Figure 4-7. Gas pressure sensitivity study with BeO reflector. Shown is the effect of gas pressure on (A) k-effective, and (B) percentage of fissions caused by neutrons in three energy groups normalized to the average in each group.

The gas pressure is varied from 10 to 60 bars. With the increase of the gas pressure, the gas density increase. This compresses the fuel particles and essentially decreases the mean free path of neutrons in the fuel, resulting in the increase in the number of fissions. This is observed in Figure 4-7A where k-effective increases with the increase in pressure. Gas pressure reaches a saturation value where further increases in gas pressure yields much smaller increases in the value of k-effective.

The influence of the gas pressure on the percentage fission by energy region is shown in Figure 4-7B. The gas pressure has a linear relationship with the percentage of fissions caused by neutrons in three energy ranges. The percentage of fissions caused by neutrons with energy less than 0.625 eV decreases as the pressure increases. The percentage of fissions caused by neutrons in the other two energy ranges increase with the increase in gas pressure. The neutrons that are thermalized by the reflector/moderator are reflected back into the core. These neutrons have low kinetic energy and their mean free path in the core is relatively small compared to more energetic neutrons that have just been “born” from fission. When the thermal neutrons are reflected back into the core they almost immediately cause fission. On the other hand, more energetic neutrons need to travel a larger distance to experience interactions with the fuel, and sometimes the mean free path is so large that these neutrons do not interact with the fuel before it sees the reflector. Increasing the gas pressure increases the gas density and decreases the mean free path of neutrons in the core. This increases the chances that a more energetic neutron will cause fission. At lower gas density an energetic neutron have such a large mean free path that it would have to travel first to the reflector and lose some of its kinetic energy in order to cause fission. At higher gas density the same energetic neutron would have a shorter mean free path and experience an

interaction with the fuel before it interacts with the reflector. Thus, increase in gas pressure will lead to increase in the percentage of fissions caused by more energetic neutrons.

An increase in the gaseous fuel pressure does not increase the percentage of fissions caused by slower neutrons. This is because slow neutrons are reflected into the core, and they almost immediately cause fissions. Their mean free path in the fuel is so small that neutron interaction with the fuel is guaranteed. Thus, increasing the gas density does not significantly affect the percentage of fissions caused by neutrons in the thermal range. The data presented in Figure 4-7B seems to show a decrease in the percentage fissions caused by neutrons in the thermal region. However, these are relative numbers; if there is an increase in the number of fissions caused by more energetic neutrons (> 0.625 eV), and if the number of fissions caused by slow neutrons (< 0.625 eV) is unchanged, the percentage of fissions caused by slow neutrons will still decrease. Nevertheless, one definite conclusion is that any increase in the gaseous fuel pressure will increase the number of fissions induced by energetic neutrons. Unlike the reflector thickness study, increase in the gaseous fuel pressure does not cause the relative distribution of the percentage of fissions to saturate. Thus, increasing the gaseous fuel pressure will yield a proportional increase in the percentage of the fissions induced by energetic neutrons (>0.625 eV), and a proportional decrease in the percentage of fissions induced by slow neutrons (<0.625 eV). Since the percentage of fissions by energy region does not approach an asymptotic value as the gaseous fuel pressure increases, the gas pressure is an effective design parameter for obtaining the desired spectrum, with an upper limit of 155 bars.

Table 4-5. Percentage increase in the number of fissions caused by neutrons in three energy ranges due to increase in gaseous fuel pressure.

pressure (bars)	% reactivity increase	% increase relative to 10 bars			
		U-235 mass	<0.625 eV	0.625 eV-100 KeV	>100 KeV
10.0	0.0000	0	0.0000	0.0000	0.0000
12.0	5.4391	20	-0.5023	10.3723	11.7647
14.0	9.3409	40	-0.9941	20.7447	25.0000
16.0	12.1721	60	-1.5278	31.9149	36.7647
18.0	14.6337	80	-2.0406	42.5532	51.4706
20.0	16.4648	100	-2.4801	51.5957	64.7059
22.5	18.3182	125	-3.0871	64.0957	79.4118
25.0	19.9689	150	-3.5894	73.6702	97.0588
27.5	21.2138	175	-4.1335	84.3085	113.2353
30.0	22.2325	200	-4.6777	95.7447	129.4118
32.5	22.8661	225	-5.2428	106.6489	147.0588
35.0	23.6207	250	-5.6718	115.4255	160.2941
37.5	24.0589	275	-6.1637	124.7340	176.4706
40.0	24.7045	300	-6.6555	134.5745	191.1765
42.5	24.9336	325	-7.1787	144.6809	208.8235
45.0	25.3190	350	-7.6706	154.5213	223.5294
47.5	25.7824	375	-8.0787	162.2340	238.2353
50.0	25.9145	400	-8.5810	172.0745	254.4118
52.5	26.0398	425	-8.9787	179.5213	267.6471
55.0	26.1650	450	-9.4705	189.6277	282.3529
57.5	26.4082	475	-9.9205	197.8723	301.4706
60.0	26.5279	500	-10.2972	205.0532	313.2353

Shown in Table 4-5, the neutrons with energies greater than 100 KeV is the energy range most sensitive to the increases in pressure among the three energy ranges. With a two bar increase in pressure, from 10 bars to 12 bars, the percentage of fissions caused by neutrons with energy greater than 100 KeV increases by 11.8%. The energy ranges greater than 0.625 eV exhibit noticeable changes as the pressure increases (relative to 10 bars), while the energy range <0.625 eV are relatively insensitive to increases pressure. This is due to increase in the U-235 mass, or density of fissile atoms. The relationship between the percentage of fissions caused by neutrons in all energy ranges and the U-235 mass is linear, similar to that with the gas pressure from Figure 4-7B.

When the gas pressure is not yet saturated, increasing the pressure is an effective way to increase the reactivity in the core. For example, a 2-bar increase in pressure from 10 to 12 bars increases the reactivity by 5.4% $\Delta k/k$. However, when the pressure is saturated, a 2.5-bar increase in pressure from 57.5 to 60 bars only increases the reactivity by 0.12% $\Delta k/k$.

Fuel Enrichment

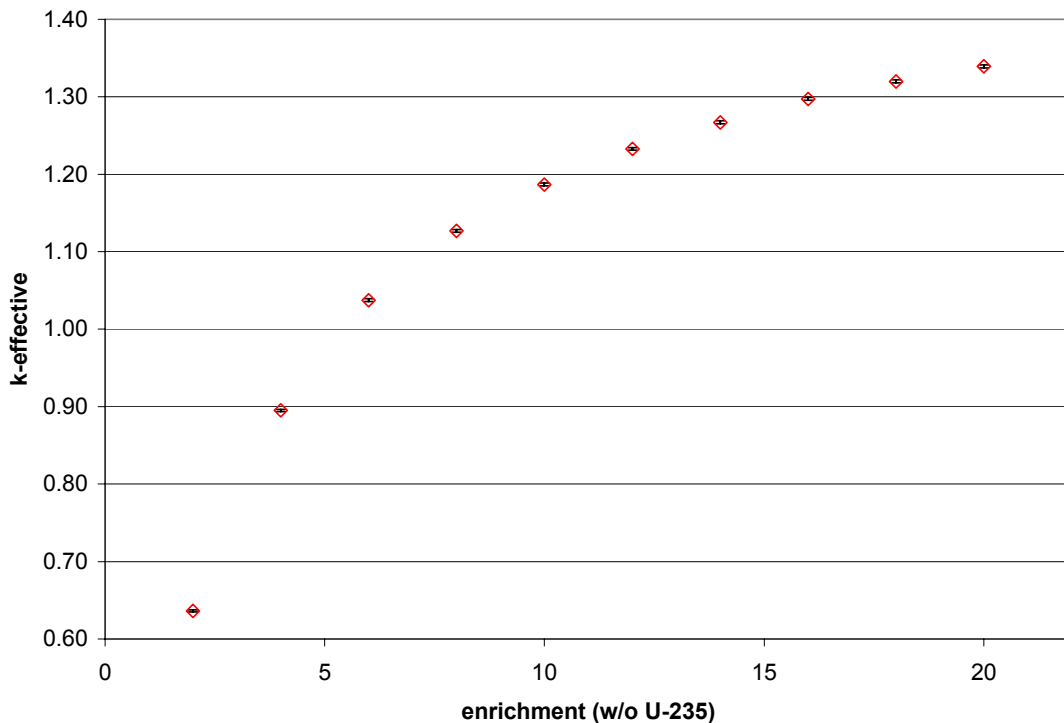
To determine the effect of the fuel enrichment on the percentage fission by energy region in the core, the reactor parameters listed in Table 4-4 were used for this analysis. The gas pressure is fixed at 12 bars and the fuel enrichment is varied between 2 and 20 w/o.

Figure 4-8 shows that fuel enrichment follows similar trends to gas pressure. The reactivity gain from increasing the fuel enrichment eventually saturates. The percentage of fissions caused by energetic neutrons increases proportionally to the increase in enrichment. Increasing the fuel enrichment has the same effect as increasing the fuel density. It may be more appropriate to envision the increase in enrichment as an increase in atom density of fissile isotopes. As the fuel enrichment increases, the number of fissile atoms (U-235) per unit volume increases relative to the other fuel atoms, specifically those that have significant neutron interaction cross section (U-238). This increases the probability that an energetic neutron causes fission before it is thermalized by interactions in the reflector.

In the gas pressure sensitivity study, the trends in the percentage of fissions from two energy ranges: 0.625 eV-100 KeV and greater than 100 KeV are very similar with respect to the proportionality that the percentages increase due to the increase in gas pressure. In Figure 4-7B the plots for the two energy ranges have a similar slope; the gas pressure has similar effects on both energy ranges. However, the enrichment study shows that increase in fuel enrichment greatly increases the number of fissions caused by neutrons with energies between 0.625 eV and 100 KeV. This energy range is roughly the range where uranium has

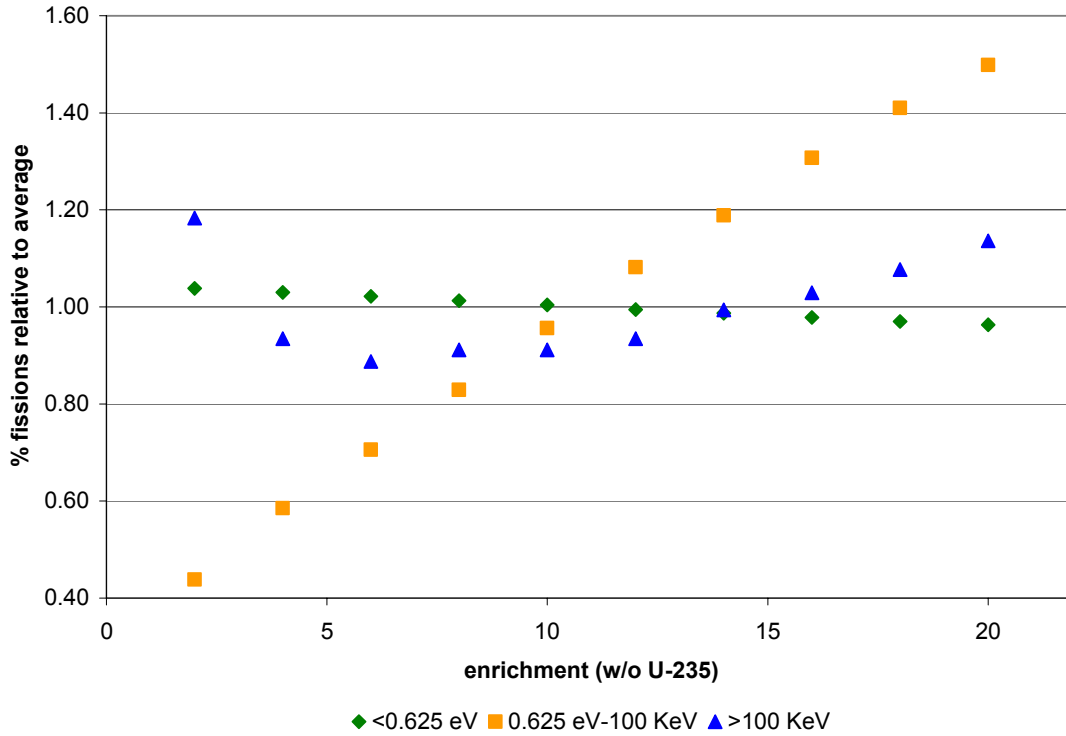
many resonances. By increasing the enrichment, the U-235 atom density increases and thus increasing the probability that a neutron will be absorbed by one of these resonances.

Table 4-6 shows that neutrons with energies between 0.625 eV and 100 KeV are significantly more sensitive to the increase in fuel enrichment than neutrons in the other two energy ranges. Compared to the data in Figure 4-7B, neutrons in this middle energy range are more sensitive to increases in gas pressure than increases in fuel enrichment. For example, a 400% increase in U-235 mass due to increase in pressure results in a 172% increase in the percentage of fissions caused by neutrons in the middle energy range, compared to a 118% increase due to increase in enrichment. With the pressure increase, there is a 400 % increase in both U-235 and U-238 mass. With the enrichment increase, the 400 % increase in U-235 is accompanied by an 8 % decrease in U-238.



A

Figure 4-8. Fuel enrichment sensitivity study with BeO reflector. Shown is the effect of enrichment on (A) k-effective, and (B) percentage of fissions caused by neutrons in three energy groups normalized to the average in each group.



B

Figure 4-8. Continued.

Table 4-6. Percentage increase in the number of fissions caused by neutrons in three energy ranges due to increase in fuel enrichment.

enrichment (w/o)	% reactivity increase	% increase relative to 10 bars			
		U-235 mass	<0.625 eV	0.625 eV-100 KeV	>100 KeV
2	0.0000	0	0.0000	0.0000	0.0000
4	33.8185	100	-0.7802	33.4495	-21.0000
6	47.9528	200	-1.5604	60.9756	-25.0000
8	55.6508	300	-2.4134	89.1986	-23.0000
10	60.3978	400	-3.2872	118.1185	-23.0000
12	63.8367	500	-4.1610	146.6899	-21.0000
14	66.2863	600	-4.9412	171.0801	-16.0000
16	68.3850	700	-5.7838	198.2578	-13.0000
18	69.9003	800	-6.5224	221.6028	-9.0000
20	71.1746	900	-7.1778	241.8118	-4.0000

To design a reactor with mostly neutrons in the 0.625 eV-100 KeV range, the system needs to be high in both pressure and enrichment. However, if the goal is to maximize the neutron population with energy greater than 100 KeV, high pressure alone will suffice due to the weak sensitivity of these neutrons to increases in enrichment.

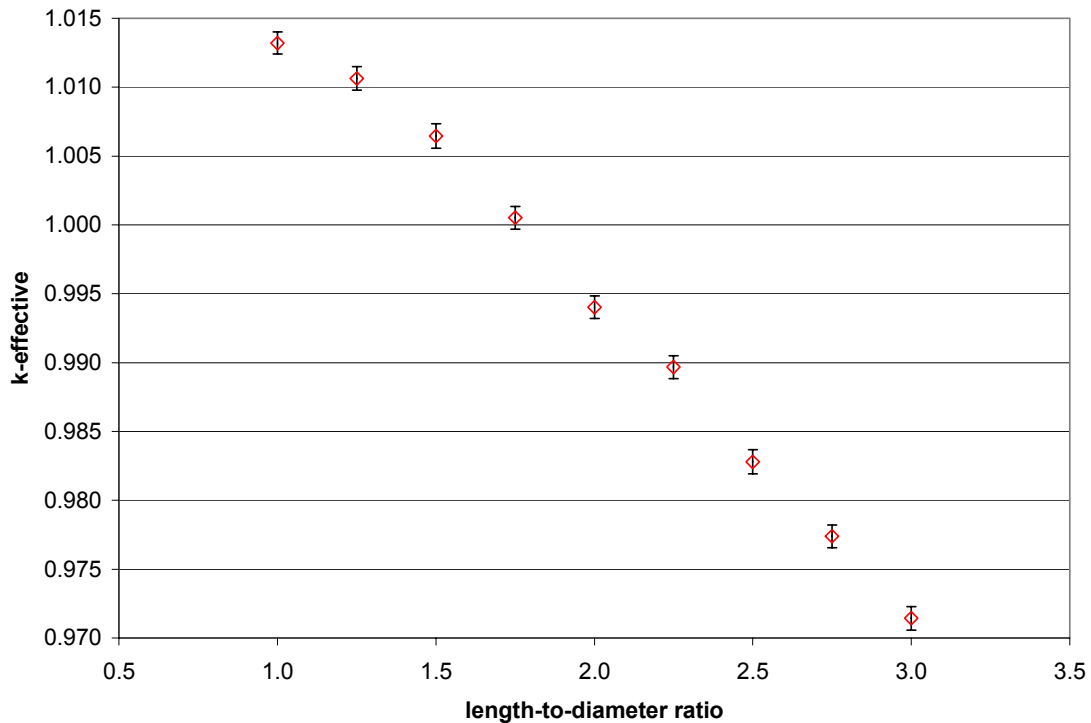
Length-To-Diameter Ratio

The length-to-diameter (L/D) ratio is varied from 1.0 to 3.0. The reactor parameters in Table 4-4 are used, except the core cavity length and diameter are changed according to the L/D ratio, and the gas pressure is at 14 bars so that most of the resulting reactor configurations will have k-effective values close to unity. For all configurations the volume from previous studies is conserved.

As expected, the core with an L/D ratio of 1.0 had the highest k-effective value (see Figure 4-9A). This is because an L/D ratio of 1.0 results in the lowest surface area to volume ratio among all the reactor configurations analyzed. The lower is the surface area to volume ratio, the lower is the neutron leakage.

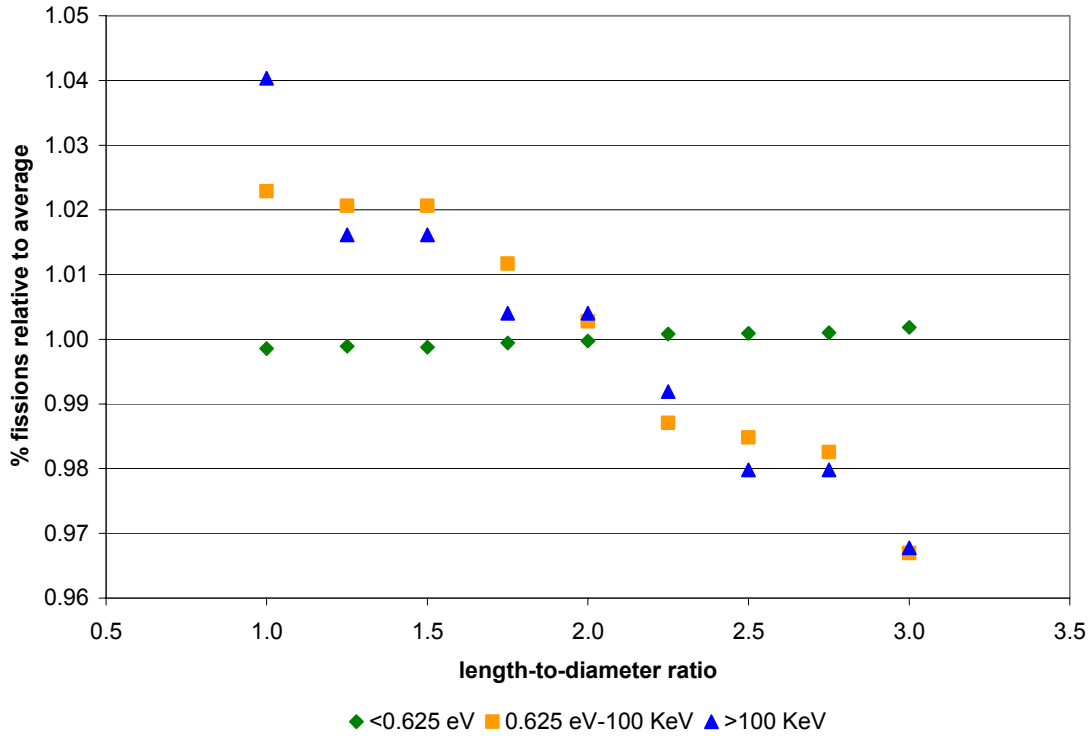
Figure 4-9B shows that there is a slight increase in the percentage of fissions caused by neutrons with energy less than 0.625 eV. However, this is only relative to the larger (but still small in absolute magnitude) decrease in the fissions caused by neutrons in other energy ranges. Although the data shown in the plot for the energy ranges 0.625 eV-100 KeV and greater than 100 KeV does not seem to have converged, this is only because the MCNP5 outputs consists of only two decimal digits; miniscule changes in the percentage of fissions caused by neutrons with energy greater than 0.625 eV could not be observed. That said, two observations may be gathered from Figure 4-9B. First, the increase in core L/D ratio decreases the percentage of fissions caused by energetic neutrons. Second, this decrease in the percentage of fissions caused by energetic neutrons is very small and not very sensitive to the L/D ratio. This can be observed in Table 4-7 where a 25% increase in the surface area to volume (SA/V) ratio only resulted in a maximum of 7% decrease in the percentage of fissions caused by neutrons with energy greater than 100 KeV, and insignificant changes in the percentage of fissions caused by slow neutrons.

The small decrease in energetic neutrons in the core with an L/D ratio of 3 is due to increased leakage at the expense of a reactivity (ρ) loss of 4.21% $\Delta k/k$ relative to the core with an L/D ratio of 1; this is equivalent to a 10% increase in fuel enrichment, 10.7% increase in gaseous fuel pressure, or 28% increase in fuel volume. However, it is easier to make even larger changes in the reactivity and core neutronic properties by changing the reflector thickness, gas pressure, and/or fuel enrichment.



A

Figure 4-9. Core length-to-diameter ratio sensitivity study with BeO reflector. Shown is the effect of L/D ratio on (A) k-effective, and (B) percentage of fissions caused by neutrons in three energy groups normalized to the average in each group.



B

Figure 4-9. Continued.

Table 4-7. Percentage increase in the number of fissions caused by neutrons in three energy ranges due to increase length-to-diameter ratio.

L/D ratio	% reactivity increase	% increase relative to L/D of 1.0			
		SA/V	<0.625 eV	0.625 eV-100 KeV	>100 KeV
1.00	0.0000	0.0000	0.0000	0.0000	0.0000
1.25	-0.2540	3.4129	0.0317	-0.2188	-2.3256
1.50	-0.6684	6.8400	0.0211	-0.2188	-2.3256
1.75	-1.2603	10.1779	0.0846	-1.0941	-3.4884
2.00	-1.9121	13.3929	0.1163	-1.9694	-3.4884
2.25	-2.3506	16.4774	0.2221	-3.5011	-4.6512
2.50	-3.0471	19.4344	0.2326	-3.7199	-5.8140
2.75	-3.5999	22.2708	0.2432	-3.9387	-5.8140
3.00	-4.2103	24.9950	0.3278	-5.4705	-6.9767

The percentage of fissions caused by energetic neutrons (>0.625 eV) is maximum in the core with an L/D ratio of 1.0. This is the core with the minimum surface area to volume ratio. Similar to other sensitivity studies, slow neutrons (<0.625 eV) are guaranteed to cause fission because of its small mean free path in the gaseous fuel. Thus, geometrical advantages, such as the minimum L/D ratio, will not significantly impact the number of

fissions from slow neutrons. On the other hand, a small L/D ratio will minimize the leakage of energetic neutrons (>0.625 eV) and thus maximize the number of fissions caused by these neutrons.

Internal Moderation

The classical GCR consists of a single fuel cavity surrounded by the reflector. In an attempt to increase the thermal neutron population, reactors with multiple cavities are analyzed. The presence of internal moderator material that are positioned in between fuel cavities will aid in the thermalization of neutrons in the area where it is needed the most, i.e. at the center of the reactor core.

For this study a simple design of three fuel cavities is employed, shown in Figure 4-10. The most efficient use of the moderator material is to distribute it homogeneously throughout the reactor core. Notice that the reactor configuration using three fuel cavities is not the ideal design for efficient use of moderator material. A reactor with seven cavities, one central cavity surrounded by six others, is a reactor design that distributes the moderator more homogeneously. However, for scoping studies the simpler design will be used.

The gap thickness is the minimum distance between adjacent fuel cavities, and it is filled with the moderator material. The core diameter is the diameter of the smallest cylinder that encases all of the fuel cavities, and the core length is determined based on the L/D ratio and the core diameter. For comparison purposes, the total fuel volume for all configurations in this study is preserved, and it is the same fuel volume used for the pressure, enrichment, and L/D ratio sensitivity studies. Table 4-8 lists the design parameters used for this study.

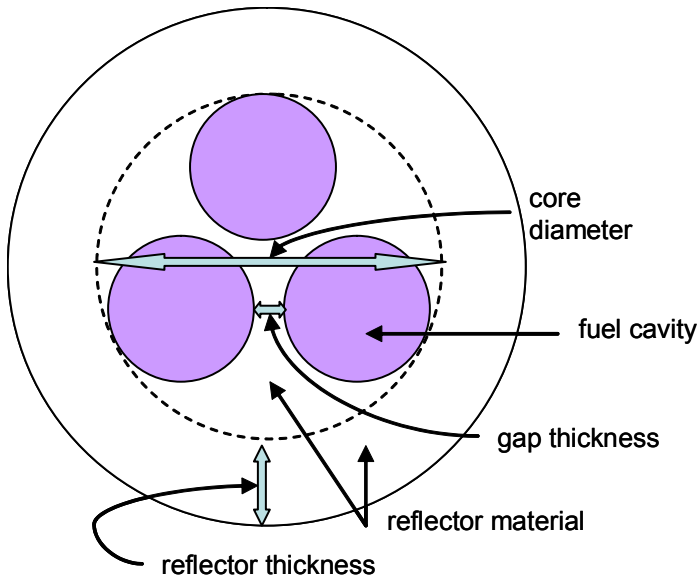
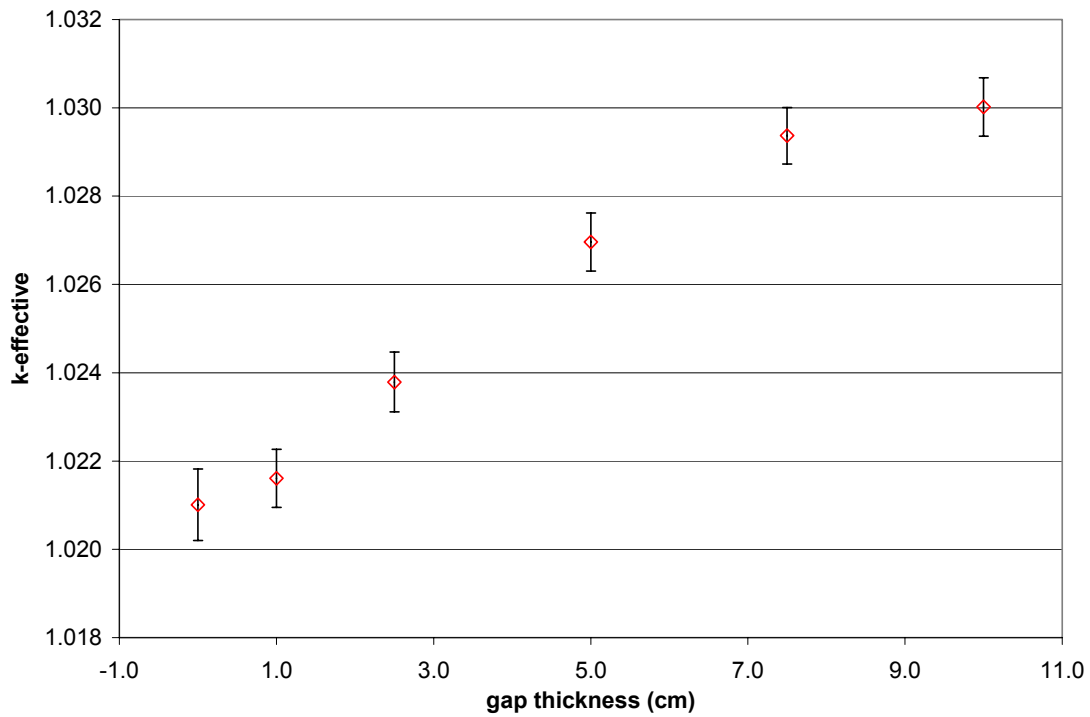
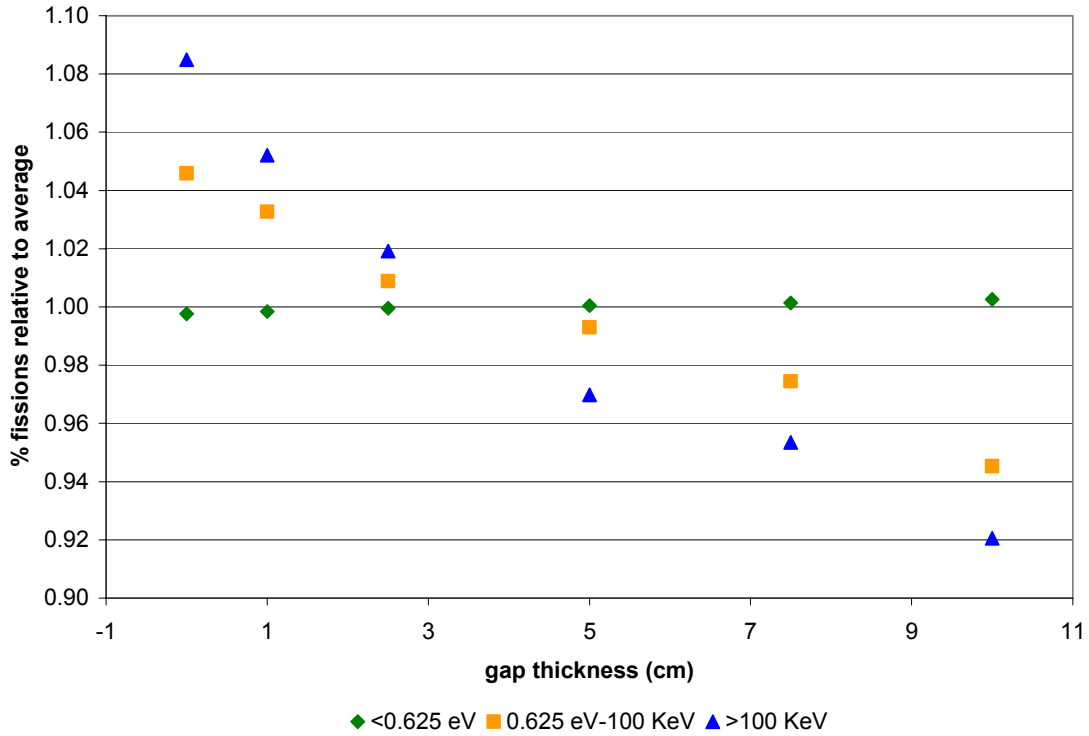


Figure 4-10. Cross sectional view of a GCR model with three fuel cavities used in the gap thickness sensitivity study.



A

Figure 4-11. Gap thickness sensitivity study using 3 fuel cavities and a BeO reflector. Shown is the effect of gap thickness on (A) k-effective, and (B) percentage of fissions caused by neutrons in three energy groups normalized to the average in each group.



B

Figure 4-11. Continued.

Table 4-8. Reactor parameters used for gap thickness sensitivity study.

design parameter	value
total fuel volume (cc)	21,205,750
reflector thickness (cm)	80
L/D ratio	1
gas pressure (bars)	14
enrichment (w/o)	5
gas temperature (K)	2,000
reflector temperature (K)	1,500

The gap thickness is varied between 0 and 10 cm, and its effect on the k-effective is shown in Figure 4-11A. The gap size saturates at a thickness of 10 cm; however, the difference in reactivity gain when the gap thickness is doubled (going from 5cm to 10 cm) is only 0.30% $\Delta k/k$. Thus, a gap thickness of 5 cm is a good compromise between reactivity gain and reduction in reflector material, which in the case of BeO is quite expensive.

Table 4-9. Percentage increase in the number of fissions caused by neutrons in three energy ranges for a three-cavity reactor relative to a single-cavity reactor due to increase gap thickness.

gap (cm)	% reactivity increase	% increase relative to single cavity			
		reflector vol	<0.625 eV	0.625 eV-100 KeV	>100 KeV
0.0	0.7669	46.9085	0.8565	-13.5667	-23.2558
1.0	0.8256	48.4896	0.9411	-14.6608	-25.5814
2.5	1.0388	50.8842	1.0574	-16.6302	-27.9070
5.0	1.3479	54.9370	1.1420	-17.9431	-31.3953
7.5	1.5823	59.0681	1.2372	-19.4748	-32.5581
10.0	1.6454	63.2785	1.3641	-21.8818	-34.8837

In reality, going from single cavity to multiple cavities is just an increase in moderator volume, and an attempt at a more homogeneous distribution of such volume. The difference in reflector volume between a single-cavity and three-cavity reactor is at least 47%. This added moderation, especially in the center of the core, decreases the percentage of fissions caused by neutrons with energies greater than 0.625 eV.

The percentage of fissions caused by neutrons with energies greater than 100 KeV is most sensitive to the increase in gap size. Table 4-9 shows that the fissions from energetic neutrons are extremely sensitive to a multiple cavity environment, but relatively insensitive to the increase in gap thickness, as shown in Table 4-10.

Table 4-10. Percentage increase in the number of fissions caused by neutrons in three energy ranges for a three-cavity reactor relative to a reactor 0 cm gap thickness.

gap (cm)	% increase relative to 0 cm Gap			
	reflector vol	<0.625 eV	0.625 eV-100 KeV	>100 KeV
0.0	0.0000	0.0000	0.0000	0.0000
1.0	1.0762	0.0839	-1.2658	-3.0303
2.5	2.7062	0.1992	-3.5443	-6.0606
5.0	5.4649	0.2831	-5.0633	-10.6061
7.5	8.2770	0.3774	-6.8354	-12.1212
10.0	11.1430	0.5033	-9.6203	-15.1515

Table 4-10 shows that increasing the gap thickness from 2.5 to 5 cm results in the largest percentage decrease in the percentage of fissions from neutrons with energies greater than 100 KeV; there is a 4.5% difference between 2.5 cm and 5 cm gap thicknesses, while

others are about 3% for this energy range. Internal moderation will be used to create a reactor with a very thermal spectrum. Thus, this will only be used in the design of the BeO reflected GCR. Since the gap thickness has a weak impact on the percentage of fissions by energy range and BeO is an expensive material, a compromise between slightly increasing the percentage of fissions induced by thermal neutrons and using the less moderator material is made and gap thickness of 5 cm will be used.

Summary Of Sensitivity Studies

The sensitivity studies provide insight into the effect of reflector material, reflector thickness, gas pressure, fuel enrichment, core L/D ratio, and gap thickness on the neutronic characteristics of the core. The change in neutronic characteristics due to changes in reactor design parameters are reported in terms of the percentage of fissions caused by neutrons in three energy ranges: less than 0.625 eV, 0.625 eV to 100 KeV, and greater than 100 KeV.

The following are the highlights of the observations.

- Reflector material dictates the critical fuel volume and the ultimate core neutronic characteristics that can be achieved at saturation thickness.
- Reflector material is the most important design parameter in determining core spectral characteristics. Also very important is the reflector temperature.
- An increase in the reflector thickness increases the percentage of fissions caused by neutrons of the dominant energy range, and this increase approaches an asymptotic value as the reflector thickness approaches its saturation thickness.
- The gas pressure and fuel enrichment are effective ways in controlling core reactivity. Gas pressure is much easier and faster to change than fuel enrichment.
- Increase in gas pressure causes an increase in the percentage of fissions caused by energetic neutrons with energies greater than 0.625 eV.
- Increase in fuel enrichment increases the percentage of fissions from neutrons in the range 0.625 eV-100 KeV.
- An increase in L/D ratio weakly decreases the percentage of fissions caused by neutrons with energies greater 100 KeV.

- Considering the reactivity penalty from the increase of the L/D ratio, and its minimal effects on the percent fission by energy region, an L/D ratio of 1.0 is optimum.
- A multiple cavity core decreases the number of fissions caused by energetic neutrons (> 0.625 eV) relative to a single cavity core.
- An increase in gap thickness between adjacent cavities mildly decreases the fissions caused by energetic neutrons.
- A gap thickness of 5 cm will be used for BeO reflected GCR.

Gas Core Reactor Design

Using the information from the sensitivity studies, and all the reflector materials, design of reactors are aimed to achieve a wide range of characteristic spectra. Starting from the natural spectral distribution provided by each reflector material, the reflector thickness, gas pressure, and fuel enrichment are varied to achieve two goals:

- A small critical volume so that the reactor design is practical according to today's power production standards. For example, a core 3 meters in diameter and 3 meters in height meets this goal.
- Obtain a wide range of neutron spectra with reactor designs that have mostly thermal, epithermal, or fast neutrons.

The L/D ratio is fixed at 1.0, and if multiple cavities are used, the gap thickness will be fixed at 5 cm, for reasons stated in the previous section.

Minimization of the Critical Fuel Volume

To achieve the first goal, relatively high gaseous fuel pressure and enrichment is needed. However, doing so will increase the population of energetic neutrons. In order to design a thermal reactor the critical volume will need to be compromised. Fortunately, reflector materials that naturally gravitate towards a thermal spectrum require small critical volumes because of the minimal leakage.

To minimize the critical volume the reflector must be at its saturation thickness, to yield the maximum reactivity gains due to reflector savings. This automatically defines the

core in terms of the dominant neutron energy group. At saturation thickness, the neutron population in the dominant energy group is very close to the maximum population achievable. This can be further maximized with the correct choice of pressure and enrichment. In the case where a thermal spectrum is desired, multiple cavities will also increase the population in the thermal range.

Since the second goal is an essential part of the objective of this research, this will have priority over minimizing the critical volume. The critical volume depends on the reactivity advantages provided by the reflector thickness, gas pressure, and fuel enrichment. The small critical volume is sacrificed in order to accomplish the second goal. The maximum pressure and enrichment minimizes the critical volume. The maximum pressure considered in the current research is 155 bars, and the maximum enrichment is 20 w/o. Even under the maximum fuel loading reactivity conditions, the use of some reflector materials with high resonance absorption peaks like ZrC, would require the critical diameter of the order of 10 m. Other reflector materials such as Pb and ^7LiH have critical diameters greater than 6 m. However, since these materials yield a fast spectrum, the critical volume is the compromise that must be made with a thermal reactor system to accomplish the second goal.

Obtaining a Wide Range of Neutron Spectra

To accomplish this second goal the number of neutrons in the reflector materials' dominant energy group is maximized with the correct choice of reflector thickness, gaseous fuel pressure, and enrichment. With the dominant energy group at saturation thickness as a starting point, the knowledge from the sensitivity studies is applied to maximize the neutron population in this energy group.

To maximize the thermal neutron population both gas pressure and fuel enrichment should be as low as reasonably possible. Additionally, multiple cavities increase the chances

that energetic neutrons encounter the moderator inside the core and are thermalized before leaking out of the system.

For an epithermal core the enrichment and pressure should be maximized. Increases in enrichment affect this energy range the most. However, this energy range is most sensitive to pressure changes. Regardless of the effectiveness of these two design parameters on the epithermal neutron population, both are needed in order to keep the volume to a minimum.

Increases in gas pressure affect fast neutrons the most. A maximum pressure must be used to maximize the fast neutron population. However, due to large mean free path of fast neutrons in the core, decreased fast neutron leakage poses a big threat to maintaining a reasonable critical volume. Thus, added reactivity from maximizing the enrichment must be used in attempt to minimize the critical volume.

Reactor Dimensions

Keeping the two design goals in mind, and applying the design guidelines from the previous sections, the optimal reactor parameters for each reflector material are listed in Table 4-11.

Table 4-11. Final reactor designs for each reflector material. All systems produce 3000 MW of thermal energy.

design parameter	reflector material						
	BeO	⁷ LiH	⁷ LiD	C	W	ZrC	Pb
core press (bars)	12.76	155	26.49	80	155	155	155
core temp (K)	2,000	2,000	2,000	2,000	2,000	2,000	2,000
refl thick (cm)	80	20	80	26	40	62.5	130
refl temp (K)	1,500	750	750	1,500	1,500	1,500	600
enrichment (w/o)	5	19.95	19.95	19.95	95	19.95	19.95
core dia (cm)	349.23	937.32	300.00	407.16	450.55	952.44	673.59
fuel volume (cc)	2.1E+07	6.5E+08	2.1E+07	5.3E+07	7.2E+07	6.8E+08	2.4E+08
U-mass (MT)	0.38	143.50	0.80	6.07	15.94	150.56	53.26
desired spectrum	thermal	thermal	thermal	therm/epi	fast	fast	epi/fast

Since preliminary calculations in the reflector thickness study indicates that a BeO reflected system is the most thermal among all reflector materials, it is the only design with multiple cavities. Other reflector materials that yield relatively thermal spectra such as graphite and ^7LiD are used for comparison purposes to bridge thermal and epithermal systems. This is the reason that the graphite reflector is not at its saturation thickness of 110 cm. Since the thermal range is the dominant range for graphite, a reflector thickness smaller than the saturation thickness decreases the number of thermal neutrons. This is due to a decrease in the amount of moderation. At a 26 cm thickness, the percentage of fissions caused by low energy neutrons becomes less than 50%. The three reflector materials, BeO, ^7LiD and graphite, which yield a thermal spectrum, have the three lowest critical volumes, without the aid of high pressure. These cores also have the lowest uranium inventory.

All reflector materials with mostly energetic neutrons need the aid of saturation reflector thickness, maximum pressure, and maximum enrichment to achieve criticality at reasonable core size. Even with all the reactivity help possible, the tungsten-reflected system is unable to accumulate enough fuel mass to become critical. For this system a fuel enrichment of 95 w/o is necessary. Thus, tungsten reflected GCR system will not be further analyzed in fuel cycle studies.

Originally, ^7LiH was expected to yield a relatively thermal spectrum. This is because both lithium-7 and hydrogen are light elements that are effective neutron moderators. Additionally, ^7LiH has a relatively low neutron capture cross section. However, the critical core volume is one order of magnitude larger than that for the BeO reflected system. Thus, ^7LiD was added to the list of reflector materials hoping that its critical volume would be comparable to that for the BeO reflected GCR. Indeed, a ^7LiD -reflected system has a higher

percentage of thermal neutrons, while the critical volume is one order of magnitude smaller than the ${}^7\text{LiH}$ system. Hence, ${}^7\text{LiH}$ is not used in further fuel cycle studies.

Reference LWR Description

The objective of this research is to alleviate the waste problems faced by today's LWRs. This includes minimizing the amount of waste and improving the waste characteristics. Table 4-12 contains a description of a typical PWR, using 15x15 assemblies. This reference PWR serves as a basis for comparing results from the GCRs described in Table 4-11.

Table 4-12. Description of the reference PWR using 15x15 fuel assemblies.

	material	inner radius (cm)	thickness (cm)	avg temp (K)
fuel	UO ₂	0	0.4096	990
cladding	zirconium	0.4178	0.0572	600
reflector	water	168.5	38.1	588
enrichment (w/o)	3.2			
pitch (cm)	1.2573			
assembly height (cm)	365			
core diameter (cm)	337			
total fuel volume (cc)	1.1E+07			
total U-mass (MT)	97.53			

Core Spectrum Characteristics

The energy spectra for the designs in Table 4-11 and the reference PWR are obtained using 660 energy bins. This bin structure is obtained from previous GCR studies found in reference [54]. A sample MCNP5 input for the BeO-reflected core described in Table 4-11 along with the energy bin structure is in Appendix B. The spectra are shown in Figure 4-12. From Figure 4-12 and Figure 4-13, it is apparent that a thermal cutoff of 0.625 eV is too low. To include all materials, the value should be at least at about 2 eV.

The reference PWR is supercritical because at the BOL the reactor needs to have enough reactivity to last one cycle of about 18 months. To suppress this extra reactivity three

methods are used: control rods, chemical shim, and burnable poisons. For simplicity the effect of control rods and burnable poisons are not simulated.

In Table 4-13, the values highlighted in green represent the maximum value in each row; the values highlighted in blue represent the minimum value in each row. From this simple table, it is apparent that the BeO system has the most thermal spectrum, the Pb system has the most epithermal spectrum, and the W system has the hardest spectrum.

The average neutron energy causing fission in the BeO reflected system is about 20 times lower than that in the reference PWR. Another GCR design with a high percentage of thermal fissions is the ^7LiD -reflected system. However, the percentage of thermal fissions in the ^7LiD system is 11% lower than the percentage of thermal fissions in the BeO system and the average neutron energy causing fission is about 3 times larger.

Among the reflector materials, W had the largest capture-to-total cross section ratio, followed by ZrC, and then Pb. The majority of these resonances for these materials are in the epithermal region (2 eV to 100 KeV). The effect of these resonances are illustrated in Table 4-13 (see also Figure 4-3). As it is shown in this table, W has the lowest percentage of epithermal fissions, followed by ZrC, and Pb had the largest percentage of epithermal fissions, not only among these three materials, but among all reflector materials.

The spectra resulting from each of the GCR designs along with the reference PWR spectrum are plotted in. The average standard deviation values are 0.037, 0.0047, and 0.0818 for the thermal, epithermal, and fast regions, respectively. For the thermal and epithermal regions the tungsten data is not included in the calculation of the average standard deviation values. In the tungsten reflected system there are practically no tallies in these two energy ranges due to high capture cross section. Because the tally values in these two energy ranges are

insignificant for the tungsten reflected system, excluding this data in the calculation of the average standard deviation is a better representation of the data in the thermal and epithermal ranges.

These spectra are averaged over the entire fuel cavity for the GCRs and over the entire core (pins and moderator) for the reference PWR. To compare the spectra generated, the tallies are first normalized to the total number of counts in each reflector material. Then each tally value is divided by the bin width since the bin widths vary. This is because, with all things equal, narrower bins get fewer counts than wider bins. Thus, all counts need to be normalized to the bin width to correctly represent the energy spectrum. In all of the spectrum plots, the gray vertical lines represent the energy bin limits.

Thermal energy range

For purposes of this research the thermal range has an upper energy limit of 2 eV. Figure 4-13 shows the spectra in this range. The BeO-reflected system has the most thermal spectrum and the W-reflected system does not have any thermal neutrons. The ${}^7\text{LiD}$ -reflected system is very similar to the reference PWR. There are slightly more neutrons in the range $1\text{E-}9$ to $1\text{E-}8$ MeV, and fewer neutrons in the range $1\text{E-}8$ to $1\text{E-}7$ MeV in the ${}^7\text{LiD}$ spectrum when compared to the PWR spectrum. The ${}^7\text{LiH}$ and graphite spectra are somewhat similar, with graphite having significantly more neutrons towards the higher end of the thermal range.

Table 4-13. Neutronic characteristics of final GCR designs compared to the reference PWR.

	PWR	BeO	⁷ LiH	⁷ LiD	graphite	W	ZrC	Pb
k-effective	1.03236	0.99761	0.99950	0.99974	0.99989	0.99882	0.99885	0.99972
standard deviation	0.00024	0.00016	0.00011	0.00013	0.00014	0.00014	0.00012	0.00012
removal lifetime (sec)	1.5E-05	4.0E-03	9.4E-05	7.9E-04	1.9E-04	1.1E-06	6.8E-05	7.3E-05
avg enrg causing fission (MeV)	2.7E-01	1.4E-02	3.5E-01	4.0E-02	1.8E-01	6.6E-01	4.6E-01	4.3E-01
# nts produced per fission	2.462	2.434	2.470	2.437	2.451	2.499	2.480	2.477
% fissions from nts with enrg. <0.625 eV	72.75	95.86	51.02	85.23	48.45	0.00	6.70	0.78
0.625 eV to 100 KeV	17.78	3.58	30.28	12.84	41.41	45.93	65.52	71.23
>100 KeV	9.46	0.56	18.69	1.93	10.14	54.07	27.78	27.99

Table 4-14. Core spectral characteristics for all GCR designs and the reference PWR.

	PWR	BeO	⁷ LiH	⁷ LiD	graphite	W	ZrC	Pb
avg. energy of neutrons (MeV)								
<2 eV	1.7E-07	1.6E-07	2.6E-07	1.7E-07	4.2E-07	1.3E-06	6.5E-07	1.0E-06
2 eV - 100 KeV	1.1E-04	1.1E-04	4.8E-04	1.4E-04	2.8E-04	1.1E-02	1.3E-03	2.0E-03
>100 KeV	5.8E-01	5.2E-01	5.4E-01	5.5E-01	5.3E-01	5.0E-01	5.0E-01	4.8E-01
fraction of nts w/ energy								
<2 eV	0.9277	0.9875	0.8668	0.9434	0.7920	0.0001	0.5143	0.2428
2 eV - 100 KeV	0.0723	0.0125	0.1332	0.0566	0.2080	0.9902	0.4856	0.7570
>100 KeV	1.5E-06	1.7E-07	2.1E-05	1.1E-06	1.0E-05	9.7E-03	1.1E-04	2.3E-04
avg standard deviation								
<2 eV	0.0125	0.0177	0.0252	0.0188	0.0549	0.2381	0.0582	0.0718
2 eV - 100 KeV	0.0045	0.0058	0.0050	0.0057	0.0036	0.1030	0.0041	0.0041
>100 KeV	0.0542	0.0616	0.0752	0.0930	0.0935	0.1001	0.0792	0.0978

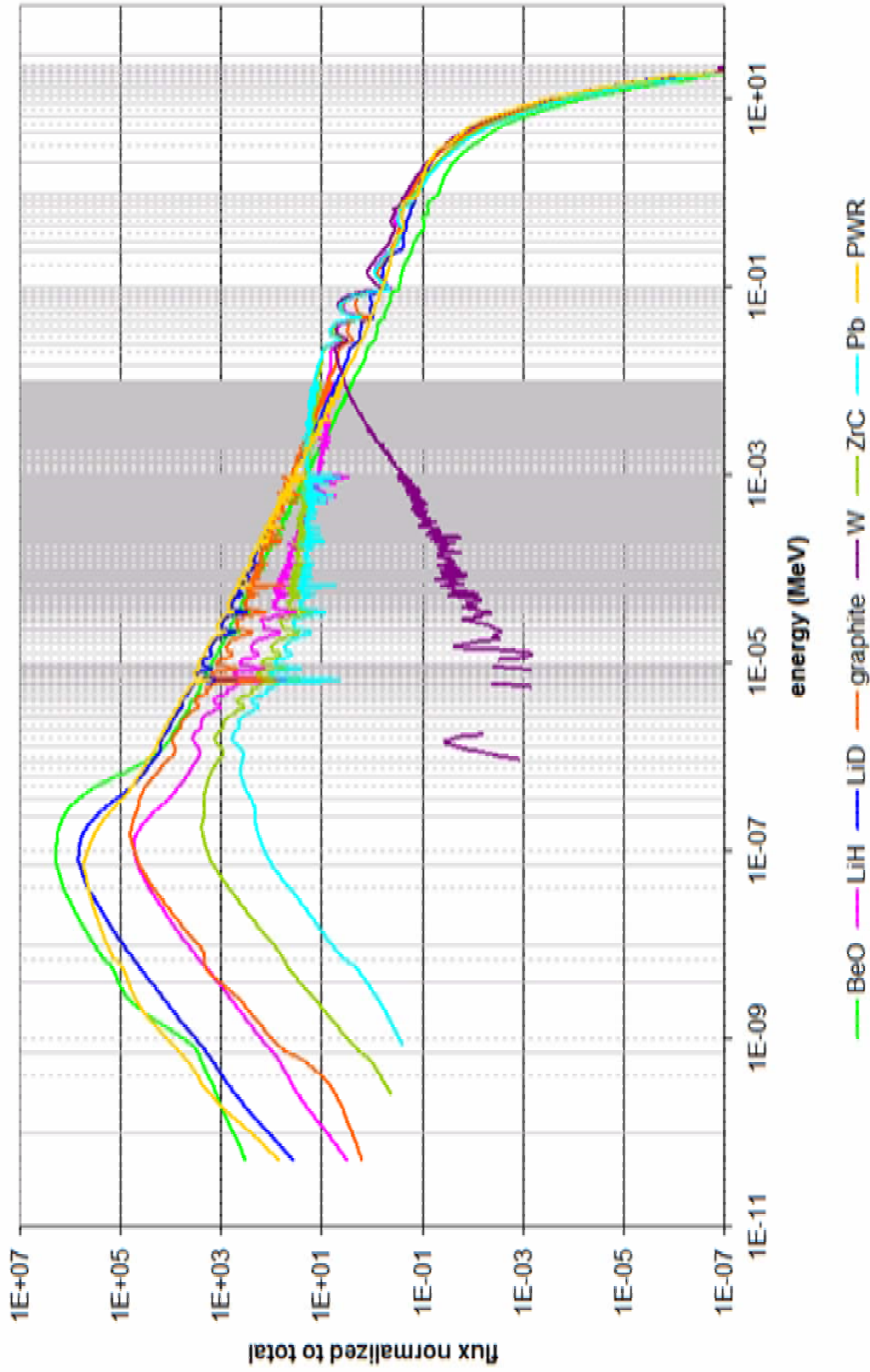


Figure 4-12. Average core spectrum obtained for each of the obtained for each of the reflector materials using design parameters in Table 4-11. The average standard deviations are 0.037, 0.0047, and 0.0818 in the thermal, epithermal, and fast ranges. Tungsten not included in the average standard deviation value in the thermal and epithermal ranges.

In all the spectra that have a significant percentage of the neutron population in the thermal range, the familiar Maxwellian-like shape can be observed; such is the case for the spectra in the BeO, ⁷LiD, and PWR. This is especially true for the PWR spectrum where the Maxwellian shape is followed by the 1/E tail that can be clearly observed in Figure 4-13 for energies greater than about 0.5 eV. In the BeO spectrum the Maxwellian part extends further than the other two thermal spectra, to about 1 eV.

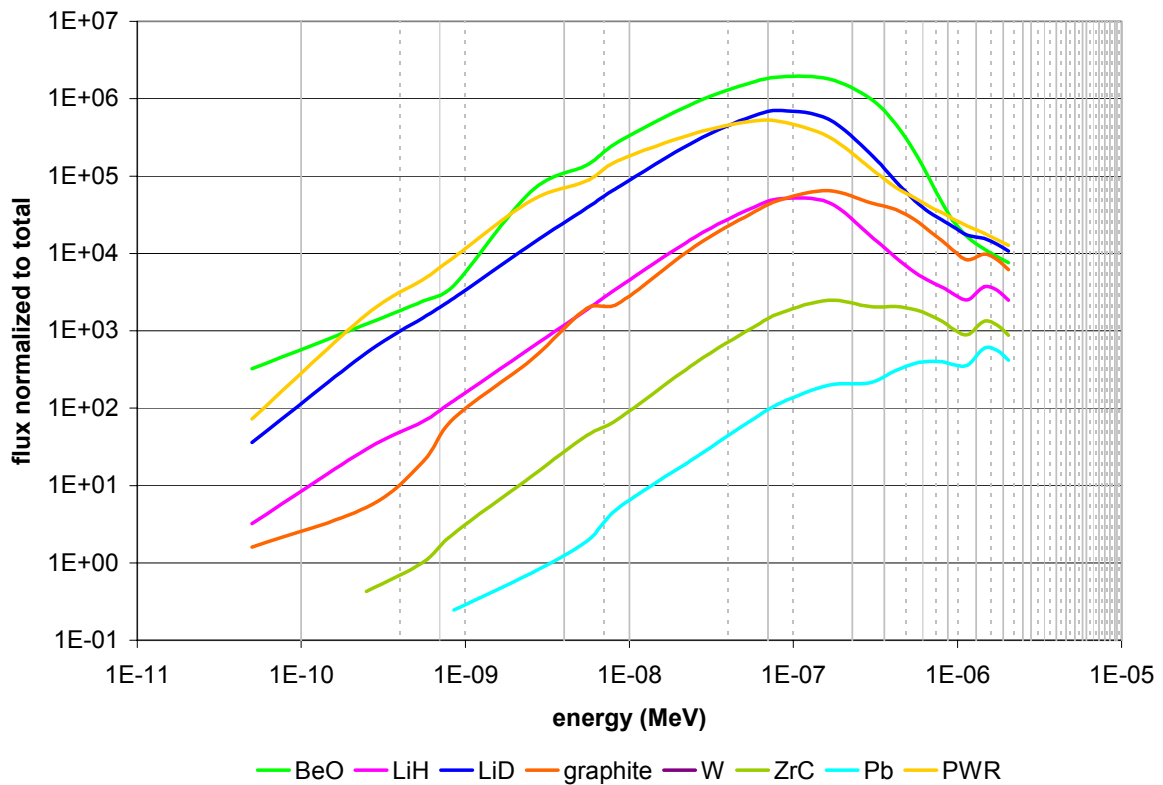


Figure 4-13. Average core spectrum obtained from each of the reflector materials for energies <2 eV. Average standard deviation of 0.037 (excluding tungsten).

The Maxwellian-like thermal shape is less and less prevalent as the reflector material yields a harder spectrum as could be seen in the case of ZrC and Pb reflected systems. The Pb reflected spectrum has no resemblance to the Maxwellian shape, and for W the thermal part of the spectrum is nonexistent.

Epithermal energy range

The epithermal range is from 2 eV to 100 KeV. The spectra are shown in Figure 4-14. The energy bins in this range are significantly smaller than in the other ranges. This is done to correctly illustrate the effect of the resonances. The neutron flux is depressed at the energies that resonances in the fuel exist. This is clearly shown in Figure 4-14 where a resonance at 6.674 eV in U-238 depresses the flux by about one order of magnitude in each of the reflector materials, except for W. Another sharp depression in the fluxes occurs at 66.032 eV in U-238. U-238 resonances are prevalent in the spectra because of the large magnitudes, and these resonances are well separated from each other so that they can easily be identified. This is especially true for resonances below 100 eV, shown in Figure 4-15.

Similar to the thermal range, the behaviors of the spectra can be separated into two groups. The BeO, ⁷LiD, graphite, and PWR systems exhibit the classical 1/E slowing down behavior, common in LWR systems. LWRs are well known thermal systems. In this energy range, graphite has the lowest fraction of lower energy neutrons and the highest fraction of higher energy neutrons among the thermal systems. ⁷LiD and graphite start behaving like the fast systems at energies greater than 10 KeV. In the 10 KeV to 100 KeV range the fast systems have two depressions in the flux at about 28 KeV and 48 KeV. This is expected, since ⁷LiD and graphite are intended to serve as a bridge between thermal and fast systems.

The BeO, ⁷LiD and PWR behave similarly in this energy range; the slope of the 1/E behavior is about the same. All thermal systems have a dramatic increase in neutron population as the energy decreases.

The second group of GCRs exhibit eccentric trends in this energy range. The spectra from the ⁷LiH, ZrC, and Pb reflected systems do not follow a 1/E behavior in the epithermal range. Instead, these spectra seem to follow an exponential pattern below 10 keV where the

flux exponentially increases as the energy decreases, approaching a relatively flat slope. At about 200 eV to about 2 KeV the Pb spectrum is flat. For this energy range the thermal systems experience more dramatic changes in the neutron spectrum than harder systems. Other than flux depression from resonances, the neutron population in the harder systems is more evenly distributed than for thermal systems in the energy range. This is especially true for Pb. Pb has the maximum percentage of fissions caused by neutrons in the epithermal range because the majority of its neutrons exist in and are evenly distributed across this range. This is because when neutrons interact with the heavier nuclides such as Zr, Pb, and W, the energy loss is smaller than with the lighter nuclides such as Be, graphite and H. On average, energetic the neutrons need to experience more scattering interactions with the heavier nuclides in order to thermalize. Hence more neutrons stay in the epithermal range.

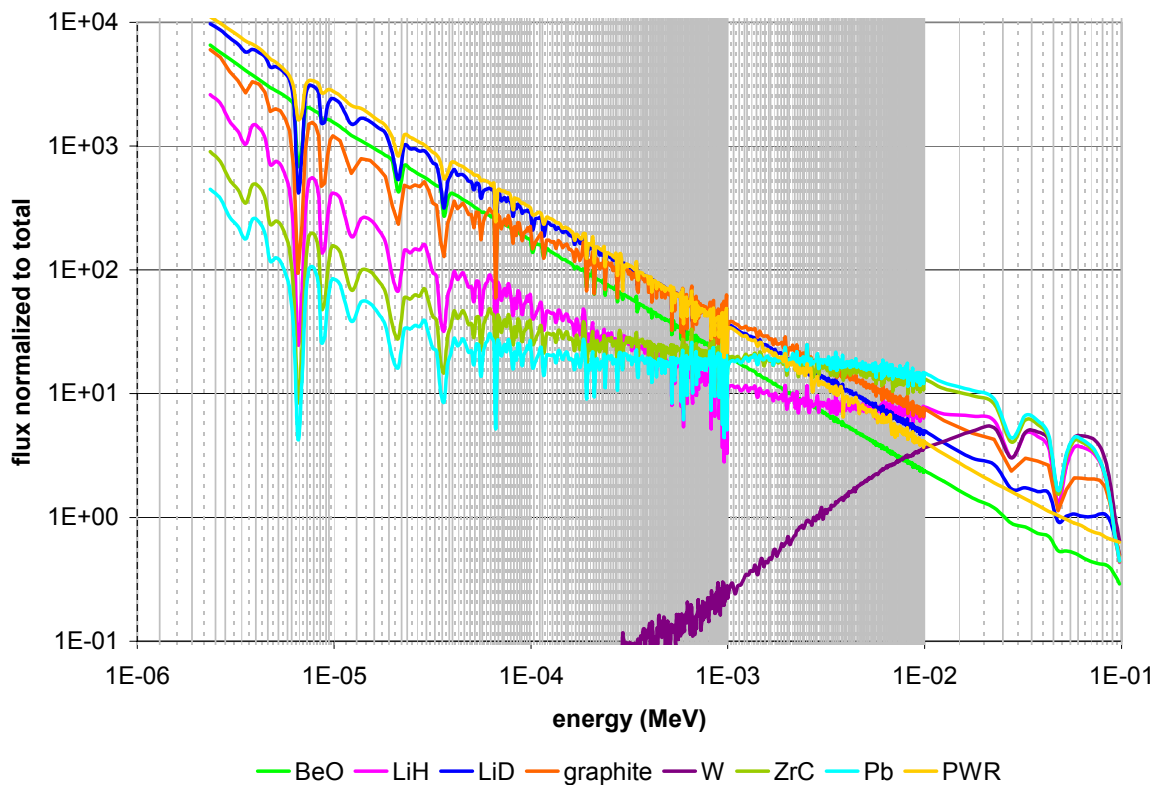


Figure 4-14. Average core spectrum obtained from each of the reflector materials from 2 eV to 100 KeV. Average standard deviation of 0.0047 (excluding tungsten).

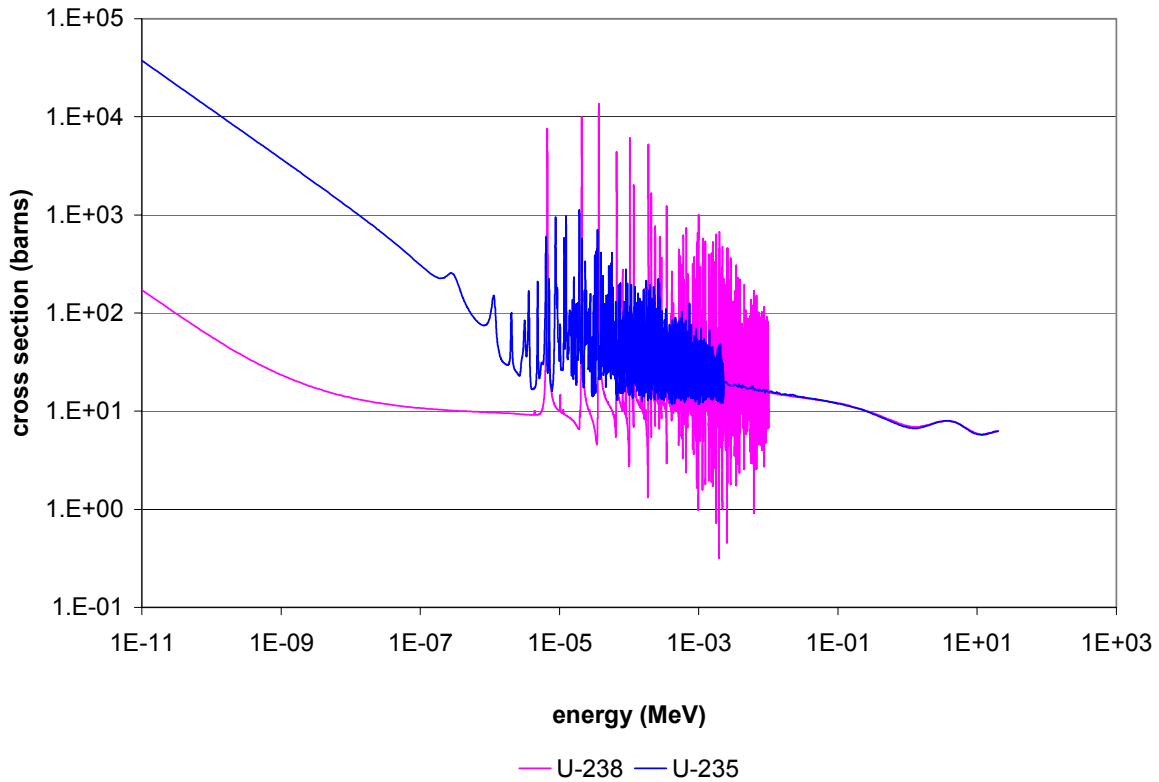


Figure 4-15. U-235 and U-238 total cross section. Data is at 300 K from ENDF/B-VI [39].

The W spectrum has decreased significantly as energy falls below a few hundred eV and has almost disappeared by about 10 eV. This is because of the abundance and intense magnitude of the resonances of in W. At energies less than about 1E-4 MeV the resonances increase to greater than 100 barns and almost all neutron interactions result in capture. Thus, low energy neutrons do not survive.

Fast energy range

The fast region has a lower energy limit of 100 KeV. It is apparent that BeO has the smallest neutron population in this region. Surprisingly, the neutron population in ZrC and Pb decreases rapidly with increasing energy, and it is below some of the thermal systems such as ^7LiD , graphite, and PWR for energies greater than 1 MeV. The part of the spectra above 1 MeV represents the neutron population from fission. Fission neutrons in ^7LiD have

a very similar distribution to those in W. At high energies the neutron population in the PWR slightly surpasses that in W. Most of the region shown in Figure 4-16 (down to several hundreds of keV) is the fission spectrum region. Down to 1 MeV, inelastic scattering tends to be very important (to even lower energies with heavy mass nuclides); an important type of inelastic scatter in BeO is the (n,2n). These are the effects responsible for the differences shown. Below about an MeV (to lower energies in high mass substances) differences in elastic scatter begin to take hold.

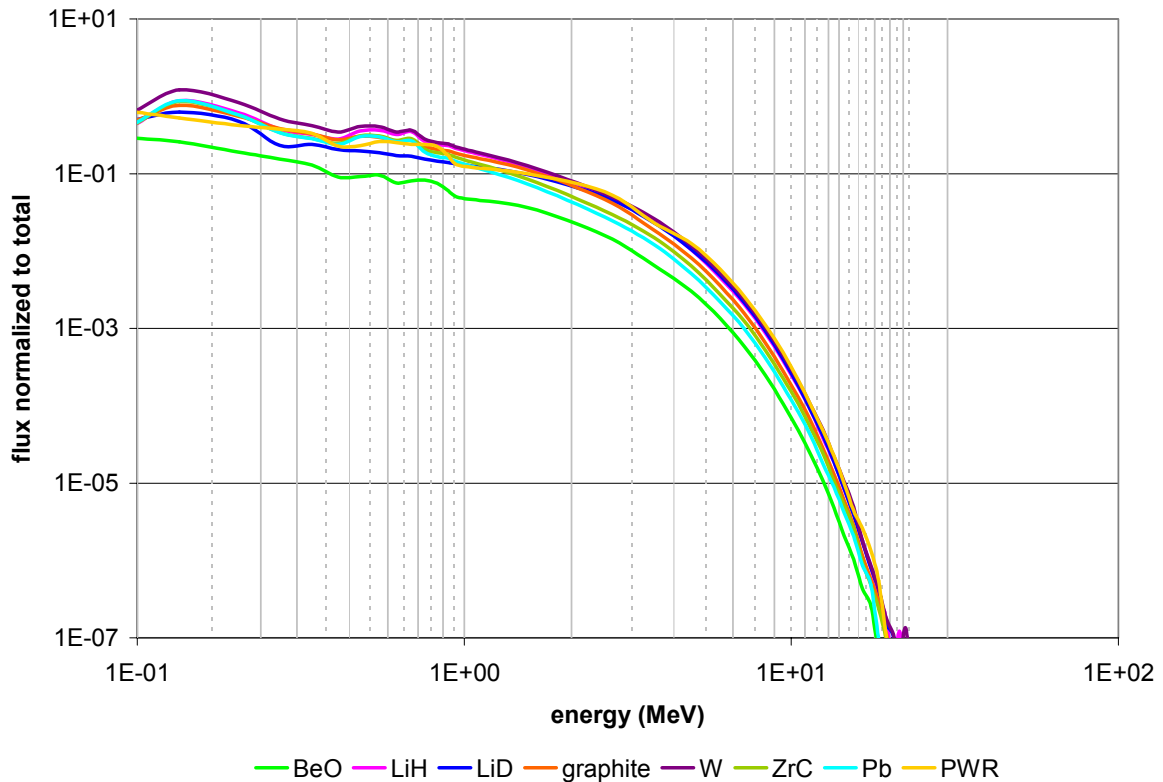


Figure 4-16. Average core spectrum obtained from each of the reflector materials for energies >100 KeV. Average standard deviation of 0.0818.

Spectral summary

One succinct way to compare spectral characteristics is to determine the average neutron energy of in each of the energy ranges. This information along with the average standard deviation is tabulated in Table 4-14.

In Table 4-14 The green highlight represents the maximum value in that row and the blue highlight represents the minimum value in that row. This confirms that BeO has the most thermal spectrum with the lowest average neutron energy in the thermal group, and the highest percentage of thermal neutrons.

The characteristics of the PWR and the ^7LiD spectra are similar. The average thermal neutron energy is the same, but the ^7LiD system has a higher percentage of neutrons in the thermal range than the PWR. The PWR has a harder spectrum than ^7LiD moderated GCR, which features maximum average neutron energy in the fast region among all of the examined systems. Among the GCRs, the reflector materials with a lower percentage of thermal neutrons actually produce spectra with lower average neutron energy in the fast region. The lowest average neutron energy in the fast region comes from a Pb-reflected system. This may be because many neutrons in these systems have high energy, causing increased leakage relative to thermal systems, and decreasing the average energy of fast neutrons. Additionally, neutrons in these systems tend to migrate to the epithermal range, indicated by the high average neutron energy and the high fraction of neutrons in this range. Thus, the average energy of fast neutrons is not a good indicator of how fast the neutron population actually is. The average energy of thermal neutrons and epithermal neutrons will be used to compare spectral characteristics of the GCRs.

Even from preliminary studies it has been evident that a W-reflected system would produce the fastest spectrum. This is because thermal neutrons are all captured by tungsten's resonances. The W system uses HEU to achieve criticality. The enrichment is 95 w/o. Recall from sensitivity studies that enrichment increases the percentage of fissions induced by neutrons with energy between 0.625 eV and 100 KeV. Indeed, 99% of the neutron

population in the W system is epithermal. However, W reflected GCR system will not be used for depletion studies because it is not practical.

The other fast spectra are from the ZrC and Pb systems. Aside from W, Pb has the lowest average thermal neutron energy, the lowest fraction of neutrons in the thermal range, and the highest fraction of neutrons in the epithermal and fast ranges. Although the ZrC spectrum has a high average thermal neutron energy, it is still quite different from the Pb spectrum. It still has the majority of its neutron in the thermal range, and its average thermal neutron energy is one order of magnitude less than that of Pb.

One goal of this part of the research is to obtain a wide range of neutron spectra for fuel cycle studies. This range must, of course include the extremes: a very thermal spectrum and a very fast spectrum. The two spectral extremes are obtained from the BeO and Pb systems. Because the W system is too impractical and the ^7LiH reflector did not serve the original intent of producing a thermal spectrum, these two materials will not be used for fuel cycle studies. Other reflector materials such as ^7LiD , graphite, and ZrC will serve as a bridge between the thermal and fast spectra.

Reflector Spectrum Characteristics

Figure 4-17 shows the average reflector spectra in for all GCRs and the PWR, even though in the PWR, the reflector is mainly used as a reflector and not a moderator. In the plots, the effect of the resonances in the reflector material itself is shown. In the epithermal region, where the core spectra are filled with depressions in the flux due to uranium resonances, the spectra are now fairly smooth for most reflector materials. The reflector with the most resonances of highest magnitude, tungsten, displays very strong depressions in the reflector spectrum. Among the reflector materials with resonances, the material with a lower average magnitude in the capture resonances than W is ZrC, and the lowest is Pb. This can

be observed in Figure 4-3. The spectrum for ZrC also shows prevalent depressions in the epithermal range. There are a few small depressions in the Pb spectrum.

The ${}^7\text{LiH}$ and ${}^7\text{LiD}$ reflector spectra are very similar. Both show a depression at about 0.26 MeV due to a resonance in ${}^7\text{Li}$. However, the ${}^7\text{LiH}$ shows a significantly larger fraction of fast neutrons.

Both BeO and graphite thermal spectra show a dramatic drop in the thermal neutron population at about $1\text{E-}9$ MeV. This is because both materials experience a sudden increase in their total cross sections close to this energy.

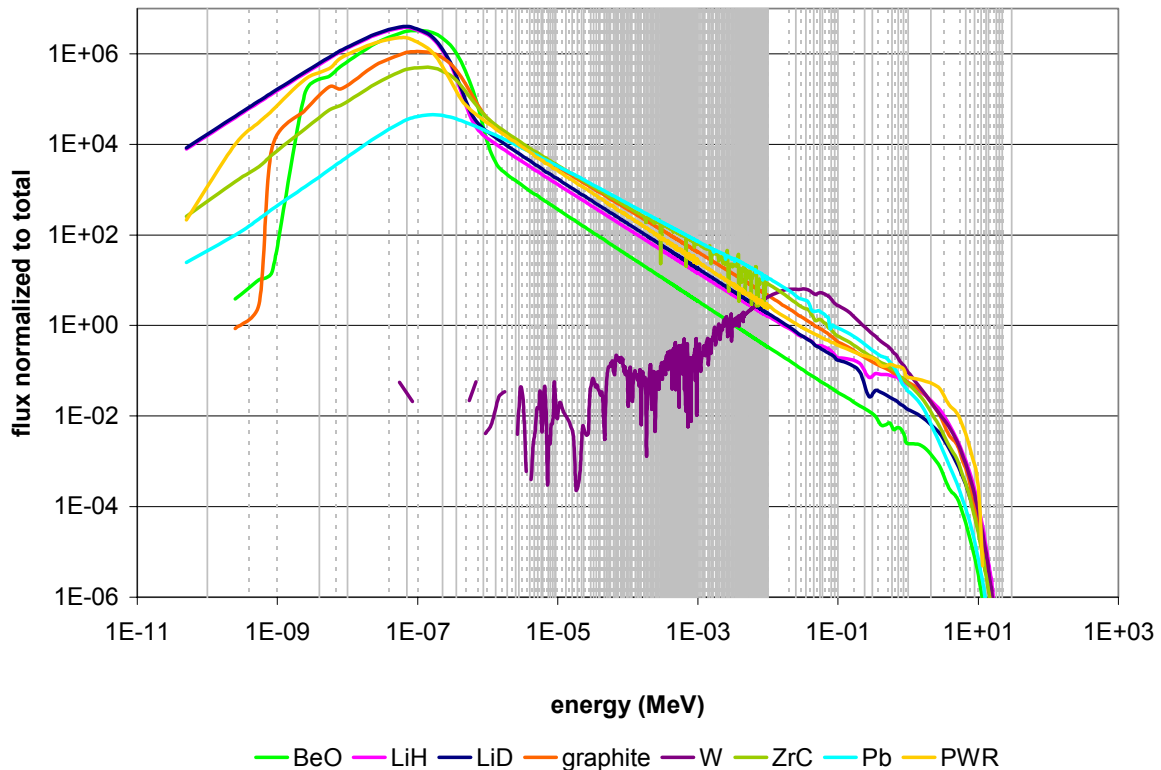


Figure 4-17. Average reflector spectrum of the reactor designs in Table 4-11. Average standard deviation excluding the tungsten data are 0.0231, 0.0069, and 0.0837 for the thermal, epithermal, and fast region, respectively.

In the epithermal range Pb yields the maximum neutron population. This is expected since epithermal neutrons cause the 71% of the fissions in the core, and constitute 76% of the neutron population.

The designs analyzed in this chapter yield a wide range of spectra, from the very thermal spectrum in the BeO system to a very fast spectrum in the Pb system. Other GCR designs such as ^7LiD , graphite, and ZrC, in their respective order, will serve as a bridge to show the transition between the thermal and fast spectra.

CHAPTER 5 FUEL CYCLE ANALYSIS

Five reflector materials are used for fuel cycle analysis: beryllium oxide (BeO), lithium-7 deuteride (Li^7D), graphite, zirconium carbide (ZrC), and lead (Pb). The design process using each reflector material is described in Chapter 4. The fuel cycle of these five GCRs are analyzed using MONTEBURNS.

Fuel Cycle Simulation

There are many ways to simulate the fuel cycle using MONTEBURNS. The variables include the burn step size, fuel feed format and enrichment, and the elements to be removed from the system.

Burn Step Size

The burn step size is the number of days that the fuel is “burned” or depleted. The user must specify the burn step size for each burn step. The smaller the burn step size, the more accurate the results. However, the computer time needed to obtain these results will increase. The choice of burn step size is a delicate balance between the accuracy desired and the time available. Actinides build in at the beginning of life; thus, shorter step sizes are required during this period. Current fuel cycles for most LWRs consist of three batches of fuel; each cycle is irradiated in the reactor for about 18 months. When the fuel is discharged it would have been irradiated for three cycles and a total of 1,643 days or 4.5 years. This is equivalent to a discharge burnup of about 40 to 50 GWD/MTU.

The actinide inventory experiences the most changes towards the beginning of the fuel cycle. Simulation of the first cycle for the PWR consists of 9 burn steps. The first 2 burn

step size is 30 days long, and the rest is 60 days long. The remaining burn steps gradually in step size. The step sizes are shown in Appendix C.

The GCRs are burned beyond 1,643 days. This is because the fuel is in gaseous form; fuel feed and fission product removal can be done online. Similar to the PWR, the actinide inventory experiences the most changes toward beginning of life. Thus, for the first 540 days (length of the first cycle in LWRs), the burn step sizes in the GCR simulation will coincide with those of the PWR. This is useful for comparing the actinide inventories of the GCRs to the actinide inventory of the PWR. After the first 540 days the step size increases gradually. This is done because of the long burn time necessary for the analysis of the GCR fuel cycle. The equilibrium actinide inventory for all the important actinides is desired. The important actinides are chosen based on criteria described in Chapter 3, and these actinides are listed at the end of the same chapter.

Feed Fuel

Because the fuel in GCRs are in gaseous form, refueling of the reactor can be done online. MONTEBURNS is able to simulate feeding fuel into the core continuously or at discrete times. The main objective is to keep the GCR critical at all time. If the fuel is fed into the core at discrete time intervals there must be enough excess reactivity in the core to maintain criticality until the next time the core is refueled. This excess reactivity must be suppressed via control drums so that the core does not become supercritical. Thus, simulating such a system would be laborious and superfluous.

A simpler way to simulate fuel feed is to continuously inject fuel into the core. Enough fuel would be fed into the core to maintain criticality. Using continuous feed also minimizes the uranium inventory in the core at any given time.

In MONTEBURNS the amount of fuel to be added into the core is indicated by the user in the feed file. Two feed values in units of grams per day are expected for each burn step. The first value is used for the beginning of the burn step and the second feed value is used for the end of the burn step. For continuous feed, the intermediate feed values are interpolated. In the MONTEBURNS output, two k-effective values are reported for each burn step: one for the middle of the burn step, and one for the end of the burn step. By changing the feed values for each burn step, the system is maintained critical throughout the life of the core. In fact, it is essential that the core k-effective is as close to 1.0 as possible, for proper simulation of the fuel cycle. Preliminary analysis show that if criticality is not maintained throughout the fuel cycle, large oscillations appear in the actinide inventories of the GCRs.

The feed fuel can be of any enrichment up to 20 w/o. However, to reduce the number of variables affecting criticality, the fuel enrichment throughout the fuel cycle is the same as the enrichment at the beginning of life (BOL).

Removal of Elements

MONTEBURNS have the capability to remove any atomic species indicated by the user. However, specific isotopes cannot be removed. This feature is not needed, because, in practice, filtering out specific isotopes from the fuel/fission product/actinide gaseous mixture is not possible. For example, removing Pu-240 from a Pu mixture is impossible because there is not enough mass difference between Pu isotopes.

For this research fission products are removed from the system for three reasons. First, some fission products are considered neutron poisons, having large capture cross sections. Removing fission products would improve neutron economy and decrease the amount of uranium required to maintain criticality. Second, filtering out fission products ensures that

the release of radioactivity during an accident is minimal. Last, fission products are short-lived compared to actinides. Thus, transmutation of fission products by increasing their neutron exposure (i.e. leaving them in the core) is not necessary. On the other hand, actinides are left in the core because they require neutron exposure to be able to transmute or fission into shorter-lived isotopes.

The fuel in the GCR circulates in the fuel loop between the core and the power conversion system. The fuel is also the thermal energy transport medium. The circulation of the fuel cannot be simulated in MONTEBURNS. Nevertheless, to approximate this behavior, the fuel that has not been burned is removed from the core, and new fuel is fed in. This method will not account for the overestimation of k -effective due to delayed neutrons that would not have been present in the core if circulation of the fuel was simulated.

MONTEBURNS Output

In the MONTEBURNS input file, with '.inp' file extension, the user indicates the important isotopes for which one group cross sections are obtained from MCNP. For an example of the MONTEBURNS input file see Appendix D. Generic cross sections from one of the libraries in ORIGEN are used for the isotopes not listed in the input file. These cross sections are used for fuel cycle calculations. The inventory for the isotopes listed in the input file are printed in the MONTEBURNS output. One of the tables from the MONTEBURNS output indicates the net amount of isotope inventory throughout the fuel cycle simulation. The table named "Monteburns Grams Produced (or Destroyed)" contains information on the mass of actinide for each burn step. The total actinide inventory for a particular time in the fuel cycle is obtained by adding the actinide inventory from the previous steps.

Burnup Calculation

The MONTEBURNS output also reports the burnup for each time step. However, if continuous fuel feed is used the value reported by MONTEBURNS is incorrect. This value is only based on the initial amount of fuel present in the core. The fuel fed into the system is not taken into account. For the correct burnup value the user must sum up the total fuel isotopes for each burn step. For uranium-based fuel the user must sum up the total mass of U-235 and U-238 isotopes for each burn step obtained from the table named “Monteburns Grams Produced (or Destroyed).” The burnup for burn step i is then:

$$BU_i = \frac{P \sum_{j=1}^i T_j}{\sum_{j=1}^i MTU_j},$$

where P is the thermal power in gigawatts, T_j is the burn step size in days for burn step j , and MTU_j is the net mass of uranium in for step j in metric tons. The burnup for step i is simply the thermal power multiplied by the total number of days from BOC to step i , divided by the total amount of uranium (initial and feed) from BOC to step i .

Issues with BeO Fuel Cycle Analysis

Results for the BeO reflected system could not be obtained. The k-effective of the BeO reflected system encountered much difficulty maintaining critical regardless of the amount of fuel that was fed into the system. The culprit was suspected to be that the burn step size was so large that the simulation method became invalid. However, even when the burn step size was shortened to less than 1 day, the system could not maintain critical.

Recall that the feed fuel enrichment for all GCRs is the same as the initial enrichment. All other GCRs with a fuel enrichment of 20 w/o were able to maintain critical throughout

the 20-year fuel cycle analyzed. It must be that the feed fuel (5 w/o enriched in U-235) in the BeO reflected GCR did not provide enough positive reactivity to counter the negative reactivity due to the presence of actinides. For future work the same system with higher feed fuel enrichment must be analyzed. Also, a new BeO reflected GCR design with an initial enrichment higher than 5 w/o can be obtained. An enrichment of 10 w/o is recommended so that comparisons can be made between the actinide inventories from the 20 w/o enriched GCRs and a 10 w/o enriched GCR.

Neutron Spectrum

The neutron spectra of all the GCR designs changes throughout the fuel cycle. This is due to absorption hardening as a result of the build up of actinides. The spectra of the GCRs compared to the reference PWR throughout the fuel cycle is shown in Figure 5-1. These are obtained from MONTEBURNS, with a fixed energy structure. There are six energy groups with the following upper energy limits:

- 0.1 eV,
- 1 eV,
- 100 eV,
- 1 MeV, and
- 20 MeV.

The BOL spectra shown in Figure 5-1A coincides with the more detailed spectra from Chapter 4. The ${}^7\text{LiH}$ and W reflected GCRs are exempt from fuel cycle studies due to the inability of these systems to meet the objectives of this research, and the BeO reflected GCR was unable to produce results. Of the GCR designs that remain, the Pb reflected GCR yields the hardest neutron spectrum and the ${}^7\text{LiD}$ reflected GCR yields the softest neutron spectrum

at BOL (0 days). The spectrum from the ^7LiD reflected design is also most similar to the spectrum from the reference PWR.

At the end of 4.5 years, the time at which fuel is discharged from the PWR, the GCRs' spectra are significantly harder than the PWR spectrum. Among the GCRs the Pb system still yields the hardest spectrum and the ^7LiD system the softest spectrum (see Figure 5-1B).

After 20 years the spectra from the ^7LiD and graphite reflected GCRs become harder than the spectrum from the ZrC reflected GCR.

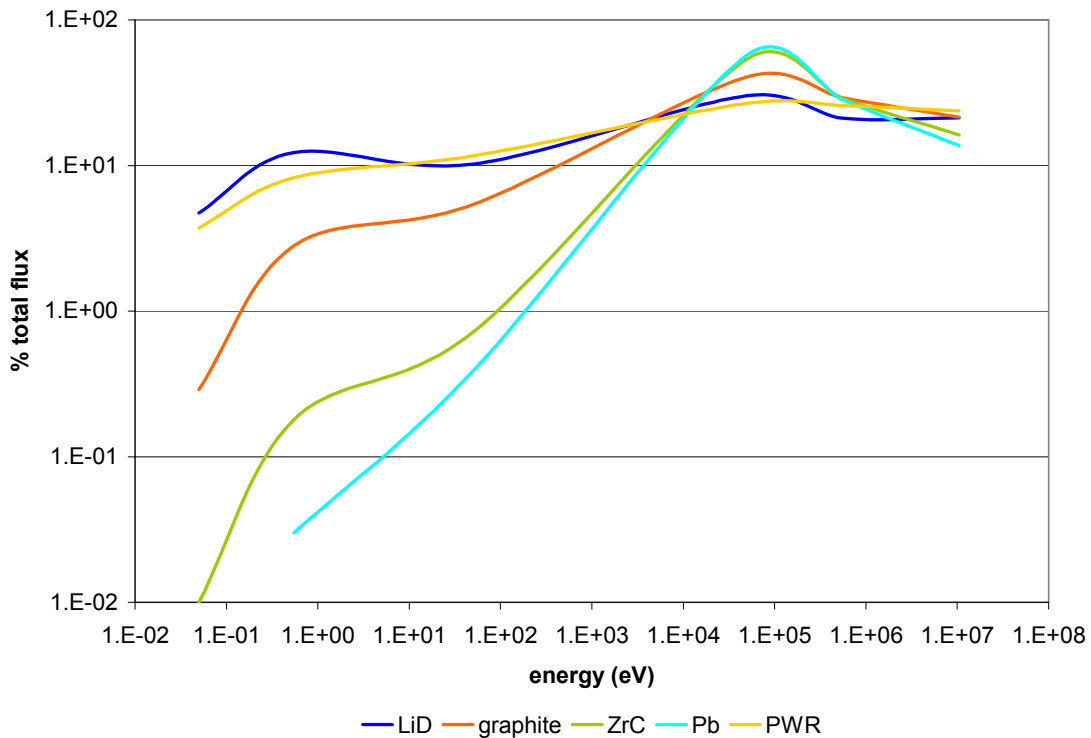
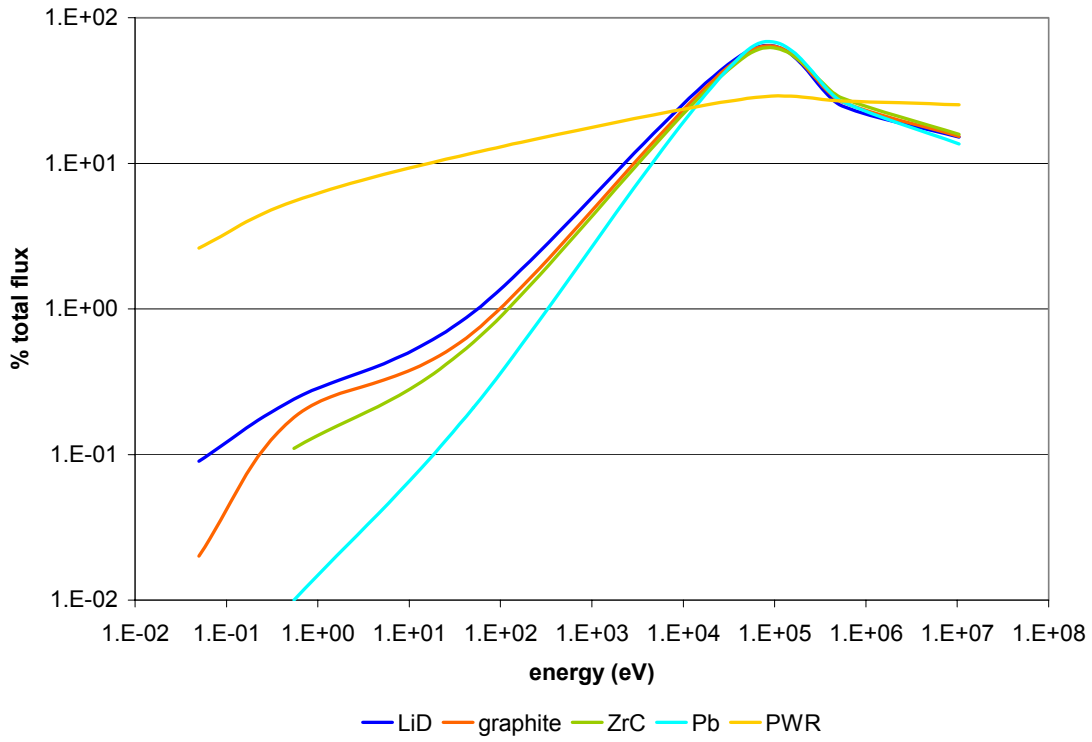
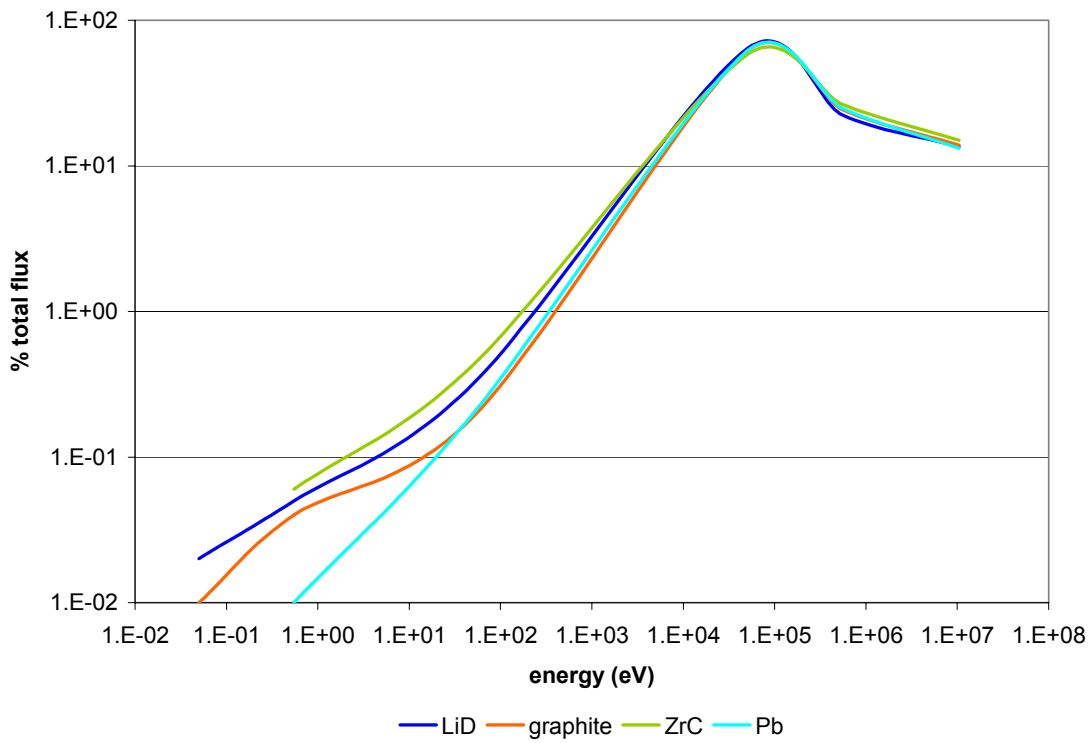


Figure 5-1. Six group core spectra at (A) BOL (0 days), (B) 4.5 years, and (C) 20 years. A



B



C

Figure 5-1. Continued.

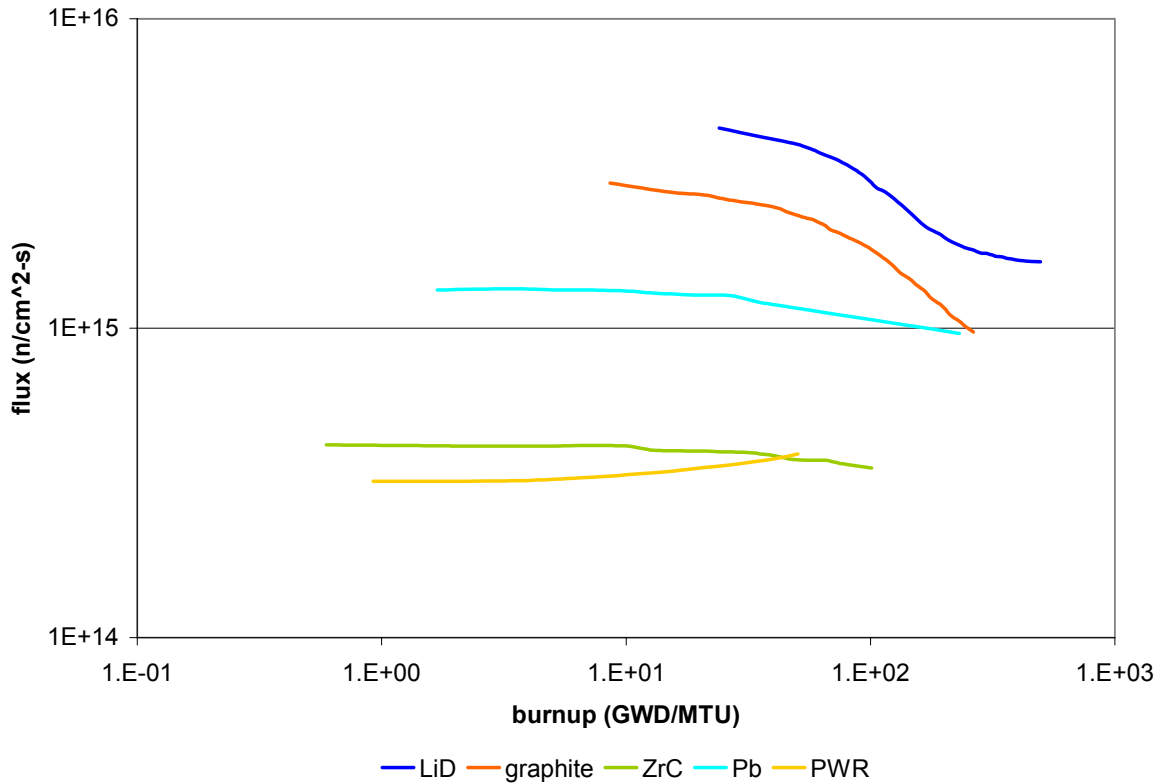


Figure 5-2. Total neutron flux as a function of fuel burnup.

A high neutron flux, on the order of $10^{15} \text{ cm}^{-2}\text{s}^{-1}$, is essential for the transmutation of actinides [16, 53]. Figure 5-2 shows that the ${}^7\text{LiD}$, graphite, and Pb reflected GCRs meet the flux level criteria. The ZrC reflected GCR design yields a flux level very similar to the reference PWR. Of the three GCRs that have a flux level on the order of $10^{15} \text{ cm}^{-2}\text{s}^{-1}$, both the graphite and Pb reflected systems show a decrease in the flux level potentially below $10^{15} \text{ cm}^{-2}\text{s}^{-1}$ beyond 20 years. The flux level of the ${}^7\text{LiD}$ reflected system show an approach to an equilibrium state where it reaches a value on the order of $10^{15} \text{ cm}^{-2}\text{s}^{-1}$.

Actinide Inventory

All actinides are left in the core with the intention of converting long-lived isotopes into shorter-lived isotopes through transmutation or fission. To determine the effectiveness

of the GCR in reducing waste and improving waste characteristics, the actinide inventories from GCRs must be compared to the actinide inventory from the reference PWR.

The fuel in the reference PWR is depleted during three cycles of 18 months in length. The burnup attained from MONTEBURNS is 50 GWD/MTU. This value is on the high end of the burnup values attained by current LWRs. However, since all GCRs are depleted for 20 years (or 7,300 days), using a burnup value of 40 GWD/MTU in the LWR as opposed to a burnup value of 50 GWD/MTU makes little difference when making comparisons with the GCRs. To compare the inventories of the PWR with the GCRs, the cumulative actinide inventory must be used. The 20-year fuel cycle in the GCRs is equivalent to 4.44 PWR fuel cycles. The cumulative PWR actinide inventory is 4.44 times the inventory of the spent fuel discharged per cycle. The fuel burnups achieved are shown in Table 5-1.

Table 5-1. Maximum fuel burnup attained for GCRs and the reference PWR. GCR values result from continuous feed of 19.95 w/o enriched fuel for 20 years. PWR burnup is the value obtained after 4.5 years of depletion.

reflector material	burnup (GWD/MTU)
LiD	495.43
graphite	263.41
ZrC	101.13
Pb	231.16
PWR	50.53

92-Uranium (U)

Other than the fuel isotopes, uranium isotopes result from decay of Pu isotopes or neutron capture by U-235. Almost all of the U-236 isotopes come from neutron capture interactions in U-235. This is because the parent nuclide of U-236 is Pu-240 with a long half life of 6.6E3 years. U-234 and U-237 have parents with relative short half lives of 87.7 years (Pu-238) and 14.4 years (Pu-241), respectively. Thus, during the time span encompassed by the fuel cycle analysis, some U-234 and U-237 isotopes have built-in from the decay of its

parent nuclides. At the end of 20 years for the GCRs and 4.44 cycles for the PWR, the uranium inventory is tabulated in Table 5-2.

Table 5-2. Inventory of uranium isotopes at the end of 20 years.
actinide inventory (g)

$T_{1/2}$ (yrs)	U-234	U-236	U-237	total
${}^7\text{LiD}$	2.46E+05	2.34E+07	1.85E-02	1.90E+06
graphite	1.58E+04	1.88E+06	1.96E+03	1.90E+06
ZrC	1.84E+04	2.97E+06	1.66E+03	2.99E+06
Pb	1.31E+04	4.92E+06	1.18E+03	4.93E+06
Pb	1.47E+04	3.63E+06	2.02E+03	3.64E+06
PWR	2.45E+03	1.75E+06	4.72E+03	1.76E+06

The U production in the the PWR and the GCRs is comparable. When only those isotopes with half lives greater than 1E4 years are considered such as U-234 and U-236, the PWR inventory is in the GCRs is larger by one order of magnitude for U-234 and comparable for U-236. When these inventories are normalized to the fuel burnup, the differences in the PWR and GCRs actinide inventories become more apparent.

Table 5-3. Inventory of uranium isotopes per unit burnup at the end of 20 years.
inventory per unit burnup

$T_{1/2}$ (yrs)	U-234	U-236	U-237	total
${}^7\text{LiD}$	2.46E+05	2.34E+07	1.85E-02	total
${}^7\text{LiD}$	3.19E+01	3.79E+03	3.96E+00	3.83E+03
graphite	6.99E+01	1.13E+04	6.30E+00	1.14E+04
ZrC	1.30E+02	4.87E+04	1.17E+01	4.88E+04
Pb	6.34E+01	1.57E+04	8.75E+00	1.58E+04
PWR	4.85E+01	3.47E+04	9.34E+01	3.48E+04

When normalized by the fuel burnup, the values in Table 5-3 represent the uranium isotopes produced as a result of the energy production process. The burnup value is not only a measure of the energy produced, but also how efficiently this energy is produced.

Normalizing the total actinide inventories by the burnup is an unbiased way to compare actinide inventories between different GCR designs and the GCRs with the reference PWR.

Thus, discussion of the actinide inventory from this point forward refers to the inventory normalized to the maximum achievable burnup.

The GCR with the least amount of uranium isotopes is the ⁷LiD reflected system by one order of magnitude. This is mainly due to high fuel burnup. When absolute values are considered the ⁷LiD system still produced the least amount of uranium isotopes among GCRs, but is comparable to the other GCRs.

Among the long-lived uranium isotopes, the PWR yields an amount of U-234 ($T_{1/2} = 2.46E5$ years) that is comparable to the GCRs. The same is true for the U-236 ($T_{1/2} = 2.34E7$ years) inventory, but the inventory in the spent fuel is one order of magnitude greater than the inventory from the ⁷LiD reflected GCR.

The ZrC reflected system produced the most long-lived uranium isotopes amongst all reactors considered; however, the ZrC system did not produce the most U-237 isotopes—the PWR spent fuel contained the most U-237 isotopes. Although U-237 is short-lived, it decays to Np-237, a long-lived actinide, and one of the key isotopes affecting HLW disposal. Nevertheless, the total uranium inventory in the ZrC system is about 40% greater than the uranium inventory in the PWR spent fuel.

93-Neptunium (Np)

The most important neptunium isotope is Np-237 because of its long half life ($T_{1/2} = 2.14E6$ years). Table 5-4 shows that the absolute amount of Np-237 produced is comparable for all systems, including the reference PWR. The largest Np-237 inventory comes from the Pb reflected system. When normalized to burnup, the Np-237 inventory in the PWR spent fuel is one order of magnitude greater than the ⁷LiD reflected GCR, but comparable to other GCR designs.

Table 5-4. Inventory of Np-237 and inventory per unit burnup at 20 years.

	inventory (g)	inventory/burnup
⁷ LiD	3.96E+05	7.99E+02
graphite	4.72E+05	1.79E+03
ZrC	4.01E+05	3.97E+03
Pb	5.34E+05	2.31E+03
PWR	3.26E+05	6.46E+03

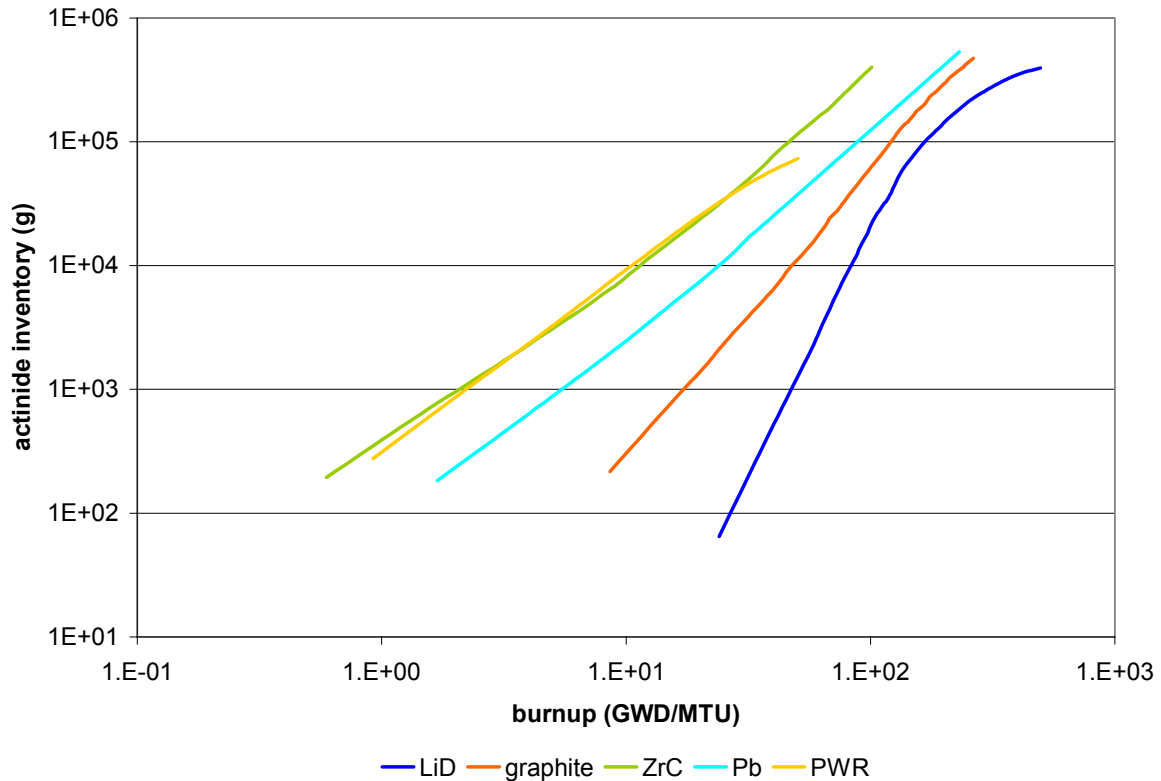


Figure 5-3. Np-237 mass as a function of fuel burnup.

The production of Np-237 is plotted in Figure 5-3. The production of Np-237 in the PWR and in the ZrC reflected GCR are very similar. Because the ZrC system achieves a higher burnup its normalized inventory value is 39% less than the inventory value in the PWR spent fuel. Notice that the curve representing the Np-237 mass in the ⁷LiD systems seems to start approaching an equilibrium value. This behavior is developing in the curve for the graphite reflected system. It is desired that the GCRs eventually achieve an equilibrium state. As energy is produced and the burnup increases, there are decreasingly smaller

increases in the Np-237 mass. Thus, when the Np-237 mass is normalized by the burnup, the ${}^7\text{LiD}$ system, and to some extent, the graphite reflected system yield the lowest Np-237 inventories amongst all systems analyzed.

The trend in Np-237 production coincides with the trends observed in the neutron flux level. Recall that the ${}^7\text{LiD}$ reflected system has the highest flux level followed by the graphite, Pb, and ZrC reflected GCRs. The lowest flux level is in the PWR core, but at the end of 4.5 years, the PWR flux level surpasses that of the ZrC reflected system. Similarly, the Np-237 inventory is minimum for the ${}^7\text{LiD}$ reflected system followed by graphite, Pb, PWR, and ZrC, for the same burnup.

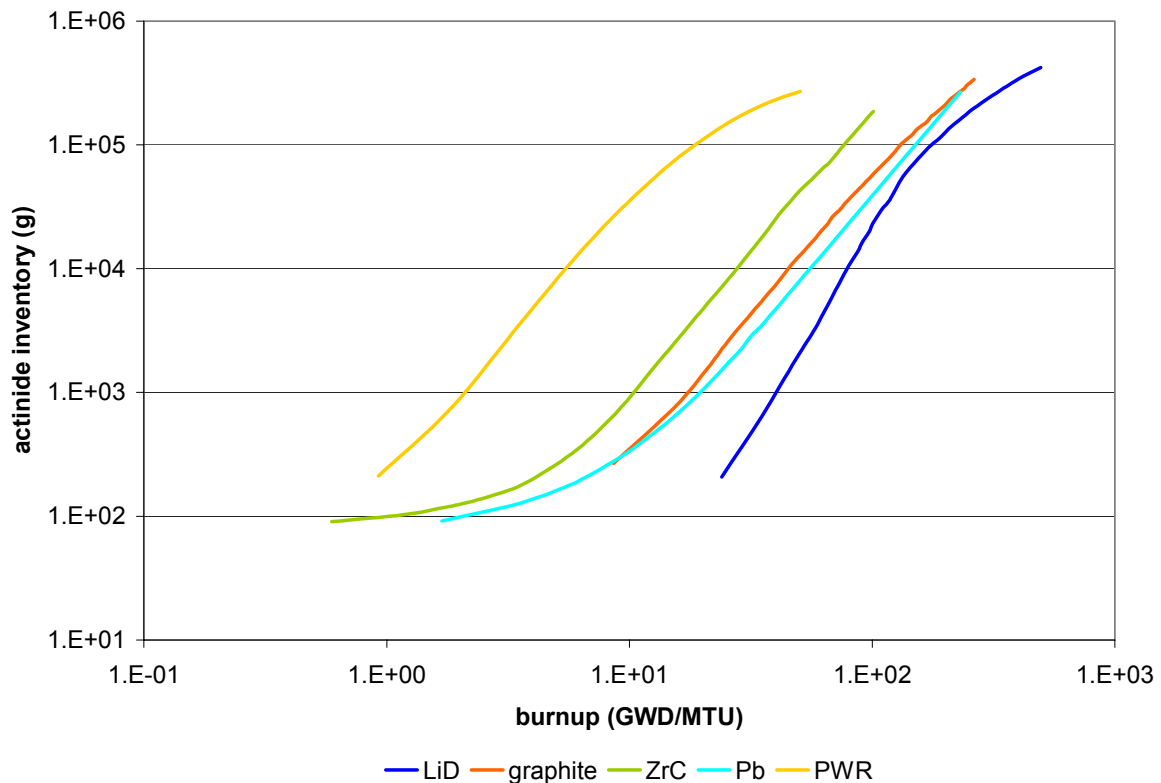


Figure 5-4. Mass of Np-237 feeders as a function of burnup. This is a sum of the masses of Am-241, Pu-241, and U-237.

Since Np-237 is a very important actinide as far as its effect on the waste disposal requirements, it is behooving to study the actinides that decay into Np-237 in a short period

of time. Figure 3-7 shows that both Am-241 and U-237 decays to Np-237 with half lives of 432.2 years and 6.75 days, respectively. However, Pu-241 decays to Am-241 rather quickly ($T_{1/2} = 23.45$ min), and Pu-241 also decays to U-237 ($T_{1/2} = 14.35$ yr). All three isotopes Am-241, U-237 and Pu-241 feed into Np-237. It is clear from Figure 5-4 that the PWR system has the largest concentration of Np-237 feeders. ${}^7\text{LiD}$, Pb, and graphite reflected systems have orders of magnitude less feeder inventory than in the PWR spent fuel for the same burnup. In fact, the feeder mass in the ${}^7\text{LiD}$ system is three orders of magnitude less than the mass in the PWR fuel.

Table 5-5. Percentage of neutrons with energy up to 1 MeV at 20 years.

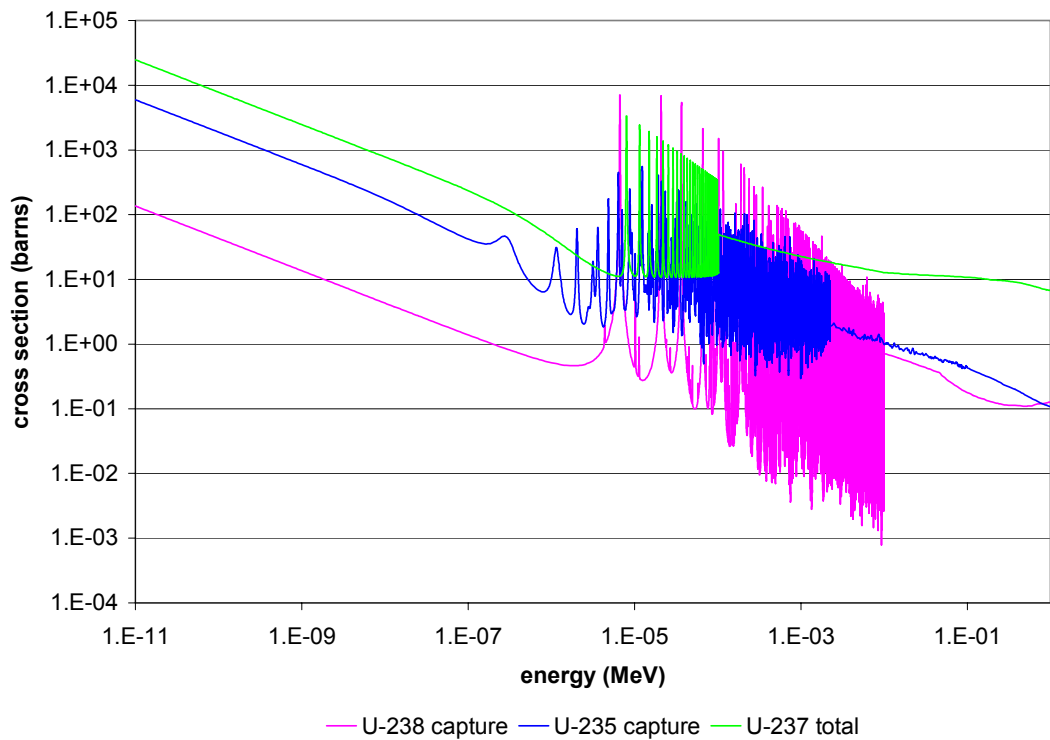
reflector	% of nts with enrg up to 1 MeV
${}^7\text{LiD}$	64.03
Pb	61.85
graphite	61.71
ZrC	58.51

The production behavior of Np-237 feeders is due to the spectral characteristics of the GCRs. Table 5-5 lists the percentage of neutrons with energy up to 1 MeV at 20 years for all GCRs analyzed. The ${}^7\text{LiD}$ reflected GCR has that highest percentage of neutrons in this energy range, followed by Pb, graphite, ZrC in decreasing order. A higher neutron population in this energy range decreases the production of Np-237 feeders (i.e. Am-241, Pu-241, and U-237).

Figure 5-5 plots the total neutron cross section for Np-237 feeders against the capture cross section of U-235 and U-238. Capture interactions in U-235 and U-238 produces actinides. Capture and fission interactions in the feeder isotopes destroy these feeder isotopes. Thus, a plot of the capture cross sections of fuel isotopes compared to the total

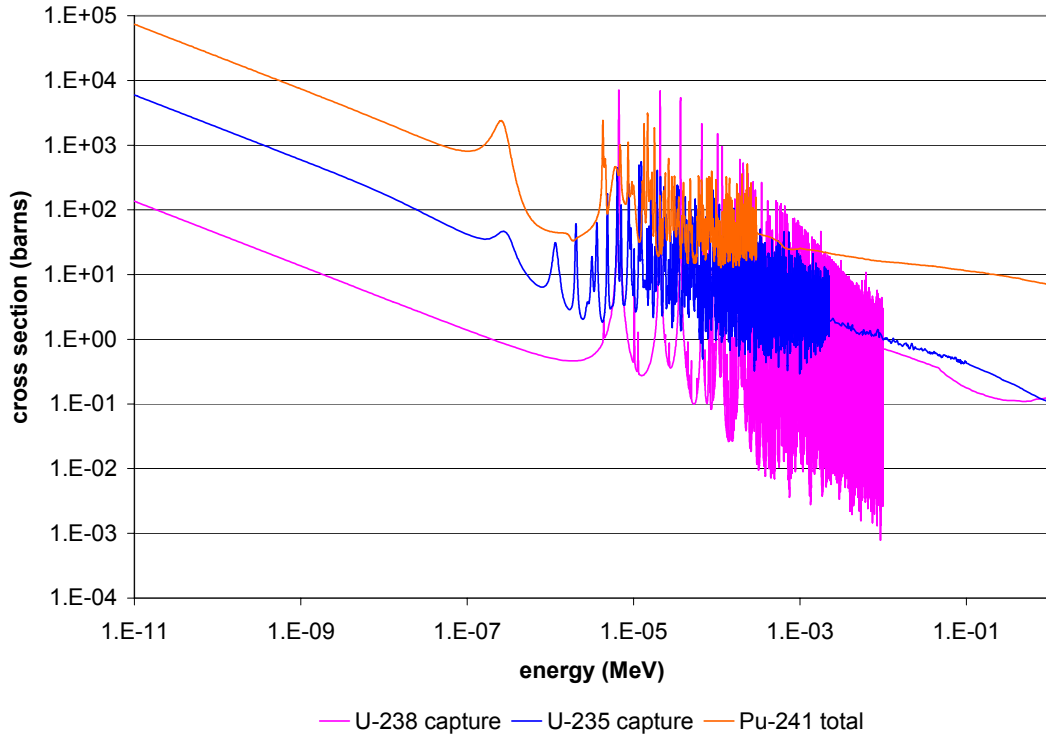
cross section of the feeder isotopes represents the competing events of feeder production and destruction.

Most of the resonances in the feeder isotopes are on average larger in magnitude than the resonances in U-235. At the lower energy end of the U-238 resonance region the magnitude of the resonances in feeder isotopes are comparable to the magnitude of the resonances in U-238. Towards both energy extremes shown in the figure the feeder isotopes have larger cross sections than both fuel isotopes. Hence, neutrons with energy up to 1 MeV are conducive to the transmutation of Np-237 feeder isotopes.

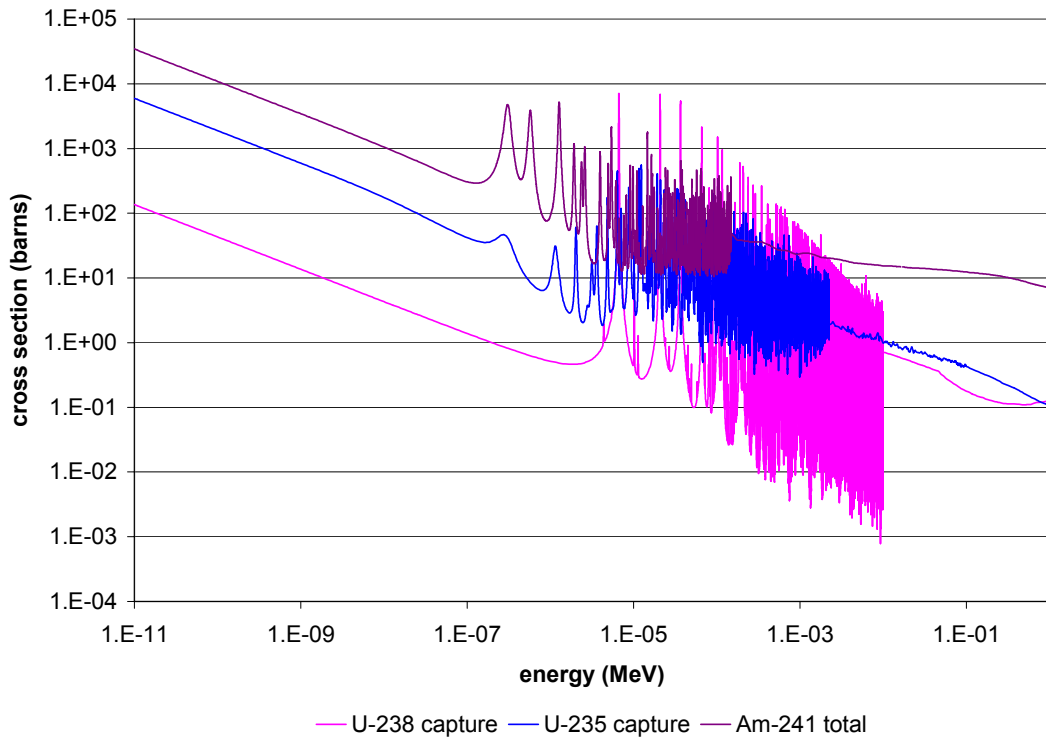


A

Figure 5-5. Total neutron cross section for (A) U-237, (B) Pu-241, and (C) Am-241 compared to U-235 and U-238 capture cross sections. Data is at 300 K from ENDF/B-VI [39].



B



C

Figure 5-5. Continued.

94-Plutonium (Pu)

Pu isotopes determine the proliferation resistance characteristics of a system. Some Pu isotopes are fissile (Pu-239 and Pu-241), and are used for nuclear weapons. The main isotope used for nuclear weapons is Pu-239. The presence of other Pu isotopes in the weapons material is considered a contaminant; this is especially true for the Pu isotopes with even mass numbers. This is because these isotopes have high specific heat and emit neutrons from spontaneous fission that complicates weapon design, and is detrimental to the reliability of the weapon. This is especially true for Pu-238 and Pu-240 isotopes. Pu isotopes are so close in mass that separation of individual isotopes is not currently possible. A high fraction of Pu-238 and Pu-240 in the Pu mixture and low fissile material inventory is the desired condition for improving proliferation resistance of the system.

Table 5-6. Inventory of plutonium isotopes at the end of 20 years.

	actinide inventory (g)					
$T_{1/2}$ (yrs)	Pu-238	Pu-239	Pu-240	Pu-241	Pu-242	total
⁷ LiD	3.07E+05	4.56E+06	2.06E+06	3.56E+05	1.16E+05	7.40E+06
graphite	2.73E+05	6.78E+06	1.84E+06	2.65E+05	6.14E+04	9.22E+06
ZrC	9.18E+04	9.82E+06	1.04E+06	1.46E+05	1.00E+04	1.11E+07
Pb	2.23E+05	8.86E+06	1.93E+06	2.20E+05	2.58E+04	1.13E+07
PWR	1.99E+05	3.58E+06	1.22E+06	1.15E+06	4.63E+05	6.62E+06
	inventory per unit burnup					
⁷ LiD	6.20E+02	9.20E+03	4.16E+03	7.19E+02	2.34E+02	1.49E+04
graphite	1.04E+03	2.57E+04	6.99E+03	1.01E+03	2.33E+02	3.50E+04
ZrC	9.08E+02	9.71E+04	1.03E+04	1.44E+03	9.89E+01	1.10E+05
Pb	9.65E+02	3.83E+04	8.34E+03	9.52E+02	1.12E+02	4.87E+04
PWR	3.94E+03	7.09E+04	2.42E+04	2.27E+04	9.17E+03	1.31E+05

Table 5-6 contains the Pu inventory. It is difficult to assess the proliferation characteristics of the systems. The systems with low fissile material inventory does not necessarily have high inventory of the even mass-numbered isotopes. One important observation from Table 5-6 is that the PWR produces the most Pu per unit burnup than all

GCRs. The Pu inventory per unit burnup is one order of magnitude greater than the GCRs, except for the ZrC reflected system. The Pu inventory in the ZrC reflected system is comparable to the inventory in the PWR spent fuel.

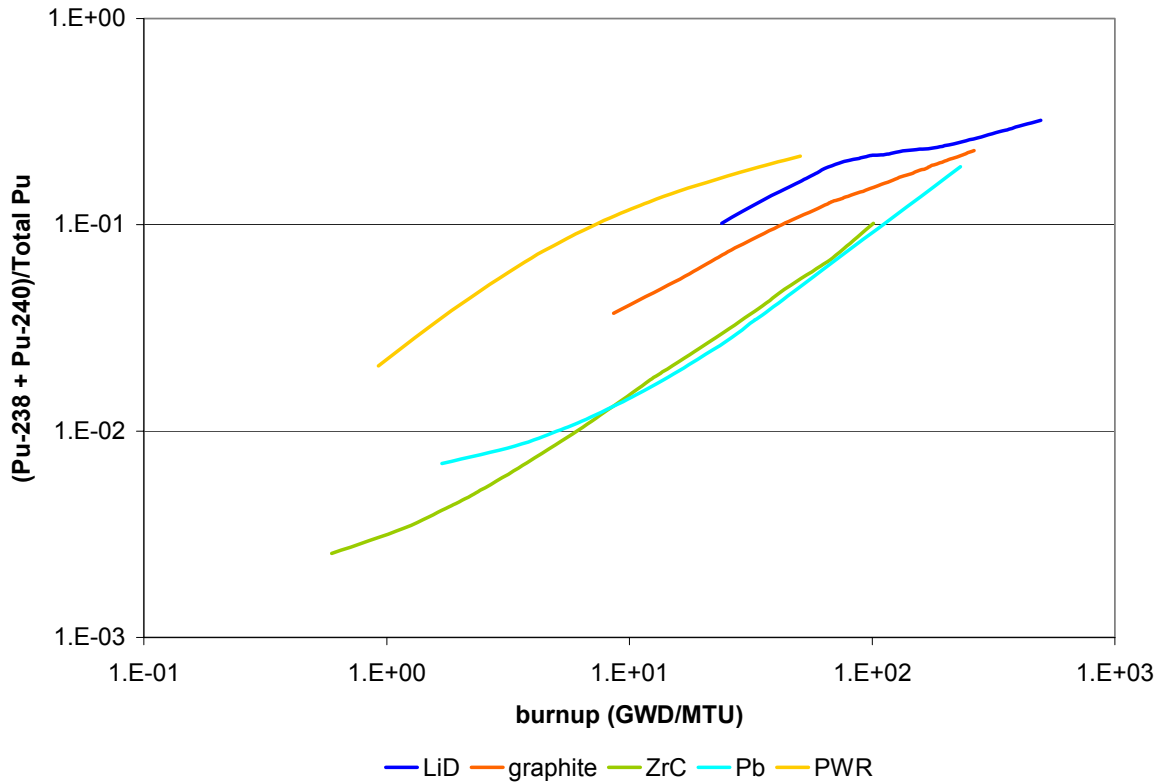


Figure 5-6. Ratio of Pu-238 and Pu-240 mass to total Pu mass.

Figure 5-6 provides more insight into the proliferation characteristics of the system considered. At the spent fuel discharge burnup the PWR system yields a Pu mixture with the highest ratio of Pu-238 and Pu-240 mass to the total Pu mass. The proliferation resistance characteristics of the GCRs improve with burnup. It is apparent that as the spectrum in the GCR is more thermal at BOL, the better is its proliferation resistance. Recall from the previous chapter that the percentage of neutrons in the thermal energy range (< 2 eV) at BOL for ${}^7\text{LiD}$, graphite, ZrC, and Pb are 99%, 79%, 51%, and 24%, respectively.

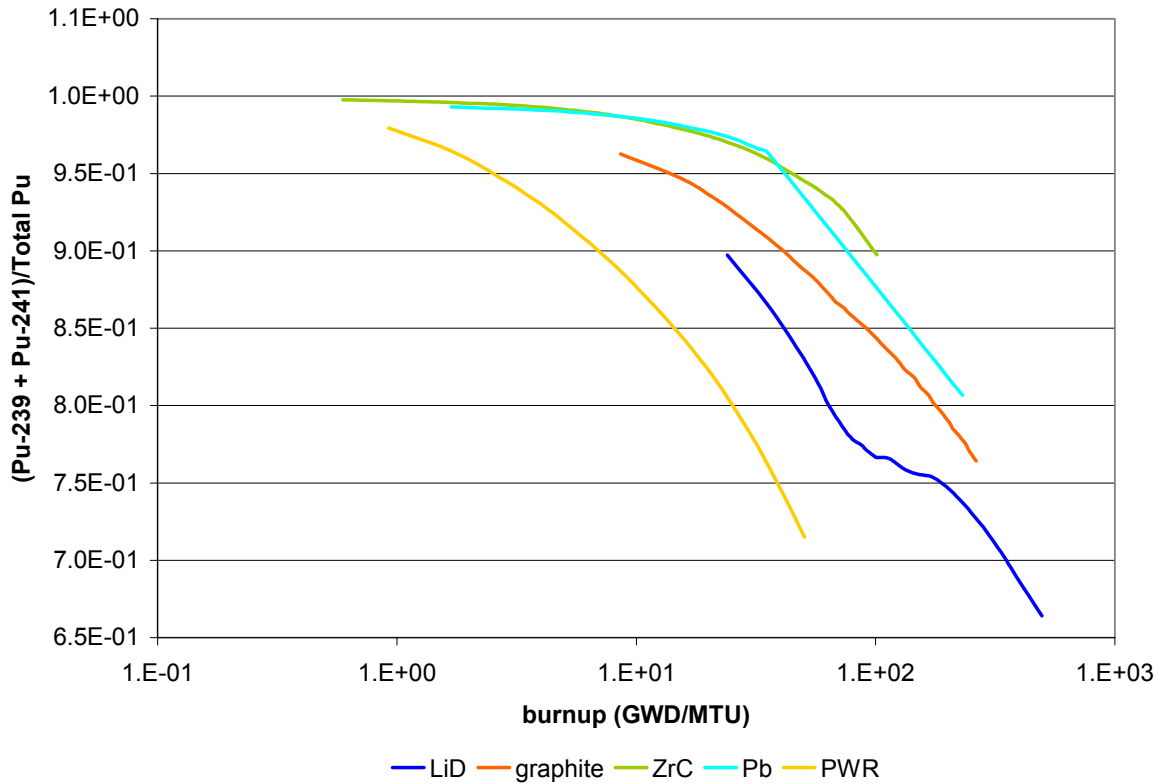


Figure 5-7. Fraction of fissile (Pu-239 and Pu-241) isotopes in Pu.

The same trend is observed with the fraction of fissile isotopes in Pu. The PWR spent fuel contains the smallest fraction of fissile isotopes. As the spectrum of the GCRs is more thermal, the fraction of fissile isotopes decreases. Thus, thermal spectrum in a GCR improves the proliferation resistance of the system.

95-Americium (Am)

Most americium isotopes are short lived. The longest half life is only 7.37E3 years (Am-243). The most important of the Am isotopes is Am-241. It decays to Np-237 ($T_{1/2} = 2.14E6$ yr).

The total Am inventory per unit burnup in the PWR spent fuel is one order of magnitude larger than the GCRs. Among the GCRs, ${}^7\text{LiD}$ produces the least amount of Am, but all GCRs yield comparable inventories of this isotope.

Table 5-7. Inventory of americium isotopes and inventory per unit burnup at 20 years.
actinide inventory (g)

$T_{1/2}$ (yrs)	Am-241	Am-242	Am-243	total
⁷ LiD	6.45E+04	1.91E+03	3.58E+04	1.02E+05
graphite	7.11E+04	2.06E+03	1.66E+04	8.98E+04
ZrC	4.07E+04	7.21E+02	1.33E+03	4.28E+04
Pb	4.57E+04	1.11E+03	3.82E+03	5.06E+04
PWR	4.78E+04	8.78E+02	1.59E+05	2.08E+05
actinide inventory per unit burnup				
⁷ LiD	1.30E+02	3.86E+00	7.23E+01	2.06E+02
graphite	2.70E+02	7.82E+00	6.30E+01	3.41E+02
ZrC	4.02E+02	7.13E+00	1.32E+01	4.23E+02
Pb	1.98E+02	4.81E+00	1.65E+01	2.19E+02
PWR	9.47E+02	1.74E+01	3.15E+03	4.11E+03

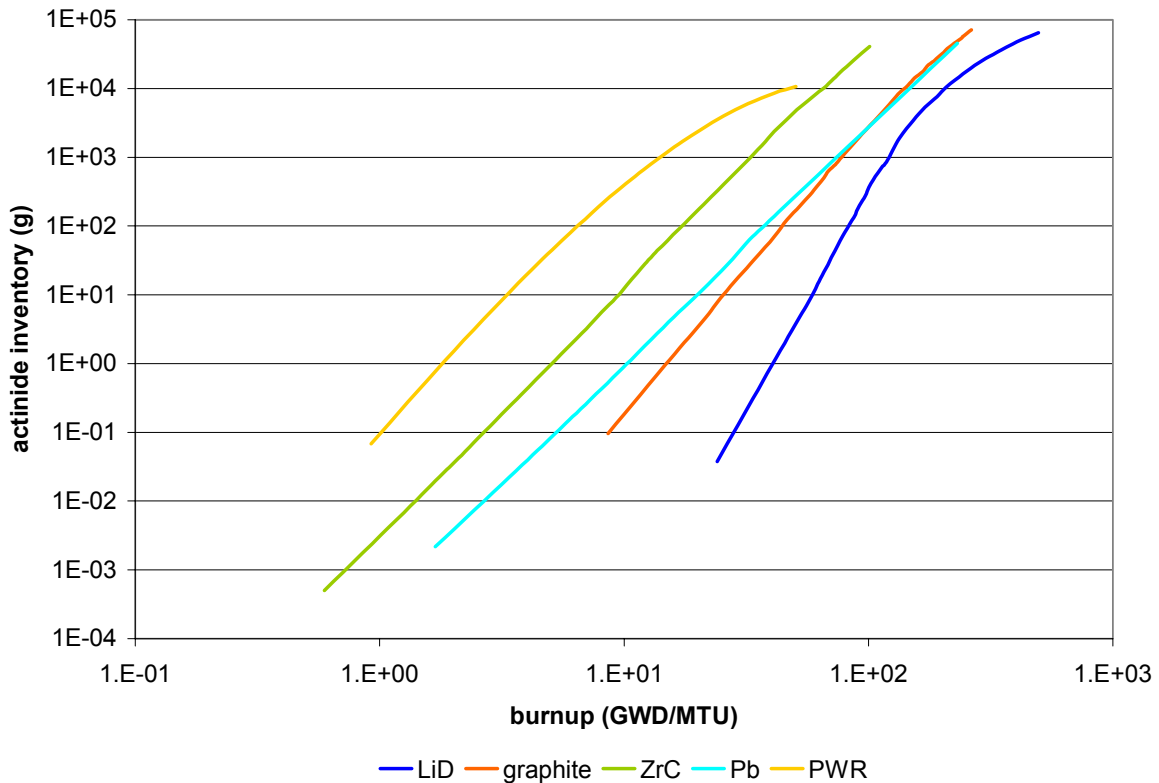


Figure 5-8. Am-241 mass as a function of fuel burnup.

The PWR spent fuel inventory of Am-241 is on the same order of magnitude as the inventories from GCRs. However, at the PWR discharge burnup of 50 GWD/MTU the spent fuel Am-241 inventory is at one order of magnitude greater than the inventory from Pb and

graphite reflected systems and five orders of magnitude greater than the Am-241 inventory from the ^7LiD reflected system. As burnup increases beyond 100 GWD/MTU, the Pb reflected system, produces less Am-241 than the graphite reflected system. This same trend is observed with the Np-237 feeders; maximizing the neutron population with energy up to 1 MeV reduces the Am-241 production. This is due to the cross section characteristics of Am-241. For more detailed discussion refer to the Np section and Figure 5-5.

96-Curium (Cm)

Table 5-8. Inventory of curium isotopes at 20 years.

$T_{1/2}$ (yrs)	actinide inventory (g)							
	Cm-242	Cm-243	Cm-244	Cm-245	Cm-246	Cm-247	Cm-248	total
^7LiD	4.8E+03	4.4E+02	2.8E+04	6.6E+03	1.6E+03	1.4E+02	2.4E+01	4.2E+04
graphite	2.7E+03	2.1E+02	8.6E+03	1.7E+03	2.0E+02	1.1E+01	9.9E-01	1.3E+04
ZrC	7.4E+02	2.2E+01	2.2E+02	1.3E+01	2.5E-01	3.2E-03	6.1E-05	1.0E+03
Pb	1.6E+03	8.6E+01	9.8E+02	9.9E+01	4.2E+00	1.1E-01	4.0E-03	2.8E+03
PWR	1.7E+04	5.3E+02	9.6E+04	9.2E+03	1.0E+03	2.0E+01	1.8E+00	1.2E+05
inventory per unit burnup								
^7LiD	9.6E+00	8.9E-01	5.7E+01	1.3E+01	3.1E+00	2.9E-01	4.9E-02	8.4E+01
graphite	1.0E+01	7.9E-01	3.3E+01	6.4E+00	7.6E-01	4.0E-02	3.8E-03	5.1E+01
ZrC	7.4E+00	2.2E-01	2.2E+00	1.2E-01	2.4E-03	3.1E-05	6.0E-07	9.9E+00
Pb	6.8E+00	3.7E-01	4.2E+00	4.3E-01	1.8E-02	4.9E-04	1.7E-05	1.2E+01
PWR	3.4E+02	1.0E+01	1.9E+03	1.8E+02	2.0E+01	3.9E-01	3.5E-02	2.4E+03

The Cm inventory per unit burnup from the PWR spent fuel is at least two orders of magnitude larger than the inventory from the GCRs. Recall that Cm isotopes are daughters of Am isotopes. Since GCRs produce less Am isotopes, they also produce less Cm isotopes. Due to lower fuel burnup, Cm in the PWR does not get enough neutron exposure to start the transmutation process. Among the GCRs the total Cm inventory decreases with flux level. A lower flux level in the GCRs is more conducive to the reduction of Cm inventory.

Waste Characteristics

The actinides are grouped according to half lives and shown in Table 5-9. The actinides which fall under the groupings shown in the table are:

- > 100 years but < 1,000 years: Am-241
- > 1,000 years but < 10 thousand years: Pu-240, Am-243, Cm-245, and Cm-246
- > 10 thousand years: U-234, U-236, Np-237, Pu-239, Pu-242, Cm-247, and Cm-248

The actinide inventory per unit burnup from the PWR discharged fuel is one order of magnitude the inventory from the GCRs. The spent fuel actinide inventory is very similar to the inventory from the ZrC reflected system. The total long-lived (>100 years) actinide inventory depends on the flux level. Recall that the system with the highest flux level and lowest long-lived actinide inventory is the ⁷LiD reflected system, followed by the graphite, Pb, PWR, and ZrC systems.

Table 5-9. Inventory of actinides grouped by half life and inventory per unit burnup of at 20 years.

T _{1/2} (yrs)	total actinide inventory (g)			
	> 1E2 yrs	> 1E3 yrs	> 1E4 yrs	total
⁷ LiD	6.45E+04	2.10E+06	6.97E+06	9.14E+06
graphite	7.11E+04	1.86E+06	1.03E+07	1.22E+07
ZrC	4.07E+04	1.04E+06	1.52E+07	1.62E+07
Pb	4.57E+04	1.93E+06	1.31E+07	1.50E+07
PWR	4.80E+04	1.39E+06	6.12E+06	7.56E+06
inventory per unit burnup				
⁷ LiD	1.30E+02	4.25E+03	1.41E+04	1.84E+04
graphite	2.70E+02	7.06E+03	3.91E+04	4.64E+04
ZrC	4.02E+02	1.03E+04	1.50E+05	1.61E+05
Pb	1.98E+02	8.35E+03	5.65E+04	6.51E+04
PWR	9.50E+02	2.75E+04	1.21E+05	1.50E+05

The isotopes with T_{1/2} > 100 years and T_{1/2} < 1,000 years only consists of Am-241.

This isotope is minimized in the ⁷LiD reflected system because it has the largest percentage of neutrons with energy under 1 MeV. For detailed discussion refer to the Np section in this chapter.

The inventory of actinides with 1E3 < T_{1/2} < 1E4 yrs from spent fuel at the PWR discharge burnup is three orders of magnitude greater than the inventory from the ⁷LiD

reflected GCR, and about one order of magnitude greater than the inventory from the graphite and Pb reflected GCRs. The production of actinides with half lives in this range is minimized as the neutron flux level is maximized.

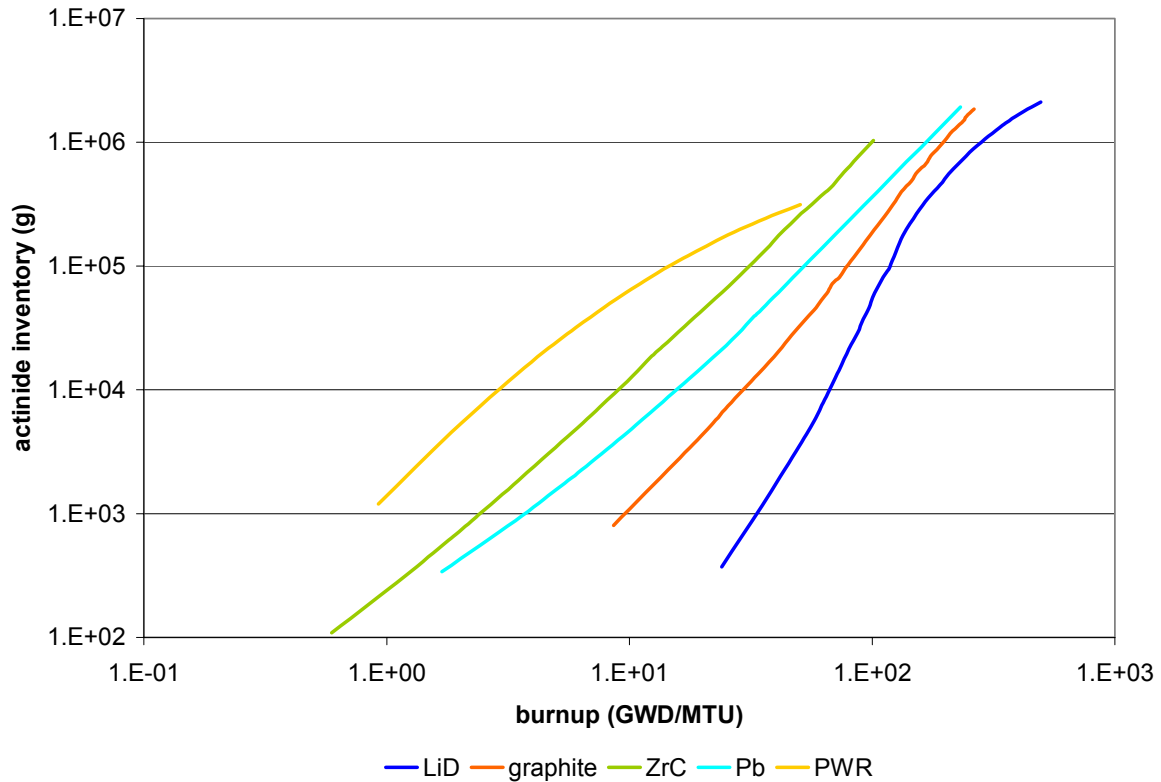


Figure 5-9. Mass of actinides with half lives greater than 1E3 years and less than 1E4 years.

One factor affecting the burner capabilities of a system is the flux level. Paternoster indicates that one important characteristic that is needed for transmutation is a flux on the order of $10^{15} \text{ cm}^{-2}\text{s}^{-1}$ [53]. Figure 5-2 shows that the ^7LiD , graphite, and Pb reflected systems meet this condition throughout the 20 years for which the fuel cycle is analyzed. The highest flux level is found in the ^7LiD system, and the lowest flux level is found in the PWR. The flux level indeed is very important to the actinide inventory. When normalized to the burnup the total amount of actinides produced increases as the flux level decreases. Thus, the most actinides produced with half lives greater than 100 years is the PWR, with the lowest flux

level, and the least actinides produced is in the ${}^7\text{LiD}$ system, with the highest flux level. The same production trend is observed for actinides with $T_{1/2} > 1\text{E}4$ yrs (see Figure 5-10).

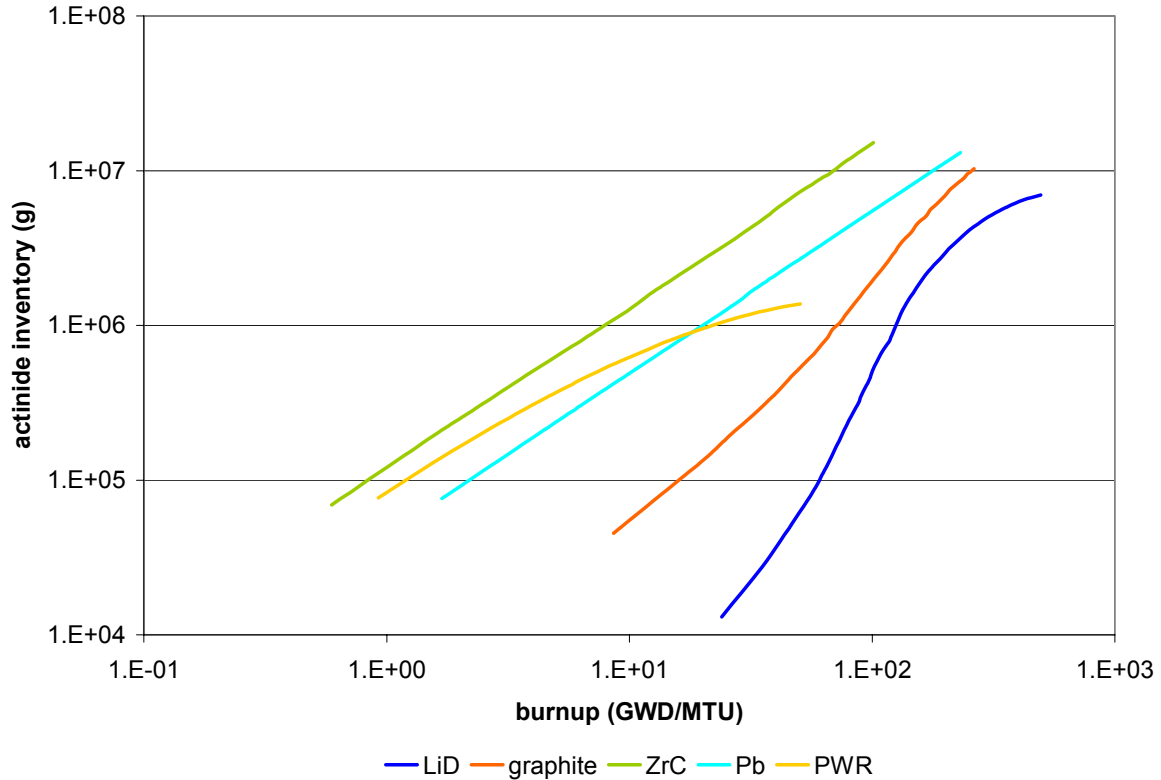


Figure 5-10. Mass of actinides with half lives greater than 1E4 years.

Most fission products are not of great concern because they are short-lived. Fission products such as I-129 ($T_{1/2} = 1.57\text{E}7$ yrs), and Cs-135 ($T_{1/2} = 2.3\text{E}6$ yrs) are long lived. The fission product inventory from the PWR is comparable to the inventory from GCRs, except for the ZrC reflected system. The ZrC reflected GCR is produces one order of magnitude more fission products than all other reactors. This is mainly due to low fuel burnup.

Fuel Utilization

Table 5-11 shows that the fuel utilization in the GCR is far superior to the PWR, except for the ZrC reflected GCR design. Even when a highly absorbent reflector is used (such as ZrC and Pb), the total amount of uranium used is less than the uranium required by the PWR.

Because ZrC has large capture resonances, the burnup at 1,643 days is less than the PWR; much more fuel is needed for the same thermal power output to compensate for the reactivity loss due to neutron captures in the reflector. In the area of fuel utilization the PWR outperforms the ZrC reflected GCR. All other GCRs show an improvement over the PWR.

Table 5-10. Inventory of long lived fission products and inventory per unit burnup at 20 years.

T _{1/2} (yrs)	fission product inventory (g)		
	I-129	Cs-135	total
⁷ LiD	1.09E+05	1.26E+06	1.37E+06
graphite	1.13E+05	9.28E+05	1.04E+06
ZrC	1.09E+05	1.20E+06	1.30E+06
Pb	6.02E+03	1.35E+06	1.36E+06
PWR	1.36E+05	3.64E+05	5.00E+05
fission product per unit burnup			
⁷ LiD	2.19E+02	2.54E+03	2.76E+03
graphite	4.29E+02	3.52E+03	3.95E+03
ZrC	1.08E+03	1.18E+04	1.29E+04
Pb	2.60E+01	5.85E+03	5.88E+03
PWR	2.69E+03	7.20E+03	9.89E+03

Table 5-11. Fuel utilization summary of GCRs and the reference PWR.

	burnup at 1,643 days	total fuel used in 20 yrs	
	(GWD/MTU)	MTU	MT U-235
⁷ LiD	162.50	44.35	8.85
graphite	116.25	83.14	16.59
ZrC	28.84	216.56	43.20
Pb	62.84	94.74	18.90
PWR	50.53	487.64	15.60

Recall that the graphite system does not use a reflector that is at saturation thickness. The saturation thickness of graphite is 110 cm, but a reflector thickness of 26 cm was used. This was done to obtain a spectrum that could be used as a transitional bridge between the thermal and fast spectra. By using a small reflector thickness, leakage of neutrons is larger than at saturation thickness. Thus, to compensate for the loss in reactivity more fuel must be

used. Even with a reactor design that results in a lot of leakage, the total fuel used and the burnup of graphite is comparable to other GCR designs.

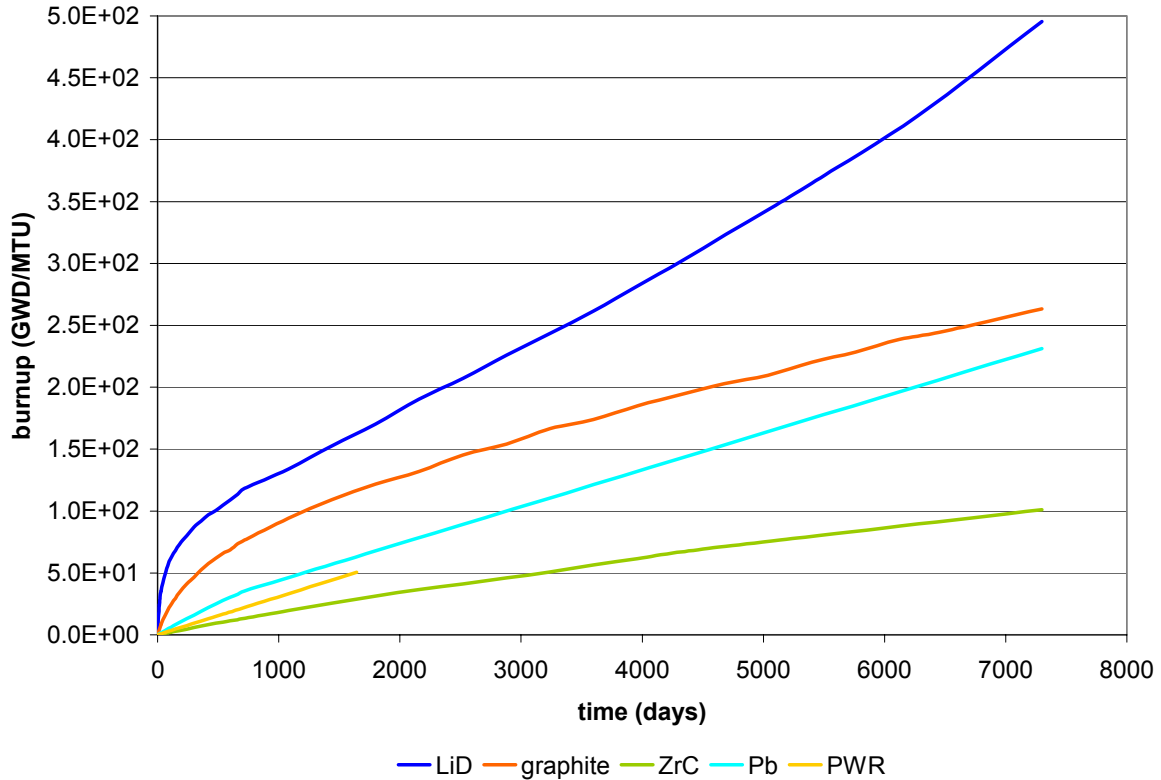


Figure 5-11. Burnup of the GCRs compared to the reference PWR.

Amongst the reactors analyzed the ${}^7\text{LiD}$ reflected system is the optimal design for fuel utilization. The burnup of this system is a factor of 3 greater than the discharge burnup of the PWR for the same amount of days, and the total amount of U-235 used is about half as much.

In general the ${}^7\text{LiD}$, graphite, and Pb reflected GCRs shows improvements over the reference PWR as far as:

- decreasing the Np-237 inventory and its feeders,
- decreasing the total waste produced,
- decreasing long-lived waste ($T_{1/2} > 100$ years), and

- increasing in fuel utilization.

The GCRs did not yield a Pu mixture that is more proliferation resistant than the PWR for a given burnup. However, the proliferation resistance characteristics of the GCRs improve with fuel burnup.

CHAPTER 6
CONCLUSIONS AND RECOMMENDATIONS FOR FUTURE WORK

Fuel Cycle Analysis Conclusions

The findings from the fuel cycle analysis are summarized in the following list.

- The reflector material is the single most important design parameter in determining the spectral characteristics of the core.
- The gaseous fuel pressure is the most effective way to control reactivity. This also has the fastest response time.
- To increase the thermal neutron population low gaseous fuel pressure, low enrichment, and internal moderation must be employed.
- To increase the epithermal and fast neutron population high fuel gas pressure and high enrichment must be employed, with an upper limit of 155 bars and 20 w/o, respectively.
- Among the reflector materials analyzed, BeO yields the softest neutron spectrum and W yields the hardest neutron spectrum.
- All GCRs studied in the fuel cycle analysis, except for the ZrC reflected system, show improved characteristics over the PWR in the areas of total long-lived actinide inventory, Np-237 inventory, Np-237 feeder inventory, and fuel utilization.
- The PWR produces a more proliferation resistant mixture of Pu at the spent fuel discharge burnup.
- In GCRs a soft spectrum is effective in improving the proliferation resistance characteristics of the Pu mixture.
- With increased burnup the Pu mixture in the GCRs becomes more proliferation resistant.
- A GCR with highest flux level produces the least amount of total actinides, the least amount of actinides with half lives greater than 1,000 years, and the least amount of Np-237.
- The increase in the neutron population with energies up to 1 MeV decreases the production of Np-237 feeders (U-237, Pu-241, and Am-241).

- A thermal spectrum in GCRs improves fuel utilization.

Recommendations For Future Work

The GCR is a very novel reactor concept. The amount of research on the GCR is miniscule compared to well-understood systems such as LWRs. Much more analysis is needed to determine the plausibility of the GCR as an economical system for commercial power production, in addition to proving that the GCR possesses improved features over current technologies.

As an extension of the reflector material sensitivity study, other moderator materials shall be investigated such as heavy water. This is because beryllium is an expensive material, much more so than heavy water. Additionally, the effect of a combination of different reflector/moderator materials should be studied. For example, reflector/moderator consisting of 15-20 cm of BeO outside the fuel cavity, surrounded by heavy water. This will reduce plant capital costs by reducing the amount of beryllium, while benefiting from the reactivity gain from (n,2n) reactions. According to Dr. Dugan, at a thickness of greater than about 15-20 cm the neutron capture reactions in BeO start to prevail over the (n,2n) reactions. Thus, BeO will provide the initial moderation of neutrons with the addition to the reactivity gain from (n,2n) reactions. Heavy water will provide the remaining moderation and also the reflection of neutrons. A combination of materials will also help reduce the critical volume of the systems that produce a fast spectrum such as ZrC and Pb. These materials may be able to benefit from a thin layer of moderating material such as BeO, ${}^7\text{LiD}$, or graphite. Although this will degrade the spectral quality desired, doing so may drastically decrease the size of the core.

Waste from GCRs should be decayed to see when it would be equivalent in activity as natural uranium ore. The spent fuel from the reference PWR should be analyzed in the same

manner to determine if the GCR indeed produces a waste with improved characteristics, reducing the time that isolation of such waste from the biosphere is required.

One area that deserves much attention is to investigate the possibility of using the GCR as a burner. Depending on the spectral characteristics of the core and the flux level, actinides can be placed in areas of the core that is most favorable for transmutation or fission. The spectrum within the core can vary drastically due to the large mean free path of neutrons and external moderation. Towards the center of the core the spectrum should consist of fast neutrons (i.e. in the KeV range) that are favorable for transmutation or fission of actinides. Additionally, most fast neutrons in the GCR leak out of the system or need to be thermalized to cause fissions; their reactivity worth is much less than thermal neutrons. Thus, using these neutrons to burn actinides placed towards the center of the core may be feasible.

One of the conclusions from Norring's research is that the initial production of actinides in a thermal spectrum is less than the production of actinides in a fast spectrum. However, for the transmutation and fission of actinides using a fast spectrum is more efficient [54]. It is necessary to investigate the effect of using both thermal and fast spectra in the fuel cycle. The fuel is initially fed into a thermal system. After the actinides have burnt-in, it is transferred to a fast system. This transfer of actinides is feasible due to the gaseous state of the fuel. The coupling of a thermal reactor to a fast reactor can theoretically decrease the amount of nuclear waste produced.

One important conclusion of this research is that the Pu mixture of the GCRs is less proliferation resistant than the Pu mixture in the PWR spent fuel. This opposes Norring's conclusion that the GCR in his research produces 28% fissile Pu, whereas the PWR produces 78% fissile Pu [54]. The discrepancy between the findings from these two research projects

may be related to the fuel cycle simulation method used. From Norring's thesis the exact method used for fuel cycle simulation is not clearly described. One can deduce from the sample MONTEBURNS input found in the Appendix of his thesis that the feed fuel is not the same enrichment as the initial enrichment at BOL. In fact, the feed fuel composition in this sample MONTEBURNS input only consists uranium and is missing the fluoride component. Additionally, the feed fuel enrichment is 65 w/o U-235. Recall that Pu-238 is mainly produced from capture interactions in U-235, and fissile Pu isotopes are produced from captures in U-238. Thus, more U-235 and less U-238 in the feed would result in an increase in Pu-238 production and decrease in fissile Pu production.

It would be interesting to determine the optimal fuel cycle conditions that would yield a Pu mixture that is more proliferation resistant than the Pu mixture resulting from the GCR fuel cycles found in this research. Feed fuel enrichment is one important fuel cycle parameter affecting the Pu characteristics. Fuel enrichment less than 20 w/o is exempt from safeguarding. Thus, the feed enrichment is limited to less than 20 w/o. As shown in this research, an enrichment of 20 w/o may not yield improvements in the Pu mixture over that of LWRs. The effects of other fuel cycle parameters on the Pu characteristics must be investigated.

Previous work on the GCRs has not considered the transmutation of fission products mainly because most fission products are short-lived and do not pose disposal problems. However, some fission products are long-lived such as Tc-99 ($T_{1/2} = 2.1E5$ years). The possibility of burning these long-lived fission products in the GCR should be investigated. This can be done simply by leaving select fission products in the core. However, MONTEBURNS requires that all isotopes of the same element must either be left in the core

or removed from it. Specific isotopes may not be selected to be filtered out of the gaseous mixture. Some of these isotopes may not pose disposal problems because they are short-lived but they may be neutron poisons. Thus, additional fuel may be needed for the negative reactivity effect caused by the presence of these fission products.

There are many ways that the GCR fuel cycle can be simulated in MONTEBURNS. The variables include feed fuel enrichment, method of fuel feed (continuous or discrete), and the elements to be removed from the core. The effect of these variables on the burnup of the fuel is unknown. For example, the fuel cycle for a reactor design could be analyzed using two methods. The first method is similar to the method used in this research where the unused uranium is removed from the core to approximate the circulation of the fuel. The second method is similar to Norring's method where all uranium isotopes are kept in the core, and more is added to maintain criticality. The total amount of fuel necessary to keep the reactor critical throughout the fuel cycle can be obtained, and the method which results in a higher fuel burnup can be determined. Similar analysis of other fuel cycle variables can be performed.

Another way to simulate depletion in the GCR is to separate the core into separate burn regions. Because most fissions occur close to the reflector, using the core-averaged cross sections in this region may not be accurate. Separating the core into at least two burn regions may improve the accuracy of results. Recall that the fuel circulates within the core. The actinides produced in the separate burn regions are eventually redistributed within the entire fuel volume. MONTEBURNS does not provide a way to simulate such a behavior. Modifications to the MONTEBURNS Perl script are necessary in order to employ this simulation method.

It is necessary to benchmark results obtained from MONTEBURNS with results from other depletion codes. Since the GCR is an unconventional system, most depletion codes are not applicable for fuel cycle analysis. This is because most depletion codes require libraries that are specific to a system. For example, in ORIGEN libraries for LWR systems are the most common, while library for gaseous fuel reactors are absent. However, MONTEBURNS solves this problem by calculating one group cross sections at each burn step using MCNP results. One may use other codes such as the SCALE package from Oak Ridge National Laboratory. However, to use the SCALE package a library must first be generated for GCRs. Additionally, it is unclear which code packages allow continuous fuel feed—an important feature of GCRs. A depletion code under development is a new feature in MCNPX coupled with CINDER. Depletion is a built-in feature in the MCNPX input, as opposed to MONTEBURNS where three input files are required. However, the current beta version of the depletion feature does not allow continuous fuel feed. It is best to use deterministic codes for benchmarking, since obtaining results from MONTEBURNS is already a time consuming process. The best way to use deterministic codes is to generate cross section libraries for GCRs using cross section processing codes such as NJOY.

APPENDIX A
TABULATED DATA FROM GCR DESIGN PARAMETERS SENSITIVITY STUDIES

The following data are from the reactor design parameters sensitivity studies presented in graphical form in Chapter 4. These design parameters include: reflector material, reflector thickness, gas pressure, fuel enrichment, and gap thickness.

Table A-1. Data from beryllium oxide reflector thickness sensitivity study.

refl width (cm)	k_{eff}	standard deviation	% fissions caused by nts with enrg in this range		
			<0.625 eV	0.625 eV-100 KeV	>100 KeV
30	0.94630	0.00131	81.60	16.05	2.35
35	0.96977	0.00128	82.08	15.62	2.31
40	0.98654	0.00137	82.44	15.29	2.27
45	0.99640	0.00130	82.54	15.23	2.22
50	1.00507	0.00132	82.75	15.04	2.21
55	1.01208	0.00131	82.87	14.91	2.22
60	1.01385	0.00135	82.86	14.94	2.20
65	1.01816	0.00130	82.98	14.82	2.19
70	1.01983	0.00128	82.97	14.84	2.19
75	1.02138	0.00131	83.11	14.71	2.18
80	1.02390	0.00131	82.93	14.90	2.17
85	1.02348	0.00131	83.01	14.82	2.17
90	1.02458	0.00130	83.09	14.75	2.16
95	1.02410	0.00128	83.08	14.73	2.19
		average	82.74	15.05	2.22

Table A-2. Data from lithium-7 hydride reflector thickness sensitivity study.

refl width (cm)	k_{eff}	standard deviation	% fissions caused by nts with enrg in this range		
			<0.625 eV	0.625 eV-100 KeV	>100 KeV
5	0.74911	0.00097	35.01	38.83	26.16
10	0.93114	0.00092	50.01	30.58	19.41
15	0.97614	0.00092	52.76	29.09	18.15
20	0.98458	0.00094	53.28	28.78	17.93
25	0.98816	0.00095	53.45	28.71	17.84
30	0.98749	0.00092	53.17	28.84	17.99
		average	49.61	30.81	19.58

Table A-3. Data from lithium-7 deuteride reflector thickness sensitivity study.

refl width (cm)	k_{eff}	standard deviation	% fissions caused by nts with enrg in this range		
			<0.625 eV	0.625 eV-100 KeV	>100 KeV
30	0.82841	0.00076	65.15	28.55	6.30
40	0.92288	0.00077	68.73	25.63	5.64
50	0.97086	0.00073	70.30	24.33	5.37
60	0.99463	0.00074	71.03	23.73	5.23
70	1.00613	0.00069	71.33	23.49	5.17
80	1.01364	0.00074	71.56	23.30	5.13
90	1.01772	0.00074	71.66	23.21	5.13
		average	69.97	24.61	5.42

Table A-4. Data from graphite reflector thickness sensitivity study.

refl width (cm)	k_{eff}	standard deviation	% fissions caused by nts with enrg in this range		
			<0.625 eV	0.625 eV-100 KeV	>100 KeV
50	0.92536	0.00184	77.70	18.91	3.39
60	0.96676	0.00179	78.38	18.36	3.26
70	0.99301	0.00181	79.12	17.73	3.15
80	1.01127	0.00171	79.24	17.63	3.13
90	1.01927	0.00189	79.61	17.31	3.09
100	1.02313	0.00183	79.76	17.14	3.11
110	1.03081	0.00177	79.73	17.21	3.06
120	1.03404	0.00181	79.87	17.08	3.05
130	1.03549	0.00194	79.88	17.07	3.05
		average	79.25	17.60	3.14

Table A-5. Data from tungsten reflector thickness sensitivity study.

refl width (cm)	k_{eff}	standard deviation	% fissions caused by nts with enrg in this range		
			<0.625 eV	0.625 eV-100 KeV	>100 KeV
5	0.82635	0.00011	0.00	38.17	61.83
10	0.95107	0.00011	0.00	43.67	56.33
15	0.98692	0.00011	0.00	45.28	54.72
20	0.99553	0.00011	0.00	45.70	54.30
25	0.99738	0.00011	0.00	45.78	54.22
30	0.99768	0.00011	0.00	45.81	54.19
35	0.99760	0.00011	0.00	45.80	54.20
		average	0.00	44.32	55.68

Table A-6. Data from zirconium carbide reflector thickness sensitivity study.

refl width (cm)	k_{eff}	standard deviation	% fissions caused by nts with enrg in this range		
			<0.625 eV	0.625 eV-100 KeV	>100 KeV
25.0	0.93559	0.00080	1.87	67.71	30.41
37.5	0.98160	0.00078	4.93	66.52	28.56
50.0	0.99393	0.00079	6.32	65.69	27.99
62.5	1.00117	0.00079	6.64	65.54	27.82
75.0	1.00121	0.00073	6.74	65.43	27.83
87.5	1.00243	0.00073	6.76	65.44	27.80
100.0	1.00211	0.00077	6.79	65.52	27.69
		average	5.72	65.98	28.30

Table A-7. Data from lead reflector thickness sensitivity study.

refl width (cm)	k_{eff}	standard deviation	% fissions caused by nts with enrg in this range		
			<0.625 eV	0.625 eV-100 KeV	>100 KeV
70	0.95496	0.00091	0.15	70.46	29.39
80	0.97178	0.00089	0.28	70.88	28.85
90	0.98298	0.00089	0.42	71.02	28.56
100	0.99159	0.00084	0.55	71.20	28.25
110	0.99626	0.00085	0.69	71.21	28.10
120	0.99962	0.00082	0.74	71.13	28.12
130	1.00008	0.00084	0.78	71.28	27.95
140	1.00036	0.00085	0.84	71.18	27.97
		average	0.56	71.05	28.40

Table A-8. Data from gas pressure sensitivity study with pressures between 10 and 60 bars.

pressure (bars)	k_{eff}	standard deviation	% fissions caused by nts with enrg in this range		
			<0.625 eV	0.625 eV-100 KeV	>100 KeV
10.0	0.92432	0.00111	95.56	3.76	0.68
12.0	0.97600	0.00116	95.08	4.15	0.76
14.0	1.01489	0.00122	94.61	4.54	0.85
16.0	1.04412	0.00119	94.10	4.96	0.93
18.0	1.07026	0.00118	93.61	5.36	1.03
20.0	1.09016	0.00127	93.19	5.70	1.12
22.5	1.11071	0.00124	92.61	6.17	1.22
25.0	1.12937	0.00120	92.13	6.53	1.34
27.5	1.14367	0.00120	91.61	6.93	1.45
30.0	1.15552	0.00125	91.09	7.36	1.56
32.5	1.16296	0.00124	90.55	7.77	1.68
35.0	1.17189	0.00127	90.14	8.10	1.77
37.5	1.17711	0.00126	89.67	8.45	1.88
40.0	1.18485	0.00125	89.20	8.82	1.98
42.5	1.18761	0.00124	88.70	9.20	2.10
45.0	1.19227	0.00125	88.23	9.57	2.20
47.5	1.19790	0.00123	87.84	9.86	2.30
50.0	1.19951	0.00127	87.36	10.23	2.41
52.5	1.20104	0.00128	86.98	10.51	2.50
55.0	1.20257	0.00120	86.51	10.89	2.60
57.5	1.20555	0.00127	86.08	11.20	2.73
60.0	1.20702	0.00122	85.72	11.47	2.81
		average	90.48	7.80	1.72

Table A-9. Data from fuel enrichment sensitivity study with enrichments between 2 and 20 w/o U-235.

enrichment (w/o)	k_{eff}	standard deviation	% fissions caused by nts with enrg in this range		
			<0.625 eV	0.625 eV-100 KeV	>100 KeV
2	0.63623	0.00118	96.13	2.87	1.00
4	0.89518	0.00154	95.38	3.83	0.79
6	1.03754	0.00172	94.63	4.62	0.75
8	1.12680	0.00171	93.81	5.43	0.77
10	1.18675	0.00191	92.97	6.26	0.77
12	1.23279	0.00187	92.13	7.08	0.79
14	1.26703	0.00183	91.38	7.78	0.84
16	1.29738	0.00183	90.57	8.56	0.87
18	1.31990	0.00193	89.86	9.23	0.91
20	1.33925	0.00195	89.23	9.81	0.96
		average	92.61	6.55	0.85

Table A-10. Data from length-to-diameter ratio sensitivity study with L/D ratios between 1 and 3.

L/D ratio	k_{eff}	standard deviation	% fissions caused by nts with enrg in this range		
			<0.625 eV	0.625 eV-100 KeV	>100 KeV
1.00	1.01321	0.00081	94.57	4.57	0.86
1.25	1.01064	0.00085	94.60	4.56	0.84
1.50	1.00646	0.00089	94.59	4.56	0.84
1.75	1.00052	0.00083	94.65	4.52	0.83
2.00	0.99402	0.00081	94.68	4.48	0.83
2.25	0.98967	0.00083	94.78	4.41	0.82
2.50	0.98280	0.00087	94.79	4.40	0.81
2.75	0.97738	0.00083	94.80	4.39	0.81
3.00	0.97143	0.00085	94.88	4.32	0.80
		average	94.70	4.47	0.83

Table A-11. Data from gap thickness sensitivity study with gap thickness between 0 and 10 cm.

gap (cm)	k_{eff}	standard deviation	% fissions caused by nts with enrg in this range		
			<0.625 eV	0.625 eV-100 KeV	>100 KeV
single cavity	1.01321	0.00081	94.57	4.57	0.86
0.0	1.02101	0.00066	95.38	3.95	0.66
1.0	1.02161	0.00068	95.46	3.90	0.64
2.5	1.02379	0.00066	95.57	3.81	0.62
5.0	1.02696	0.00064	95.65	3.75	0.59
7.5	1.02937	0.00066	95.74	3.68	0.58
10.0	1.03002	0.00063	95.86	3.57	0.56
		average	95.61	3.78	0.61

APPENDIX B
SAMPLE MCNP INPUT

This MCNP input file describes the ^7LiD GCR analyzed in Chapters 4 and 5. The energy bin structure used for spectrum tallies is also listed here. This file should not be named with a file extension when using MONTEBURNS. For depletion calculation in MONTEBURNS the tallies and energy bin structure is not necessary. Additionally, the number of histories should be decreased.

```
LiD reflector Tfuel 2000 Tmod 750, 80cm
C
C Gas avg temperature of 2000 K
C reflector temp of 750 K
C Pressure of 26.49157685 bars
C 80 cm reflector
C 19.95 w/o enrichment
C Fuel volume 21205750.41 cc
C U mass 8.0414E+05 g
C L/D 1
C
1 1 -5.0027E-02 -1 5 -6 imp:n 1 vol=21205750.41 $ fuel
4 7 -0.876 #1 -3 4 -7 imp:n 1 vol=55241765.22 $ reflector
6 0 (3:-4:7) imp:n 0 $ world

1 cz 150.0
3 cz 230.0
4 pz 0.0
5 pz 80.00
6 pz 380.0
7 pz 460.0

mode n
kcode 100000 1 10 400
ksrc 0.0 0.0 230.0
f14:n 1 Score flux tally
f24:n 4 $reflector flux tally
C
C Energy bin structure
```

C

E0	1.00E-10	4.00E-10	7.00E-10	1.00E-09	4.00E-09
	7.00E-09	1.00E-08	4.00E-08	7.00E-08	1.00E-07
	2.29E-07	3.57E-07	4.86E-07	6.14E-07	7.43E-07
	8.71E-07	1.00E-06	1.30E-06	1.60E-06	1.90E-06
	2.20E-06	2.50E-06	2.80E-06	3.10E-06	3.40E-06
	3.70E-06	4.00E-06	4.30E-06	4.60E-06	4.90E-06
	5.20E-06	5.50E-06	5.80E-06	6.10E-06	6.40E-06
	6.70E-06	7.00E-06	7.30E-06	7.60E-06	7.90E-06
	8.20E-06	8.50E-06	8.80E-06	9.10E-06	9.40E-06
	9.70E-06	1.00E-05	1.15E-05	1.30E-05	1.45E-05
	1.60E-05	1.75E-05	1.90E-05	2.05E-05	2.20E-05
	2.35E-05	2.50E-05	2.65E-05	2.80E-05	2.95E-05
	3.10E-05	3.25E-05	3.40E-05	3.55E-05	3.70E-05
	3.85E-05	4.00E-05	4.15E-05	4.30E-05	4.45E-05
	4.60E-05	4.75E-05	4.90E-05	5.05E-05	5.20E-05
	5.35E-05	5.50E-05	5.65E-05	5.80E-05	5.95E-05
	6.10E-05	6.25E-05	6.40E-05	6.55E-05	6.70E-05
	6.85E-05	7.00E-05	7.15E-05	7.30E-05	7.45E-05
	7.60E-05	7.75E-05	7.90E-05	8.05E-05	8.20E-05
	8.35E-05	8.50E-05	8.65E-05	8.80E-05	8.95E-05
	9.10E-05	9.25E-05	9.40E-05	9.55E-05	9.70E-05
	9.85E-05	0.0001	0.0001036	0.0001072	0.0001108
	0.0001144	0.000118	0.0001216	0.0001252	0.0001288
	0.0001324	0.000136	0.0001396	0.0001432	0.0001468
	0.0001504	0.000154	0.0001576	0.0001612	0.0001648
	0.0001684	0.000172	0.0001756	0.0001792	0.0001828
	0.0001864	0.00019	0.0001936	0.0001972	0.0002008
	0.0002044	0.000208	0.0002116	0.0002152	0.0002188
	0.0002224	0.000226	0.0002296	0.0002332	0.0002368
	0.0002404	0.000244	0.0002476	0.0002512	0.0002548
	0.0002584	0.000262	0.0002656	0.0002692	0.0002728
	0.0002764	0.00028	0.0002836	0.0002872	0.0002908
	0.0002944	0.000298	0.0003016	0.0003052	0.0003088
	0.0003124	0.000316	0.0003196	0.0003232	0.0003268
	0.0003304	0.000334	0.0003376	0.0003412	0.0003448
	0.0003484	0.000352	0.0003556	0.0003592	0.0003628
	0.0003664	0.00037	0.0003736	0.0003772	0.0003808
	0.0003844	0.000388	0.0003916	0.0003952	0.0003988
	0.0004024	0.000406	0.0004096	0.0004132	0.0004168
	0.0004204	0.000424	0.0004276	0.0004312	0.0004348
	0.0004384	0.000442	0.0004456	0.0004492	0.0004528
	0.0004564	0.00046	0.0004636	0.0004672	0.0004708
	0.0004744	0.000478	0.0004816	0.0004852	0.0004888
	0.0004924	0.000496	0.0004996	0.0005032	0.0005068
	0.0005104	0.000514	0.0005176	0.0005212	0.0005248

0.0005284	0.000532	0.0005356	0.0005392	0.0005428
0.0005464	0.00055	0.0005536	0.0005572	0.0005608
0.0005644	0.000568	0.0005716	0.0005752	0.0005788
0.0005824	0.000586	0.0005896	0.0005932	0.0005968
0.0006004	0.000604	0.0006076	0.0006112	0.0006148
0.0006184	0.000622	0.0006256	0.0006292	0.0006328
0.0006364	0.00064	0.0006436	0.0006472	0.0006508
0.0006544	0.000658	0.0006616	0.0006652	0.0006688
0.0006724	0.000676	0.0006796	0.0006832	0.0006868
0.0006904	0.000694	0.0006976	0.0007012	0.0007048
0.0007084	0.000712	0.0007156	0.0007192	0.0007228
0.0007264	0.00073	0.0007336	0.0007372	0.0007408
0.0007444	0.000748	0.0007516	0.0007552	0.0007588
0.0007624	0.000766	0.0007696	0.0007732	0.0007768
0.0007804	0.000784	0.0007876	0.0007912	0.0007948
0.0007984	0.000802	0.0008056	0.0008092	0.0008128
0.0008164	0.00082	0.0008236	0.0008272	0.0008308
0.0008344	0.000838	0.0008416	0.0008452	0.0008488
0.0008524	0.000856	0.0008596	0.0008632	0.0008668
0.0008704	0.000874	0.0008776	0.0008812	0.0008848
0.0008884	0.000892	0.0008956	0.0008992	0.0009028
0.0009064	0.00091	0.0009136	0.0009172	0.0009208
0.0009244	0.000928	0.0009316	0.0009352	0.0009388
0.0009424	0.000946	0.0009496	0.0009532	0.0009568
0.0009604	0.000964	0.0009676	0.0009712	0.0009748
0.0009784	0.000982	0.0009856	0.0009892	0.0009928
0.0009964	0.001	0.001036	0.001072	0.001108
0.001144	0.00118	0.001216	0.001252	0.001288
0.001324	0.00136	0.001396	0.001432	0.001468
0.001504	0.00154	0.001576	0.001612	0.001648
0.001684	0.00172	0.001756	0.001792	0.001828
0.001864	0.0019	0.001936	0.001972	0.002008
0.002044	0.00208	0.002116	0.002152	0.002188
0.002224	0.00226	0.002296	0.002332	0.002368
0.002404	0.00244	0.002476	0.002512	0.002548
0.002584	0.00262	0.002656	0.002692	0.002728
0.002764	0.0028	0.002836	0.002872	0.002908
0.002944	0.00298	0.003016	0.003052	0.003088
0.003124	0.00316	0.003196	0.003232	0.003268
0.003304	0.00334	0.003376	0.003412	0.003448
0.003484	0.00352	0.003556	0.003592	0.003628
0.003664	0.0037	0.003736	0.003772	0.003808
0.003844	0.00388	0.003916	0.003952	0.003988
0.004024	0.00406	0.004096	0.004132	0.004168
0.004204	0.00424	0.004276	0.004312	0.004348
0.004384	0.00442	0.004456	0.004492	0.004528

0.004564	0.0046	0.004636	0.004672	0.004708
0.004744	0.00478	0.004816	0.004852	0.004888
0.004924	0.00496	0.004996	0.005032	0.005068
0.005104	0.00514	0.005176	0.005212	0.005248
0.005284	0.00532	0.005356	0.005392	0.005428
0.005464	0.0055	0.005536	0.005572	0.005608
0.005644	0.00568	0.005716	0.005752	0.005788
0.005824	0.00586	0.005896	0.005932	0.005968
0.006004	0.00604	0.006076	0.006112	0.006148
0.006184	0.00622	0.006256	0.006292	0.006328
0.006364	0.0064	0.006436	0.006472	0.006508
0.006544	0.00658	0.006616	0.006652	0.006688
0.006724	0.00676	0.006796	0.006832	0.006868
0.006904	0.00694	0.006976	0.007012	0.007048
0.007084	0.00712	0.007156	0.007192	0.007228
0.007264	0.0073	0.007336	0.007372	0.007408
0.007444	0.00748	0.007516	0.007552	0.007588
0.007624	0.00766	0.007696	0.007732	0.007768
0.007804	0.00784	0.007876	0.007912	0.007948
0.007984	0.00802	0.008056	0.008092	0.008128
0.008164	0.0082	0.008236	0.008272	0.008308
0.008344	0.00838	0.008416	0.008452	0.008488
0.008524	0.00856	0.008596	0.008632	0.008668
0.008704	0.00874	0.008776	0.008812	0.008848
0.008884	0.00892	0.008956	0.008992	0.009028
0.009064	0.0091	0.009136	0.009172	0.009208
0.009244	0.00928	0.009316	0.009352	0.009388
0.009424	0.00946	0.009496	0.009532	0.009568
0.009604	0.00964	0.009676	0.009712	0.009748
0.009784	0.00982	0.009856	0.009892	0.009928
0.009964	0.01	0.015	0.02	0.025
0.03	0.035	0.04	0.045	0.05
0.055	0.06	0.065	0.07	0.075
0.08	0.085	0.09	0.095	0.1
0.16923	0.23846	0.30769	0.37692	0.44615
0.51538	0.58462	0.65385	0.72308	0.79231
0.86154	0.93077	1	2.125	3.25
4.375	5.5	6.625	7.75	8.875
10	11	12	13	14
15	16	17	18	19
20	21	22	23	30

C

C FUEL

C

C 19.95 w/o enrichment

C flourine at 293.6 K, ENDF66a

C U235 and U238 at 1200 K, ENDF62mt

C

m1 9019.66c 4

92235.17c 0.201543028

92238.17c 0.798456972

GAS=1 \$ fuel gaseous

C

C REFLECTOR

C

C H-2 and Li-7 at 293.6 K, ENDF66a

C

m7 1002.66c 0.5

3007.66c 0.5

tmp 1.72340E-07 \$ 2000 K

6.46275E-08 6.46275E-08 \$ 750 K

totnu

print

APPENDIX C
SAMPLE MONTEBURNS FEED FILE

This is the feed file corresponding to the MCNP input file of the ⁷LiD GCR design analyzed in Chapters 4 and 5. This file should be named '*filename.feed*'. The feed fuel enrichment is 19.95 w/o and all fission products together with unused fuel are removed.

Time Step	Days Burned	Power	MBMat	Feed	Begin&End	Rates	Remov.	Fraction	F.P.	Removed
			#	grams/day	Group#					
1	15.	1.00	1 1	177780.2	20244.7	1 1.0 0 0.0 0 0.0 !				
2	15.	1.00	1 1	116636.2	13478.5	1 1.0 0 0.0 0 0.0 !				
3	30.	1.00	1 1	92028.0	21576.0	1 1.0 0 0.0 0 0.0 !				
4	30.	1.00	1 1	70881.0	25781.0	1 1.0 0 0.0 0 0.0 !				
5	30.	1.00	1 1	56508.4	41832.2	1 1.0 0 0.0 0 0.0 !				
6	60.	1.00	1 1	50281.2	38961.4	1 1.0 0 0.0 0 0.0 !				
7	60.	1.00	1 1	34058.7	47509.6	1 1.0 0 0.0 0 0.0 !				
8	60.	1.00	1 1	35795.0	35528.9	1 1.0 0 0.0 0 0.0 !				
9	60.	1.00	1 1	27877.0	45018.7	1 1.0 0 0.0 0 0.0 !				
10	60.	1.00	1 1	30859.1	34944.9	1 1.0 0 0.0 0 0.0 !				
11	60.	1.00	1 1	26877.2	45995.9	1 1.0 0 0.0 0 0.0 !				
12	60.	1.00	1 1	29805.0	35598.1	1 1.0 0 0.0 0 0.0 !				
13	60.	1.00	1 1	19489.7	35228.2	1 1.0 0 0.0 0 0.0 !				
14	60.	1.00	1 1	22583.4	28707.3	1 1.0 0 0.0 0 0.0 !				
15	60.	1.00	1 1	19841.9	34619.0	1 1.0 0 0.0 0 0.0 !				
16	360.	1.00	1 1	34987.9	20290.5	1 1.0 0 0.0 0 0.0 !				
17	360.	1.00	1 1	28324.4	15629.0	1 1.0 0 0.0 0 0.0 !				
18	360.	1.00	1 1	30806.2	5718.8	1 1.0 0 0.0 0 0.0 !				
19	360.	1.00	1 1	25609.8	4519.9	1 1.0 0 0.0 0 0.0 !				
20	360.	1.00	1 1	28273.7	1668.9	1 1.0 0 0.0 0 0.0 !				
21	360.	1.00	1 1	23916.6	2002.0	1 1.0 0 0.0 0 0.0 !				
22	360.	1.00	1 1	22633.3	1690.8	1 1.0 0 0.0 0 0.0 !				
23	360.	1.00	1 1	19050.6	2123.1	1 1.0 0 0.0 0 0.0 !				
24	360.	1.00	1 1	18045.8	1815.2	1 1.0 0 0.0 0 0.0 !				
25	360.	1.00	1 1	15224.1	2277.9	1 1.0 0 0.0 0 0.0 !				
26	370.	1.00	1 1	14421.1	1947.6	1 1.0 0 0.0 0 0.0 !				
27	371.	1.00	1 1	12156.8	2483.5	1 1.0 0 0.0 0 0.0 !				
28	371.	1.00	1 1	11648.7	2155.1	1 1.0 0 0.0 0 0.0 !				
29	841.	1.00	1 1	9819.7	2748.1	1 1.0 0 0.0 0 0.0 !				
30	1027	1.00	1 1	7077.6	1786.8	1 1.0 0 0.0 0 0.0 !				

1

3
92235 0.151220897
92238 0.606778586
9019 0.242000517
1
3
9 9
92 92
28 68

APPENDIX D
SAMPLE MONTEBURNS INPUT FILE

This is the MONTEBURNS input file corresponding to the ⁷LiD GCR design analyzed in Chapters 4 and 5. This file should be named '*filename.inp*'.

```

LiD GCR
PC          ! Operating system
1          ! Number of materials for depletion
1          ! Material number (from MCNP input file) for depletion
0.0        ! Volume (if 0.0 then the MCNP volume will be used) [cc]
3000       ! Thermal power [MW]
-200.0     ! Recoverable energy per fission
0.0        ! Total number of depletion days (non zero if no feed file used)
30         ! No. of outer burn steps, must = to No. of feed steps and < 100
100        ! No. of internal burn steps (within ORIGEN)
1          ! No. of predictor steps
0          ! Outer step to restart after (if = 0 starts from beginning)
PWRU       ! ORIGEN default library
C:\Origen22\Libs ! Location of ORIGEN library
0.1        ! Fractional importance
1          ! Intermediate k-effective calculation, 0=no and 1=yes
27         ! Number of automatic tally isotopes (those deemed important)
43099.65c  ! List of the important isotopes
53129.60c
54135.54c  ! ***** These cross sections take precedence over those listed in
55135.60c  ! ***** 'mbxs.inp'
55137.60c
62149.65c
92234.65c
92235.17c
92236.65c
92237.65c
92238.17c
93237.66c
94238.65c
94239.17c
94240.65c
94241.65c
94242.65c
95241.65c

```

95242.65c
95243.65c
96242.65c
96243.65c
96244.65c
96245.65c
96246.66c
96247.65c
96248.65c

LIST OF REFERENCES

1. Cochran, R. G., Tsoulfanidis, N., *The Nuclear Fuel Cycle: Analysis and Management*, 2nd Edition, American Nuclear Society, La Grange Park, IL, 1990, pp. 210-314.
2. "Radiation Information, Uranium," *U.S. Environmental Protection Agency*, 30 Nov. 2004, accessed 8 Sep. 2005
<<http://www.epa.gov/radiation/radionuclides/uranium.htm>>.
3. "Processing of Used Nuclear Fuel for Recycling," *Uranium Information Center*, UIC Nuclear Issues Briefing Paper # 72, Dec. 2005, accessed 24 Feb. 2006
<<http://www.uic.com.au/nip72.htm>>.
4. Lamarsh, J. R., Baratta, A. J., *Introduction to Nuclear Engineering*, 3rd Edition, Prentice Hall, Upper Saddle River, NJ, 2001, pp. 188-221.
5. "Plutonium Recovery from Spent Fuel Reprocessing by Nuclear Fuel Services at West Valley, New York from 1966 to 1972," *U.S. Department of Energy*, Feb. 1996, accessed 23 Feb. 2006
<<http://www.osti.gov/opennet/document/purecov/nfsrepo.html#ZZ3>>.
6. "Nuclear Reprocessing," *Wikipedia*, accessed 24 Feb. 2006
<http://en.wikipedia.org/wiki/Nuclear_reprocessing#The_current_main_method_which_is_in_use>.
7. "Technology Pioneered at Argonne Shows Promise for Next Generation of Nuclear Reactors," *Frontiers 2002 Research Highlights*, accessed 24 Feb. 2006
<http://www.anl.gov/Media_Center/Frontiers/2002/d1ee.html>.
8. "Low-Level Waste," *U.S. Nuclear Regulatory Commission*, 2 Sep. 2004, accessed 25 Feb. 2006 <<http://www.nrc.gov/waste/low-level-waste.html>>.
9. "Why Yucca Mountain," *U.S. Department of Energy*, accessed 26 Feb. 2006
<<http://www.ocrwm.doe.gov/ymp/sr/brochure.pdf>>.
10. "IB92059: Civilian Nuclear Waste Disposal," *CRS Issue Brief for Congress*, 30 Jul. 2001, accessed 25 Feb. 2006 <http://cnie.org/NLE/CRSreports/Waste/waste-2.cfm#_1_9>.
11. "Yucca Mountain Science and Engineering Report, Rev 1, DOE/RW-0539-1," *U.S. Department of Energy*, Feb. 2002, accessed 27 Feb. 2006
<http://www.ocrwm.doe.gov/documents/ser_b/index.htm>.

12. American Nuclear Society *Nuclear News* Sept 2005, statement Nov 2005.
13. “Nuclear Performance Monthly,” *Nuclear Energy Institute*, Feb. 2006, accessed 27 Feb. 2006 <<http://www.nei.org/documents/NuclearPerformanceMonthly.pdf>>.
14. Sasa, T., “Research Activities for Accelerator-Driven Transmutation System at JAERI,” *Progress in Nuclear Energy: Proceedings of the First COE-INES International Symposium, INES-1*, Vol. 47, No. 1-4, Nov. 2004, pp. 314-326.
15. Zrodnikov, A., Gulevich, A., Chekounov, V., Dedoul, A., Novikova, N., Tormyshev, I., Orlov, Y., Pankratov, D., Roussanov, A., Smetanin, E., Troyanov, V., “Nuclear Waste Burner for Minor Actinides Elimination,” *Progress in Nuclear Energy: Proceedings of the First COE-INES International Symposium, INES-1*, Vol. 47, No. 1-4, Nov. 2004, pp. 339-346.
16. Takizuka, T., Tsujimoto, K., Sasa, T., Takano, H., “Dedicated Accelerator-Driven System for Nuclear Waste Transmutation,” Center for Neutron Science, Japan Atomic Energy Research Institute, Tokai-Mura, 1998.
17. Smith, B. M., Anghaie, S., “Gas Core Reactor with Magnetohydrodynamic Power System and Cascading Power Cycle,” *Nuclear Technology*, Vol. 145, No. 3, 2004.
18. Hassan, H. A., Deese, J. E., “Thermodynamic Properties of UF₆ at High Temperatures,” NASA-CR-2373, April 1974.
19. Nieskens, M. J. P. C., Stein, H. N., “Thermodynamic Calculations on the System Uranium-Carbon-Flourine,” FOM-nr 41.165, University of Technology, Eindhoven, The Netherlands, Feb. 1977.
20. Maya, I., Anghaie, S., Diaz, N. J., Dugan, E. T., “Ultrahigh Temperature Vapor-Core Reactor—Magnetohydrodynamic System for Space Nuclear Electric Power,” *Journal of Propulsion and Power*, Vol. 9, No. 1, Jan.-Feb. 1993, pp. 98-104.
21. Anghaie, S., “Development of Liquid-Vapor Core Reactors with MHD Generator for Space Power and Propulsion Applications,” DOE Project: DE-FG07-98ID 13635, Final Report, Aug. 2002.
22. Kahook, S. D., “Static and Dynamic Neutronic Analysis of the Uranium Tetra-Flouride, Ultrahigh Temperature, Vapor Core Reactor System,” University of Florida, Gainesville, 1991.
23. *Webelements*, accessed 29 Mar. 2006 <<http://www.webelements.com>>.
24. “Beryllium Oxide-Beryllia,” *The A to Z of Materials*, accessed 29 Mar. 2006 <<http://www.azom.com/details.asp?ArticleID=263>>.
25. “Lithium Hydride,” accessed 29 Mar. 2006 <<http://www.cmmp.ucl.ac.uk/~ahh/research/crystal/lih.htm>>.

26. "Lithium Hydride," *Wikipedia*, 21, Jan. 2006, accessed 29 Mar. 2006 <http://en.wikipedia.org/wiki/Lithium_hydride>.
27. "Zirconium Carbide," *The A to Z of Materials*, accessed 27 Apr. 2006 <<http://www.azom.com/details.asp?ArticleID=261>>.
28. "Zirconium Carbide," *Wikipedia*, 19 Mar. 2006, accessed 27 Apr. 2006 <http://en.wikipedia.org/wiki/Zirconium_carbide>.
29. Adriamonje, S., Carminati, F., "Neutron Driven Nuclear Transmutation by Adiabatic Resonance Crossing," *AIP Conference Proceedings CP447, Nuclear Fission and Fission-Product Spectroscopy: Second International Workshop*, 1998, pp. 26-34.
30. Abanades, A., Aleixandre, J., "Transmutation of Tc-99 in a Low Lethargy Medium as a Function of the Neutron Energy," *AIP Conference Proceedings CP447, Nuclear Fission and Fission-Product Spectroscopy: Second International Workshop*, 1998, pp. 35-42.
31. Anghaie, S., Knight, T. W., Norring, R., Smith, B. M., "Optimum Utilization of Nuclear Fuel with Gas and Vapor Core Reactors," *Progress in Nuclear Energy: Proceedings of the First COE-INES International Symposium, INES-1*, Nov. 2004, pp. 74-90.
32. Dugan, E. T., Kutikkad, K., "Reactor Dynamics and Stability Analysis of a Burst-Mode Gas Core Reactor, Brayton Cycle Space Power System," *Nuclear Technology*, Vol. 103, Jul. 1993, pp. 79-92.
33. Dugan, E. T., Kahook, S. D., "Static and Dynamic Neutronic Analysis of a Burst-Mode, Multiple-Cavity Gas Core Reactor, Rankine Cycle Space Power System," *Nuclear Technology*, Vol. 103, Aug. 1993, pp. 139-156.
34. Dugan, E. T., Alfakhar, M. K., "A Hybrid S_n -Diffusion Theory Computational Scheme for Efficient Neutronic Calculations of Externally Moderated Gas Core Reactors," *Nuclear Technology*, Vol. 103, Sep. 1993, pp. 417-425.
35. X-5 Monte Carlo Team, *MCNP-A General Monte Carlo N-Particle Transport Code, Version 5*, Vol. 1, Apr. 2003.
36. Croff, A. G., "ORIGEN2: A Versatile Computer Code for Calculating the Nuclide Compositions and Characteristics of Nuclear Materials," *Nuclear Technology*, Vol. 62, Sep. 1983, pp. 335-352.
37. "Some Physics of Uranium," *World Nuclear Association*, Jul. 2000, accessed 14 Apr. 2006 <<http://www.world-nuclear.org/education/phys.htm>>.
38. "Thorium," *Wikipedia*, accessed 20 Apr. 2006 <<http://en.wikipedia.org/wiki/Thorium>>.

39. "Evaluated Nuclear Data File/B-VI.8," *Brookhaven National Laboratory*, 2001, accessed 18 April 2006 <<http://www.nndc.bnl.gov/exfor3/endlf00.htm>>.
40. "Plutonium," *Wikipedia*, 18 Apr. 2006, accessed 20 Apr. 2006 <<http://en.wikipedia.org/wiki/Plutonium>>.
41. "Periodic Table of the Elements," *Los Alamos National Laboratory's Chemistry Division*, 15 Dec. 2003, accessed 20 Apr. 2006 <<http://periodic.lanl.gov/default.htm>>.
42. "Table of Nuclides," *Korea Atomic Energy Research Institute*, accessed 21 Apr. 2006 <<http://atom.kaeri.re.kr/>>.
43. "Curium," *Wikipedia*, 20 Apr. 2006, accessed 21 Apr. 2006 <<http://en.wikipedia.org/wiki/Curium>>.
44. Shmelev, A., Apse, V., and Koulikov, G., "On the Main Objectives of Transmutation Cycles for Long-Lived Fission Products and Minor Actinides," *Progress in Nuclear Energy*, Vol. 37, No. 1-4, 2000, pp. 235-240.
45. "Radioisotope Thermoelectric Generator," *Wikipedia*, 13 Apr. 2006, accessed 21 Apr. 2006 <http://en.wikipedia.org/wiki/Radioisotope_thermoelectric_generators>.
46. "Fission Product," *Wikipedia*, 12 Apr. 2006, accessed 23 Apr. 2006 <http://en.wikipedia.org/wiki/Fission_product>.
47. "Fission Product (by Element)," *Wikipedia*, 12 Mar. 2006, accessed 23 Apr. 2006 <http://en.wikipedia.org/wiki/Fission_products_%28by_element%29>.
48. "Strontium," *Wikipedia*, 11 Apr. 2006, accessed 23 Apr. 2006 <<http://en.wikipedia.org/wiki/Strontium>>.
49. Moore, P., "Going Nuclear: A Green Makes the Case," *The Washington Post*, 16 Apr. 2006, pp. B01.
50. Ezoubtchenko, A. A., Saito, M., Artisyuk, V. V., Sagara, H., "Proliferation Resistance Properties of U and Pu Isotopes," *Progress in Nuclear Energy*, Vol. 47, No. 1-4, 2005, pp. 701-702.
51. Peryoga, Y., Saito, M., Sagara, H., "Improvement of Plutonium Proliferation Resistance by Doping Minor Actinides," *Progress in Nuclear Energy*, Vol. 47, No. 1-4, 2005, pp. 693-700.
52. "Technetium," *Wikipedia*, accessed 26 Apr. 2006 <<http://en.wikipedia.org/wiki/Tc>>.
53. Paternoster, R., Ohanian, M. J., Schneider, R., Thom, K., "Nuclear Waste Disposal Utilizing a Gaseous-Core Reactor," *Transactions of the American Nuclear Society*, Vol. 19, 1974, pp. 203-204.

54. Norring, R., "Optimum Utilization of Fission Power with Gas Core Reactors," M.E. Thesis, University of Florida, Gainesville, 2004.
55. Baxter, A., Rodriguez, C., "The Application of Gas-Cooled Reactor Technologies to the Transmutation of Nuclear Waste," *Progress in Nuclear Energy*, Vol. 38, No. 1-2, 2001, pp. 81-105.
56. Broeders, C., Kiefhaber, E., Wiese, H., "Burning Transuranium Isotopes in Thermal and Fast Reactors," *Nuclear Engineering and Design* 202, 2000, pp. 157-172.

BIOGRAPHICAL SKETCH

Cindy Fung was born on February 11th, 1982, in Venezuela. She moved to Miami, Florida, at the age of eight, but moved back to Venezuela at the age of twelve and attended middle school for three years before moving back to Miami for high school. During her attendance in Advanced Placement classes in high school, she was introduced to nuclear physics. She graduated in the top ten percent of her class from Miami Senior High School in 2000.

Following graduation she moved to Gainesville, Florida, where she was admitted to the College of Engineering at the University of Florida and became a student in the Nuclear and Radiological Engineering Department. During the summers, she obtained various internship positions to gain work experience in the nuclear industry. Her employers include Entergy, General Electric, and Los Alamos National Laboratory.

Throughout her college years, she actively participated in extracurricular activities to develop leadership and interpersonal skills. Some of the leadership positions include treasurer and secretary of the Benton Engineering Council, vice-president and president of the Student Chapter of the American Nuclear Society, and member of Alpha Nu Sigma—an honor society for Nuclear Engineering students. In 2003, she received the Leadership Award from the Benton Engineering Council. During her presidency at the American Nuclear Society, she spearheaded many improvements leading the chapter to win the Samuel Glasstone Award—the highest honor a student chapter can receive from the American Nuclear Society (the national organization).

In 2004, she obtained her Bachelor of Science in nuclear and radiological engineering with a minor in computer information science and engineering. She graduated summa cum laude (highest honors) with an honors project titled “Development of Gamma Transport Factors for Boiling Water Reactor Fuels.”

She continued her studies in nuclear engineering at the University of Florida as a Master of Engineering student. She plans to obtain her M.E. in August 2006.

She has accepted a position in the Edison Engineering Development Program at Global Nuclear Fuel—a subsidiary of General Electric. The program will train her to be a successful engineer and leader in all businesses owned by General Electric, increasing both the breadth and depth of the skills she developed as a student. She is excited to start her career at General Electric.